LUND UNIVERSITY

Turbocharged HCCI Engine, Improving Efficiency and Operating Range

Johansson, Thomas

2010

Link to publication

Citation for published version (APA):
Johansson, T. (2010). *Turbocharged HCCI Engine, Improving Efficiency and Operating Range*. [Doctoral Thesis (compilation), Combustion Engines].

Total number of authors:
1

General rights
Unless other specific re-use rights are stated the following general rights apply:
Copyright and moral rights for the publications made accessible in the public portal are retained by the authors and/or other copyright owners and it is a condition of accessing publications that users recognise and abide by the legal requirements associated with these rights.
• Users may download and print one copy of any publication from the public portal for the purpose of private study or research.
• You may not further distribute the material or use it for any profit-making activity or commercial gain
• You may freely distribute the URL identifying the publication in the public portal

Read more about Creative commons licenses: https://creativecommons.org/licenses/

Take down policy
If you believe that this document breaches copyright please contact us providing details, and we will remove access to the work immediately and investigate your claim.

LUND UNIVERSITY

PO Box 117
221 00 Lund
+46 46-222 00 00

Turbocharged HCCI Engine

Improving Efficiency and Operating Range

Thomas Johansson

Doctoral Thesis

Division of Combustion Engines
Department of Energy Sciences
Faculty of Engineering
Lund University
Sweden

LUND UNIVERSITY

To my family

ISBN 978-91-7473-061-6
ISRN LUTMDN/TMHP-10/1073 – SE
ISSN 0282-1990

Division of Combustion Engines
Department of Energy Sciences
Faculty of Engineering
Lund University
P.O Box 118
SE-22100 Lund

© Thomas Johansson, All rights reserved
Printed in Sweden by Media-Tryck, Lund, November 2010

List of papers

Paper I
HCCI Operating Range in a Turbo-charged Multi Cylinder Engine with VVT and Spray-Guided DI
T. Johansson, B. Johansson, P. Tunestål, H. Aulin
SAE technical paper 2009-01-0494
Presented at the SAE world congress, April 2009, Detroit, USA

Paper II
Thermodynamic Modeling and Control of a Negative Valve Overlap Turbo Engine
H. Aulin, T. Johansson, P. Tunestål, B. Johansson
IASTED paper 651-071
Presented at Control and Applications congress, July 2009, Cambridge, UK

Paper III
Control of a Turbo Charged NVO HCCI Engine using a Model Based Approach
H. Aulin, T. Johansson, P. Tunestål, B. Johansson
IFP paper
Presented at E-COSM congress, November 2009, Rueil-Malmaison, France

Paper IV
The Effect of Intake Temperature in a Turbocharged Multi Cylinder Engine operating in HCCI mode
T. Johansson, B. Johansson, P. Tunestål, H. Aulin
SAE technical paper 2009-24-0060
Presented at the ICE congress, September 2009, Capri, Italy
Approved for SAE International Journal of Engines, March 2010

Paper V
HCCI Heat Release Data for Combustion Simulation, based on Results from a Turbocharged Multi Cylinder Engine
T. Johansson,P. Borgqvist, B. Johansson, P. Tunestål, H. Aulin
SAE technical paper 2010-01-1490
Presented at the SAE Brasil congress, May 2010, Rio de Janeiro, Brazil

Paper VI
Turbocharging to extend HCCI Operating Range in a Multi Cylinder Engine-Benefits and Limitations
T. Johansson, B. Johansson, P. Tunestål, H. Aulin
FISITA technical paper F2010-A037
Presented at the FISITA congress, May 2010, Budapest, Hungary

Other publications

Extracting Cylinder Individual Combustion Data from a High Precision Torque Sensor
H. Aulin, P. Tunestål, T. Johansson, B. Johansson
ICE paper F2010-35101
Presented at ASME, September 2010, San Antonio, Texas, USA

Abstract

Increasing fuel prices and environmental concern drives the research and development for the internal combustion engine. Even if the basic knowledge of most of the engine processes is better analyzed and understood today there is scope to improve the fuel efficiency and released exhaust pollutants.

Homogeneous Charge Compression Ignition (HCCI) is a promising combustion concept with high fuel efficiency and low emissions. In HCCI, the combustion is not the same as in the SI or Diesel engines. The auto-ignition in HCCI combustion has no flame propagation and therefore the combustible mixture is consumed rapidly, even at low temperature. This results in high peak pressure rate and therefore high combustion noise, that limits the possible operating range.

The focus of this thesis is to research how the fuel efficiency can be the improved and how the operating range can be extended for a turbocharged light duty multi-cylinder HCCI engine. In turbocharged HCCI mode the combustion noise is reduced, but at the same time the engine operation becomes very sensitive. The research evaluates how different engine settings influence the fuel efficiency, combustion noise and exhaust emissions.

It is shown which operating limitations a HCCI engine needs to fulfill regarding; combustion noise, combustion stability, peak cylinder pressure, nitrogen oxides and soot emissions. At increased boost pressure the achieved fuel efficiency has to be balanced against these operating limitations and the real operating range can be very limited, especially at high load.

Due to the low exhaust enthalpy from a negative valve overlap HCCI engine the turbocharger function is important. It is shown how efficiency and operating range can be improved by finding a better suited smaller turbocharger. At high boost pressure the pumping losses can be very high in this engine configuration.

In engine simulation of the turbocharged HCCI, the correct exhaust valve closing position is fundamental since it controls the mass flow through the engine. It is shown that by controlling the exhaust valve closing position in the engine simulation to have in-cylinder temperature of ~1000 K near firing top dead center, gives simulation results that follows experimental engine results well. The short duration exhaust valve event was identified as one source to the pumping losses. The engine simulation results showed that a change of exhaust valve timing could reduce the pumping losses. This was verified with experimental results where the

new longer duration exhaust camshaft improved the fuel efficiency and capable operating range.

The knowledge on how to operate this turbocharged HCCI engine to improve the fuel efficiency and fulfill the operating limitations, resulted in an operating range from 1000 to 3000 rpm and a load of more than 5 bar BMEP, in that speed range. It is shown that this turbocharged HCCI engine has an average improvement in fuel efficiency of 11 % in this operating range and up to 35 % improvement in fuel efficiency in some operating points, compared to a modern SI engine.

Acknowledgements

It has been a rewarding time at the division of Combustion Engines, having the opportunity to do research in my main area of interest. Many people have helped me to accomplish this work.

First I would like to thank General Motors and Saab Powertrain for financing my projects together with the Swedish Energy Agency.

I would like to thank my supervisors, professor Bengt Johansson and Per Tunestål. First for letting me start as a Ph.D. student with a very interesting project, and for always making time to help me with the research, proof reading and going through my presentation material.

Krister has been very helpful with all my computer related issues, both for the office and the test cell, and also sharing my interest in motorsport and Formula Student.

My first supervisor at GM, Richard Backman had lots of useful ideas and we had a nice times in Germany and USA.

I would like to thank the technicians who helped me during my time, Bertil, Kjell, Tommy, Jan-Erik, Thomas, Mats and especially Tom who fixed things when time was short.

I would like to thank all of my colleagues at the division for all the help and interesting discussions. I especially want to thank Carl and Patrick for being good friends, both on and off work, both helping me with my strange Matlab wishes, Carl also for showing me the best motorcycle roads and sharing many nice lunches. With Håkan and Andreas there were many interesting discussions on engines and tuning. With Mehrzad it was nice to be at a conference in Rio de Janeiro, every best evening. Hans for having the engine controllable and working hard to fix the features I wanted.

Finally I would like to thank my family, especially Lisa for standing by me with our lovely children, Jakob and Maja.

To those not mentioned here I am not less grateful.

Nomenclature

AR	Active Radicals
ATAC	Active Thermo-Atmosphere Combustion
AVS	Audi Valvelift System
BDSC	Blow Down Super-Charging
BDC	Bottom Dead Center
BMEP	Brake Mean Effective Pressure
CA10	Crank angle 10 % burned
CA50	Crank angle 50 % burned
CA90	Crank angle 90 % burned
CAI	Controlled Auto-Ignition
CFR	Cooperative Fuel Research
CI	Compression Ignition
CIHC	Compression Ignited Homogeneous Charge
CAD	1) Crank Angle Degrees 2) Computer-Aided Design
CFR	Cooperative Fuel Research
CO	Carbon monoxide
CO_2	Carbon dioxide
CoV	Coefficient of Variation
CPS	Cam Profile Switching
DI	Direct Injection
DOE	Design of Experiments
dP	Pressure derivate
EI	Emission Index
EGR	Exhaust Gas Recirculation
EVC	Exhaust Valve Closing
EVO	Exhaust Valve Opening
FEA	Finite Element Analysis
FMEP	Friction Mean Effective Pressure
FSN	Filter Smoke Number
FTM	Fast Thermal Management
FuelMEP	Fuel Mean Effective Pressure
γ	specific heat ratio C_p/C_v
GCI	Gasoline Compression Ignition
HAJI	Hydrogen Assisted Jet Ignition
HC	Hydrocarbon
HCCI	Homogeneous Charge Compression Ignition
HR	Heat Release
$IMEP_{gross}$	Indicated Mean Effective Pressure, gross
$IMEP_{net}$	Indicated Mean Effective Pressure, net
IVC	Intake Valve Closing
IVO	Intake Valve Opening
m	Mass

NA	Naturally Aspirated
NEDC	New European Driving Cycle
NO_x	Nitrogen Oxides
NVO	Negative Valve Overlap
nsfc	net specific fuel consumption
MBT	Maximum Brake Torque
O_2	Oxygen
Pa	Pascal (pressure unit)
PCCI	Premixed-Charge Compression Ignition
PCP	Peak Cylinder Pressure
P_{ex}	Exhaust Pressure
PFI	Port Fuel Injected
P_{in}	Intake Pressure
PMEP	Pumping Mean Effective Pressure
ppm	
PVO	Positive Valve Overlap
Q	Heat
QemisMEP	Emission Mean Effective Pressure (energy chemically bound in emissions)
QexhMEP	Exhaust Mean Effective Pressure (sensible exhaust energy)
Q_{HR}	Accumulated Heat Release
QhrMEP	Accumulated Heat Released Mean Effective Pressure
QhtMEP	Heat Transfer Mean Effective Pressure (heat transfer to cylinder walls)
Q_{LHV}	Lower Heating Value of Fuel
RON	Research Octane Number
RI	Ringing Intensity
SA	Spark Assisting
SACI	Spark Assisted Compression Ignition
SOI	Start of Injection
SI	Spark Ignition
STD	Standard Deviation
T	1) Temperature 2) Torque
TDC	Top Dead Center
TDC_f	Top Dead Center, firing
TDC_{GE}	Top Dead Center, gas exchange
T_{IVC}	Temperature at IVC
T_{TDC}	Temperature at TDC
TWC	Three Way Catalyst
VCR	Variable Compression Ratio
VGT	Variable Geometry Turbine
VNT	Variable Nozzle Turbine
VTEC	Variable valve Timing and lift Electronic Control
VVT	Variable Valve Timing
W	Work
x_b	Burned gas fraction

γ	Ratio of Specific Heats (CP/ CV)
η_b	Brake Efficiency
η_c	Combustion Efficiency
η_{GE}	Gas Exchange Efficiency
$\eta_{gross\ ind.}$	Gross Indicated Efficiency
η_m	Mechanical Efficiency
$\eta_{net\ ind.}$	Net Indicated Efficiency
η_t	Thermodynamic Efficiency
λ	Relative Air / fuel Ratio
ρ	Density

Table of Contents

1 Introduction

The four-stroke internal combustion engine has had the same operating principle and materials for more than 130 years but still there are many areas left for improvement. As the engine type of choice for transportation it relies heavily on the availability of a suitable energy source. This has so far been met by the vast amount of oil that has been available. The demand for reduced fuel consumption and increased efficiency becomes more important when the fuel prices are rising. Lately the green house effect has set new challenges to further increase the efficiency of the internal combustion engine. Increased environmental concern has focused more and more on the released exhaust pollutants from engines.

Development of the Spark Ignition (SI) and the Compression Ignition (CI) engines has reached substantial advantages in efficiency and exhaust emissions in the last decades. The CI engine has a fuel efficiency advantage over the SI engine due to higher thermodynamic efficiency and lower pumping losses. In regard to the exhaust emissions the SI engine holds an advantage over the CI engine.

We want the fuel efficiency from the CI engine and the emission levels from the SI engine, and this can be reached with Homogeneous Charge Compression Ignition (HCCI). HCCI combustion was first applied to two-stroke engines [1], [2] with improvement in fuel efficiency and combustion stability. When HCCI as applied to the four-stroke engine, the fuel efficiency could be improved up to 50 % compared to the SI engine [3]. The auto-ignition in HCCI combustion leads to short burn duration and therefore high combustion induced noise. This limits the possible operating range [3]. The peak pressure rate can be reduced with increased charge dilution. With increased boost pressure the operating range can be extended [4], [5], [6]. The potential for increased load range in boosted conditions has often been evaluated with an external supply of compressed air in a single cylinder test engine [5], [7], [8], [9].

For a real HCCI application on a multi-cylinder engine, the usage of a turbocharger provides a higher efficiency than a supercharger [10]. The research on turbocharged conditions for a multi-cylinder engine was normally conducted in heavy duty engines [6], [11], [12]. The research into turbocharged multi-cylinder light duty HCCI engines is limited [10]. A common way to initiate HCCI combustion is by trapping internal exhaust residuals [13]. The research into turbocharged light-duty multi-cylinder engines, with trapped internal exhaust residuals for HCCI combustion, is very limited, and this thesis set out to investigate the features in this area to increase the knowledge and understanding of HCCI combustion.

1.1 Background

HCCI was identified in the late 1970´s [1], [2] as a promising combustion concept that could combine high efficiency with low exhaust emissions for the two-stroke engine. In the 1990´s this was shown for four-stroke engines as well [14]. This lead to increased research activity in the engine community all over the world on HCCI combustion. In this awakening of the benefits with HCCI, Lund University took a front position among published research papers regarding HCCI [5], [15], [16], [17], [18], [19], [20], [21]. The shortcomings of the HCCI combustion, with its high pressure rise rate and lack of direct ignition timing control, became more and more obvious. This meant that the HCCI combustion was best suited for the lower load regime. While the stoichiometric SI engine lacks efficiency at low load due to its poor thermodynamic and gas exchange properties, the base engine could be switched over to operate in HCCI mode at low load. In this way the basic SI engine structure could be kept to have the efficiency, but not the cost of a diesel engine. On the hardware side, the main difference between operating in HCCI is some arrangement to increase the induced charge temperature. To initiate auto-ignition of the charge, the right conditions have to be set in advance, and for combustion feedback an in-cylinder pressure transducer normally gave enough information to control the auto-ignition timing in HCCI mode.

1.2 Objective

This research was in many ways a continuation of a previous HCCI research project at Lund University in collaboration with GM Powertrain.

The research was divided in to two parts, one for the combustion and one for engine control. This thesis covers the combustion part.

The main objective of the research was to understand the features of a turbocharged multi-cylinder HCCI engine, and how to improve the fuel efficiency and exhaust emissions. One other objective was to increase the capable operating range to more than 500 kPa Brake Mean Effective Pressure (BMEP), from 1000 to 3000 rpm. The turbocharging in HCCI mode is mainly intended as a way to reduce the combustion noise to extend the operating range. If the operating range could be increased to that BMEP level, a normal load regime for a passenger car could be operated in HCCI mode. Since GM wanted to take HCCI closer to production there was appropriate limitations imposed on combustion noise, combustion stability, peak cylinder pressure and emission levels. Also, the modifications to the engine hardware was limited since GM wanted to be able to compare the turbocharged results to GM:s own Naturally Aspirated (NA) HCCI research results.

1.3 Method

The main work in this research was of experimental nature with a fully instrumented engine setup. Engine simulation in GT-Power was used to find ways to improve the efficiency and operating range. Engine parts were designed in the Computer-Aided Design (CAD) program Inventor. To evaluate the strength of engine components, Inventor was used both for the dynamic simulation and Finite Element Analysis (FEA). Post-processing of data was done in Matlab.

2 Combustion Engine Fundamentals

2.1 Working Principle

The four-stroke engine is the most common engine type today for land transportation. The four-stroke engine has as the name implies four distinctive strokes, and it takes two crankshaft revolutions to complete one four-stroke cycle. Even if the combustion type differs, the basic working principle is divided into the same four parts. In Figure 1 the four different strokes are shown.

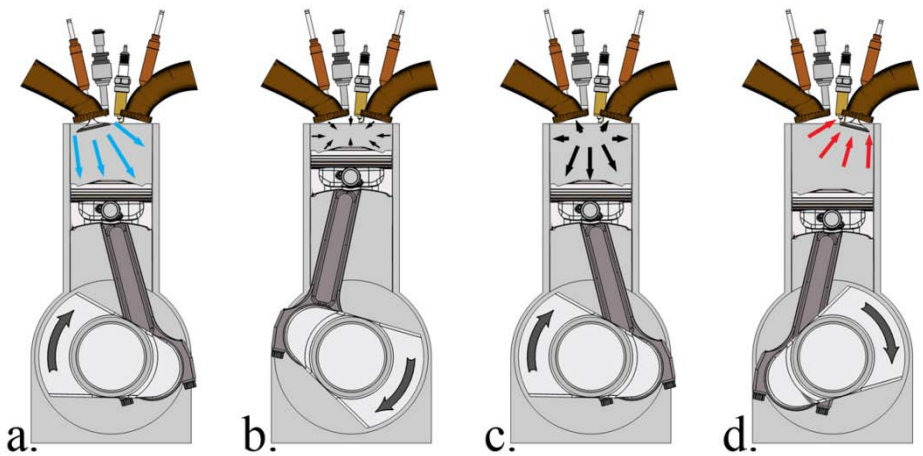

Figure 1: The four-stroke engine cycle

a. Intake stroke: the piston descends towards Bottom Dead Center (BDC) and the outside air pressure is equalizing the reduced in-cylinder pressure through the open intake valve. If the engine is Port Fuel Injected (PFI) the fuel is introduced during the intake stroke. If the engine is Direct Injected (DI) the fuel can be introduced later.

b. Compression stroke: all valves are now closed and the piston moves upwards towards the Top Dead Center (TDC), compressing the in-cylinder charge.

In the vicinity of TDC_f the fuel-air mixture is ignited and the in-cylinder pressure is increased.

c. Expansion stroke: the expanding gases force the piston towards BDC, and useful work is produced.

d. Exhaust stroke: close to BDC the exhaust valve is opened and the burned gases are released to the exhaust manifold as the piston rises upwards to TDC_{GE} where a new cycle can be started.

2.1.1 The Spark Ignition Engine

In the SI engine there is a spark discharge close to TDC_f during the compression stroke. This starts the combustion of a premixed air and fuel charge. The created flame front expands relatively slowly inside the cylinder until all ignitable mixture is consumed during a relatively long burn duration. The fuel has to withstand the increased temperature during the compression stroke and combustion without any self-ignition before the flame front reaches the fuel element. This means that auto-ignition resistant gasoline qualities are the primary fuel type for the SI engine. Since the ordinary air-fuel mixture needs to be near stoichiometric for complete flame propagation [22], this usually leads to a decreased engine efficiency when the load has to be reduced. Traditionally the power output from the SI engine is controlled by a throttle to reduce the in-cylinder air mass. This introduces a pumping loss when reduced power output is needed. Since the compression ratio is limited by knocking combustion or auto-ignition at high load, the throttled air-fuel charge has a low relative compression leading to loss of thermodynamic efficiency in throttled condition.

To sustain the flame propagation, the burned gas temperature needs to be over 1900 K [23]. Since the Nitrogen Oxide (NOx) formation increases rapidly at this combustion temperature, the SI engine will have high NOx emissions. With a normal Three-Way Catalyst (TWC) the NOx emissions can be reduced effectively when the SI engine is operated in stoichiometric condition.In the last decades, a number of features have been introduced to increase the efficiency of the SI engine. With DI of the fuel inside the cylinder, the compression ratio can be increased due to a cooler and denser air-fuel charge, which is more resistant to knocking combustion as the fuel vaporization takes away heat inside the cylinder [24]. There is less fuel loss during the valve overlap period with DI, resulting in lower Hydrocarbon (HC) emissions [25]. With DI it is possible to reduce the throttling losses by forming a stratified charge in the cylinder, with a global lean air fuel ratio. The excess air in stratified operation increases the specific heat ratio, leading to a higher thermal efficiency [26]. When operating lean in SI mode the NOx emissions can be reduced by a NOx storage catalytic converter [27]. The throttling losses can also be decreased with reduced intake valve opening duration or control of its timing [28], [29]. The base compression ratio can be increased when the effective compression ratio is controlled with a delayed intake valve closing timing to improve the fuel efficiency [30].

2.1.2 The Compression Ignition Engine

In the CI or Diesel engine the fuel is injected directly into the cylinder towards the end of the compression stroke. The compression ratio is usually higher than what is employed for the SI engine, leading to a higher temperature than the auto-ignition point of the fuels used for the CI engine. The higher compression ratio for the CI engine gives an fuel efficiency advantages over the SI engine due to higher expansion ratio.

The fuel is injected at high pressure, and air is entrained into the fuel jet. This creates a fuel-rich premixed reaction zone in the central region where soot formation and particulate growth takes place. In the periphery at the turbulent diffusion flame the soot oxidation and NOx formation occurs [31].

The injected fuel amount controls the load, and therefore the CI engine can be operated without a throttle, yielding a further advantage compared to the SI engine. The CI engine is normally operated at lean conditions, meaning that a normal TWC cannot be used. The NOx and soot emissions can be reduced with oxidizing catalysts, NOx traps, Selective Catalytic Reduction (SCR) catalysts and particulate traps. The emission reduction equipment and the high pressure fuel injection system leads to a higher manufacturing cost for the CI engine compared to the SI engine.

2.1.3 Mean Effective Pressure

The fuel efficiency of an engine can be broken down into different processes to identify problem areas. This makes it possible to compare results between different engines. To compare the results for different engine sizes and engine speeds the result can be normalized. This is achieved by comparing the results per cycle and normalizing with the cylinder displacement, giving results in mean effective pressures. The unit for the pressure is Pascal [Pa], and normally it is presented as kPa, MPa or bar. Besides knowing how much energy that is supplied, and how much energy that is usable in the end, we like to know the sources of the losses. This can be visualized by a Sankey diagram as seen in Figure 2.

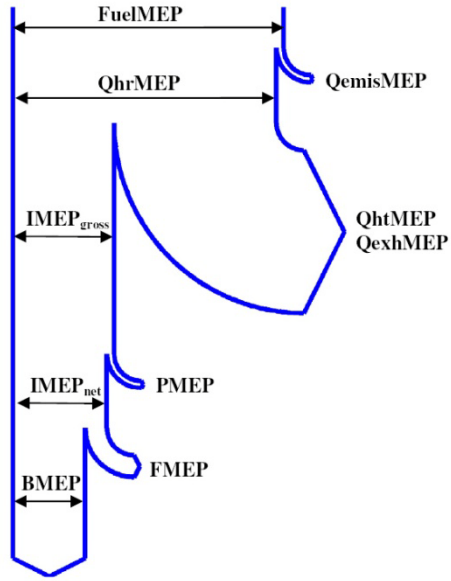

Figure 2: Sankey diagram of mean effective pressures

The supplied energy content per cycle with the fuel is normalized to give $FuelMEP$ according to (2.1), where m_f is the fuel mass per cycle, Q_{LHV} is the lower heating value of the fuel and V_d is the volume displacement.

$$FuelMEP = \frac{m_f * Q_{LHV}}{V_d} \tag{2.1}$$

Some energy is lost due to incomplete combustion, this is defined as $QemisMEP$. This can be estimated from the exhaust composition, measured by the emission equipment . The heat released $QhrMEP$ in (2.2) can be expressed as:

$$QhrMEP = \frac{Q_{hr}}{V_d} \tag{2.2}$$

After combustion there will be some additional heat transfer losses to the surrounding cylinder walls, defined as $QhtMEP$. There will also be expansion loss and exhaust loss due to the elevated temperature, $QexhMEP$.

Next the Indicated Mean Effective Pressure or IMEP is calculated. This is the normalized work (W_c) on the piston, see (2.3). With $IMEP_{net}$ the entire cycle is considered and in $IMEP_{gross}$ the gas exchange process is excluded. This is normally measured through in-cylinder pressure measurement with a piezoelectric sensor together with the estimation of cylinder volume from the crankshaft position.

$$IMEP = \frac{W_c}{V_d} = \frac{\oint pdV}{V_d} \quad (2.3)$$

The normalized pumping loss during the gas exchange process is $PMEP$, and this is the difference between $IMEP_{gross}$ and $IMEP_{net}$:

$$PMEP = IMEP_{gross} - IMEP_{net} \quad (2.4)$$

PMEP can be divided into two parts, pressure loss over the engine and throttling losses according to (2.5). The pressure loss over the engine occurs when a turbocharger is used which usually leads to a higher back pressure, $P_{exhaust}$, than intake pressure, P_{intake}.

$$PMEP = Throttling_{valves} + (P_{exhaust} - P_{intake}) \quad (2.5)$$

The normalized friction losses, or $FMEP$ from the engine is normally calculated using the measured $BMEP$ and subtracting $IMEP_{net}$, (2.6). $FMEP$ can also be estimated by measuring the motoring work of the engine, or part of the engine. But the lack of a firing pressure inside the engine affects the accuracy [32]. A large part of the friction losses are from the piston assembly due to the gas forces acting on piston rings, and this property is lost when motoring the engine. The friction losses in the journal bearings is also different without the viscosity change in the lubricating oil at firing condition.

$$FMEP = IMEP_{net} - BMEP \quad (2.6)$$

By measuring the engine torque (T) and normalizing this with engine displacement, the $BMEP$ is calculated according to:

$$BMEP = \frac{4\pi T}{V_d} \quad (2.7)$$

2.1.4 Efficiencies

By using the described mean effective pressures in previous section, the resulting efficiencies from different processes can be calculated, as shown in Figure 3.

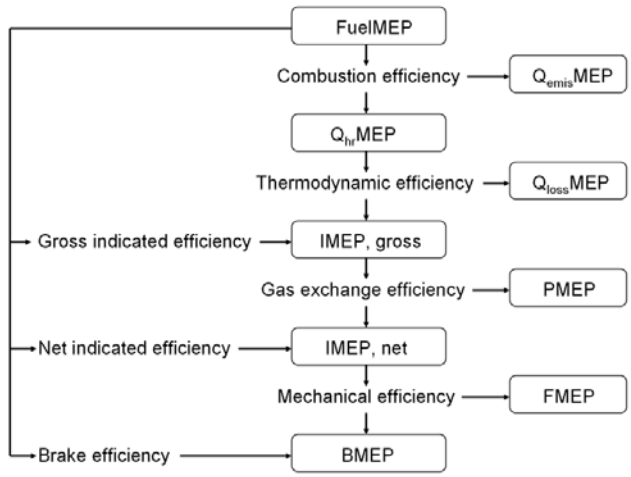

Figure 3: Efficiency breakdown

The combustion efficiency, η_c, reflects how much of the fuel energy that is converted into heat:

$$\eta_c = \frac{Q_{hr}MEP}{FuelMEP} = 1 - \frac{Q_{emis}MEP}{FuelMEP} \tag{2.8}$$

The thermodynamic efficiency, η_t, reflects the efficiency to convert the released heat to indicated work:

$$\eta_t = \frac{IMEP_{gross}}{Q_{hr}MEP} = 1 - \frac{Q_{ht}MEP + Q_{exh}MEP}{Q_{hr}MEP} \tag{2.9}$$

The gas exchange efficiency, η_{GE}, describes how well the gas exchange process of the exhaust and intake stroke is done:

$$\eta_{GE} = \frac{IMEP_{net}}{IMEP_{gross}} = 1 - \frac{PMEP}{IMEP_{gross}} \tag{2.10}$$

The mechanical efficiency, η_m, describes how much of the supplied work inside the cylinder is converted to usable work:

$$\eta_m = \frac{BMEP}{IMEP_{net}} = 1 - \frac{FMEP}{IMEP_{net}} \tag{2.11}$$

The total efficiency, η_b, can be described by the ratio of the normalized usable work $BMEP$, and the supplied energy $FuelMEP$, or by multiplying the separate efficiencies to get:

$$\eta_b = \frac{BMEP}{FuelMEP} = \eta_c \cdot \eta_t \cdot \eta_{GE} \cdot \eta_m \quad (2.12)$$

3 HCCI

In an HCCI engine, the temperature of the premixed air-fuel mixture is raised during the compression stroke until auto-ignition occurs. The combustion rate with HCCI is typically very high, and by having the ignition timing near TDC_f, the expansion ratio can be maximized. In HCCI mode, the combustion can occur in lean mixtures, up to more than four times the stoichiometric value [33]. This means that an HCCI engine can be operated without a intake throttle, addressing a main drawback for the SI engine with its high pumping losses at part load. In HCCI mode the combustion temperature is sufficiently low to avoid any major NOx formation, even at lean conditions. The HCCI engine will combine the good features from both SI and CI engines, but at the same time introduce its own issues.

In HCCI mode the charge is ignited at several locations simultaneously in the combustion chamber. The ignition starts where the temperature is highest or where the mixture is richest [34]. When the local combustion starts, the global charge is on the verge of auto-ignition. This give a very rapid combustion process once started. The high combustion rate leads to high pressure rise rate, and therefore the combustion induced noise will be high. The high pressure rate can lead to high frequency pressure oscillations [35] inside the combustion chamber that can increase the heat transfer losses to the walls [36]. The heat losses during combustion for HCCI are less than for SI due to a lower combustion temperature. This is offset to some extent by the higher heat losses during compression and the overall heat losses for the HCCI combustion can be higher than for the SI combustion[37].

To keep the combustion rate at an acceptable level, the mixture has to be diluted, leading to a reduction of the power density for an HCCI engine. The dilution is achieved with air or Exhaust Gas Recirculation (EGR). The EGR can be in the form of internal or external recirculation of burnt gases. The external EGR is re-routed to the intake manifold while the internal EGR has not left the exhaust system. Dilution with EGR reduces the combustion temperature through the thermodynamic cooling effect when the in-cylinder heat capacity is increased [38]. With EGR the thermal efficiency is reduced, but at the same time the combustion efficiency is improved while the influence on combustion duration is negligible [11]. The addition of EGR

can increase the NOx emissions for well mixed HCCI at a constant load and combustion phasing [39].

The auto ignition timing depends on initial pressure and temperature and the increase of those due to compression of the charge during the compression stroke. To be able to control the ignition timing with HCCI, the combustion has to be monitored. By using an in-cylinder pressure sensor, all the needed combustion parameters can be measured [40]. The combustion monitoring can be done in other ways, for example with ionization measurement [41], [42], a knock sensor signal [43], an instant torque signal [44], engine speed variation [45] or even by measuring the valve movements [46].

The auto ignition in HCCI mode can be controlled with; intake temperature heating [47], [48], variable compression ratio [20], [49], [50], [51], dual fuels with different auto-ignition properties [21] or with EGR [52].

When operating with a homogenous charge, the appropriate conditions for the auto-ignition combustion timing are normally set before the intake valve closing (IVC) timing. Direct fuel injection gives an increased control space [53], [54] and even a possibility to change the operating conditions after IVC, and the preferred charge composition either does not have to, or will be homogeneous at the time of combustion [55].

3.1 HCCI History

Auto-ignition of an air-fuel charge has been known before the first internal combustion engine. Even the inventor of the four-stroke engine, Nicolaus Otto is reported to have encountered problems with violent combustion in his early tests [56].

The auto-ignition of gasoline was widely seen as a combustion problem until 1979 when two concepts were presented that used the auto-ignition for combustion initiation. Both the Active Thermo-Atmosphere Combustion (ATAC) by Onishi et al. [1] and the Toyota-Soken [2] set out with auto-ignition as a new combustion concept, that differed from ordinary SI and Diesel combustion. This was documented by optical experiments, showing how the ignition started at numerous points around the combustion chamber. The auto-ignition was done by EGR dilution in a gasoline fueled two-stroke engine in an effort to reduce the fuel consumption, reduce the HC emissions and increase the combustion stability. It was believed that some radical components in the retained exhaust were the ignition triggers. The ATAC combustion process was also taken into production with a portable engine generator by Onishi.

In 1983 Najt and Foster [14] repeated the auto-ignition process in a four-stroke engine by using EGR and intake heating. This was accomplished in a Cooperative Fuel Research (CFR) engine and the combustion process was called Compression Ignition Homogenous Charge (CIHC). They also concluded that it was unlikely that any chemical species in the exhaust significantly alters the ignition process, meaning that the charge temperature was more important than composition.

In 1989 Thring [57] showed that a gasoline four-stroke engine with intake heating and EGR operating with auto-ignition could have an efficiency level comparable to the diesel engine at part load due to the un-throttled operation. Thring concluded that the particulate emissions should have a big advantage over the diesel engine due to the homogenous charge. Knocking combustion was a limiting factor, and the combustion timing could advance until misfire was encountered, even if the load during the tests was only 1.4 bar BMEP. Thring suggested that an engine for a passenger car could be designed to use auto-ignition at idle and part load to obtain diesel economy, and switched over to conventional SI operation at full power for good specific power output. Thring set the acronym for this combustion mode to HCCI that become the synonymous for this type of combustion later on.

The first multi-cylinder results with HCCI combustion was presented in 1992 by Stockinger et al. [3]. In these experiments, a 1.6*l* four-stroke engine could be operated up to 5 bar BMEP in HCCI mode. This meant that the normal operating load range for a passenger car could be covered in HCCI mode. Higher loads than 5 bar was not possible due to the high pressure oscillations during combustion. The fuel efficiency could be increased up to 50 % in HCCI mode compared to SI. The engine could be operated without any EGR, with only intake air heating. The NOx emissions were shown to decrease drastically in HCCI mode.

The paper "The Knocking Syndrome- Its Cure and Its Potential" [58] by Willand et al. in 1998 responded to Oppenheimers earlier proposals [59], [60], [61] by outlining how the practical implementation of HCCI could be done. Achieving HCCI with an increased compression ratio was not recommended, as the relative cylinder volume changes faster, and then leaves the combustion less time to occur at constant volume. Pre-inlet heating was not recommended due to the large amounts of energy that would be required for transient control of homogeneous combustion. The recommended approach was to retain internal EGR with Negative Valve Overlap (NVO) together with variable valve timings with reduced valve opening duration. With internal EGR the combustion would have a self-stabilizing effect since, if one cycle has a late combustion it provides a hotter exhaust gas, causing the next cycle to ignite earlier and reduce exhaust temperature again. Direct injection was proposed as a way to control the combustion. By injecting the fuel in the NVO

period the increased activation energy would advance the combustion timing without any soot penalty due to the relatively low temperature.

The operating range had so far been limited to part load. In 1998, Christensen et al. [5] showed that it was possible to reach up to 14 bar $IMEP_{gross}$ by supercharging a heavy duty engine. The in-cylinder peak pressure rate at 14 bar IMEP was about 40 bar/CAD due to an early combustion timing that had to be used to increase the combustion stability. This was done in a single cylinder engine with external supply of compressed air up to 3 bar and no throttling on the exhaust side. The tests were carried out with three different fuels.

The first results from HCCI combustion using NVO were presented in 2000 by Lavy et al. [13]. They named this Controlled Auto-Ignition (CAI), which became somewhat synonymous for this type of HCCI. Their operating range was limited to 4 bar IMEP, but it was proposed that variable Valve Timing (VVT) and Cam Profile Switching (CPS) could overcome this.

3.2 HCCI Concepts

3.2.1 Exhaust Diluted- Two-strokes

HCCI combustion with exhaust dilution was successfully applied to two-stroke engines. First the ATAC [1] concept was used for power generators, then Honda introduced its Active Radicals Combustion (AR Combustion) to motorcycle engines [62], [63]. Honda used a variable exhaust port to trap sufficient amount of residuals for auto-ignition. The variable exhaust valve was a standard feature for two-stroke engines and was first introduced by Yamaha [64] to improve the performance of the two-stroke engine. Honda increased the closed portion of the exhaust port to get AR Combustion with the retained exhaust gases. At high load the exhaust port height was increased and the engine was operated in SI mode. The combustion stability with AR combustion was increased substantially and the fuel consumption was reduced. Honda proved the AR combustion in the grueling Granada-Dakar rally with the EXP-2 motorcycle and finished fifth overall in 1995. The AR Combustion was used in series production with the scooter Honda 125 FES, sold in Sweden in 1998 [65].

3.2.2 Exhaust Diluted- Four-strokes

If HCCI is used for part load in combination with SI at high load, the compression ratio has to be chosen to suit both combustion modes to avoid any torque limitations by knocking combustion in SI mode. To be able to switch between these combustion modes, the trapping of residuals can be controlled by appropriate valve timings [13], [66], [67], [68], [69], [70] . There are different strategies to trap these residuals. A common way to increase the in-cylinder temperature is by trapping some exhaust residuals from the previous cycle through early Exhaust Valve Closing (EVC).

To increase the expansion work the Exhaust Valve Opening (EVO) timing needs to be as late as possible, but not to late since this will increase the pumping loss during the exhaust stroke. The chosen exhaust valve duration will depend on what HCCI load and engine speed the engine is going to be operated at [71] and has to be a compromise in an engine with fixed valve duration. If the duration is short it will be suitable for low HCCI load, but at high load it will increase the pumping losses. If the duration is too long some expansion work is lost at low load.

The valve opening and closing rate should be as high as possible but it is limited by the valve spring performance. High acceleration leads to high force and therefore high strain on the valve spring. High strain on the valve mechanism reduces the durability and the friction losses increase at the camshaft interface. For acceptable acceleration levels with reduced valve duration the maximum valve lift is reduced to approximately 4 mm in HCCI engines with ordinary camshafts. This reduced valve lift can introduce throttling losses on both the intake and exhaust sides depending on load and engine speed.

An issue with NVO is the resulting recompression of the exhaust gas that will introduce additional heat losses and thermal stress on engine components. With NVO there is also a need to have very different valve timings in HCCI and SI modes. This can be accomplished by a CPS system that Honda presented in 1989 [72] known as VTEC (Variable valve Timing and lift Electronic Control) or Porsche´s VarioCam [73]. In these systems two different cam profiles can be used for one valve.

To be able to control the combustion timing precisely in NVO HCCI mode, the control of the valve timing is crucial. VVT was first introduced in production with a mechanical system in 1980 [74] by Alfa-Romeo. Also, the camshaft timing wheel position can be changed by using hydraulic control in two chambers between the camshaft and the camshaft timing wheel [75]. This leads to a robust and cheap solution and this became more wide-spread. Since the system uses pressurized oil

from the engine lubrication system, the valve position during startup cannot be controlled and the response time depends on the oil viscosity, which changes with oil temperature. The introduction of an electric motor to control the VVT timing [76] has further improved the response and precision of the VVT system, and this can be controlled during engine start up as well.

Besides using NVO for internal EGR, a re-breathing of the exhaust gas during the intake stroke can be made in a number of ways. The exhaust closing timing can be delayed into the intake stroke and the intake valve opening can either be in conjunction with EVC or well before EVC [77] thus creating a Positive Valve Overlap. (PVO). The downside with this delayed EVC is the needed increase of clearance height for the valve. A deeper valve pocket in the piston limits the combustion chamber design and it can be hard to reach the targeted compression ratio. Also, a deeper valve pocket can lead to an increased top land height for the compression ring which increases the crevice volume, leading to higher HC emissions [22], [78]. This feature is solved by having a normal valve overlap and then re-opening the exhaust valve during the intake stroke to trap enough residuals for the auto-ignition. The intake valve lift and duration can then be reduced. Volkswagen has used this type of system for their auto-ignition concept calling it GCI (Gasoline Compression Ignition) [79] using the Audi Valvelift System (AVS) with a sliding cam.

3.2.3 Air Diluted

A common way to operate HCCI is to heat the intake charge and have a suitable compression ratio [3], [5], [15], [19], [20]. The intake heating can be obtained with an electrical heater, but a more practical solution is to increase the temperature of the intake air with a heat exchanger coupled to the hot exhaust gases [3], [47], [48]. With a Fast Thermal Management (FTM) system [48] it is possible to have transient load and speed changes with just a few engine cycles of delay for the combustion timing. A downside with exhaust heat utilization is the added complexity of the intake and exhaust system together with the dependence on thermal inertia in this type of system.

Auto-ignition can be reached and controlled by changing the engine effective compression ratio. This can be made with a Variable Compression Ratio (VCR) mechanism [20], [49], [50]). With higher compression ratios, the Carbon Oxides (CO) emissions increase as the rapid expansion reduces the reaction time [49], [80]. The higher cost with a VCR equipped engine has so far prevented mass production. It is also possible to change the effective compression ratio by using variable valve timing. If the intake valve closing is delayed into the compression stroke some air

can be pushed out of the cylinder leading to a reduction of effective compression ratio. The control actuation is limited in HCCI mode and cannot be used without the aid of inlet air conditioning [81].

The benefit with air as dilution compared to exhaust, is the higher ratio of specific heats, γ, which leads to higher thermodynamic efficiency.

3.3 Boosted HCCI

When the load is increased in HCCI mode the combustion noise can be very high due to the high peak pressure rate. Increased dilution will reduce the reaction rate and also the relative pressure rise rate (i.e. the peak pressure rate relative to the peak cylinder pressure) is decreased leading to a reduction of the combustion noise. To increase the in-cylinder dilution, the intake pressure can be increased with a mechanical supercharger. This consumes additional power from the engine and increases the FMEP. A turbocharger functions by converting the exhaust gas enthalpy to mechanical work and uses this to compress the intake charge. This normally leads to an increase of back-pressure and therefore the pumping losses are increased. When operating in HCCI mode the exhaust enthalpy is low due to the low combustion temperature and fast combustion rate so the turbocharger needs to be designed for HCCI operation.

In the early results from Aoyama et al. [4] in 1996 a supercharger was used to extend the operating range with auto-ignition for their single cylinder engine. They named the HCCI combustion Premixed-Charge Compression Ignition (PCCI). Nothing was mentioned about the combustion noise but with supercharging the pressure rise rate was slower than in the case of intake air heating, i.e. it was easier to place the combustion timing right. The big jump of possible operating range came in 1998 when Christensen et al. [5] showed that it was possible to operate up to 14 bar IMEP with HCCI combustion with natural gas. The experiments were conducted in a single cylinder heavy duty engine, supercharged up to 300 kPa with an external compressor. Olsson et al. [6] used a turbocharger in a multi-cylinder heavy duty engine and the load was increased up to 16 bar BMEP and 20.4 bar $IMEP_{gross}$, with blending of n-heptane and ethanol to control the combustion timing. Wilhelmsson et al. [12] showed the effect of combustion timing on efficiency and engine out NOx in a turbocharged heavy duty HCCI engine.

Hyvönen et al. [82] used a mechanical supercharger to increase the operating range in HCCI for a light duty engine. The operating range could be increased compared to the NA setup. The limiting factor were the allowed peak cylinder pressure and the high parasitic losses of the compressor, in the used engine. In 2005 Hyvönen

used a turbocharger to increase the brake efficiency compared to the mechanical supercharger [10]. By using a turbocharger with Variable Nozzle Turbine (VNT) the trade-off between engine back-pressure and inlet boost pressure could be optimized at different operating points. This was done with operating limits on Peak Cylinder Pressure (PCP), peak pressure rate (dP) and NOx emissions.

It is possible to supercharge an HCCI engine with the exhaust blow-down process. With this Blow Down Super-Charging (BDSC) the exhaust system is interconnected between the cylinders and after the intake valve is closed, one exhaust valve is re-opened in one cylinder so the blow-down process from the another cylinder can increase the in-cylinder pressure. With this system the operating range is reported to increase up to 650 kPa IMEP [83], [84] for a NA HCCI engine.

3.4 Assisted HCCI

The auto-ignition combustion can be initiated or supported by additional supply of energy into the cylinder. If normal spark ignition is used, this is called Spark Assisted Compression Ignition (SACI) [68], [85], [86]. This can be used for a mode switch between HCCI combustion and SI by initiating the auto-ignition with a spark [87]. The drawback is that the typical SI combustion cycle to cycle fluctuations are increased and the lean or otherwise diluted in-cylinder conditions for SI combustion makes these worse [87]. The HCCI ignition can also be triggered by a small stratified charge near the spark plug for an initial SI combustion [88] but then the NOx emissions increase.

The auto-ignition combustion can be initiated by focusing a laser beam inside the cylinder [89], [90]. The practical application of laser assist is limited due to cost and weight, plus the need of a clean optical window into the cylinder. The auto-ignition can be initiated through igniting part of the fuel inside a small pre-chamber that is connected to the main combustion chamber by small orifices. This creates multiple jets of burnt gases into the combustion chamber which initiates the main ignition. The hydrogen fueled pre-chamber is called Hydrogen Assisted Jet Ignition (HAJI) [91] and with propane it is called Turbulent Jet Ignition [92].

3.5 Direct Injection and NVO

When the engine is equipped with DI, there is large freedom to choose when to inject the fuel during the cycle. Normally the fuel is injected during the intake stroke to promote fuel vaporization and homogeneity. If the HCCI engine has a re-compression with NVO the fuel can be injected during this part to alter the combustion timing. Since HCCI is normally operated with lean mixtures, the

trapped residuals in NVO contains excess oxygen. If the fuel is injected into this environment, the fuel composition can be changed and any heat release can influence the main combustion timing.

Fuel injection during the NVO was proposed by Willand et al. [58] and results were shown by Urushihara et al. [54] and Koopmans et al. [93] . In these results an earlier injection in the NVO period resulted in an advancement of the combustion timing. The fuel consumption improved by splitting up the injection with one part of the fuel injected during the NVO and the rest during the intake stroke. The low load limit can be lowered by fuel reforming during the recompression, as the NVO heat release improves auto-ignition conditions in the main compression but at the price of increased cyclic variability for the main combustion [94].

4 Experimental Setup

4.1 Engine System

The test engine is a General Motors in-line four cylinder LNF 850, Mule1, gasoline engine with a total displacement of 2.2 *l*. The cylinder head is a 4-valve design with a pent-roof combustion chamber. There are some small squish areas on the intake and exhaust sides. The piston has a raised dome with a small bowl in the center. The intake channel is side-drafted with a low tumble design. The engine has DI of spray-guided type with a centrally placed injector. The eight-hole solenoid fuel injector has a cone angle of 60°, see Figure 4.

The spark plug is located close to the fuel injector and has an extended tip. The spark is always operated as a safety measure against misfires and it can also improve the combustion stability with late combustion timing.

To achieve HCCI combustion the engine is operated with NVO with low lift (4 to 5 mm) and short duration camshafts (125° to 155°) as seen in Figure 5 where the minimum and maximum valve timings are plotted. The VVT is controlled by hydraulic actuators at the camshafts giving a 50 Crank Angle Degree (CAD) adjustment for both intake and exhaust valve timings.

The engine has been turbocharged with different units. In the start of the research, a 90 hp (diesel) Variable Geometry Turbine (VGT) turbocharger was used. This was later on changed to a 47 hp (diesel) unit with fixed turbine, The exhaust manifold is of pulse type with short individual runners straight to the turbine inlet as seen in Figure 6. On the intake side there is a water cooled intercooler. The heated aluminum intake manifold has short intake runners and a small volume as seen in Figure 7. The cooling system has an electrically driven water pump and the coolant temperature is adjusted by the control system. Engine specifications are listed in Table 1.

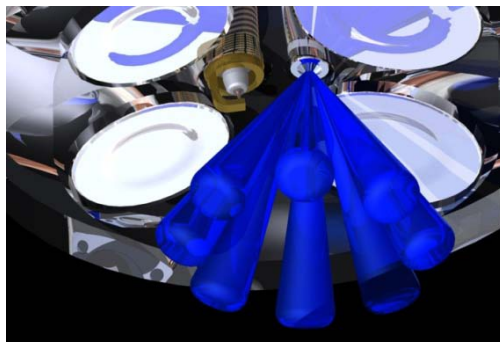

Figure 4: Spray-guided fuel injection

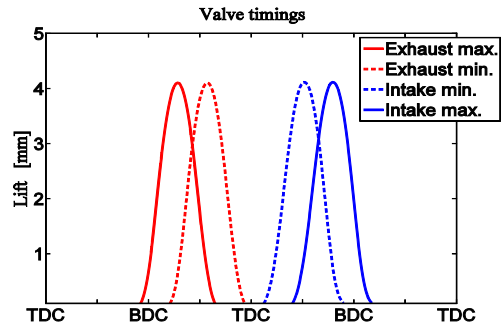

Figure 5: Valve timing range

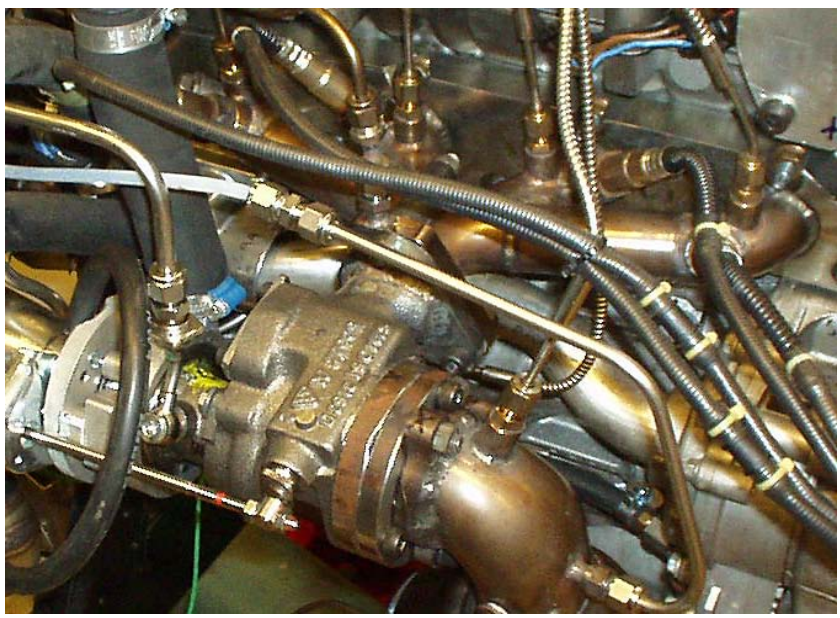

Figure 6: Exhaust manifold

Figure 7: Intake manifold

Table 1: Engine specifications

Number of cylinders	4
Displacement	2198 cm^3
Bore x Stroke	86 mm x 94.6 mm
Compression Ratio	11.75:1
Valve duration IN	125 CAD
Valve duration EX	125 or 155 CAD
NVO range	50-100 CAD
Turbochargers	B&W BV35, KP31
Fuel Supply	DI, up to 20 MPa
Fuel Type	Gasoline, 95 RON

4.1.1 Measurement

The control system is a combined data acquisition and engine control unit from dSPACE. The base structure for the control system is programmed in Simulink environment. There are several engine sensors measuring the operating conditions, see Table 2.

The temperature is measured by chromel-alumel (type K) thermocouples which are calibrated using boiling water before first usage. The temperature is measured in the test cell, before and after the compressor, after the intercooler, inside the intake manifold and downstream the intake channels (40mm from the intake valve). On the exhaust side the temperature is measured after the cylinders separately plus before and after the turbine. The coolant temperature is measured on the ingoing and outgoing side. The oil temperature is measured in the engine sump. The EGR temperature is measured before and after the cooler.

The pressure is measured with piezoresistive transmitters which are compared to a weather station reading to get the daily atmospheric pressure. The pressure is measured in the test cell, after the compressor, before and after the turbine and in the oil system. The pressure levels are presented in absolute scale meaning that 100 kPa is 1 bar or nearly atmospheric condition.

The air-fuel ratio is measured by broad band lambda sensors in the exhaust manifold, cylinder separated plus after the turbine. The lambda sensors are checked by grouping all of them at the same distance from the turbine. The emissions are measured after the turbine and before any catalyst. The Carbon Dioxide (CO_2) in the intake is measured in the center of the intake manifold. The emission analyzer is calibrated against appropriate reference gases before any engine measurement. The emission pre-filter is changed after one day of engine testing. The soot measurements are done after the turbine with extended sampling volume. The fuel flow is measured by a laboratory grade scale for more than three minutes at every operating point. The location of TDC is determined by having the peak cylinder pressure for motored conditions at 0.8 CAD before TDC. The presented results are based on average results from all four cylinders up to 2000 cycles. No combustion with misfires is allowed in the results.

The most important sensors for combustion feedback is the individual in-cylinder pressure sensors. These piezoelectric sensors are connected to an A/D converter that is connected to the control system. The control system has an in-cycle resolved heat release calculation where main parameters; combustion timing for 10, 50, 90 % heat released (CA10, CA50, CA90), peak cylinder pressure (PCP) and peak pressure derivative (dP) are calculated with a resolution up to 0.2 CAD. Emission analysis and soot measurements are collected on an external PC and the data is sent to the control unit.

Table 2: Measurement and control system

ECU and data logging	dSPACE Rapid Pro
Cylinder pressure sensor	Kistler 6043Asp
Charge amplifier	Kistler 5011B
Emission analyzer	Horiba 9100 MEXA
Soot analyzer	AVL 415 S

On the test screen, see Figure 8, all the main data and calculated parameters are presented together with the engine control settings.

The first step before the HCCI engine was turbocharged, was to test it in NA HCCI setup and compare the results to GM:s previous data for the same engine. This was done in a 10-point test at different engine speeds and loads. The results were comparable. For example, fuel consumption was only 2 % higher in the 10-point test. The main difference was the calculation of the peak pressure rate, this was found to be higher due to a finer crank angle resolution, and was adjusted with a suitable calculation process.

Before any results are collected, the engine was run at a reference point at 2000 rpm and $IMEP_{net}$ 340 kPa.

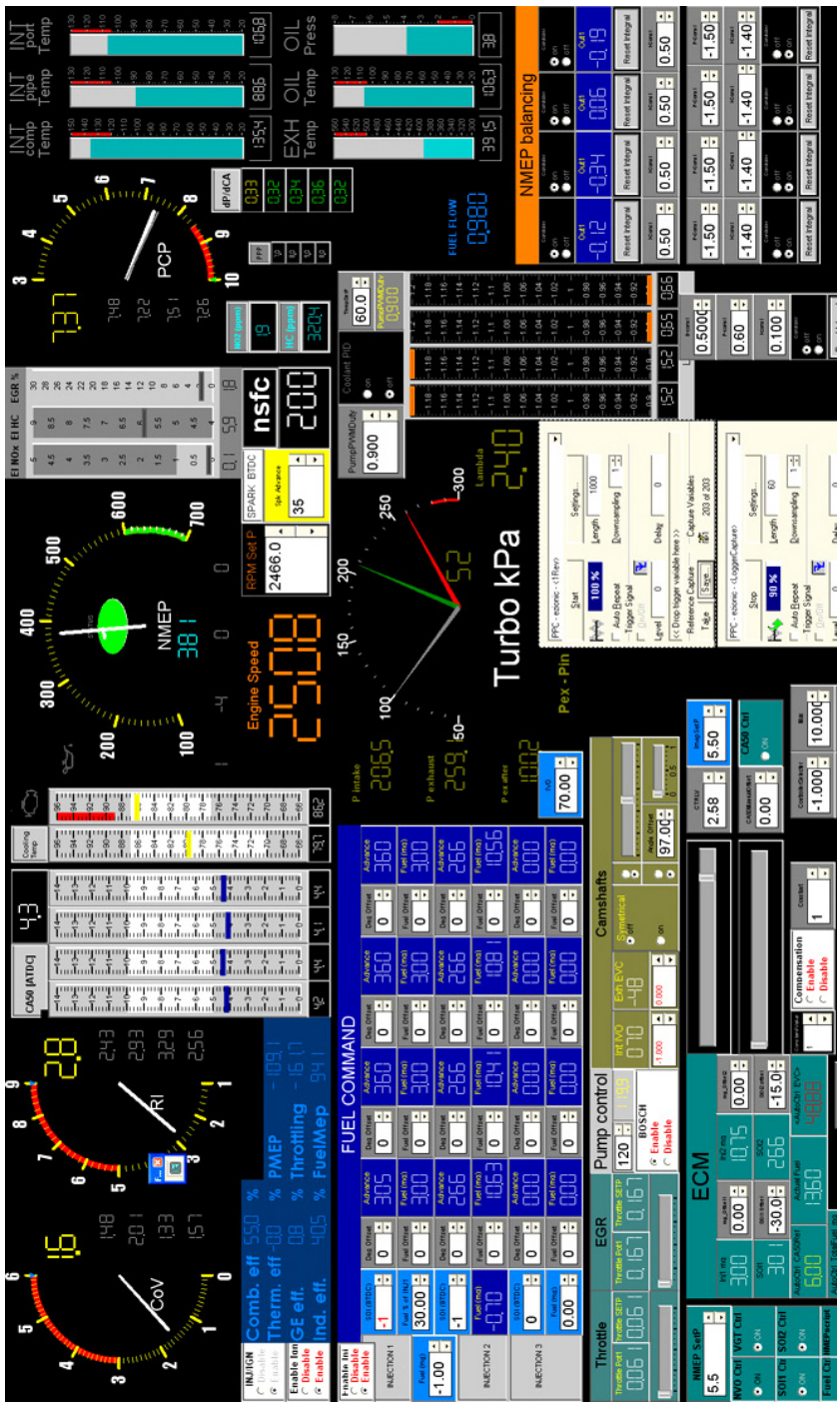

Figure 8: Control and engine parameter display

4.1.2 Cylinder Balancing

To increase the operating range it is important that all the cylinders operate identically, meaning that they have the same combustion phasing, indicated mean effective pressure and peak pressure rise rate. This means that the control system has to perform cylinder balancing. Injecting some of the fuel in NVO can give a reformation of the fuel with an increase in charge temperature and a reduction in effective octane number leading to more advanced combustion timing. The combustion timing will also be more advanced if the fuel is injected in the beginning of the NVO than in the end of NVO. The excess air during NVO injection influences the fuel reformation and the effect of combustion phasing is more pronounced at lean mixtures.

The fuel injection timing also has an influence on efficiency and soot. When injecting the fuel in the NVO sector leads to increased heat losses. It can also increase the pumping losses from the exhaust blow-down with this type of short duration camshaft operating at high load. The additional heat from fuel reformation leads to that less internal EGR is needed for a set combustion timing. If the exhaust valve opening becomes too late, the pumping work from the exhaust stroke is increased.

By splitting up the fuel injection and injecting a part of the fuel in the NVO, it is possible to achieve cylinder balancing and injection timing with the highest fuel efficiency .

The control system sets the CA50 position and uses the cylinder with the most advanced CA50 position for the EVC set point. The other cylinders are then advanced by adjusting the injection timing and/or fuel amount in the first injection, until all cylinders have the same CA50 position. Since there will be some differences in injection timing when using CA50 balancing there will also be some differences in efficiency between the cylinders. This results in different load, IMEP, in the cylinders. To maximize the load range there has to be cylinder balancing of IMEP as well. This is done at the main injection event. Obviously this affect the CA50 balancing since increasing the fuel amount will raise the combustion heat, leading to earlier CA50 for that cylinder. Therefore the cylinder balancing has to be constantly monitored and adjusted by the control system. The implementation of the cylinder balancing to the control system was done by H. Aulin. This is described in Paper II and Paper III.

When operating the engine at a global $\lambda=1$ in conjunction with above described cylinder balancing of IMEP, there will be local difference in cylinder to cylinder

lambda that can lead to an increased Coefficient of Variation (CoV), and even to misfire from the cylinder running richest, see Figure 9.

The lambda differences between all the cylinders when balancing with IMEP or lambda in two tests are shown in Figure 10. When operating near λ=1 there should be lambda balancing instead of IMEP balancing for stable engine conditions.

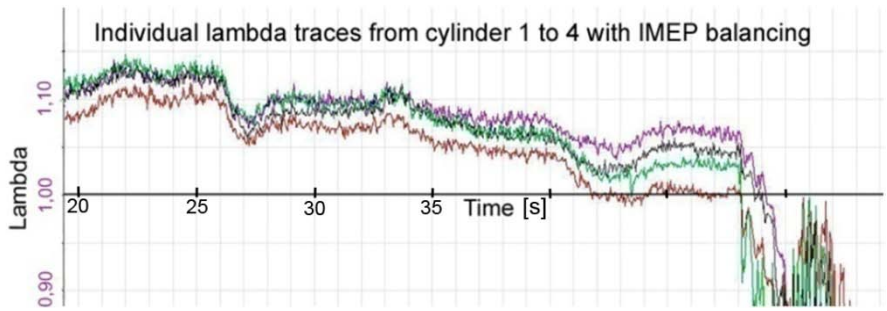

Figure 9: Cylinder individual lambda traces, lambda difference between the cylinders

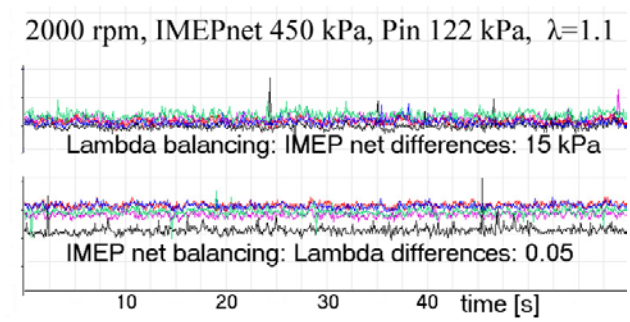

Figure 10: Cylinder individual lambda traces, lambda balancing vs. IMEP balancing

The lambda measurements are done with individual lambda sensors in the exhaust runners, see Figure 11. The signal quality could be reduced due to interference but in reality it did not seem to impose any problem due to the short response time of the sensors. In the future it could be possible to extract cylinder to cylinder information from only one lambda sensor using this fast response.

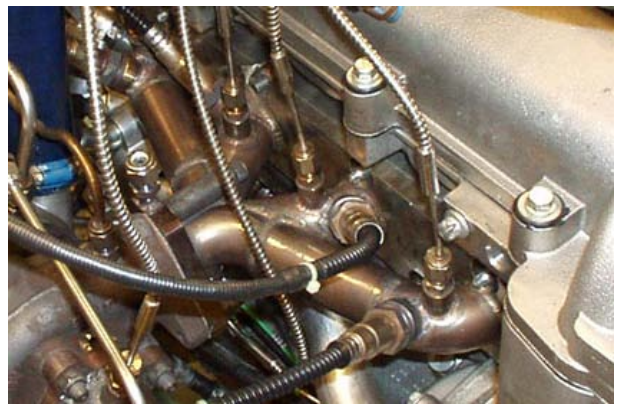

Figure 11: Individual lambda sensors in the exhaust manifold

The torque measurement has during a period been done with an ABB Torductor, as seen in Figure 12 and in the CAD drawing in Figure 13. This sensor measures the instant engine torque when it is delivered out from the crankshaft by measuring the change of the magnetic flux in the shaft . Figure 14 shows a graph of the engine out torque together with the cylinder pressure for the same sampling period.

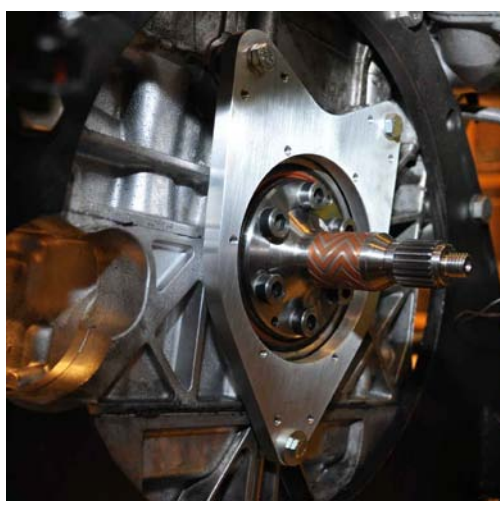

Figure 12: ABB Torductor on the turbocharged HCCI engine

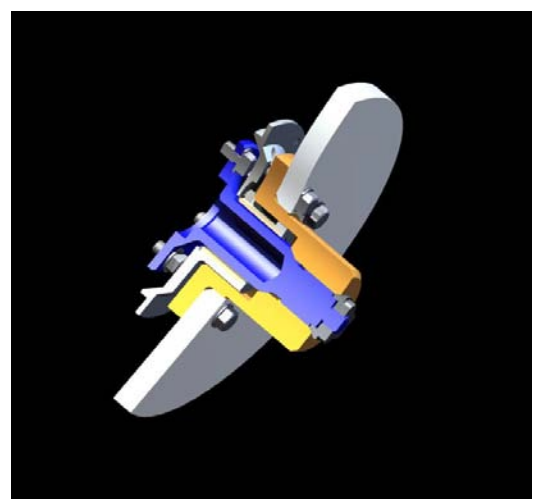

Figure 13: CAD rendering of ABB Torductor

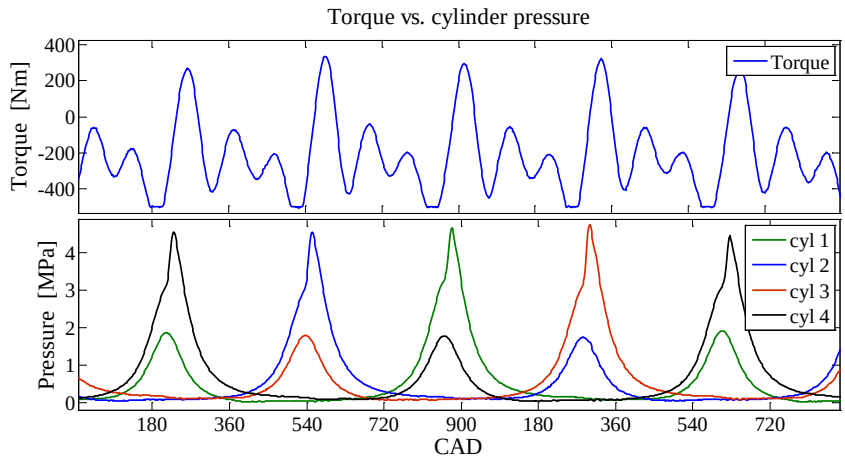

Figure 14: Torque and cylinder pressure at 2000 rpm, $IMEP_{net}$ 350 kPa

The goal with this Torductor torque sensor was to extract cylinder individual data like combustion timing, that could be used for cylinder balancing.

4.1.3 Temperature and EGR Control System

Two types of EGR routing are common: short and long route. The short route EGR diverts the exhaust gas before the turbine inlet and routes it to the compressor outlet on the intake side. This means there is a loss of exhaust energy to the turbine, something that is already low in HCCI mode due to the low combustion temperature and mass flow.

The long route EGR system takes exhaust gas after the turbine and routes it to the compressor inlet. To get a positive displacement of exhaust gas there is a throttle in the exhaust system to increase back pressure. The compressor inlet can be used as an ejector to enhance the EGR flow, and the required back pressure is quite small, about 3 kPa. The external EGR routing is cooled by the engine cooling circuit and is controlled by an EGR valve near the turbocharger, see Figure 17. The external EGR is used when the engine is operated stoichiometric or when the pumping losses need to be reduced. The pumping losses can be reduced with these types of short duration valve timings by adding cooled EGR to get more beneficial valve timings. If the turbocharger builds more back pressure than boost pressure due to a choked turbine the external EGR will reduce the mass flow since more internal EGR is needed for a given combustion timing as the heat capacity of the intake charge is increased.

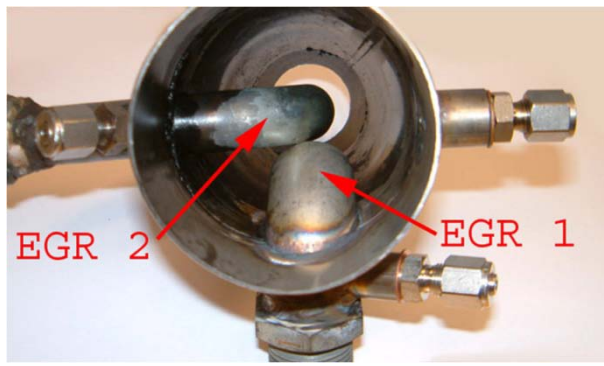

Figure 15: Compressor intake with long route EGR (1)

A drawback with EGR in HCCI mode is the relatively slow response in a system that is normally cycle to cycle controlled, especially during transients. Another drawback is the added weight and cost. Instead of using external EGR the boost pressure should be as high as possible to increase the air dilution and suppress the NOx emissions, but this has to be weighted against any increased pumping losses.

The intake temperature is controlled by an electrical throttle in the bypass routing to the water-cooled intercooler circuit, see Figure 16. When the throttle is fully open the main air flow goes through the bypass routing due to less flow resistance compared to the intercooler circuit. By closing the throttle, the airflow is forced through the intercooler circuit and the air temperature is decreased.

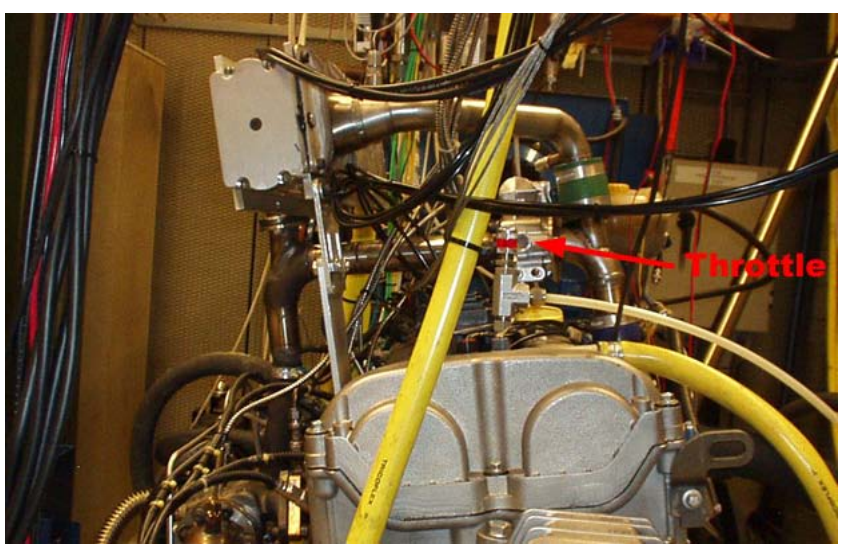

Figure 16: Throttle controlled intake temperature

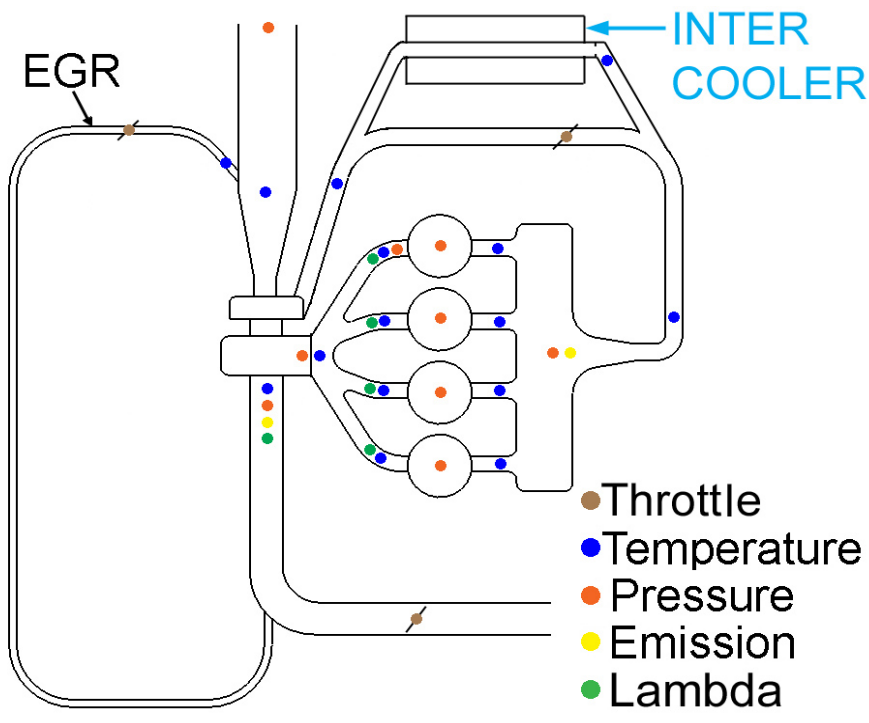

Figure 17: Engine layout

5 Diagnostic Methods

5.1 In-cylinder Pressure and Heat Release Calculation

To be able to predict the in-cylinder conditions, the cylinder pressure is measured with a piezo-electric sensor and the crankshaft position is estimated from the crank angle sensor. From this in-cylinder pressure and calculated volume, the IMEP and gas exchange efficiency can be obtained directly. With a Heat Release (HR) calculation the percentage burnt and combustion duration is available.

The heat release analysis in this work was based on a single zone model which is based on the first law of thermodynamics for a system. The energy or heat released from the combustion (Q), can be expressed as a function of the internal energy (U), the performed work (W), the heat transfer to the cylinder walls (Q_{HT}) and the mass loss to crevices ($Q_{Crevice}$):

$$\partial Q = \partial U + \partial W + \partial Q_{HT} + \partial Q_{Crevice} \quad (5.1)$$

Then by using the equation of state and assuming the in-cylinder content to be an ideal gas with a constant trapped mass and neglecting the crevice losses, the change of internal energy per CAD:

$$\frac{\partial Q}{d\theta} = \frac{\gamma}{\gamma-1} p \frac{\partial V}{d\theta} + \frac{1}{\gamma-1} V \frac{\partial p}{d\theta} + \frac{\partial Q_{HT}}{d\theta} \quad (5.2)$$

Where V and p are the cylinder volume and pressure, γ is the specific heat ratio (C_p/C_v).

The heat transfer to the walls is estimated by assuming a homogenous temperature in the combustion chamber (T_{gas}) and a constant wall temperature (T_{wall}):

$$\frac{\partial Q_{HT}}{dt} = h A_{wall} (T_{gas} - T_{wall}) \quad (5.3)$$

Where h is the heat transfer coefficient and A_{wall} is the exposed wall area. The heat transfer coefficient , h, is estimated by the relationship introduced by Woschni [95] shown in (5.4). C is an engine dependent constant, B is the bore and w is a characteristic gas velocity, see (5.5).

$$h = C B^{-0.2} p^{0.8} T^{-0.55} w^{0.8} \quad (5.4)$$

$$w = C_1 S_p + C_2 \frac{V_d T_r}{V_r p_r} (p - p_m) \quad (5.5)$$

C_1 and C_2 are correlation coefficients that need to be tuned for the individual engine model. For non swirling in-cylinder conditions C_1 can be set to 2.28 and C_2 to 0.00324 for the combustion and expansion phase. S_p is the mean piston speed. V_d is the cylinder displacement, V_r, p, T_r are reference conditions for volume, pressure (kPa), and temperature at a reference point, p_m is the motored pressure.

In this way the HR can be estimated by tuning some constants. When the engine is operated in HCCI with internal EGR, the residual fraction is high, leading to a reduction of the specific heat ratio , γ. The residual fraction can be estimated by the exhaust lambda together with the air or fuel flow. The volume near TDC_f can be influenced by the deformation of engine components due to high cylinder pressure [96].

6 Results

This section is a summary of the results from the research on turbocharged HCCI.

In the first section, "Engine Operation Variables", the responses for different engine settings for combustion timing, injection timing, valve timing etc. are investigated regarding their effect on fuel efficiency, combustion noise and emissions. These results indicate how the turbocharged HCCI can be operated and where the best efficiency and lowest emissions can be found. The results presented here are an extension of those presented in Paper I, where the possible operating range with turbocharging was examined. This is followed by the "Operating Limitations" chapter where appropriate operating limitations for HCCI are described in the same way as in Paper I.

The "Turbocharger and Operating regime" chapter shows how the operating limitations vary with different operating variables and where the usable and efficient operating range is with increased boost pressure. This is a extension of the results presented in Paper VI.

In the "Pumping losses" chapter discusses the high pumping losses for the turbocharged HCCI setup and is related to the results in Paper VI. The losses are identified by dividing the total pumping loss into two parts, from the turbocharger and from the valve timings. In the "Effect of Intake Temperature" chapter the results from other engine speeds and loads than in Paper IV are covered. The results are complemented with additional results from other intake valve timings and EGR.

The "HCCI Simulation" chapter describes how GT-Power simulations were used for this engine. The simulation results are compared to the measured results and the errors for the simulation are identified. This resulted in a description of how HCCI engine simulation can be done in Paper V. The temperature calculation for the engine simulation program is more detailed and visualized here.

In the final chapter, "Results from Final Operating Range", the engine parameters and results are presented in the same way as in Paper I, but now with the final results. The progress in possible operating range during the evolution of the work is shown here.

6.1 Engine Operating Variables

When operating with turbocharging and HCCI mode, the available experimental hardware had many degrees of freedom to influence the combustion. The valve timing on both the exhaust and intake side can be adjusted in both symmetrical and asymmetrical ways. The injection timing can be almost anytime during the cycle and it can be split into multiple parts. The limitations are on the injector duration which has to be more than 2 ms, and the dwell time has to be more than 3.3 ms between two injections. The intake temperature can be changed using a throttle controlled cooling circuit to get the desired intake temperature. With a VGT turbocharger, the boost pressure and therefore the back pressure can be adjusted in certain intervals. With the fixed turbocharger, a wastegate can be controlled. External EGR can be re-circulated and cooled at different levels. The coolant temperature can be increased to 110 ℃ with the electrical engine coolant pump. At certain operating conditions the ignition timing can be used to influence the combustion. For every operating point the EVC timing, IVO timing, injection timings and amounts, intake temperature, turbocharger setting, external EGR setting and coolant temperature have to be chosen. In this multi dimensional control space, engine operation can be challenging, especially at high load. At high load, a too advanced combustion timing can in worst case break the engine, and if the combustion is too late there is risk for misfires so severe that the combustion quenches entirely.

6.1.1 Exhaust Valve Closing Timing, EVC

Since the EVC timing controls the amount of internal EGR it has a very strong influence on the combustion timing, as seen in Figure 18. For every degree of change in the EVC timing the CA50 timing changes close to one degree. The combustion timing influences the peak pressure rate, dP, in this example it varies from 3 to 10 bar/CAD with a change of 12 ° on the EVC timing . Since RI is chosen to quantify the combustion noise, it can be varied from 3 to 20 MW/m^2 at this operating point.

From a subjective perspective, when the RI level is below 3 MW/m^2 the engine noise is comfortable, when the RI level is around 5 to 8 MW/m^2 it sounds quite hard, comparable to a diesel engine. If the RI level is in the region of 10-13 MW/m^2, the engine noise is quite hard and starts to feel uncomfortable. When the RI level approaches 20 MW/m^2, the engine noise is very uncomfortable and sounds unsafe. In Figure 18 it can be seen that the peak cylinder pressure increases with earlier combustion timings.

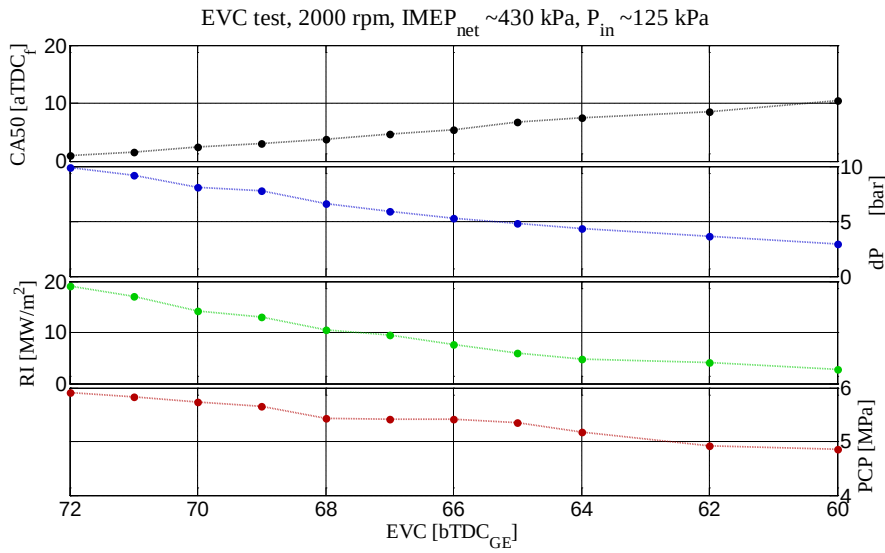

Figure 18: Effect of exhaust valve closing timing, EVC

6.1.2 Combustion Timing, CA50

The EVC timing is the main parameter for controlling the combustion timing and the IVO timing can be chosen to be symmetrical or asymmetrical with respect to EVC. In Figure 19, the results from these two valve strategies are compared and presented as a function of CA50 timing instead of EVC timing. The asymmetrical IVO means that IVO is fixed at 72 °aTDC$_{GE}$. The used intake cam profile gives a valve duration of 125°. In the results the peak pressure rate is reduced with asymmetrical timing due to increased in-cylinder dilution with late IVC. The NOx emissions are almost the same for both conditions but the NOx emissions rise at early combustion timings due to increased combustion temperature at this rather high HCCI load. The combustion stability expressed as CoV of IMEP$_{net}$, is lowest at a CA50 timing of 6 to 8 °aTDC$_f$. The CA50 timing could not be delayed later than ~10 °aTDC$_f$ due to unstable combustion, resulting in misfire or complete loss of combustion. The net specific fuel consumption (nsfc) is improved with delayed combustion timings in this test and an asymmetrical timing has slightly higher fuel consumption reflecting the overexpansion of the exhaust gases after the recompression phase.

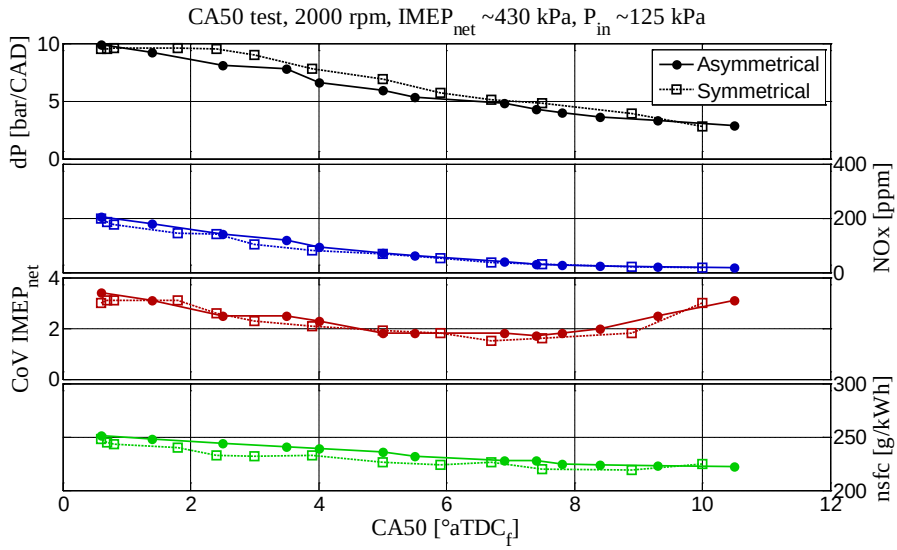

Figure 19: CA 50 test with symmetrical and asymmetrical valve timings

6.1.3 Injected Fuel Mass, m_{fuel}

The effect on load from increased fuel amount is shown in Figure 20. The load increases almost linearly with injected fuel, and NOx emissions rises exponentially with load in these results without turbocharging. The HCCI combustion is normally lean. If a normal TWC is used the NOx reduction is limited at lean conditions, this needs to be considered when the NOx rises. CA50 has to be delayed with increasing load to maintain the peak pressure rise at acceptable level.

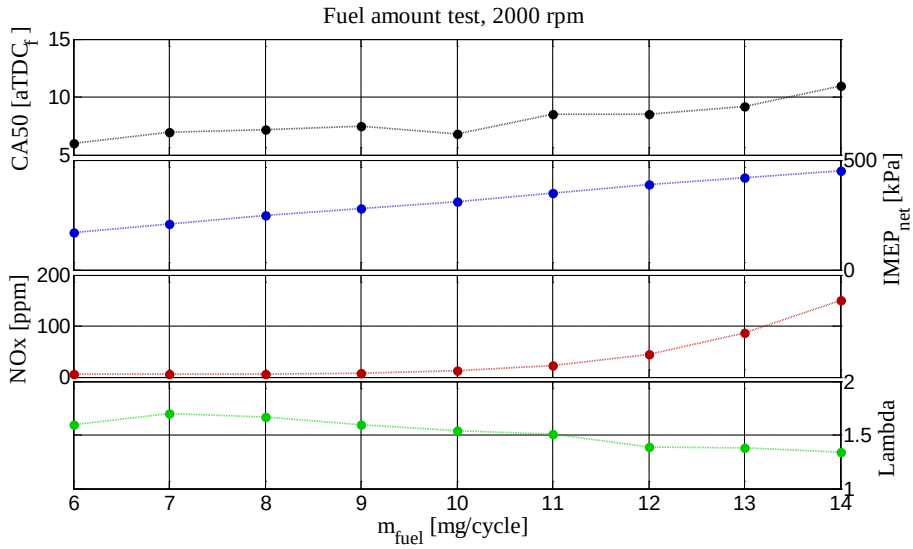

Figure 20: Effect of injected fuel amount vs. load

6.1.4 Start of Injection, SOI

The influence of Start of Injection (SOI) timing is seen in Figure 21. This is tested with a constant fuel amount of 8 mg/cycle with maximum possible NVO in this setup (200 °). At this engine speed of 2000 rpm it is possible to have combustion when injecting the fuel during the entire engine cycle due to the large amounts of internal fuel rich EGR. Obviously it is not advisable to inject fuel during the expansion or the exhaust stroke, and this is evident from the loss of capable load. Quite naturally the HC emission measurement reaches its maximum threshold level of 2000 ppm but this can be used to some extent if a reduced load is the goal i.e. idle operation. The best efficiency and lowest NOx emissions in these results are when the fuel injection is in the beginning of the intake stroke.

In Figure 22, the same fuel amount is used, 8 mg/cycle, but now with a reduced engine speed of 1500 rpm. The difference is that the fuel injection has to be before 180 °bTDC$_f$ to avoid misfires. In Figure 23, the fuel amount is increased to 10 mg/cycle at 1500 rpm but here the EVC timing is used to control the combustion timing. It is now possible to compensate the influence from SOI on the combustion timing with the EVC timing. The SOI timing has strong influence on used EVC timing during the recompression phase, which reflects the added fuel reformation or heat release in this part that gives a reduction of needed internal EGR for a set combustion timing.

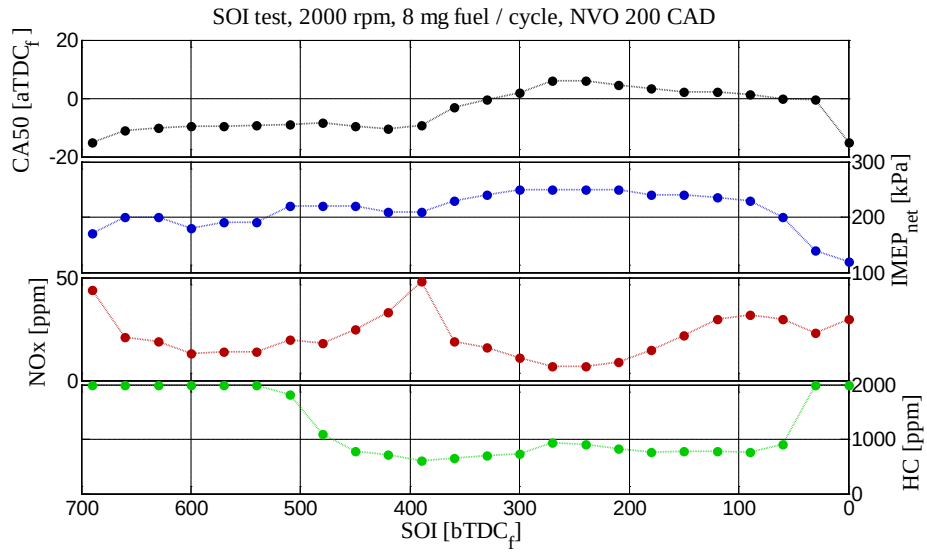

Figure 21: Effect of start of injection timing, SOI at 2000 rpm

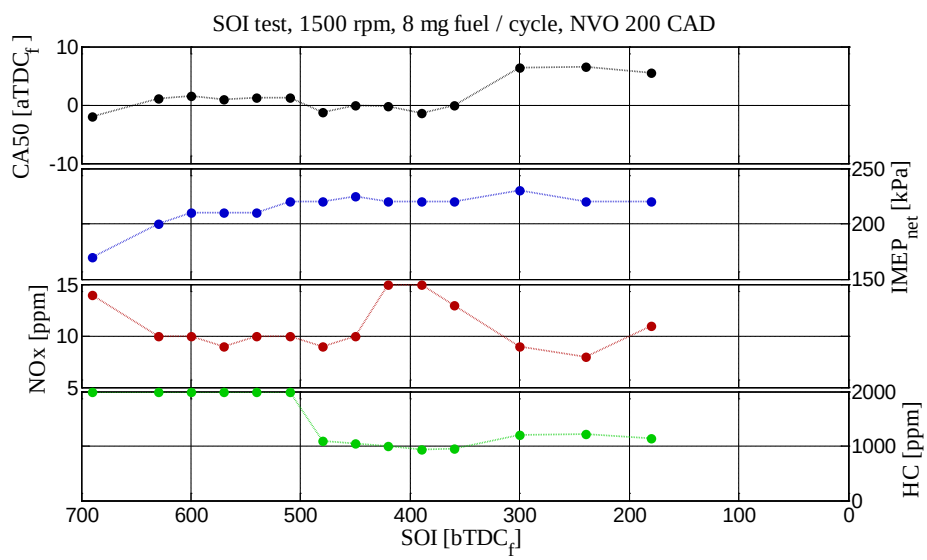

Figure 22: Effect of start of injection timing, SOI at 1500 rpm

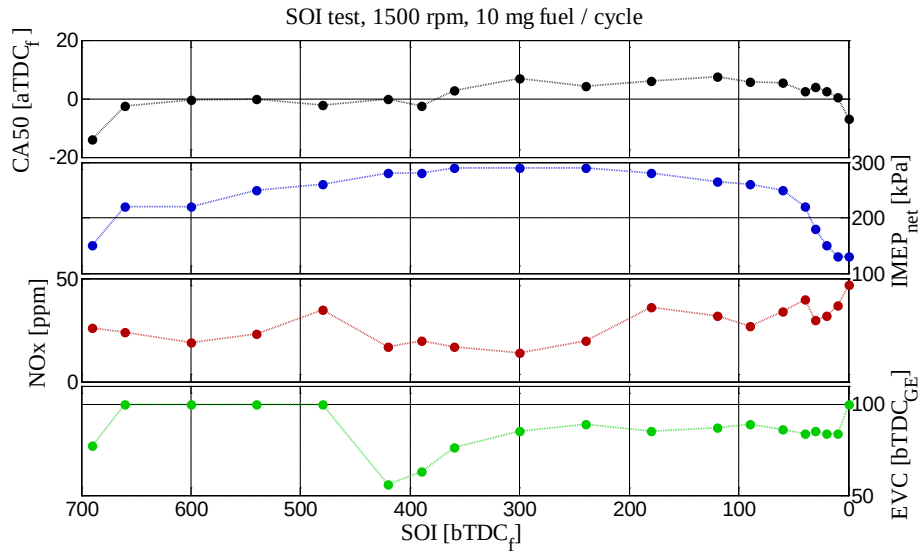

Figure 23: Effect of start of injection timing, SOI at 1500 rpm

These first injection experiments with single injection, indicate that an injection timing around 300 °bTDC$_f$ can be a starting point for a split injection test. Figure 24, shows the results from injecting 50 % of the fuel at 300 °bTDC$_f$ and the rest in a second injection. The results with single and split injection are quite similar but with split injection the second injection, SOI2, can be very late without losing efficiency when 50 % of the fuel is injected in SOI1.

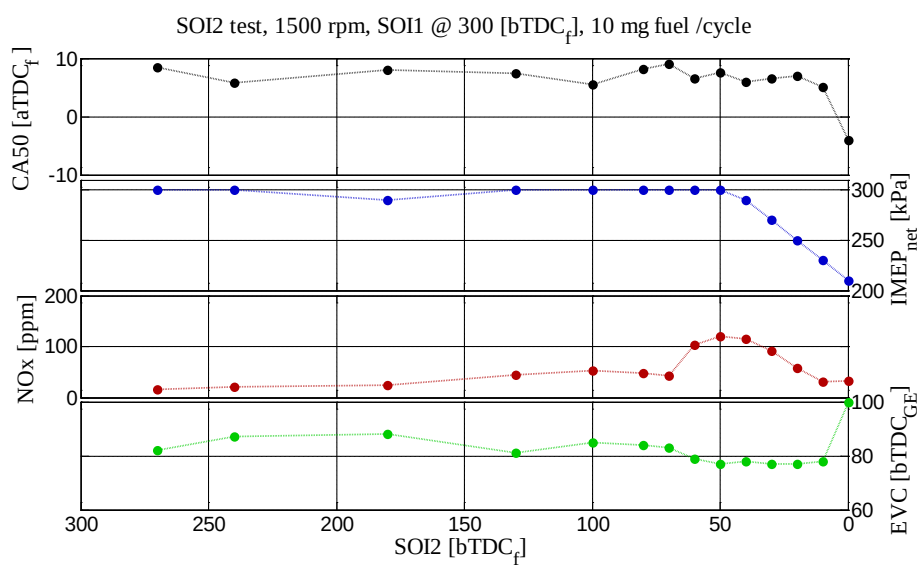

Figure 24: Effect of start of second injection, SOI2 at 1500 rpm

Fuel injection during the NVO period can give a fuel reformation with an increase in charge temperature leading to an advancement of the combustion timing. It will be more advanced if the fuel is injected in the beginning of the NVO than in the end, as seen in Figure 25. This fuel injection experiment is done with fixed valve timings. The excess air during NVO injection influences the fuel reformation and the effect on combustion phasing is more pronounced at lean mixtures [93]. This effect on the combustion timing by the SOI timing can be used for the cylinder individual balancing of the combustion timing.

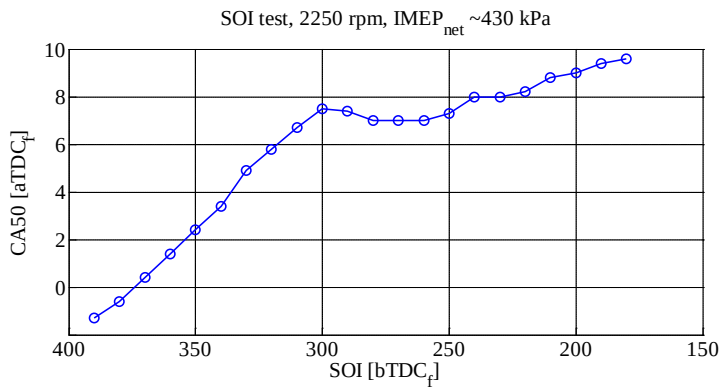

Figure 25: Start of injection vs., combustion timing, SOI vs. CA50

6.1.5 Coolant Temperature

The influence of engine coolant temperature is seen in Figure 26. The coolant temperature out from the engine is varied from 70° to 95 °C and at the same time the combustion timing is kept constant at 8.5 °aTDC$_f$ by adjusting the EVC timing. A higher coolant temperature reduces the heat losses and therefore less internal EGR is needed, as seen in the delayed EVC timing. With less internal EGR the mass flow through the engine is increased. The higher coolant temperature leads to a higher intake pressure and back pressure and this is reflected in the higher nsfc with increasing coolant temperature.

6.1.6 Ignition Timing

Normally the spark ignition timing has little or no effect on the HCCI combustion and can be turned off. As a precaution against misfires and loss of combustion, the ignition was normally on. At high load or when operating near stoichiometric conditions it can have a pronounced effect as seen in Figure 27. At this relative high HCCI load it was possible to delay the combustion timing by adjusting the ignition timing, in an effort to reduce the combustion noise with the used single injection at 300 °aTDC$_f$. The RI could be decreased from 10 to 6.5 MW/m^2 by adjusting the

ignition timing from 40° to 15°bTDC$_f$ in this test. Without spark assist it was not possible to delay the CA50 timing more than 8 degrees without misfire.

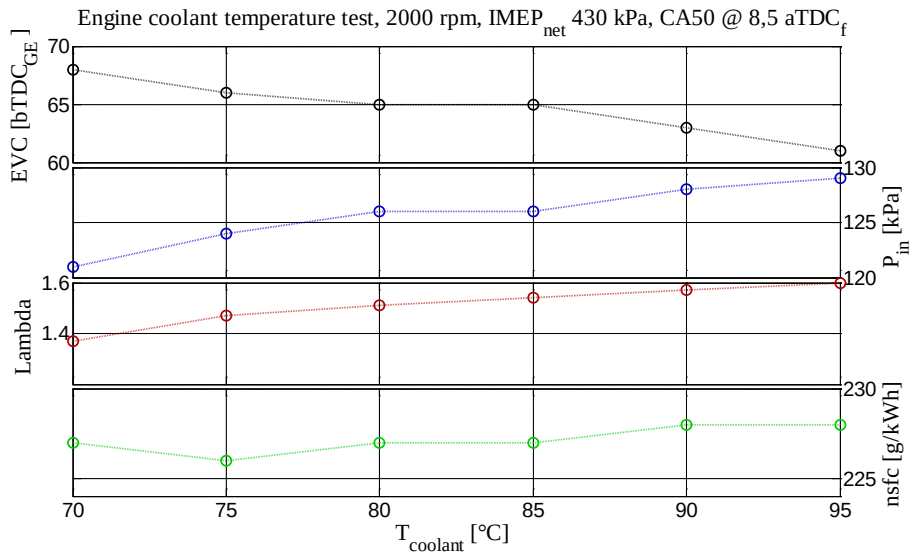

Figure 26: Effect of coolant temperature

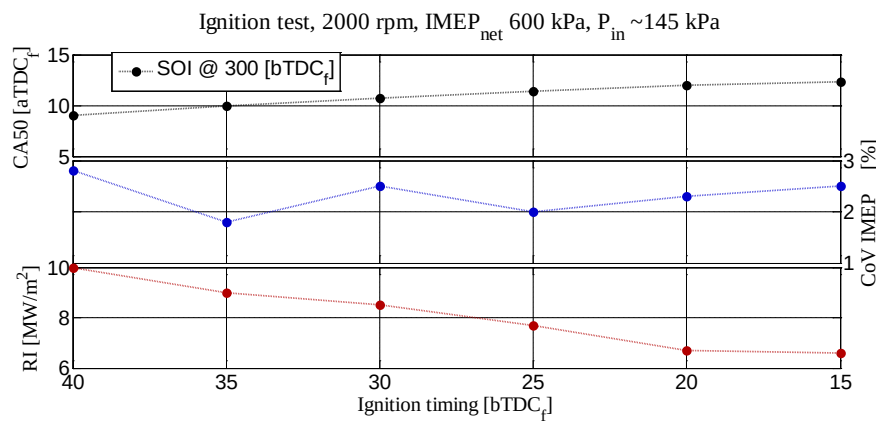

Figure 27: Effect of ignition timing

6.1.7 Stratified HCCI

The result from fuel stratification and Spark Assist (SA) in HCCI is seen in Figure 28. The split fuel injection used had ~5 % of the fuel injected just before TDC_f to form a stratified mixture near the spark plug. The ignition timing is 5 ° to 10 ° after the second injection. The combustion noise, RI, could be decreased by an delayed second injection timing even if the CA50 timing was advanced. Since it was expected that SA and stratification could lead to an increase of soot formation due to fuel rich burning zones, the soot measurement equipment was used. This showed increased soot formation as measured with Filter Smoke Number (FSN). The ignition timing had to be positioned exactly right and the fuel pressure had to be increased from the normal 12 MPa to 16 MPa. It might be possible to decrease the soot in this stratified spark assisted HCCI combustion with other fuel injectors and higher fuel pressure but that was not available at the time of the tests.

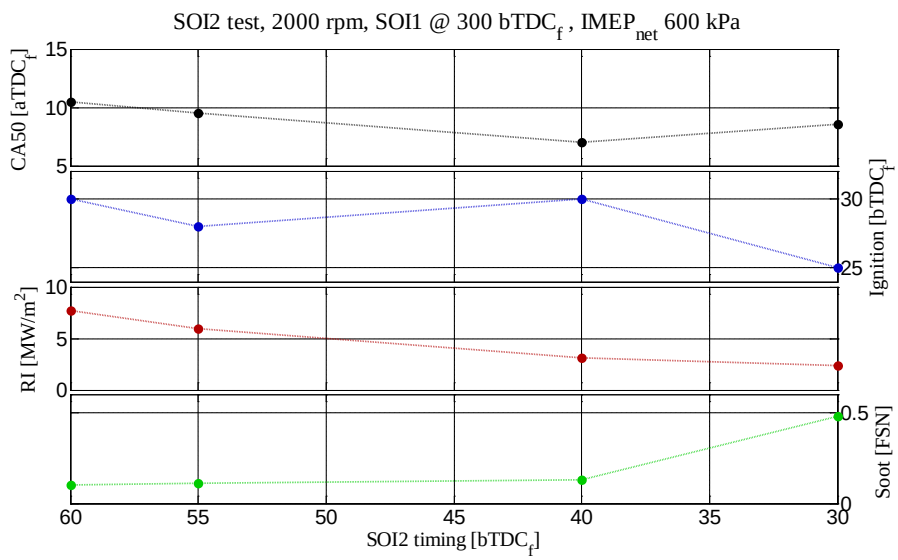

Figure 28: Effect of stratifying with spark assist, SOI2 timing

The HR for this type of stratified SACI can be seen in Figure 29. The initial HR progresses slowly as in SI combustion up to a certain point where it changes to the HCCI type of rapid HR.

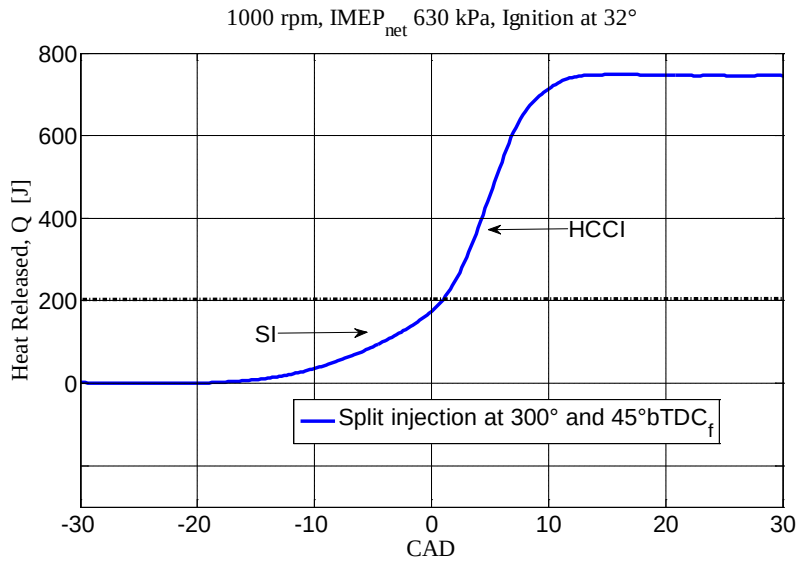

Figure 29: Heat release for stratifying with spark assist

6.1.8 Soot Emission

As the stratified SA combustion gave significant soot levels it can be of interest to also measure soot in normal HCCI operation. It was belivied that HCCI combustion was free from soot due to the homogenous condition. In Figure 30, a single injection experiment with constant CA50 timing is shown. By injecting the fuel near TDC_{GE} the soot formation increases. This is when the piston is close to the fuel injector and fuel impingement on piston surface is believed to leave a liquid film that burns rich during the main combustion. The combustion noise, RI, is also increased when injecting the fuel during the NVO sector due to shorter burn duration with the pre-reacted fuel. The lowest fuel consumption is when the fuel is injected in the region of 250 °$bTDC_f$ with low soot levels as well.

With split injection, the soot is higher than for single injection, see Figure 31. The first injection is set at 300°, where ~25% of the fuel is injected to avoid soot formation. Both low fuel consumption and RI could be reached when injecting the fuel at 230° $bTDC_f$.

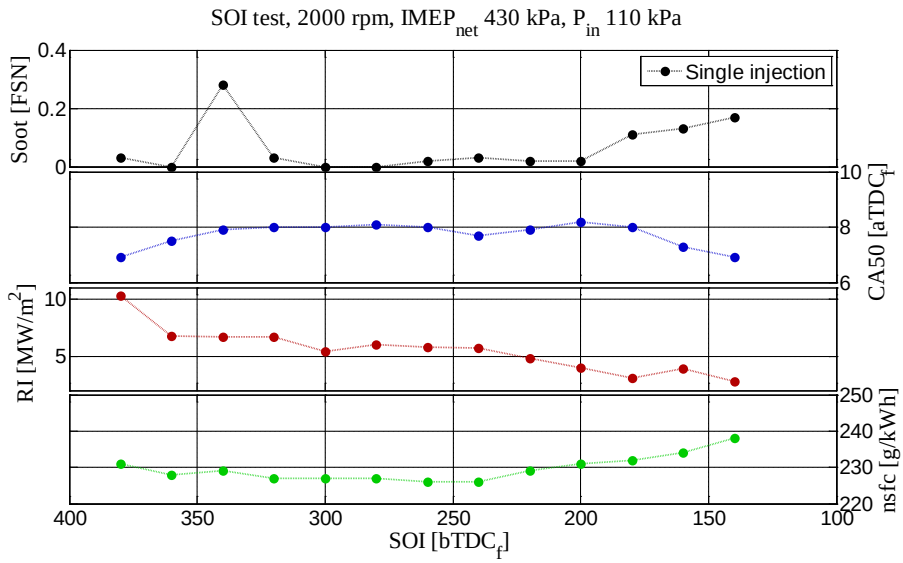

Figure 30: Effect on soot with single injection

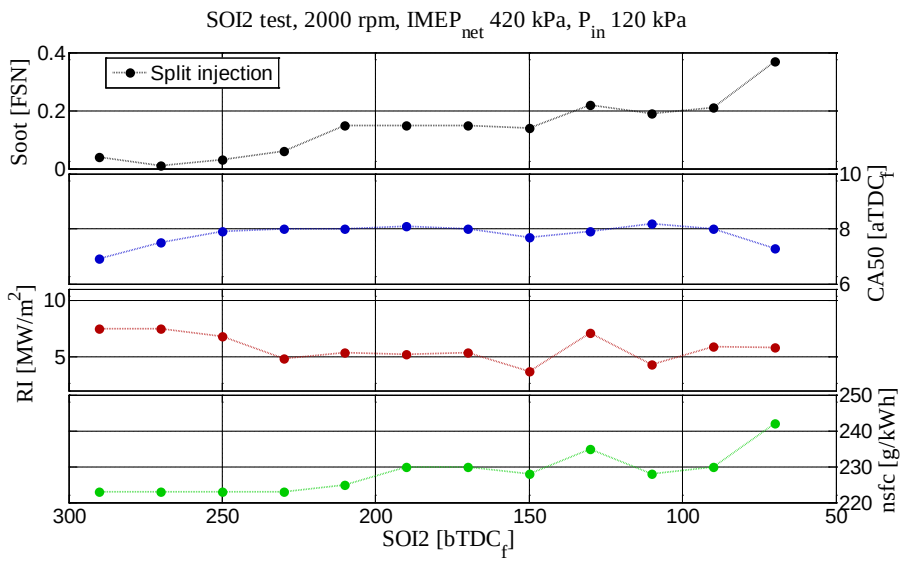

Figure 31: Effect on soot with split injection

6.1.9 Boost Pressure and Lambda

In Figure 32, a comparison between lean and stoichiometric (achieved with external EGR) operation is shown,. When external EGR is added, the heat capacity of the in-cylinder charge is increased. This is a result from the increased water vapor and CO_2 content when the air dilution is replaced. With external EGR the internal EGR needs to be increased to keep the combustion timing, as reflected in the earlier EVC timing. The earlier EVC timing leads to a reduction of the mass flow through the engine and the VGT has to be adjusted to keep the boost pressure. This increases the back pressure for a given intake pressure as seen in the pressure loss over the engine, P_{ex}-P_{in}, when operating stoichiometric. nsfc is higher for the stoichiometric case due to increased pumping losses and also from increased heat losses due to the extended recompression phase.

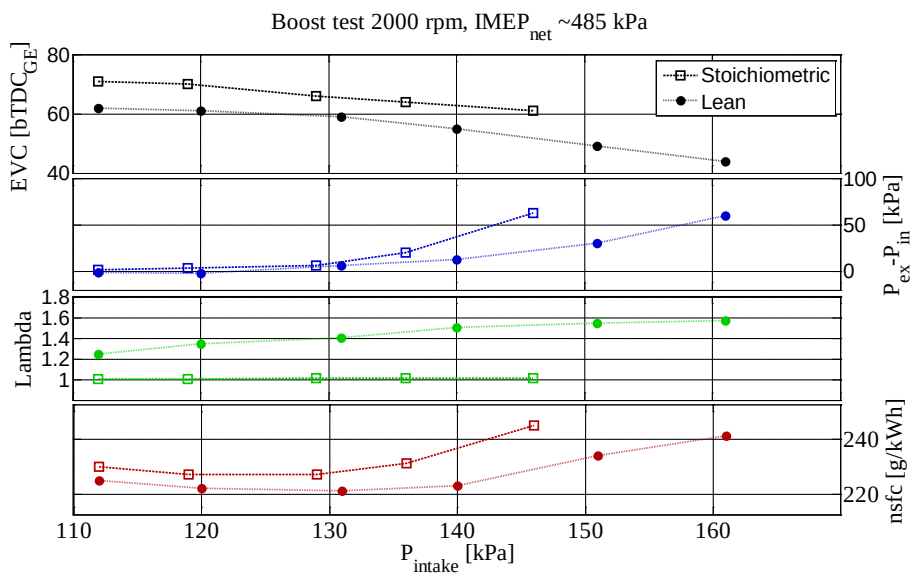

Figure 32: Lean and stoichiometric boost test

6.1.10 Boost Pressure and Valve Timings

It is normal to operate NVO HCCI with almost symmetrical valve timings, meaning that the EVC timing is as much before TDC_{GE} as IVO is after TDC_{GE}. As the load is increased, a later EVC is needed to keep the combustion timing. With these short duration camshafts the IVC can then be before BDC. As seen in Figure 33, the boost pressure is increased by delaying IVC with asymmetrical valve timing due to increased cylinder filling.

The achievable boost pressure has to be weighted against pumping losses due to turbocharger inefficiency and throttling losses over the valves, to keep engine efficiency as high as possible.

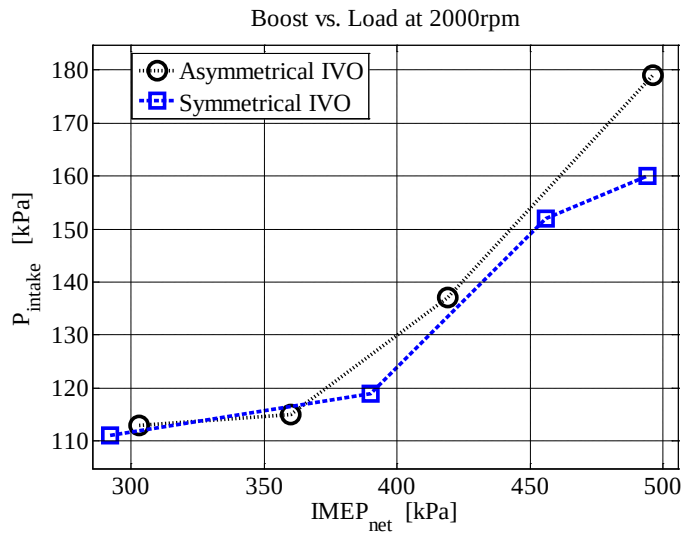

Figure 33: Boost pressure vs. valve strategy

6.1.11 Boost Pressure and Stoichiometric Condition

When a TWC is used to reduce the engine out NOx emissions the engine has to be operated near stoichiometric conditions. At low HCCI load i.e. below $IMEP_{net}$ 350 kPa, the NOx emissions are usually insignificant but at higher loads they can impose a problem. Stoichiometric operating can be a problem with increased boost pressure as seen in Figure 34. In this operating point, at 2000 rpm, $IMEP_{net}$ of 450 kPa and an intake pressure of 145 kPa, the lambda traces for all four cylinders and the mean lambda after the exhaust turbine are shown. A richer mixture is imposed by external EGR until stoichiometric is reached. This leads to misfiring as seen from the oscillating lambda trace in the end. The NVO is 118 CAD when stoichiometric condition is reached. If the intake pressure is reduced to 120 kPa, see Figure 35, less external EGR is needed and the NVO is 144 CAD at the end. It is now possible to operate richer than stoichiometric and it seems like the increased internal EGR has a stabilizing effect on combustion stability.

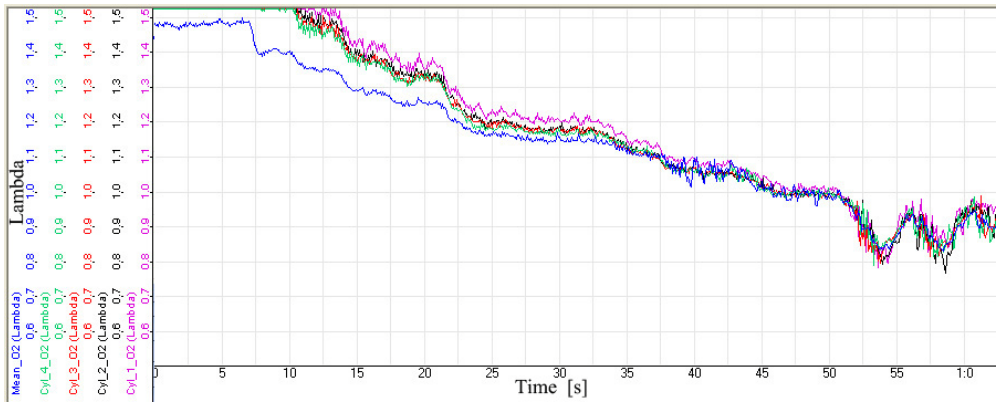

Figure 34: Individual lambda traces at 2000 rpm, $IMEP_{net}$ 450 kPa, P_{intake} 145 kPa

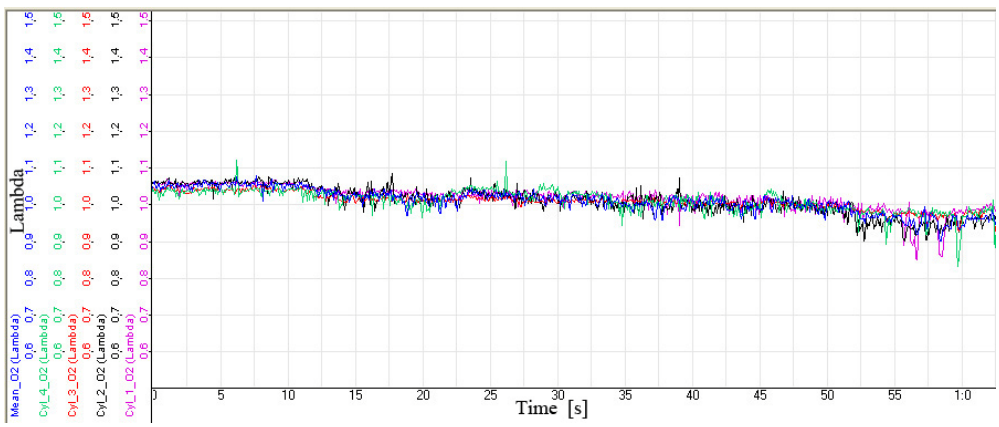

Figure 35: Individual lambda traces at 2000 rpm, $IMEP_{net}$ 450 kPa, P_{intake} 120 kPa

6.1.12 Summary of Basic HCCI Operation

The strategy on how to operate this turbocharged HCCI engine is based on the previously described results. Some parameters could be varied more than others depending on operating point.

The EVC timing directly controls the amount of internal EGR and therefore has a strong effect on the combustion timing in a NVO HCCI engine. A delayed combustion timing reduces the peak pressure rate and therefore the combustion noise or RI. The combustion timing will influence the NOx emissions, the combustion stability, the peak cylinder pressure and the fuel efficiency.

The injection timing influences efficiency, RI, soot, NOx and HC emissions. Injecting the fuel during in NVO period advances the combustion timing and increases RI.

The cooling temperature influences the heat losses and therefore sets how much internal EGR is needed for a given combustion timing. This also influences the mass flow through the engine. The mass flow influences the efficiency of the turbocharger and thus attainable boost pressure. The boost pressure in turn influences the fuel efficiency.

With spark assist, the ignition timing can, at certain operating points, influence the combustion timing and can be used to delay the combustion timing if reduced combustion noise is wanted.

If spark assist is used in association with a late fuel injection to create a stratified charge, there is risk of significant increase of soot formation.

With increased boost pressure, the combustion noise is reduced and the pressure loss over the engine is increased. This means that more fuel has to be burned at a constant load, which counteracts the reduced noise to some extent. With stoichiometric condition instead of lean burn the mass flow through the engine is reduced as internal EGR is needed, leading to a reduction of the fuel efficiency for a set boost pressure level.

If a TWC is used for stoichiometric conditions, higher boost pressures can lead to misfire when external EGR is added. An increase of the internal EGR fraction seems to have a stabilizing effect on the combustion.

In these results it has been shown that all the engine operating variables influence fuel efficiency, peak pressure rate and emissions and therefore need to be tuned at every operating point to obtain low fuel consumption, low combustion noise and emission levels at the same time.

6.2 Operating Limitations

Much research has been performed on the HCCI combustion concept the last decades. However, most publications are not focused on maximum load range and what limitations that are most important. In this chapter the combustion noise, combustion stability, soot, NOx and PCP limitations will be defined and discussed.

6.2.1 Combustion Noise

Due to the nature of the high energy release rate in HCCI mode the combustion induced noise can be very high. A measure of combustion noise is given by the pressure rise rate.

Eng [97] analyzed the relation between combustion-generated pressure waves and the audible noise with HCCI combustion. He concluded that these pressure oscillations cause the engine structure to vibrate and therefore generate audible engine noise. In Eng´s analysis it was shown why Christensen et al. [5] could tolerate a higher peak pressure rate when the engine was supercharged. He concluded that the combustion-generated noise was at the same level as the NA set-up used by himself. By using the equation for the intensity of a harmonic wave he presented the Ringing Intensity (RI) as a measurement of combustion noise:

$$RI \approx \frac{1}{2\gamma}\frac{\left(\beta\frac{dP}{dt_{max}}\right)^2}{P_{max}}\sqrt{\gamma R T_{max}} \qquad (6.1)$$

Where γ is the ratio of specific heats, β is a scale factor for the measured pressure oscillation amplitude relative to the maximum rate of pressure rise. dP/dt_{max} is the maximum rate of pressure rise in the time domain, meaning that this is also a function of engine speed. P_{max} is the maximum cylinder pressure. Since the cylinder pressure is a function of the intake pressure a higher intake pressure/ P_{max} will reduce the RI. T_{max} is the maximum cylinder temperature and R is the universal gas constant. Eng used an RI limit of 2 MW/m^2 in his experiments.

Another method to quantify combustion induced noise was presented by Andreae et al. [98]. They proposed to use only the peak pressure rate in time as noise threshold, giving the expression a function of engine speed but not boost pressure:

$$\left(\frac{dP}{dt}\right)_{max} \qquad (6.2)$$

It was concluded that the audible noise was not from transmission of the in-cylinder pressure wave through the engine structure. It was rather the sound radiation from

the structural vibration excited by the first few waves of cylinder gas vibration. The threshold of 5 MPa/ms was recommended by Andreae et al.

Normally the pressure rise rate is measured in bar/CAD or MPa/ms, and can be used to impose an operating limit. But neither of these catch the real combustion noise when the engine is supercharged The Ringing Intensity, RI (MW/m²) on the other hand compares the pressure rise rate to peak cylinder pressure and engine speed. The RI has been used as criterion to limit the pressure rise rate due to the fact that it reflects the audible combustion noise in a good way. In Figure 36, a comparison of these different pressure rise rate expressions are shown when the load is constant and boost pressure is varied.

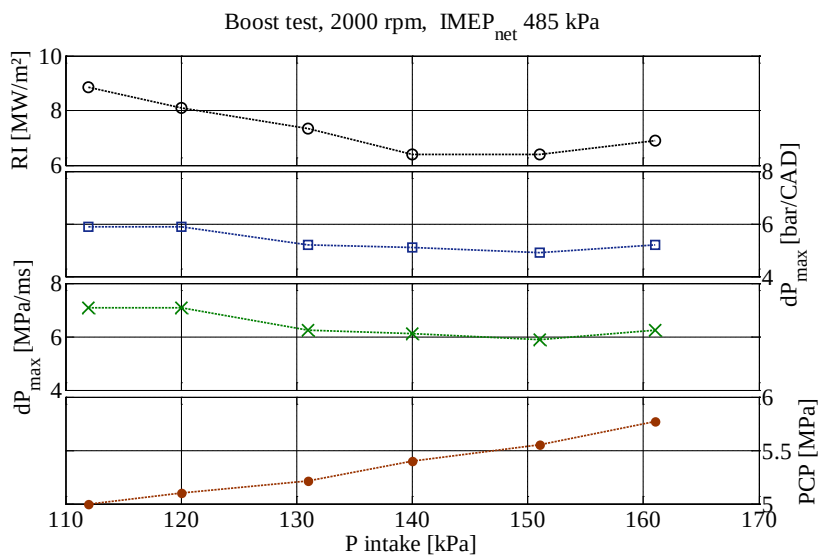

Figure 36: Boost result with different pressure rate expressions

To be able to increase the load range, a high intake pressure is advantageous to keep the combustion noise at an acceptable level, i.e. a low RI number. It was decided that RI had to be limited to 5 MW/m², since any higher level has too high engine noise. In Figure 37, the influence of intake pressure on RI is seen as an exponential trend line fitted to experimental data. This test is done with a constant CA50 timing at 8.5 °aTDC$_f$. When intake pressure is increased the PCP is also increased.

With increased intake pressure it is possible to decrease the combustion noise as seen in Figure 36. The RI goes from 9 MW/m^2 to 6.5 MW/m^2 when the intake pressure is increased from 110 kPa to 140 kPa in this test and the variation in units are less for the peak pressure rate in CAD or time. As expected the PCP increases with higher intake pressure.

The achievable boost pressure has to be weighted against pumping losses due to turbocharger inefficiency and throttling losses over the valves.

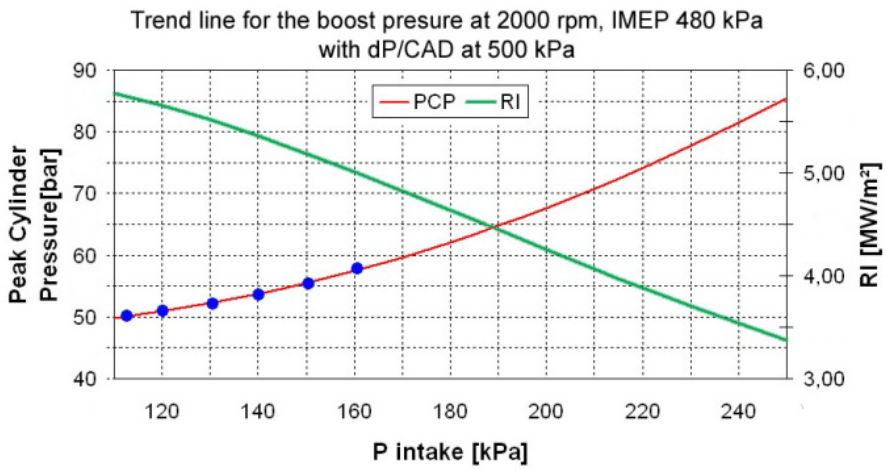

Figure 37: Trend line for Ringing Intensity

6.2.2 Combustion Stability

Since the HCCI engine is operated unthrottled, the relative pressure oscillations in the intake and exhaust are decreased. This leads to reduced in-cylinder temperature and turbulence fluctuations. The SI combustion is started in a small joint where the plasma channel is formed between the spark plug electrodes. Thus it is very sensitive to the local conditions of air/fuel ratio, turbulence and mean velocity. HCCI has multiple ignition kernels and is thus much less sensitive to the local conditions. This results in reduced cycle to cycle variations for HCCI combustion [3].

But when the load is maximized together with late combustion timing, CoV increases. At higher engine speeds where the time window for proper combustion phasing is reduced, it is more difficult to retard the combustion. There is less risk for misfire when the CoV is under 3 %, see Figure 38. The CoV is calculated by comparing the deviation of IMEP to the average values of the previously measured IMEP. In Figure 38, CoV is shown versus cycle number with a calculation of fifteen previously measured IMEP values. Misfires at high HCCI load results in violent combustion the subsequent cycles, and must be avoided at all times. For loads near idle operation the combustion is limited by the Standard Deviation (STD) of $IMEP_{net}$ instead of CoV. The limit is set to 15 kPA of $IMEP_{net}$ for stable combustion.

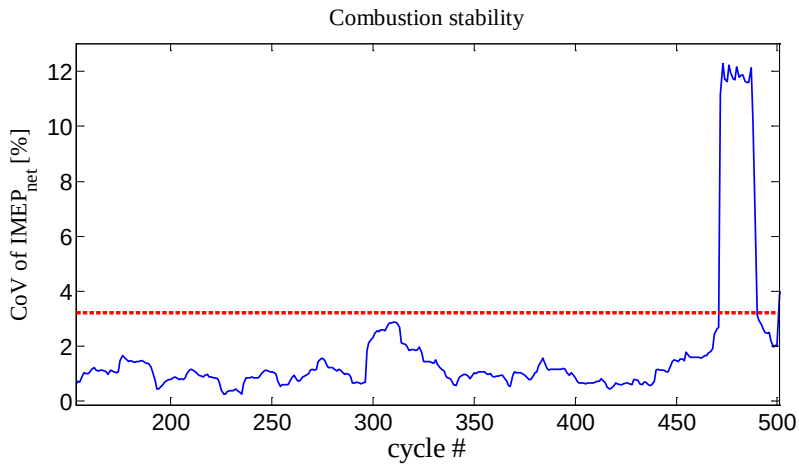

Figure 38: Combustion stability, CoV of IMEP$_{net}$

6.2.3 Soot Emissions

To estimate the soot limit in the FSN scale the Euro 5 and 6 limits of 0.005 g/km must be converted. If a vehicle with a fuel consumption of 0.06 l/km or 44 g/km and operating at λ=1.5 is assumed, the smoke opacity is at 0.25 [99] which corresponds to a FSN value of 0.05 [100]. The maximum soot level is set at 0.1 FSN for a single operating point and 0.05 FSN for the average results from a complete speed and load range test.

As can be seen in Figure 30 and Figure 31, a late injection timing will increase the soot level and lower the efficiency. Injecting the fuel around TDC$_{GE}$, when the piston is close to the injector, raises the risk for fuel impingement on the piston surface.

The heat release rate can be decreased with a spark assisted stratified injection, but the risk for high soot levels is seen in Figure 39. The fuel spray during NVO is visualized in Figure 40.

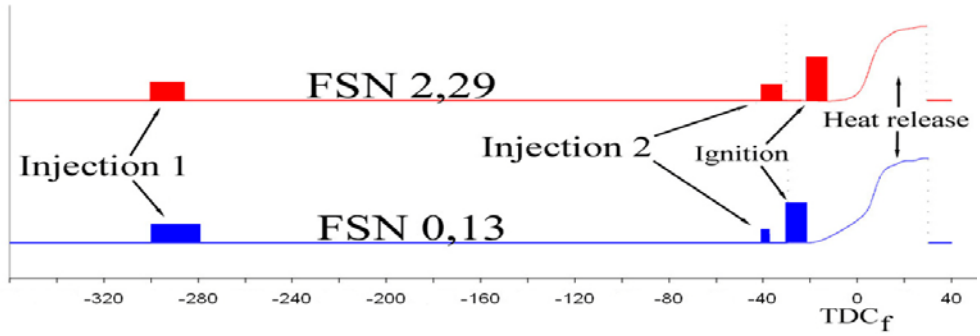

Figure 39: Late second fuel injection vs. soot

Figure 40: Fuel spray during the negative valve overlap

6.2.4 Nitrogen Oxide Emissions

HCCI is known for low NOx emission levels, but as the load increases, NOx emissions increases due to higher temperature and less dilution. This means that there will be a NOx limit when operating lean HCCI. The Euro 5 and 6 limits the NOx emissions at 0.06 g/km, if a fuel consumption of 44 g/km is assumed, the corresponding NOx level will be 1.36 g/kg$_{fuel}$. To have margin, the Emission Index (EI) NOx limit is set at 1.0 g/kg$_{fuel}$. This correspond to NOx levels below 15 to 20 ppm depending on air/fuel ratio. With higher intake pressure the dilution increases and NOx levels are reduced, as seen in Figure 41.

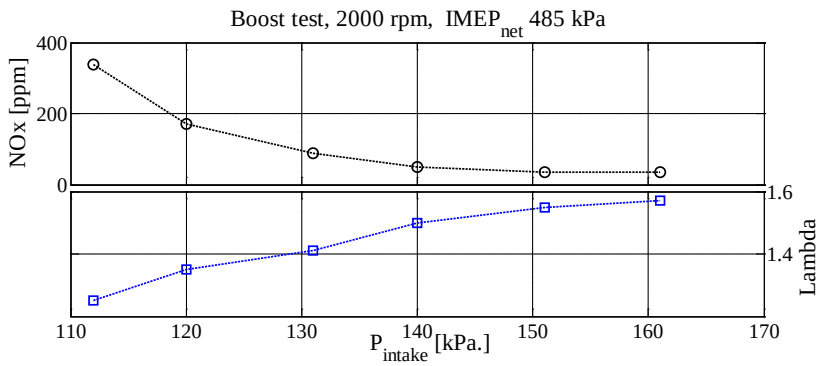

Figure 41: Boost variation vs. NOx and Lambda

If the NOx emissions becomes too high, the engine has to be operated stoichiometric to meet the NOx legislation. There can be some concerns regarding the low temperature in HCCI mode and TWC but for this engine, the light off temperature of the TWC is reached at high load. To operate the engine stoichiometric the engine was equipped with a long route EGR system.

HCCI combustion is sustained without a spark to ignite the charge but SA can reduce CoV and thus enable a later combustion phasing. Especially at low engine speed and high load, a delayed combustion phasing is possible with low CoV using SA. At low engine speed and high load the NOx emissions are usually high since the turbocharger cannot increase the intake pressure. This means that the engine is operated stoichiometric. At higher engine speeds the NOx is below the limit but any influence from SA on the NOx emissions has to be considered.

6.2.5 Peak Cylinder Pressure

The peak cylinder pressure scales with intake pressure, see Figure 36, and it can become a limiting factor. There is risk for structural damage of the engine if the design limit is exceeded. An example of consequences of high PCP can be seen in Figure 42. The engine was operated at 2000 rpm and $IMEP_{net}$ 600 kPa, the intake pressure was 220 kPa and the PCP was 10.5 MPa, when a piston failure occurred.

FEA revealed that the piston stress level was above the fatigue limit (~60 MPa) as seen in Figure 43. A redesign of the piston was made with increased top land height, see Figure 44, and the PCP limit was reduced to 9.5 MPa to prevent further problems at the piston top.

Figure 42: Damaged piston due to high PCP

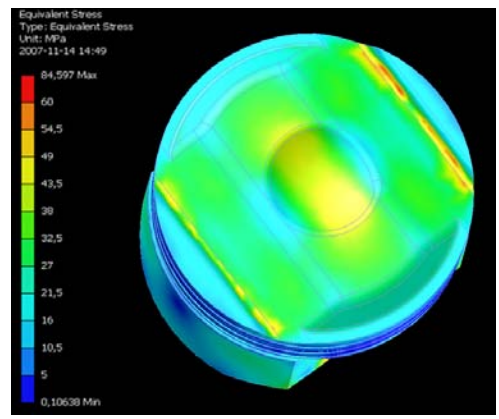

Figure 43: Finite element analysis of broken piston

Figure 44: Piston modification

6.2.6 Summary Operating Limitations

The limits on HCCI operation are the following:

Combustion noise:	RI < 5 MW/m^2
Combustion stability:	CoV of $IMEP_{net}$ < 3 % or STD of $IMEP_{net}$ < 15 kPa
Soot emissions:	FSN < 0.10 for a single operating point FSN < 0.05 average, for the entire operating range
NOx emission:	EI NOx < 1.0 g/kg_{fuel}
Engine stress:	PCP < 9.5 MPa

6.3 Turbocharging and Operating Regime

To increase the maximum load range in HCCI, the combustion noise has to be reduced. The boosted HCCI engine can on the other hand, for a given RI, use a more beneficial combustion timing compared to a naturally aspirated HCCI engine, and therefore improve thermal efficiency.

In this chapter it will be shown how the intake pressure can be influenced from different operation variables and how this affects the resulting fuel efficiency, combustion noise and stability. Also included is experiments to increase the boost pressure and evaluation of different turbochargers. The following results are made with cylinder individual balancing as described in the experimental setup.

6.3.1 CA50 Timing

The combustion phasing, CA50, is an important combustion parameter when operating in HCCI mode, a later CA50 can raise the upper load limit by decreasing RI and PCP as seen in Figure 18. This has to be weighted against an efficiency loss when moving away from the timing for Maximum Brake Torque (MBT) as seen in Figure 45. Here a CA50 variation test is performed at 2500 rpm where the load is held constant by the injected fuel amount. A delayed combustion timing reduces the heat losses but on the other hand the thermodynamic efficiency is reduced due to less expansion ratio. Increased intake pressure leads to increased back pressure, as seen in the Figure 46, as P_{ex} - P_{in}.

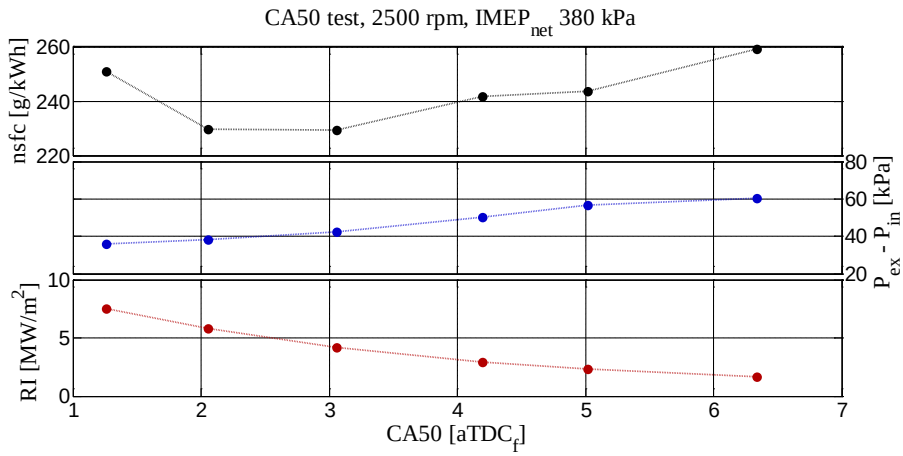

Figure 45: Combustion timing test, CA50

Controlling the combustion timing with the amount of internal residuals influences the mass flow and therefore available boost pressure as seen in Figure 46. A later CA50 timing requires less internal residuals which is arranged with a delayed EVC timing. As a result the mass flow is increased together with boost pressure, but here the turbocharger sizing plays an important role. The RI level is directly affected by CA50 timing, and is over the limit with early combustion. The CoV increases with late CA50 timing so the chosen CA50 timing has to be between 3 and 5 degrees. At this operating point with relatively high boost pressure the NOx level is low, independent of the CA50 timing.

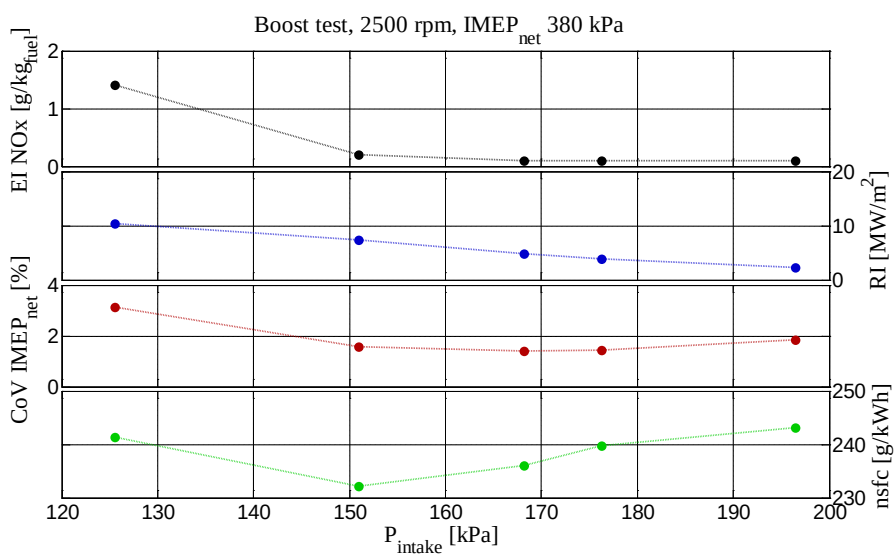

Figure 46: Intake pressure test, CA50

6.3.2 IVO Timing

When load and boost pressure are increased the exhaust and intake temperatures are increased meaning that less hot residuals are needed and hence a later EVC can be used. With the short duration valve timing camshaft, the IVC can be before BDC. This will reduce the volumetric efficiency and reduce the in-cylinder pressure. In Figure 47, an IVO test is performed from a symmetrical starting point to latest possible IVO timing when the CA50 timing is kept constant at 5 degrees by changing the EVC timing. This implies that the EVC timing has to be changed continuously as the IVO timing is delayed to keep the chosen combustion timing. The RI level is over the limit with symmetrical valve timings and the combustion stability, CoV, is too high with the latest IVO timings where also the fuel consumption is high. For this operating point a slightly asymmetrical IVO timing is preferred.

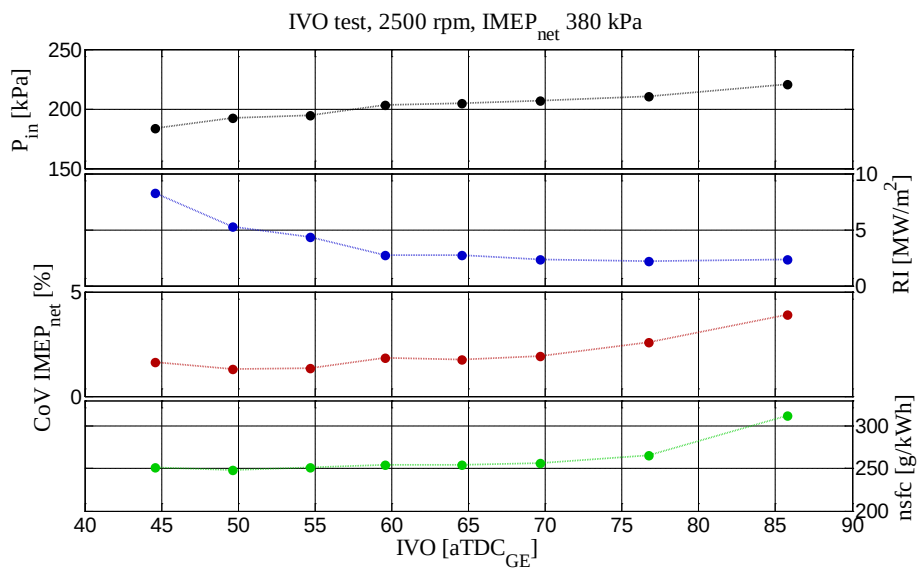

Figure 47: Intake valve opening timing test, IVO

6.3.3 Intake Temperature

When the boost pressure is increased, the intake temperature will increase if an intercooler is not used. Higher intake temperature reduces the need for internal EGR for a chosen CA50 timing, leading to increased mass flow. Thus a higher intake pressure can be reached as seen in Figure 48. The CA50 timing is constant at 5 degrees by adjusting the EVC timing. The intake temperature is measured 40 mm from the intake valve and the temperature is regulated in the intercooler circuit. The IVO timing is at latest possible timing. Since both RI and CoV are low in these

results, the intake temperature can be set for the lowest specific fuel consumption at 50 °C.

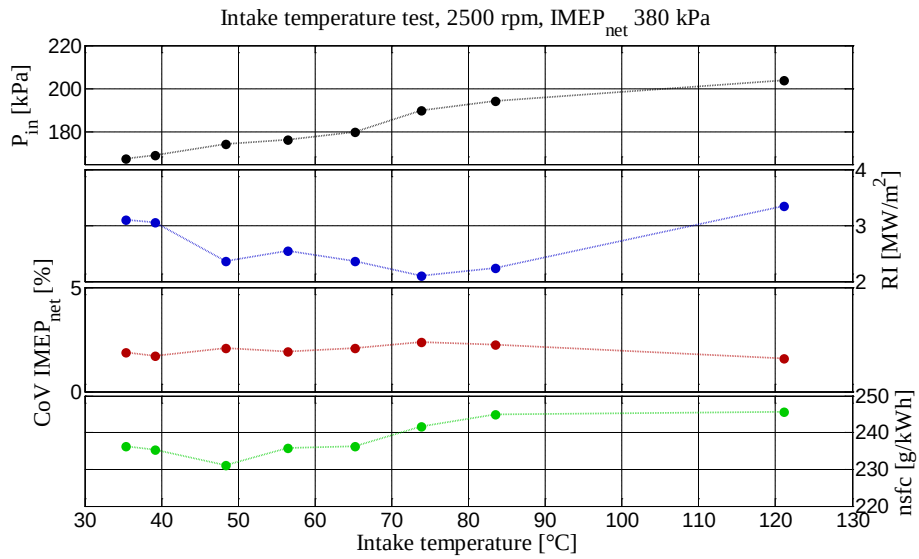

Figure 48: Intake temperature test

6.3.4 EGR

External cooled EGR can be used when the engine is operated stoichiometric due to high NOx emissions or to influence the pumping losses. When external EGR is increased, the mass flow through the engine is reduced due to the increased heat capacity of the intake charge, leading to more internal EGR to keep the combustion timing constant as seen in Figure 49.

This reduction of intake pressure increases RI but at the same time the CoV is decreased due to the higher internal EGR content, which has a stabilizing effect. The fuel consumption can be reduced in these results with EGR due to more beneficial valve timings and reduced pressure loss over the engine.

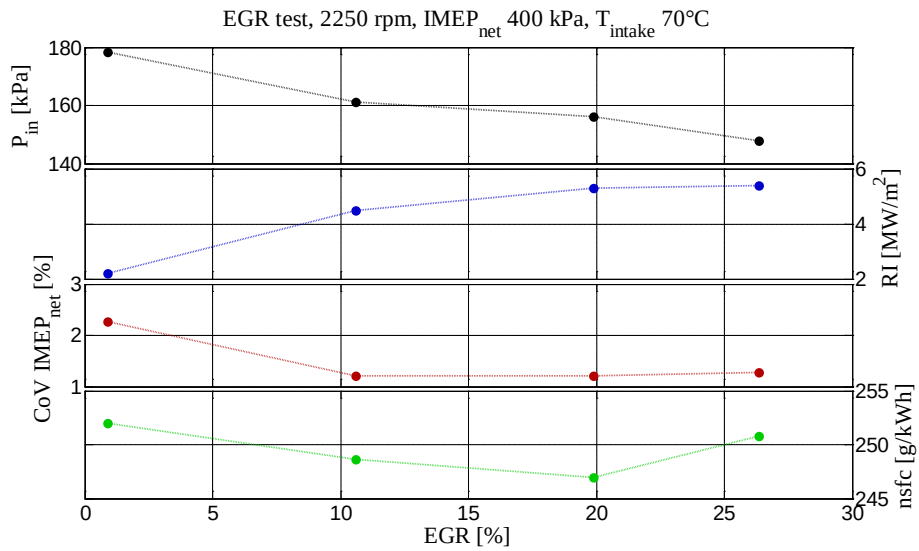

Figure 49: External EGR test

6.3.5 Intake Pressure

A higher intake pressure will not always automatically reduce the combustion noise for a given load since the pumping losses normally increase as well. With increasing pumping losses there is a need to burn more fuel to keep the load and this can counteract the effect on RI with increased intake pressure. In Figure 50, a boost variation test is done at 2500 rpm. This is done by actuating the wastegate. The CA50 timing is constant at 5 degrees by changing the EVC timing. At the lowest boost pressure the NOx emissions are above the limit. The RI is reduced by 8 MW/m² when going from low to high intake pressure. The CoV is stable except at the lowest intake pressure. In this test an intake pressure at 170 kPa gives the lowest fuel consumption for RI below 5 MW/m^2.

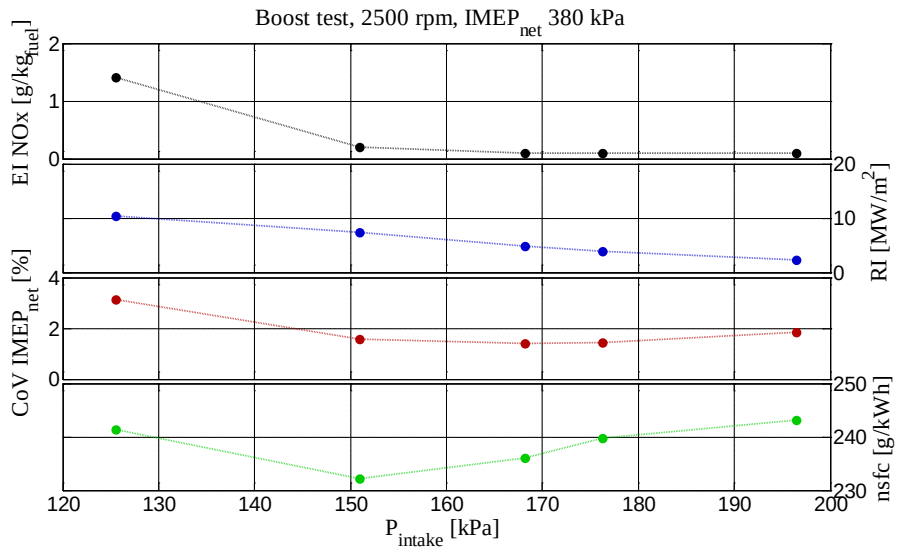

Figure 50: Ringing Intensity and peak pressure rise vs. intake pressure

6.3.6 Boost for Transient

A challenge during a load transient with a turbocharger is that the boost pressure is normally delayed due to turbocharger inertia etc. This delayed boost pressure can lead to increase of combustion noise, reducing available practical load range. Recall that there is cylinder balancing by the control system, where part of the fuel is injected during the NVO for fuel reformation. Normally we try to minimize this fuel reformation quantity to increase the efficiency and reduce engine out soot emissions. But for a load transient we can increase this fuel reformation quantity by advancing the first injection timing as seen in Figure 51. In this operating point, 2000 rpm and $IMEP_{net}$ of 400 kPa, the mass flow increased more than 25% with the more advanced injection timing. This leads to an increase of boost pressure by 20 kPa (the combustion timing is constant at 6° $aTDC_f$ here). The increased fuel reformation with more advanced injection has to be counteracted by a later EVC to trap less hot residuals for the same combustion phasing. As the EVC timing directly controls the mass flow the boost pressure can then be increased even before the actual load transient. As there is a limited amount of fuel that can be used for this reformation depending on exhaust conditions together with the EVC timing, a balanced fuel quantity has to be chosen. The drawback with this increased boost pressure is the reduced fuel efficiency with nsfc increasing from 235 to 250 g/kWh.

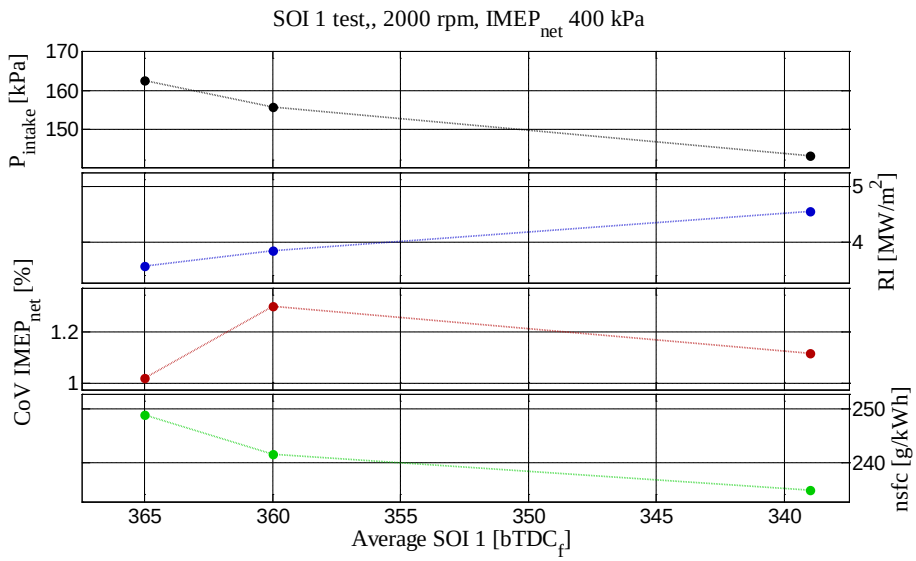

Figure 51: First injection timing test

In an effort to increase the intake pressure with higher exhaust mass flow, a test was conducted with water injection. In this experiment the mass flow was increased with water injection into the turbine inlet. With this system it was possible to have an instant increase of boost pressure, as seen in Figure 52. But this rather low boost increase was not enough to influence RI, and from a practical standpoint this kind of system is unsuitable.

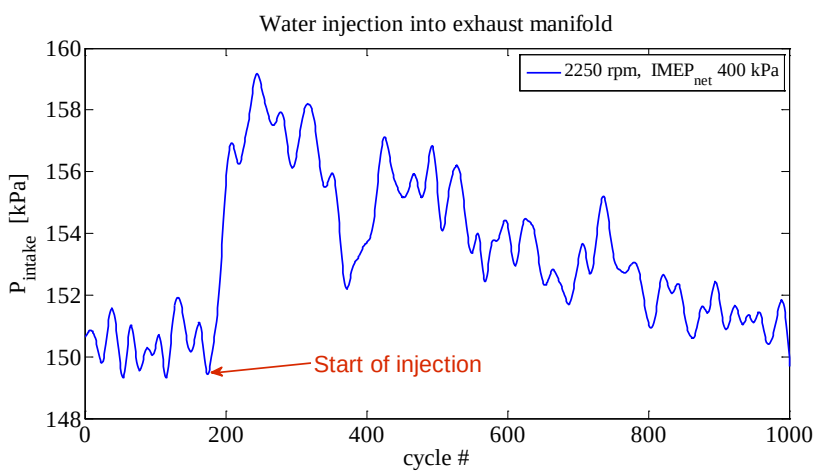

Figure 52: Water injection into exhaust manifold

Another solution to increase the boost pressure was also tested. An extra volume was added to the exhaust manifold and it was connected to the intake manifold. In

some early experiments with a short route EGR system it was possible at certain operating points to have a higher intake pressure than exhaust pressure. With short duration valve timings the turbine gets a very uneven exhaust flow and by damping it with an additional exhaust volume and feed it with a small amount of air from the intake manifold, it might be possible to increase the overall turbocharger function.

This system was first evaluated in a GT-Power model where the results indicated that it could be possible to achieve both higher and lower boost pressure with this type of system as seen in Figure 53. In this figure an optimization is showed between damping volume length (ex-chamber) and the orifice diameter in the interconnecting pipe (sr-strypning) resulting in different intake pressures. This system was the manufactured and connected to the engine, see Figure 54. It was tested with two different damping volumes with no gain. The boost pressure decreased 5 kPa in both setups, the reason might have been that the surface heat loss from the damping volume was not modeled accurately in the simulation .

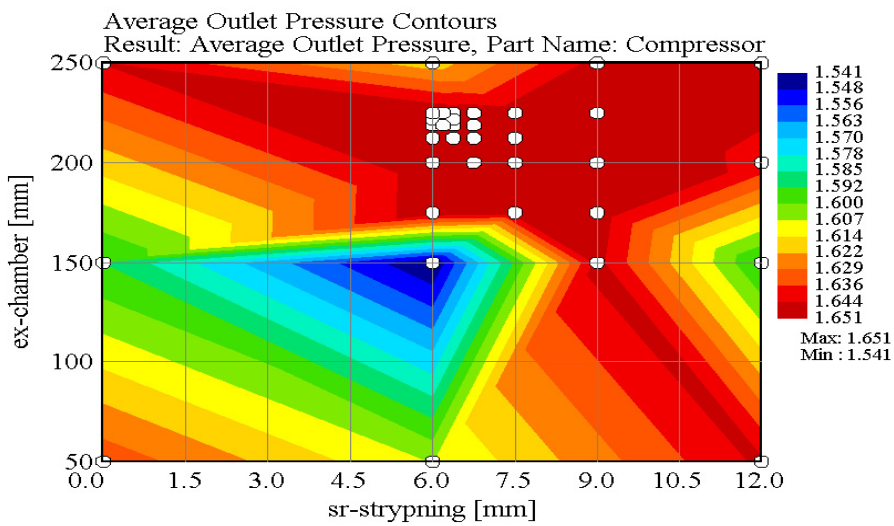

Figure 53: GT-Power simulation of boost pipe

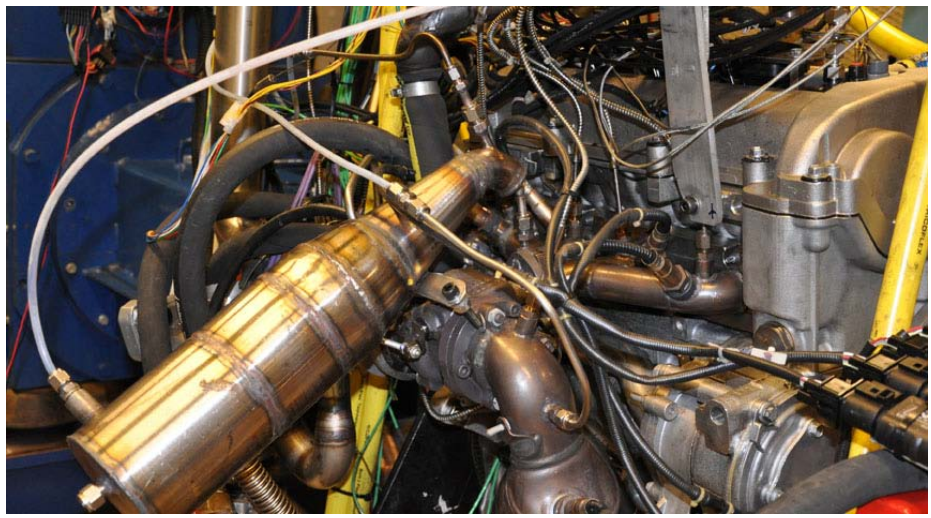

Figure 54: Boost pipe at exhaust manifold

6.3.7 Turbocharger Performance

To increase the load range of HCCI there is a need for high boost pressure at very low mass flows. There has not been a demand for this type of small turbocharger so far, and this limits the availability of suitable units. Our experiments has been with off the shelf diesel turbochargers. Figure 55 shows a comparison of two turbochargers, the BV35 is a 90 hp unit with Variable Geometry Turbine (VGT) and the KP31 is a 47 hp unit with fixed geometry turbine. A VGT unit in HCCI mode is an interesting control task as the VGT constantly needs to be adjusted. This requires adjustment of EVC timing to hold the combustion timing position. This adjustment of EVC timing influences the mass flow and therefore the VGT need to be adjusted again.

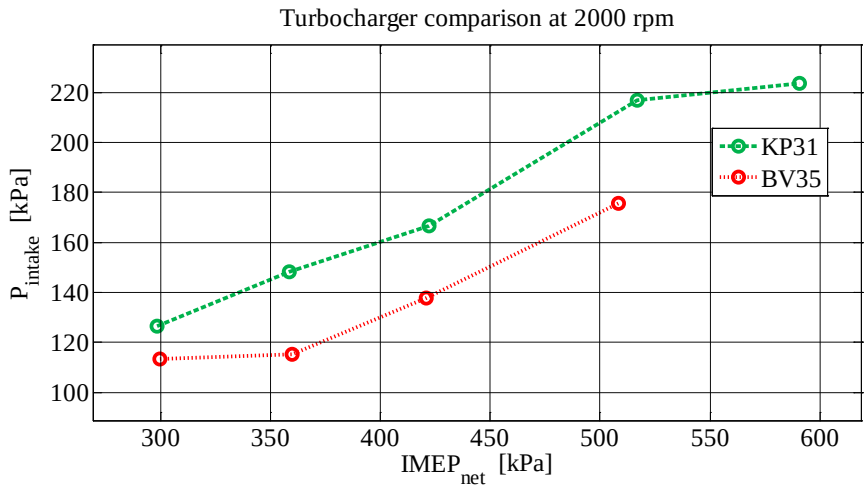

Figure 55: Turbocharger comparison

The intake pressure could be increased substantially with the smaller KP31 turbocharger in comparison to the larger BV35, see Figure 56. The intake pressure could be increased up to 70 kPa with the KP31. The increased intake pressure reduced the NOx emissions as seen in Figure 57. This meant that the engine could be operated lean in almost the entire operating range. The maximum load range could also be extended with the KP31 turbocharger as seen in Figure 58. The limitation for the small turbocharger starts at higher engine speeds where the turbine can become choked, leading to increasing pumping losses. But as described above, the mass flow can be adjusted by appropriate settings for the EVC timing, IVO timing, intake temperature, cooling temperature and external EGR level.

Even if the intake pressure was much higher with the KP31, the combustion noise was just slightly reduced as seen in Figure 59. The reason is that a more advanced combustion timing could be selected with the KP31 turbocharger to increase the thermodynamic efficiency, leading to improvement for the fuel consumption as seen in Figure 60.

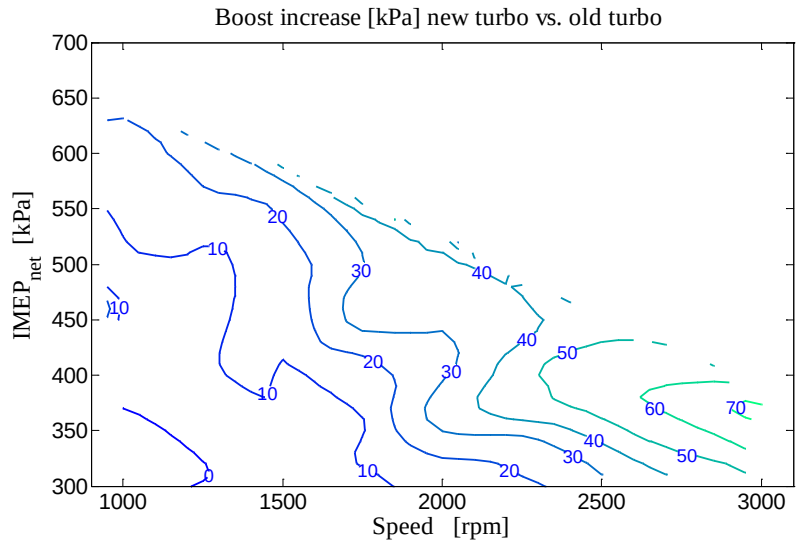

Figure 56: Increase of intake pressure with new turbocharger

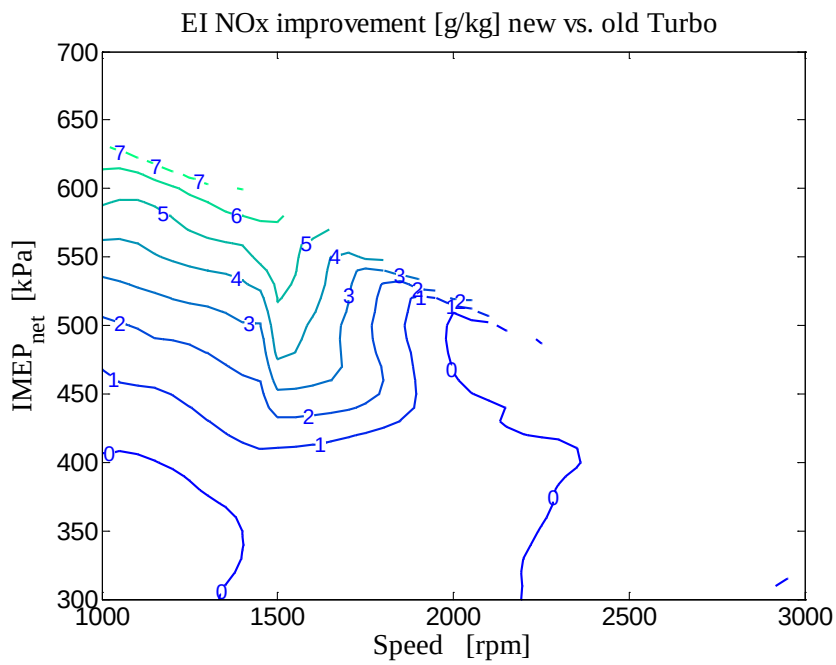

Figure 57: Improvement of NOx with new turbocharger

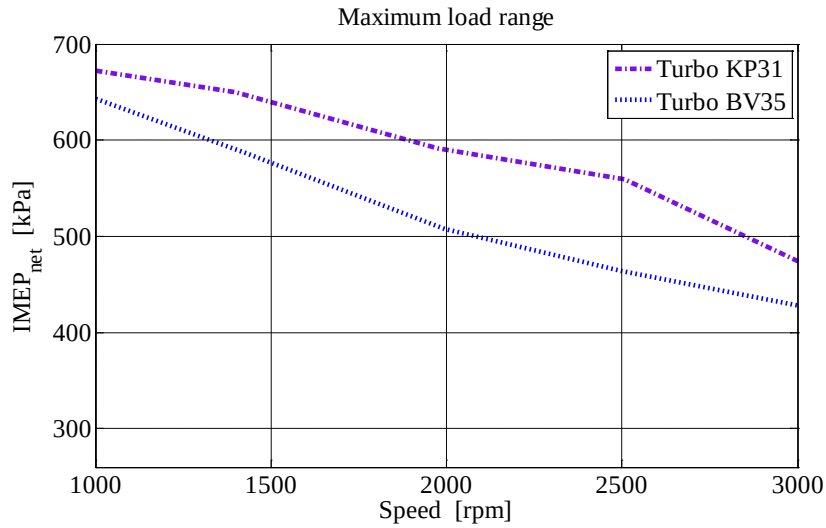

Figure 58: Maximum load range

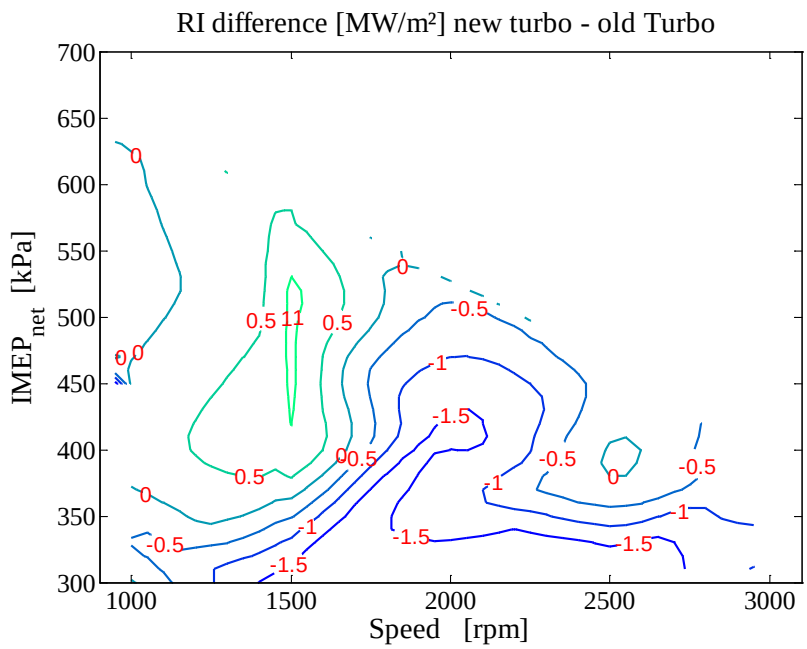

Figure 59: RI difference

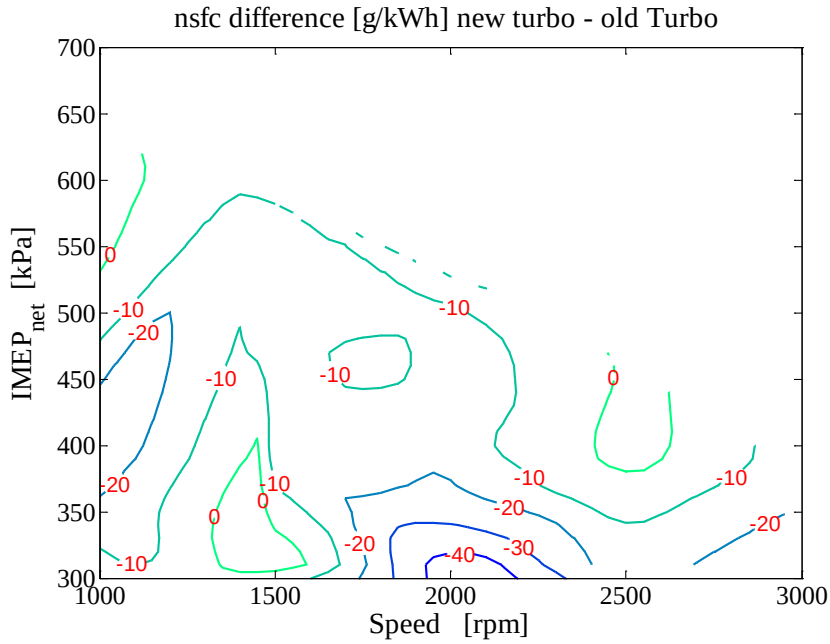

Figure 60: nsfc difference with new turbocharger vs. old turbocharger

6.4 Pumping Losses

In a NVO HCCI engine the valve durations are short compared to SI engine durations and this can lead to throttling losses for the HCCI engine. For example, at low HCCI load the EVC position needs to be in the region of 100° before TDC_{GE} and the EVO need to be before BDC not to lose efficiency. This implies an exhaust valve duration of ~80° is suitable for low load. At high HCCI load we might need a 40° EVC timing and the EVO timing also needs to be before BDC to keep the efficiency. This implies an exhaust valve duration of more than 140° is suitable for high load. To cover all loads we might choose an exhaust valve duration of 120° but this means that the EVO position will be at 20° after BDC at high load.

If the exhaust valve duration is too long the expansion work is reduced at low load, but on the other hand the expansion work at low load is quite small so it is possible to operate with a relative long duration or early EVO timing. In the end the chosen exhaust valve duration has to be a compromise in an engine with fixed valve duration.

On the intake side, similar balancing of the valve duration has to be made. If the IVO is done before the expansion work from the recompression phase is recovered there will be loss of efficiency. If the IVC is delayed after BDC the effective

compression ratio is reduced. In the end the intake valve duration ends up to be similar to the exhaust valve duration with the same compromise.

For a NVO HCCI engine with short valve duration the valve lift is in the region of 4 mm to have acceptable accelerations levels. This reduced valve lift can introduce throttling losses on both the intake and exhaust side depending on load and engine speed.

With the addition of a turbocharger there is usually an increase of the pumping losses due to the low efficiency of the turbine and the compressor. In Figure 61 it can be seen that the pumping losses increase with load at a fairly high rate in this particular turbocharged HCCI setup with the low duration exhaust camshaft (125° duration). In this result with the KP31 turbocharger, no intake cooling was used.

The pumping losses are divided into two parts as described earlier to get additional information:

$$PMEP = Throttling_{valve} + (P_{ex} - P_{in}) \quad (6.3)$$

$P_{ex} - P_{in}$: The pressure loss over the engine from turbine and compressor,

$Throttling_{valve}$: The pressure loss over inlet and exhaust valves

The pressure loss over the engine, $P_{ex} - P_{in}$, with the KP31 turbocharger becomes a problem at higher engine speed and load due to the choked turbine as seen in Figure 62.

The throttling losses over the valves at high load can be very high, even higher than what is possible in an SI engine as seen in Figure 63. The throttling losses originates from the short duration valve timings. At high HCCI load the EVO timing can be after BDC, leading to an increase of the pumping work from the blow-down process.

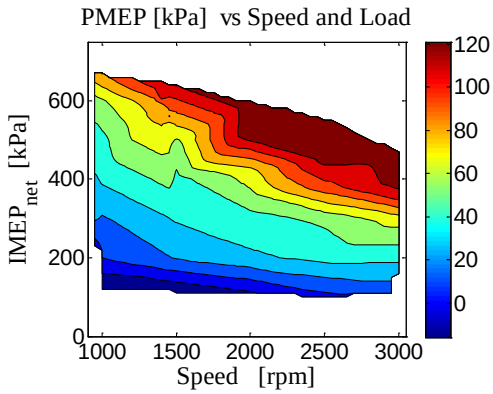

Figure 61: PMEP

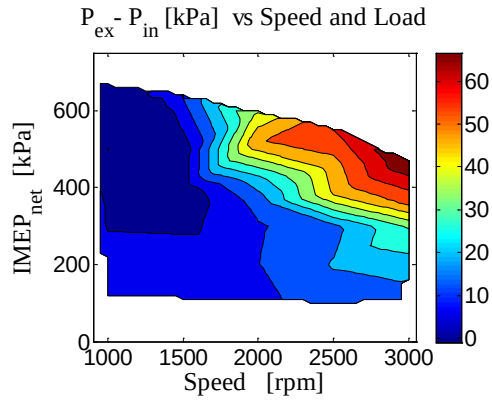

Figure 62: Pressure loss over the engine

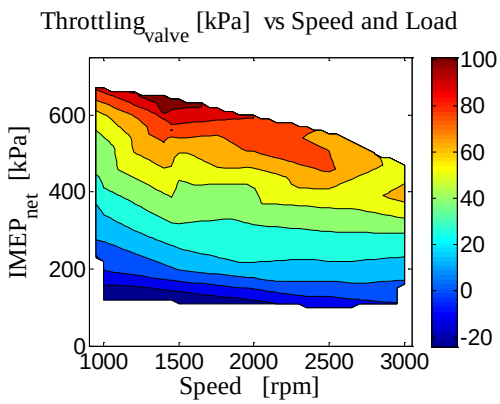

Figure 63:Throttling losses

6.4.1 Pumping Loss Reduction

To reduce the throttling losses, a wide span of valve timings was evaluated in the GT-Power simulation program. The boundary conditions were taken from the real engine testing except for the exhaust profile. This was done by using a discrete-grid optimization for a multiplier of the valve lift (ex_lift_factor) and valve duration (ex_dur_factor) of the used 125°/ 4 mm valve profile. The resulting PMEP from some of these simulations are seen in Figure 64 to Figure 67. where the simulation points are white dots. It was concluded that a longer exhaust valve timing was beneficial. The valve duration should not be extended to more than 130 % to be able to operate at low load as well. By using a valve timing with 125 % longer duration the valve lift could also be increased 125 %, for the same valve acceleration as seen in Figure 68. A new exhaust camshaft was manufactured based on these results.

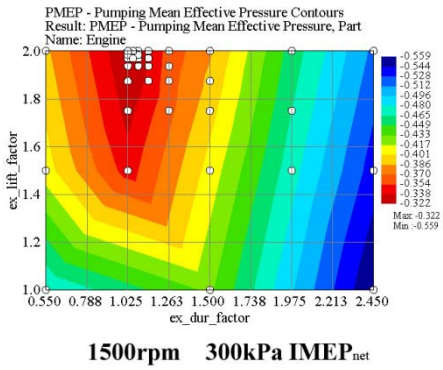

Figure 64: GT-Power simulation

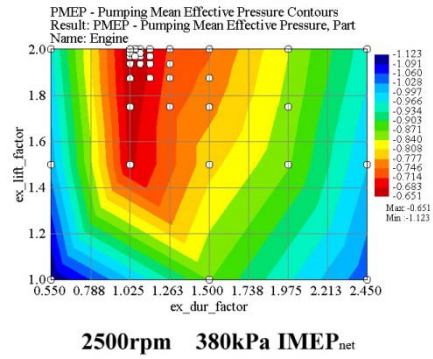

Figure 65: GT-Power simulation

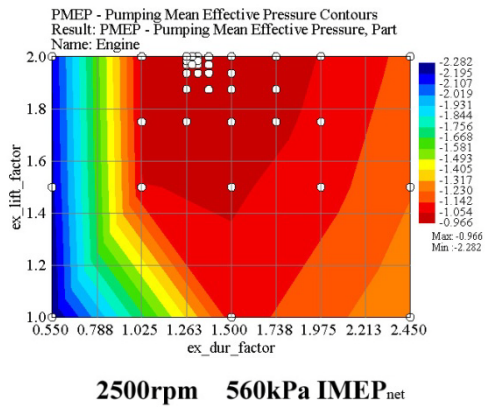

Figure 66: GT-Power simulation

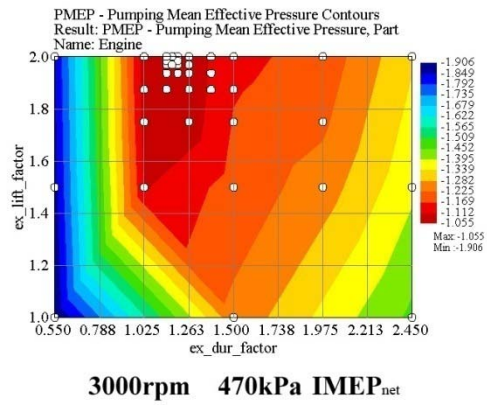

Figure 67: GT-Power simulation

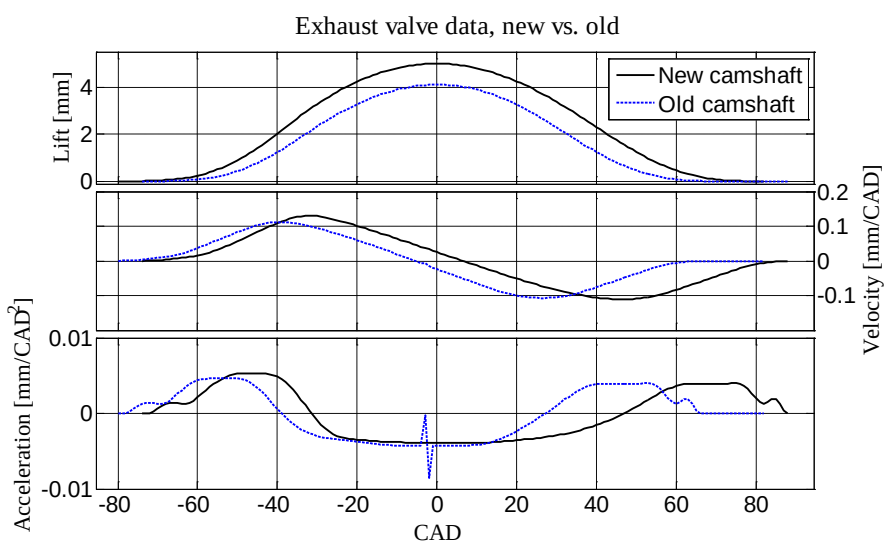

Figure 68: Exhaust valve data comparison

With the new longer duration camshaft the pumping losses could be reduced up to 70 kPa as seen in Figure 69. In this comparison the new exhaust camshaft is compared to the old exhaust camshaft final operating range. External EGR and intake cooling were used to decrease the pumping losses for both camshafts in this result. The pressure loss over the engine, P_{ex}-P_{in} in Figure 70, was also reduced due to a slight reduction of the boost pressure.

In Figure 71 it can be seen that the new longer duration camshaft manages to reduce the throttling losses substantially. Since the main part of the pumping losses orginate from the throttling losses in this turbocharged setup, these could be reduced up to 60 kPa with the new exhaust camshaft.

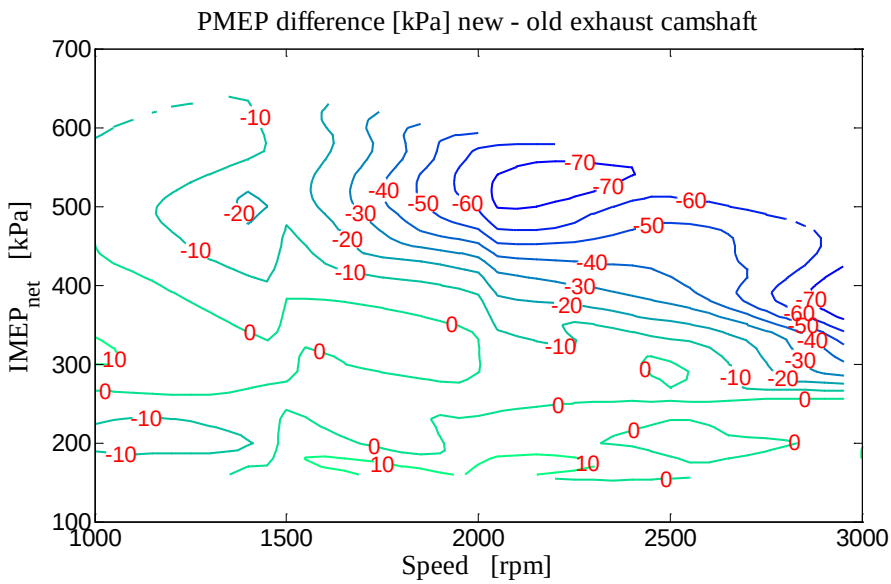

Figure 69: Pumping loss difference

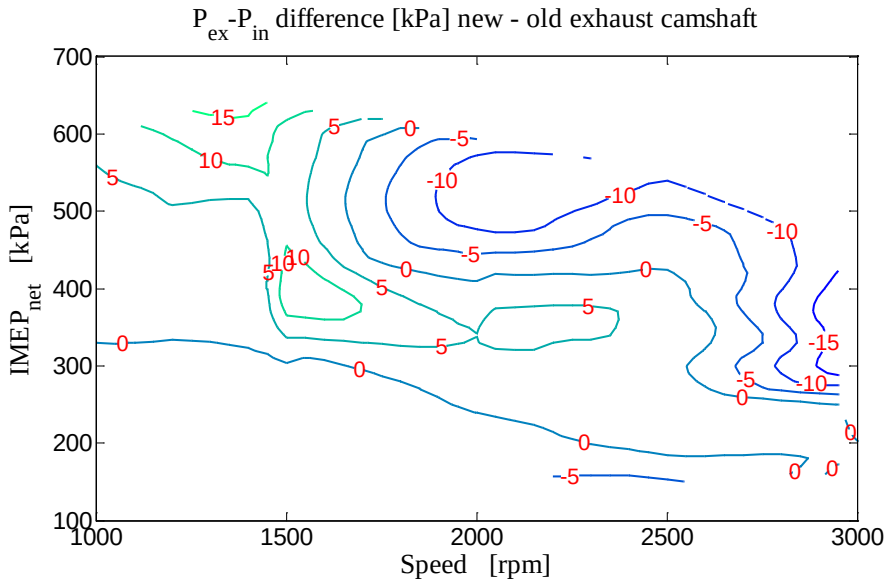

Figure 70: Pressure loss difference over the engine

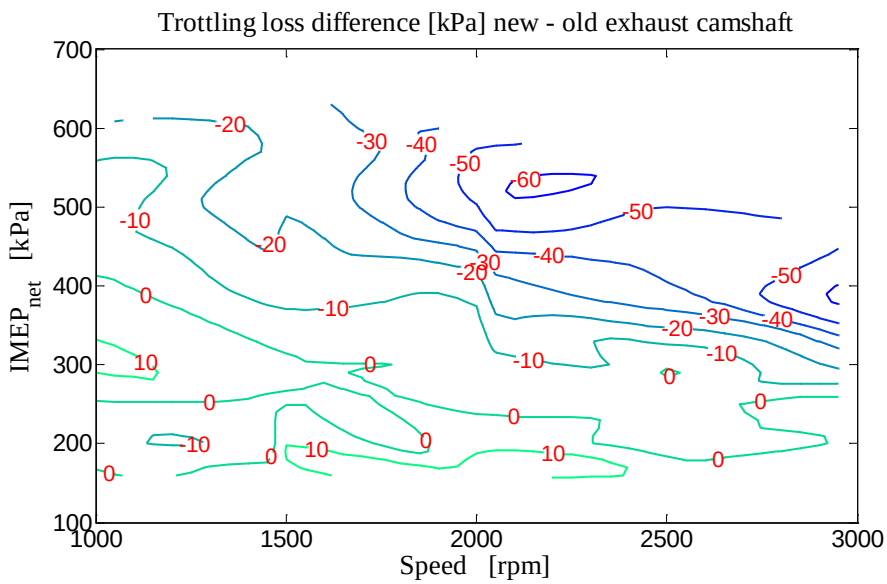

Figure 71: Throttling loss difference

By this reduction in pumping losses, the maximum load could be extended in almost the entire engine speed range as seen in Figure 72. But at 1000 rpm the capable load was reduced due to higher soot formation. The reason for this could be small differences in injection strategy.

The reduction in pumping losses lead to a reduction of the fuel consumption in almost the entire operating range as seen in Figure 73. It could be anticipated that the high reduction of pumping losses would have improved the fuel consumption even further, but the reduced expansion ratio with an earlier exhaust valve opening timing together with the slight decrease in boost pressure meant that the combustion timing had to be delayed, further reducing the expansion ratio.

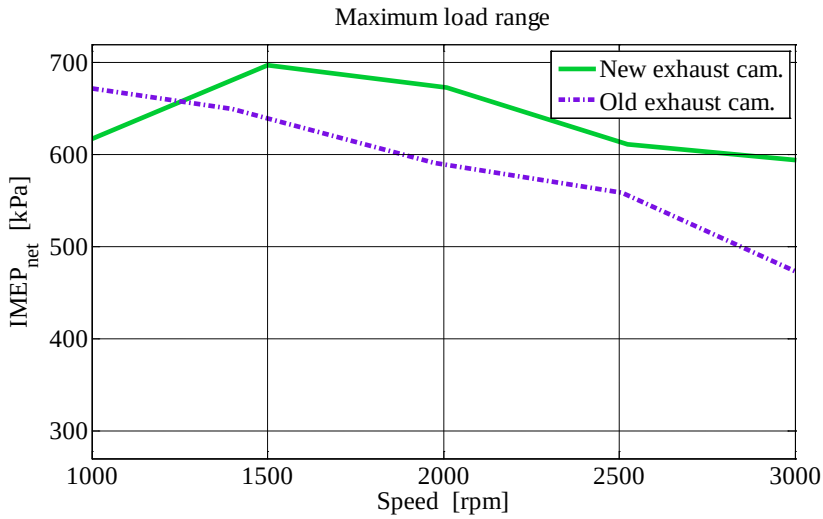

Figure 72: Improvement in maximum operating range

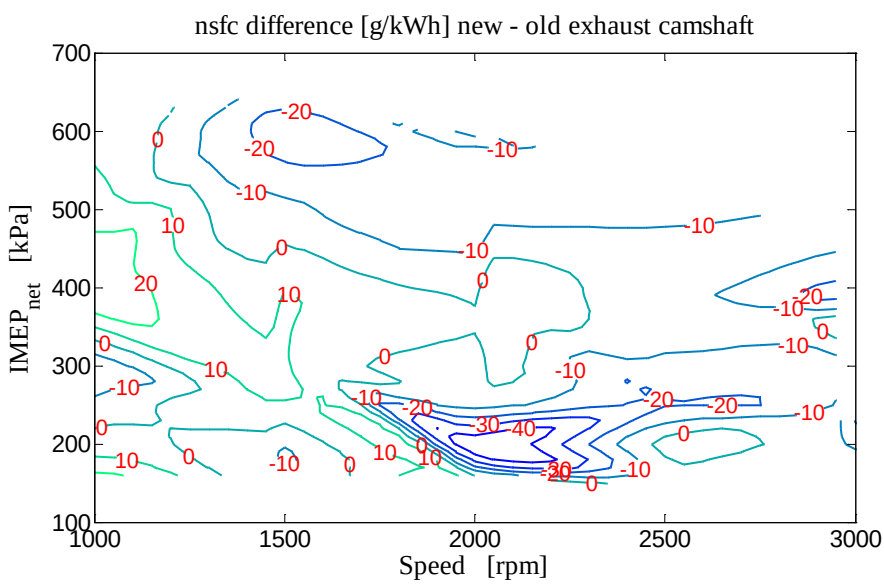

Figure 73: Difference in fuel consumption with the new exhaust camshaft

6.4.2 Turbocharger Modification

The limitation for the KP31 turbocharger was apparent at 3000 rpm and high load where the turbine became choked i.e. the backpressure rose without any increase in boost pressure. This increase of pumping losses reduced the maximum load.

In an effort to reduce the high backpressure at high engine speed, the turbine housing was modified with shortcut holes as seen in Figure 74. The idea behind this was to divert some of the exhaust flow directly to the turbine but still use some of the kinetic energy of this diverted flow when losing expansion work. In tests with these drilled shortcut holes, the backpressure reduced 10 to 20 kPa together with the boost pressure. In the end there was only some small gain in turbocharger efficiency at high rpm, at lower rpm it was worse.

This test gave the author the idea for a new wastegate solution. A normal wastegate consists of many parts, a sealing valve, a leverage arm, sealed spring-loaded pressure chamber, meaning a rather high manufacturing costs. With this valve type of wastegate there can be some sealing issues as well.

Since the proposed solution only uses one part, a shaft with some holes drilled through, this should reduce the manufacturing costs significantly. The sealing should be improved as well and the obvious problem of galling could be avoided by using a ceramic shaft. This is proposed as a simple, cheap and leak free solution for turbocharger manufactures that can be servo actuated instead of pressure actuated.

Figure 74: Proposed wastegate solution

6.5 Intake Temperature Effect

The combustion timing in an NVO HCCI engine is mainly controlled by the EVC timing. The combustion timing in turbocharged HCCI mode is even more important due to the direct influence it has on boost pressure and therefore the intake temperature. A late combustion timing will increase the available exhaust enthalpy for the exhaust turbine leading to higher boost pressure. When the intake temperature is increased it can be cooled to a chosen level. The results for the combustion timing and chosen intake temperature are presented at different engine speeds and loads. The presented results are; intake pressure, RI, NOx emissions and nsfc.

6.5.1 Different Load and Engine Speed

These graphs represent the possible CA50 timing and intake temperature with a fixed IVO timing at 86 °aTDC_{GE}. Even if it is possible to operate this turbocharged HCCI engine at a higher load, this is unsuitable for a wide CA50 variation due to the small operation window between very high RI and misfire. The maximum temperature is without charge cooling and the lowest intake temperature is with maximum charge cooling.

Since the VVT adjustment is limited to 50 CAD, the outer limits can be reached at some operating point. The low limit for the cooling of intake temperature is set to 40°C, since this minimum level is expected for a real application. When the intake pressure is in the region of 200 kPa the turbine starts to get choked, leading to increasing pumping losses. When the pumping losses increase there is a need to burn more fuel to keep the load constant, leading to even higher pumping losses and therefore it is not possible to broaden the operating range.

As can be seen in the graphs the variation in intake pressure can be very high for a given operating point, up to more than 50 kPa. The achievable boost pressure is directly connected to both the combustion timing and the intake temperature.

The intake pressure at 2000 rpm and 360 kPa $IMEP_{net}$ scales both to the CA50 timing and intake temperature, Figure 75, while the RI scales to the CA50 timing, see Figure 76. At this relatively low load the NOx level in Figure 77 is below our NOx limit at 1 g/kg_{fuel} and it scales with the intake pressure. The best fuel efficiency is found with an intake temperature of 55°C and CA50 timing of 5 degrees, see Figure 78. It can be seen how precise the operating conditions have to be for best fuel efficiency. Notable is also that it is not possible to delay the CA50 timing to more than 8 degrees in this turbocharged setup to avoid misfires.

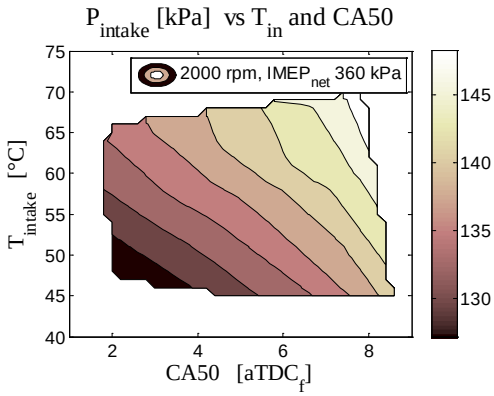

Figure 75: Intake pressure, P_{in}

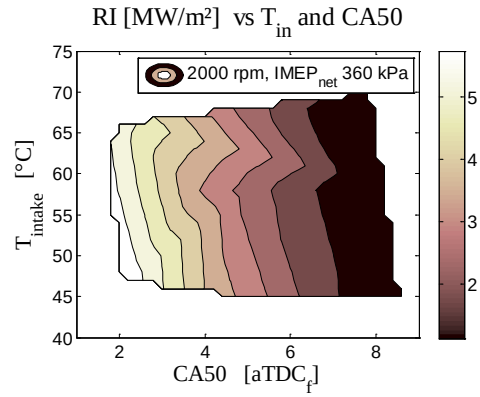

Figure 76: Combustion noise, RI

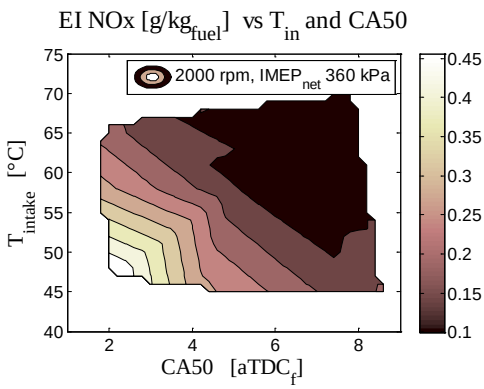

Figure 77: Nitrogen oxides emission, EI NOx

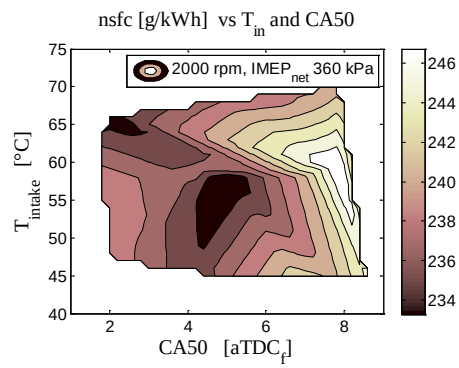

Figure 78: Fuel consumption, nsfc

The results at 2000 rpm and 420 kPa $IMEP_{net}$ are quite similar to the 360 kPa load point, except RI now limits the usable CA50 timings to just a few degrees, see Figure 79. The RI scales to CA50 timing and is limiting the operating range after 5 degrees, see Figure 80. The worst fuel consumption, Figure 82, is now found with intake temperatures near 60 degrees due to slightly reduced thermodynamic efficiency.

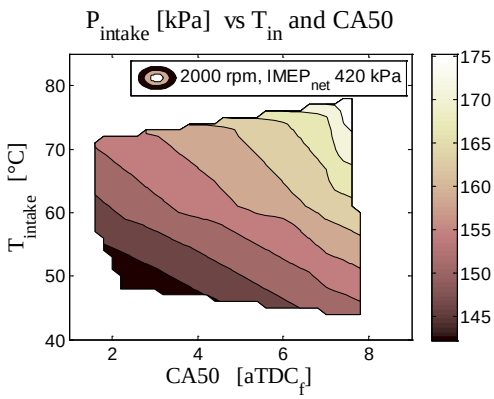

Figure 79: Intake pressure, P_{in}

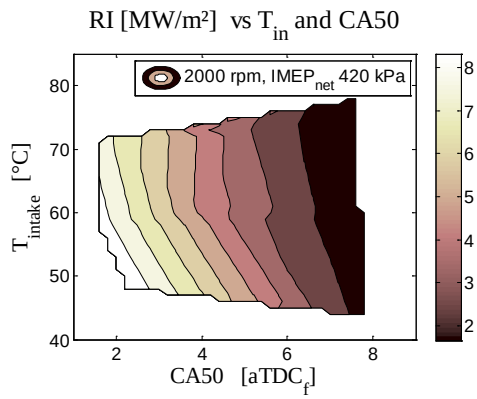

Figure 80: Combustion noise, RI

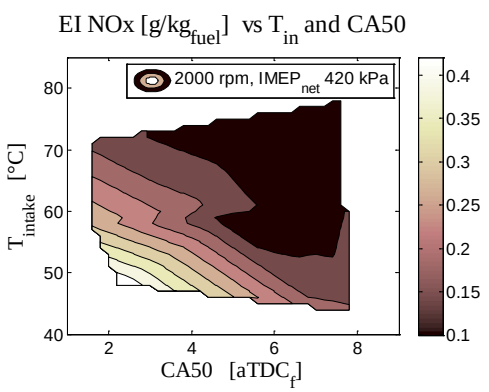

Figure 81: Nitrogen oxides emission, EI NOx

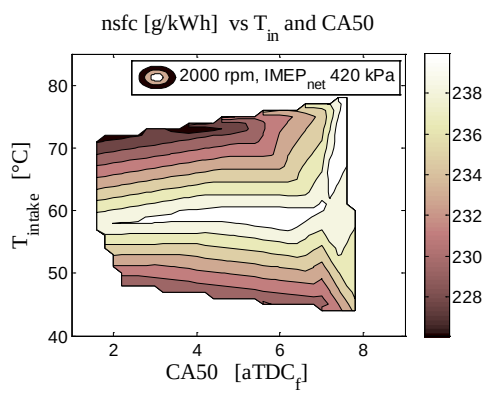

Figure 82: Fuel consumption, nsfc

When the load is increased up to 500 kPa, the high intake pressure is near the maximum available with this turbocharger, see Figure 83. The window for the CA50 timing with allowable RI is now down to just one degree, see Figure 84. The NOx in emission in Figure 85, at this relative high load is below the limit due to the high intake pressure,. The best fuel consumption is at low intake temperatures due to the reduced pumping losses, see Figure 86.

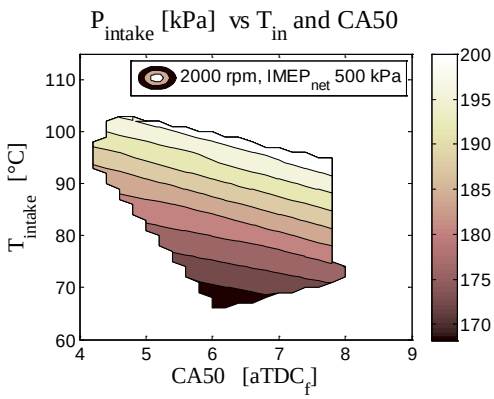

Figure 83: Intake pressure, P_{in}

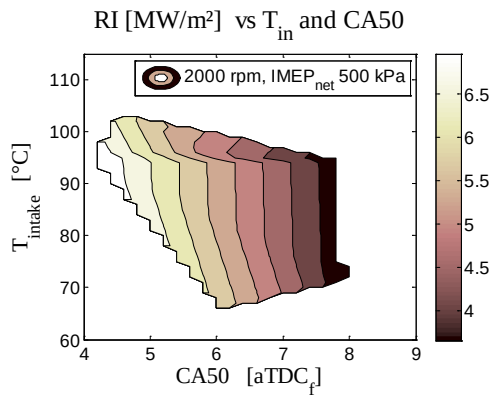

Figure 84: Combustion noise, RI

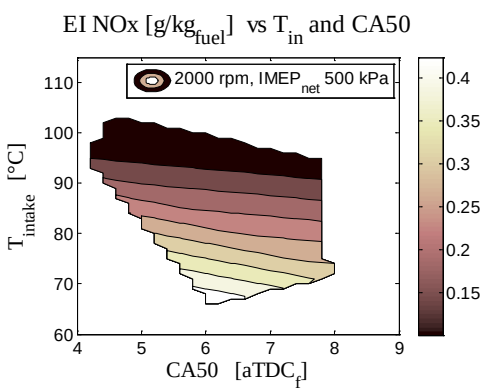

Figure 85: Nitrogen oxides emission, EI NOx

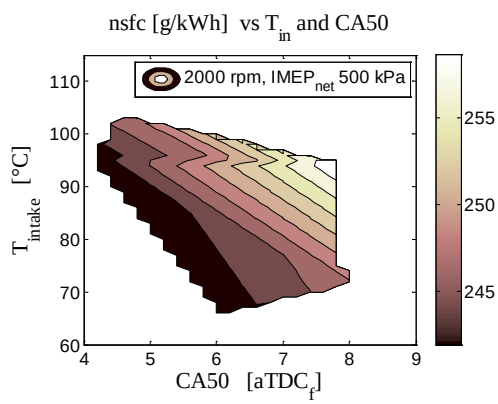

Figure 86: Fuel consumption, nsfc

At 2500 rpm and 300 kPa $IMEP_{net}$ the intake pressure, RI and NOx are not limiting the operating range (Figure 87, Figure 88, Figure 89). The highest fuel efficiency is found with either low or high intake temperature, see Figure 90.

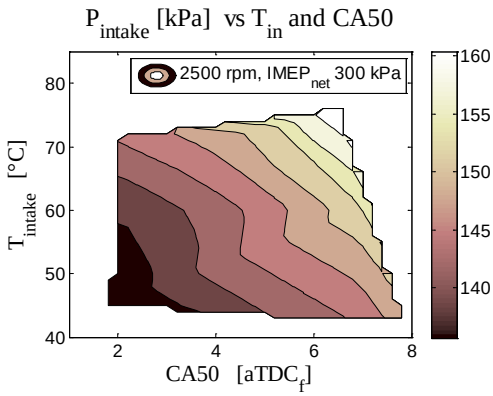

Figure 87: Intake pressure, P_{in}

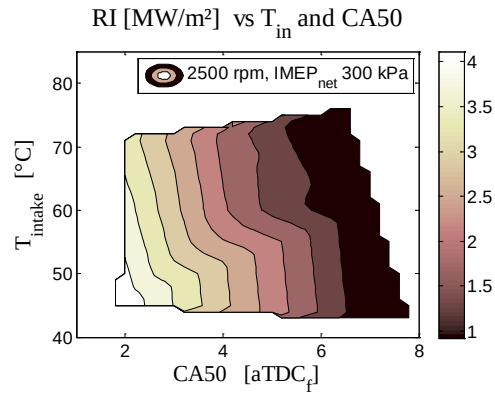

Figure 88: Combustion noise, RI

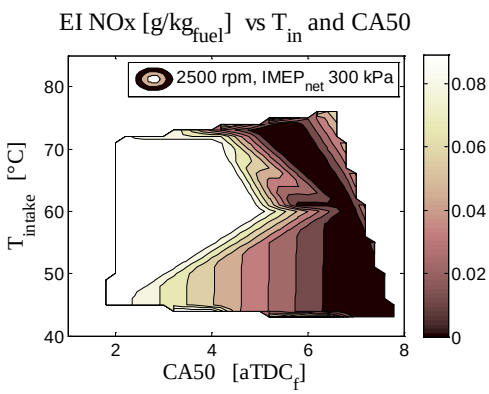

Figure 89: Nitrogen oxides emission, EI NOx

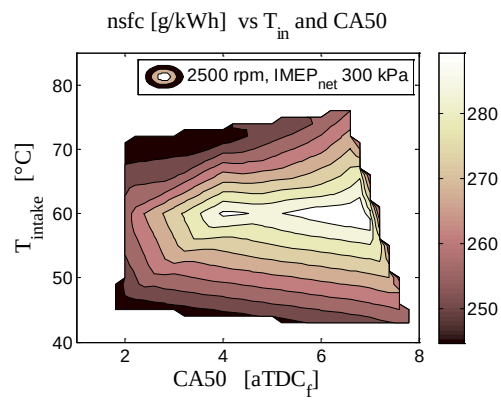

Figure 90: Fuel consumption, nsfc

At 2500 rpm and 360 kPa $IMEP_{net}$ there is substantial difference in the intake pressure dependence on CA50 timing and intake temperature as seen in Figure 91. The RI limit is reached only at the most advanced CA50 timings, see Figure 92. NOx is extremely low here, see Figure 93, and is below 5 ppm in these results. The fuel efficiency, in Figure 94, is now strongly influenced by the pumping losses at higher intake temperatures and the lowest fuel consumption is found with low intake temperatures.

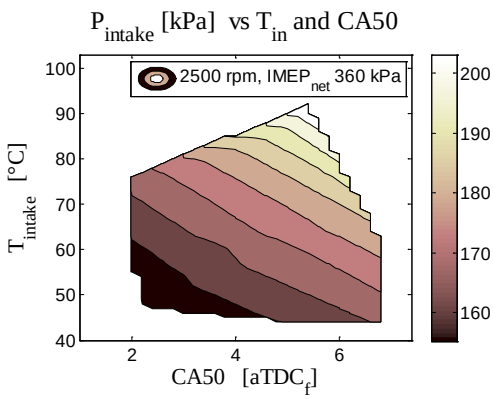

Figure 91: Intake pressure, P_{in}

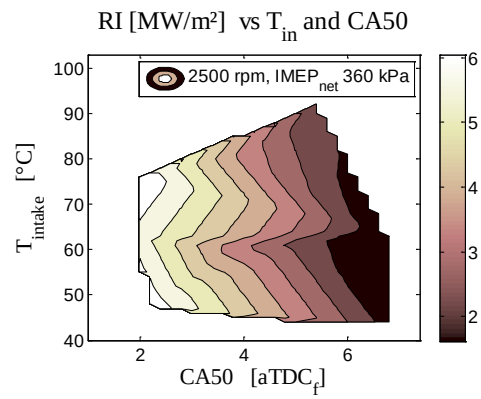

Figure 92: Combustion noise, RI

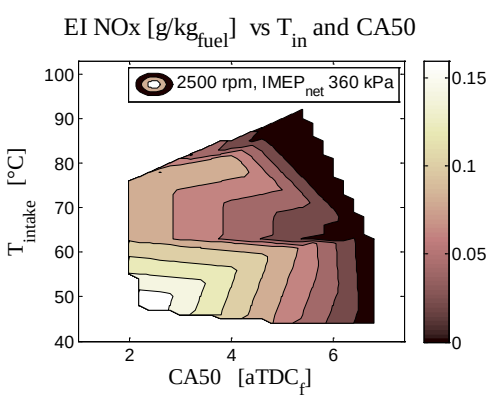

Figure 93: Nitrogen oxides emission, EI NOx

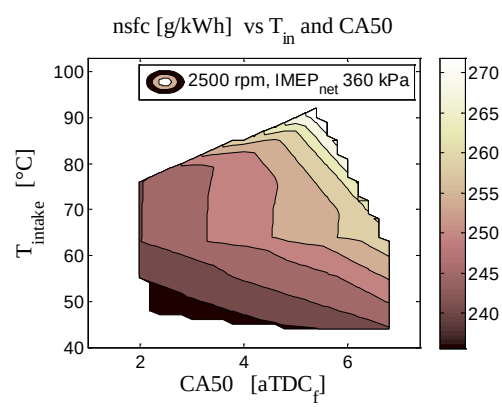

Figure 94: Fuel consumption, nsfc

At 2500 rpm and 500 kPa $IMEP_{net}$ the turbine is more or less choked and the CA50 timing or the intake temperature have a reduced influence on the intake pressure, see Figure 95. Due to the choked turbine it was not possible to test with any higher temperatures. The RI scales to the combustion timing, se Figure 96. The NOx emissions are hardly measurable at this engine test point as seen in Figure 97. The best fuel efficiency is found when the pumping losses are reduced, at low intake temperatures, Figure 98.

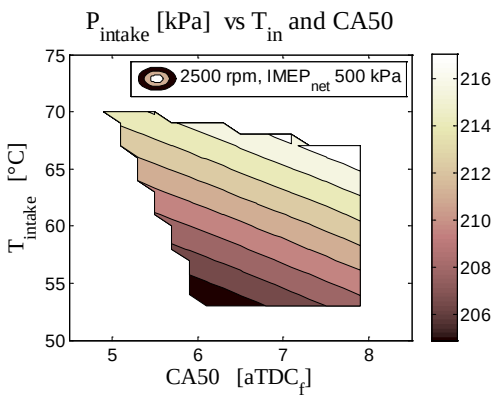

Figure 95: Intake pressure, P_{in}

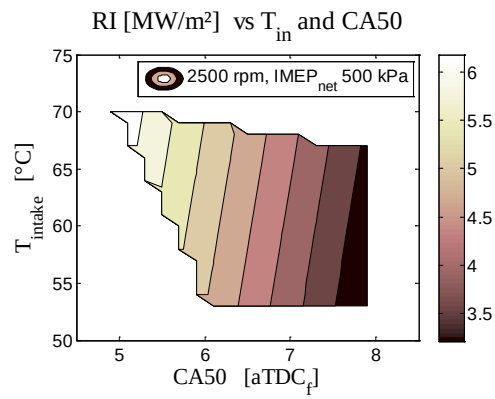

Figure 96: Combustion noise, RI

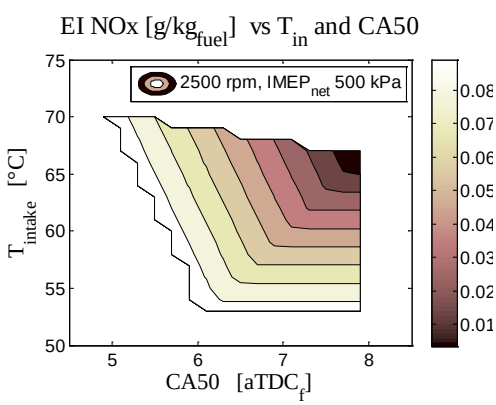

Figure 97: Nitrogen oxides emission, EI NOx

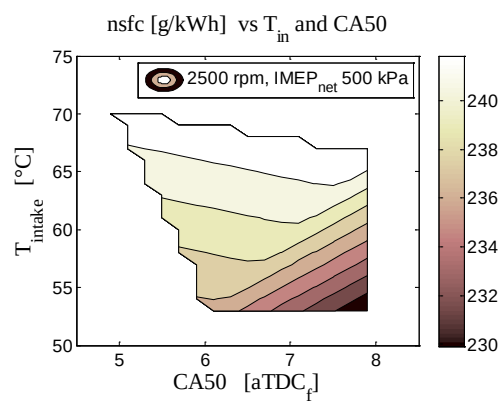

Figure 98: Fuel consumption, nsfc

From these graphs it can be seen that for this kind of turbocharged HCCI, the real operation window depends on load and engine speed and the combustion timing range can be just a few degrees. The intake pressure is increased with higher intake temperature and delayed combustion timings due to increased mass flow with delayed EVC timings. The NOx emissions are seldom any problem when there is boost pressure and NOx levels below the limit in all shown load points. The operating point for lowest fuel consumption varies in these examples, this is due to differences in pumping losses, thermodynamic efficiency and expansion ratio.

6.5.2 Symmetrical and Asymmetrical Valve Timing

In the previous section IVO was held at latest possible position at 86 °aTDC_{GE} to maximize the intake pressure in order to provide the highest possible intake temperature. The question is then, how will symmetrical IVO and external EGR influence the results?

In Figure 99, there is a comparison of symmetrical and asymmetrical valve timings, with and without long route EGR. These results are from 2250 rpm and $IMEP_{net}$ at 400 kPa. The intake temperature is 60 °C and the 125° duration exhaust camshaft is used. This operating point is chosen due to the wide variation of intake pressure and CA50 timings that is possible here. It is also shown in Paper IV that this is a preferred intake temperature at this operating point.

Symmetrical valve timings and EGR leads to a reduction of the intake pressure due to decreased mass flow. Since the intake temperature is constant, the reduced in-cylinder pressure with symmetrical valve timings means that the effective compression is reduced, lowering the temperature at ignition and therefore more internal EGR is needed for a given combustion timing.

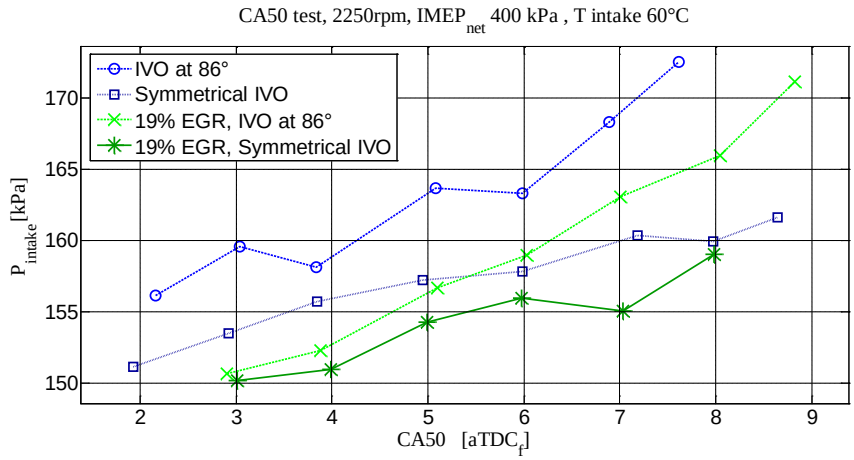

Figure 99: Intake pressure, P_{intake}

As a direct result of increasing intake pressure, the pumping losses increase, as seen in Figure 100. At this operating point the pumping losses depend on the pressure loss over the engine, see Figure 101. The throttling losses are not influenced to the same extent by the used valve timings and EGR at this operating point, as seen in Figure 102.

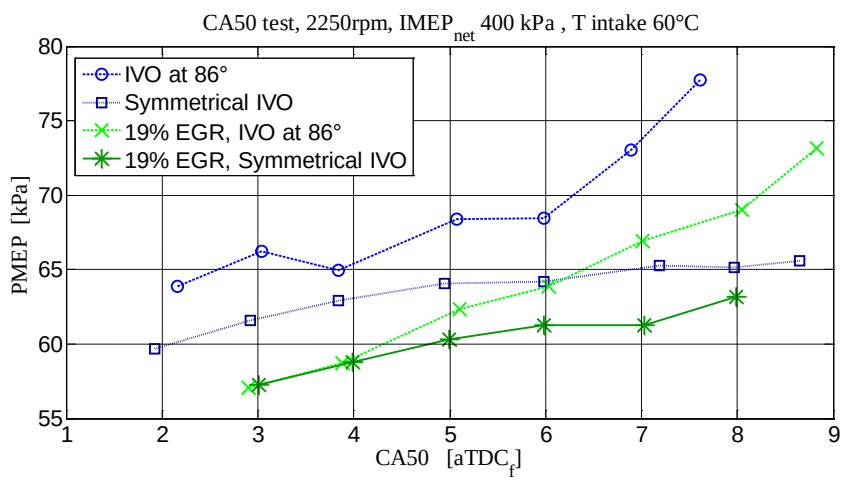

Figure 100: Pumping losses, PMEP

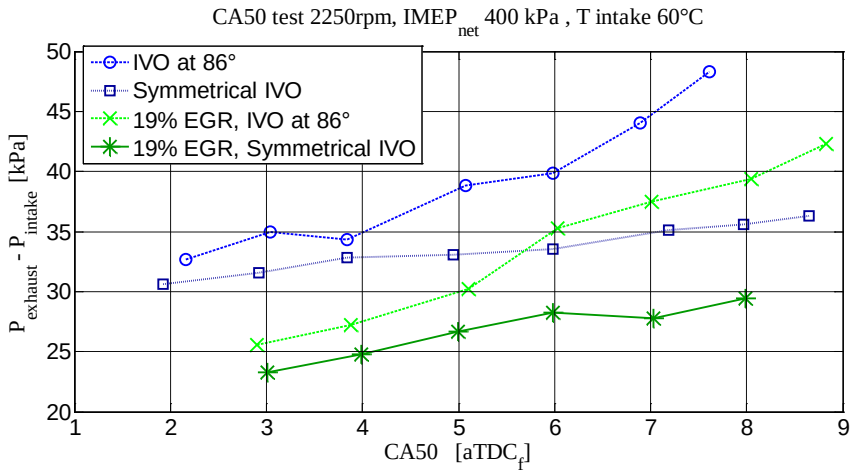

Figure 101: Pressure loss over engine, $P_{exhaust}$ - P_{intake}

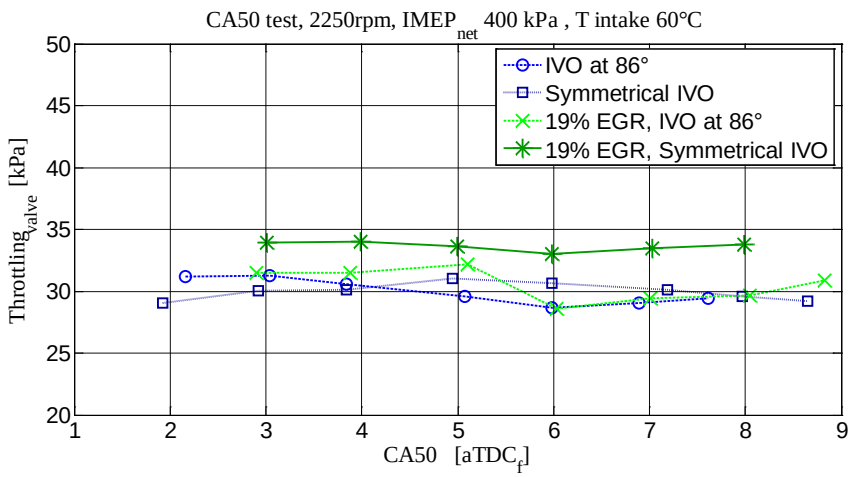

Figure 102: Valve throttling losses

The resulting combustion noise, RI, is highest for the symmetrical case without EGR as seen in Figure 103. With EGR the intake pressure is reduced but still the RI level is the same as for the asymmetrical case without EGR. The explanation to this is seen in Figure 104, where the combustion duration, CA10 to CA90, is slightly increased with addition of EGR

.

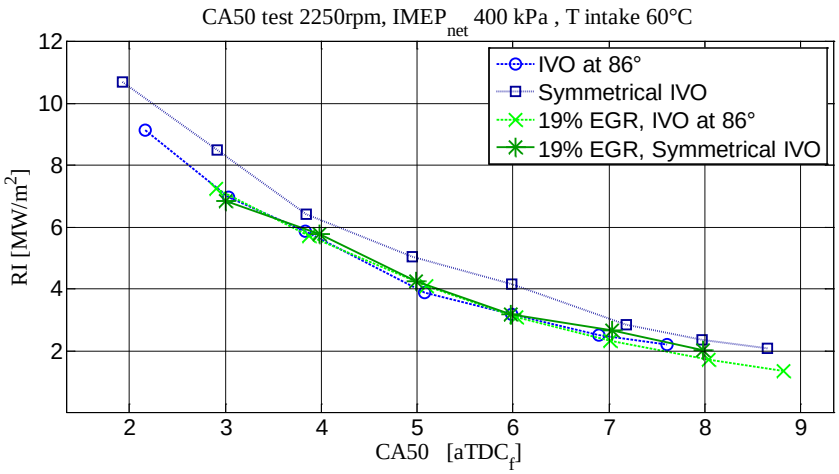

Figure 103: Combustion noise, RI

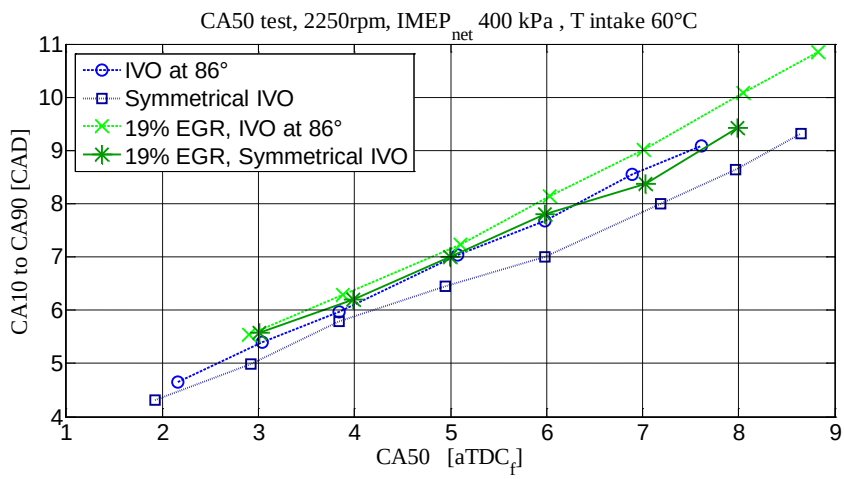

Figure 104: Combustion duration, CA10 to CA90

The combustion stability is normally viewed as CoV of $IMEP_{net}$, as in Figure 105. The combustion seems most stable at a CA50 timing of 4 to 5 degrees and the addition of EGR improves the combustion stability. By complementing the CoV of IMEP with the STD of CA50, more information on combustion stability is given in Figure 106. Now the combustion seems even more stable with the addition of external EGR due to higher internal EGR content. It was found in Paper IV that STD of CA50 complement CoV of IMEP at certain operating conditions since the CoV of IMEP does not always give enough information about the combustion stability.

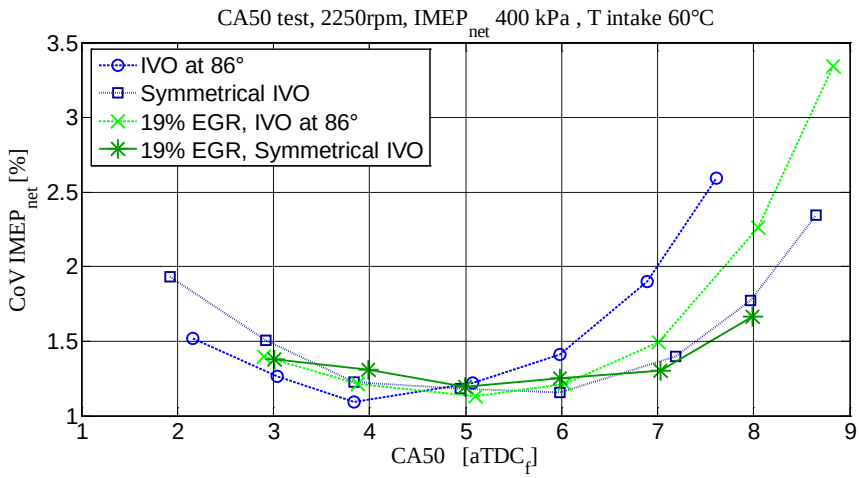

Figure 105: Combustion stability, CoV

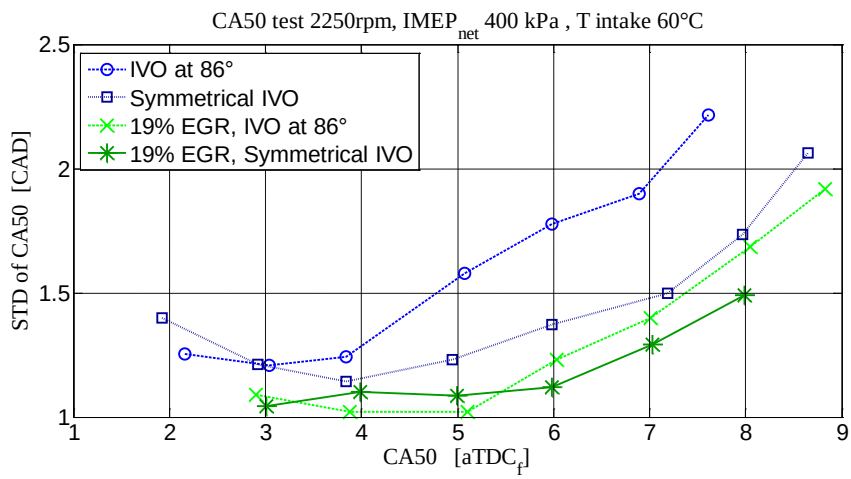

Figure 106: Standard deviation of CA50, STD

The NOx emissions are below the limit as seen in Figure 107, and decrease with delayed CA50 timing except for the asymmetrical case without EGR, where the higher CA50 deviation leads to increasing NOx emissions. The HC emissions in this turbocharged DI setup are generally low as seen in the figure. It is believed that the applied injection strategy minimize the crevice losses.

Finally, Figure 108 shows the efficiency breakdown for these results. The combustion efficiency decreases slightly with delayed CA50 timing. The thermal efficiency is highest for the symmetrical case without EGR due to higher specific heat ratio and higher expansion ratio since the EVC timing and therefore the EVO timing is delayed compared to the other examples. The gas exchange efficiency is directly connected to the intake pressure as seen in the graph. The resulting indicated efficiency shows quite even results for all examples and the case with symmetrical valve timings and 19% EGR has low combustion noise and high efficiency in a wide CA50 range.

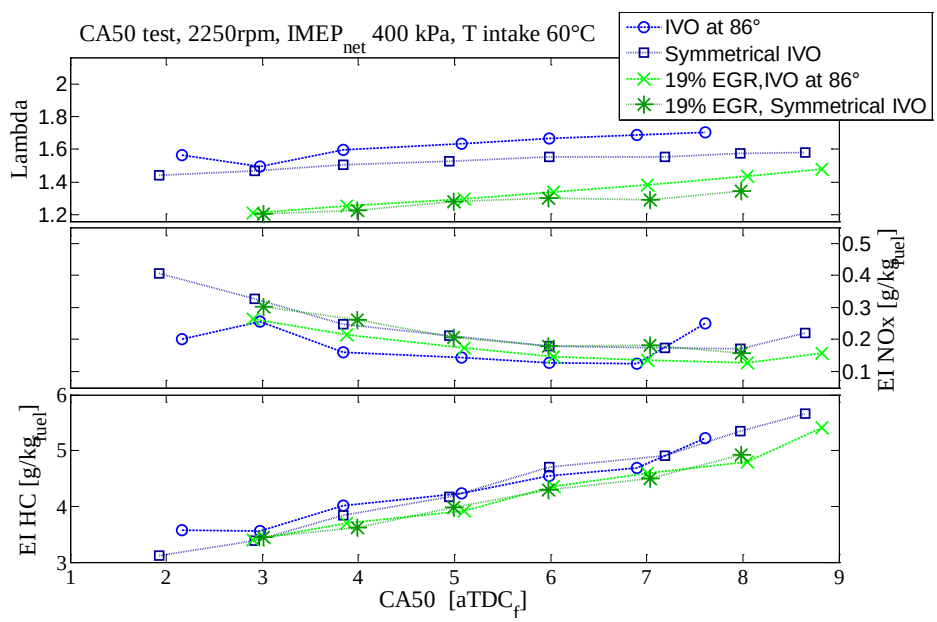

Figure 107: Lambda, NOx and HC emissions

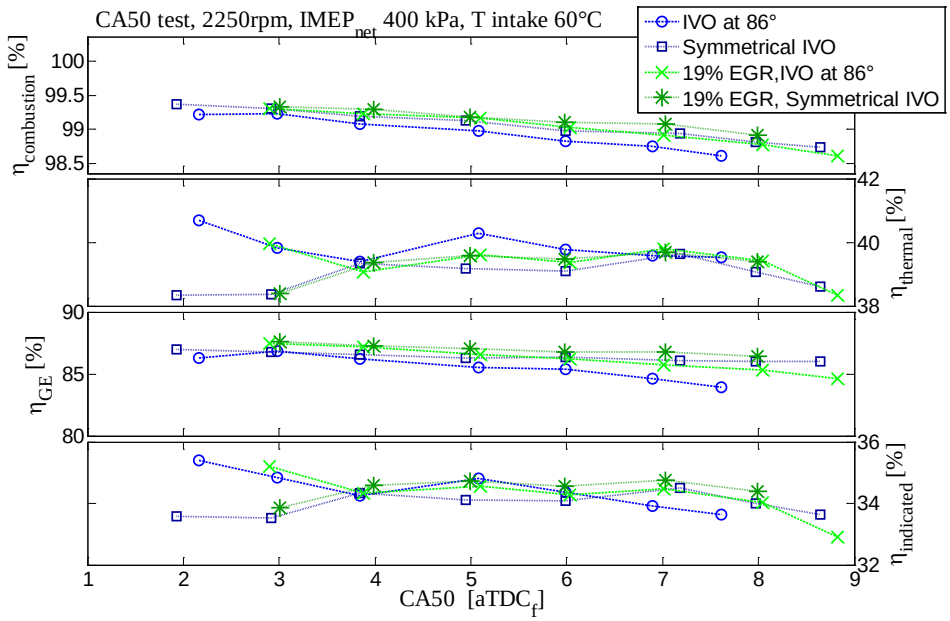

Figure 108: Efficiency breakdown

In these results the intake temperature was held constant at 60°C. In Figure 109, the resulting fuel efficiency and RI from other intake temperatures are shown. The intake temperature is set at 50, 70 and 90 °C, with both symmetrical and asymmetrical valve timings and the resulting fuel efficiency and RI vary substantially. When the intake temperature is 90 °C with asymmetrical valve timings the increased turbocharger backpressure limits the available CA50 range and the fuel efficiency is reduced.

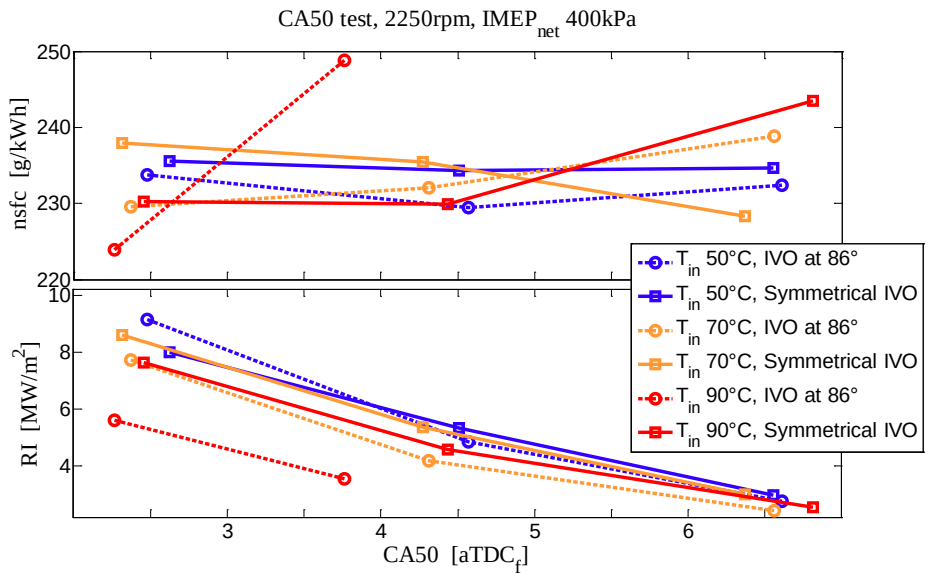

Figure 109: Fuel consumption and combustion noise with different intake temperatures and valve strategies

6.5.3 Discussion

When operating a turbocharged HCCI engine with NVO, the extra freedom to adjust the intake temperature is attractive from a combustion perspective to be able to operate the engine at the most beneficial setting. For example, if the pressure rise rate is high, a high intake pressure is needed. Choosing a higher intake temperature leads to higher intake pressure and the combustion noise can be reduced. However, this has to be weighted against any increasing pumping losses with associated reduction in fuel efficiency.

When the intake pressure is too high it can result in loss of turbocharger performance. This was the case at 90 °C where the increasing backpressure limited the available combustion timing range. This can be circumvented by appropriate intake valve timings. A shrinking combustion timing range puts even higher demands on the control system, especially during transients where a broad combustion timing range is desired.

The loss of combustion stability is not really obvious when only using the CoV of IMEP as an indicator. The STD of CA50 visualizes the combustion stability more clearly. The combustion timing range and stability can be increased by using external EGR. The combustion timing is the major variable during these tests, it directly controls the dilution level and what intake temperature level can be reached. This gives the combustion timing a huge impact on test results in turbocharged

HCCI mode. This further emphasizes the importance of robust combustion timing control.

To find the optimum intake temperature and combustion timing, one has to balance factors like: pressure rise rate, efficiency, combustion stability and range plus the emissions level, against each other.

6.6 HCCI Simulation

In an engine simulation program it is possible to evaluate how different operating settings and hardware changes influence the results. To improve the operating range or fuel efficiency, it is possible to virtually test many combinations in an effective way compared to real engine experiments.

When setting up an engine model in a simulating program it is advisable to build a detailed model of the engine. In Figure 110, the GT-Power model for the turbocharged HCCI engine is shown. In this model the long route EGR system is included with controllers for EGR recirculation and backpressure. The issue with this detailed layout comes from the long simulation time to get the results to converge, for example this model takes 45 minutes until the results have converged to within 2%, using three 2,1 GHz CPU:s.

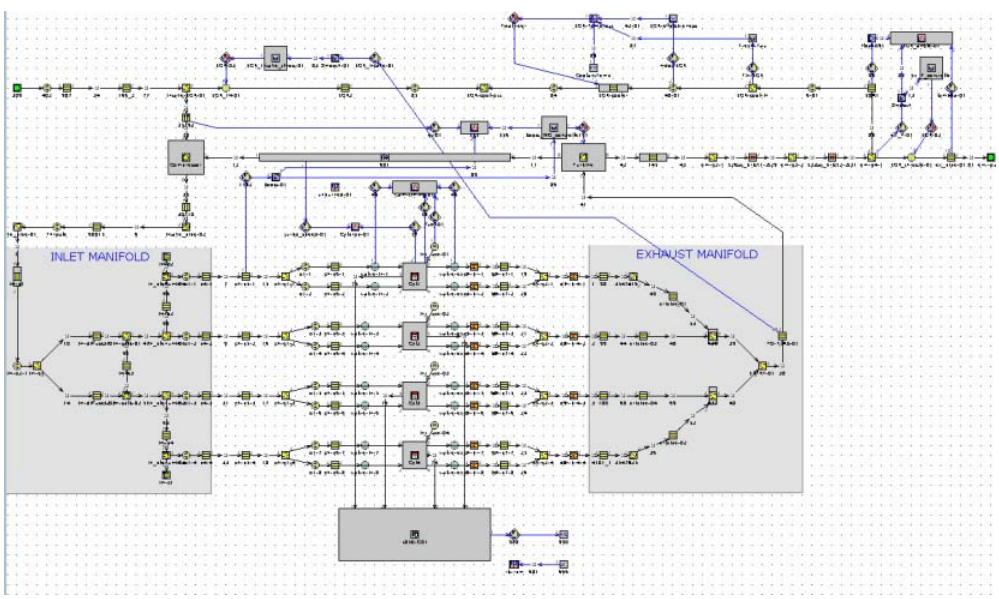

Figure 110: GT-Power turbocharged HCCI model

6.6.1 Simulation of Exhaust Valve Timing and Result

When experimental data are available it might be possible to simplify the engine model and feed the model with combustion data and other boundary conditions to speed up the calculation time. The model in Figure 111 was used to evaluate different valve durations and lifts before the real camshaft was made, see Figure 64 to Figure 67. The simulation time was only a couple of minutes, and it is possible to do a full factorial Design of Experiments (DOE) analysis in a couple of hours instead of days with this simplified GT-Power model, compared to the full GT-Power model in Figure 110.

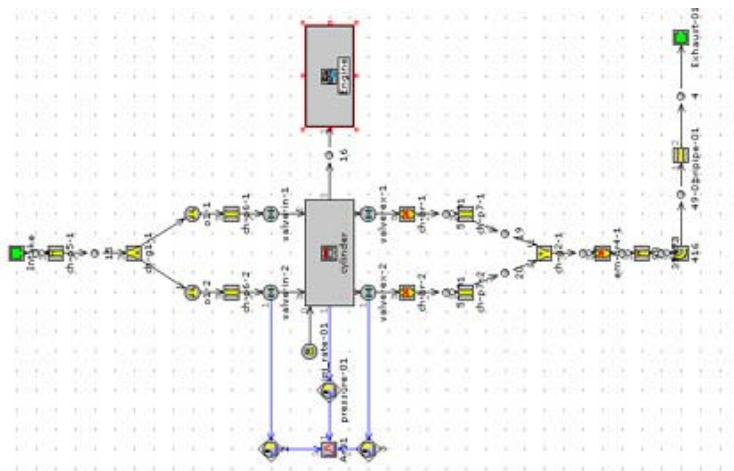

Figure 111: GT-Power simplified HCCI model

When analyzing the turbocharger performance, a more complete model is needed to predict the turbocharger performance. This was also done in an effort to improve the KP31 turbocharger to avoid the turbine choking at high mass flows. In Figure 112 and Figure 113, the results from the KP31 turbocharger with current turbine, a larger turbine, short and long duration exhaust valve timing with 4 and 5 mm valve lifts, are compared to a TD02 turbocharger with different turbine sizes and exhaust valve timings. From the results, the combination with the highest possible intake pressure and the lowest pumping losses was the KP31 turbocharger together with the long duration exhaust valve timing.

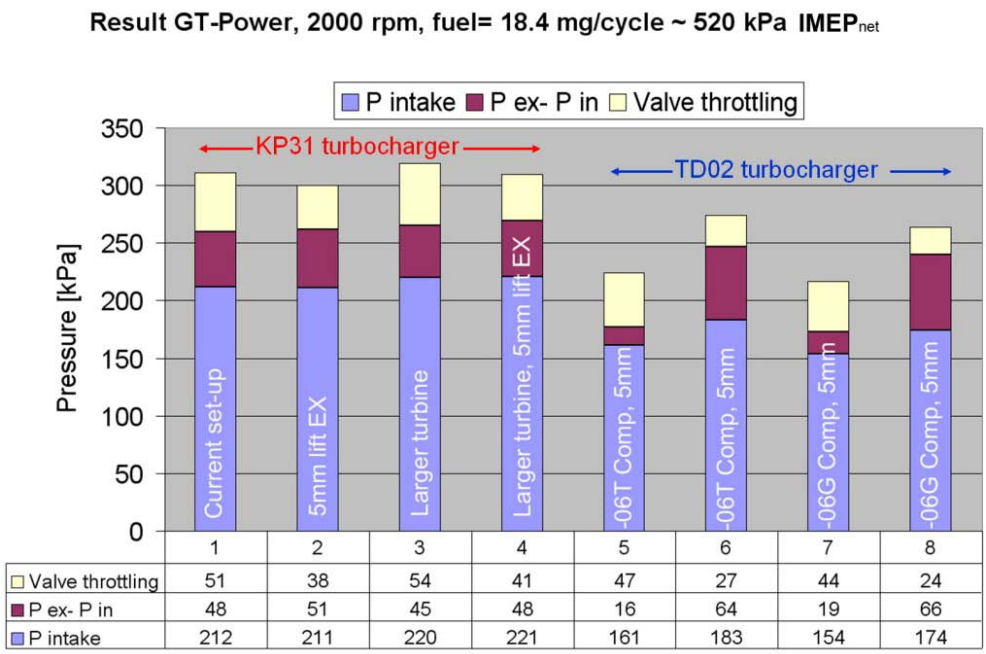

	1	2	3	4	5	6	7	8
Valve throttling	51	38	54	41	47	27	44	24
P ex- P in	48	51	45	48	16	64	19	66
P intake	212	211	220	221	161	183	154	174

Figure 112: GT-Power turbocharger and valve timing simulation

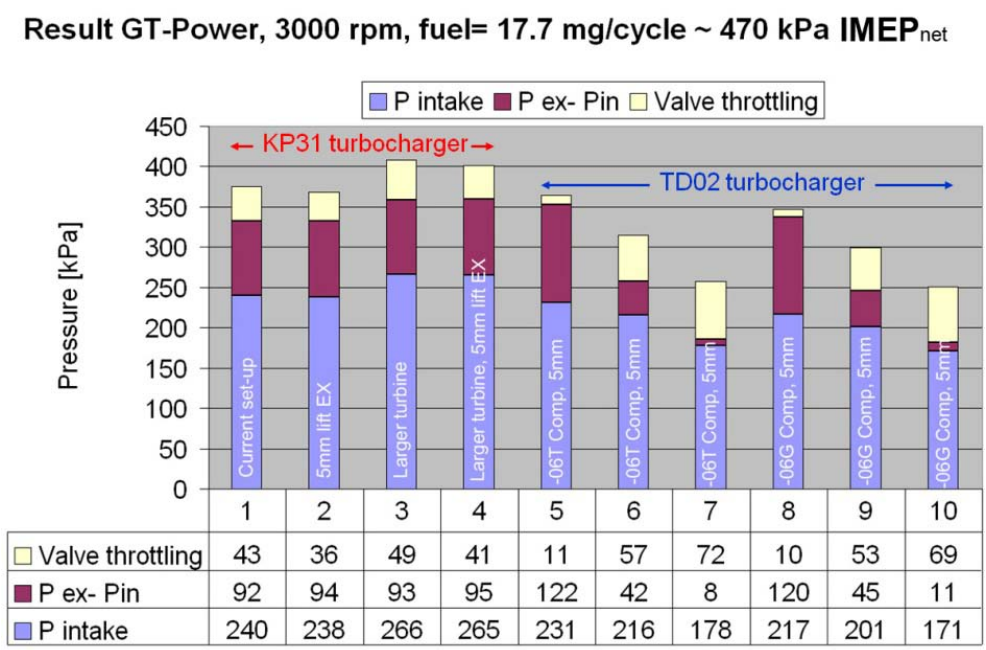

	1	2	3	4	5	6	7	8	9	10
Valve throttling	43	36	49	41	11	57	72	10	53	69
P ex- Pin	92	94	93	95	122	42	8	120	45	11
P intake	240	238	266	265	231	216	178	217	201	171

Figure 113: GT-Power turbocharger and valve timing simulation

The compressor efficiency contours from GT-Power simulation, for two of the turbocharger combinations are seen in Figure 114 and Figure 115. The arrows points to the simulated operating point. It can be seen that the operating location for the KP31 is near the highest compressor efficiency, whereas for the TD02, it is at a reduced efficiency, near the surge line.

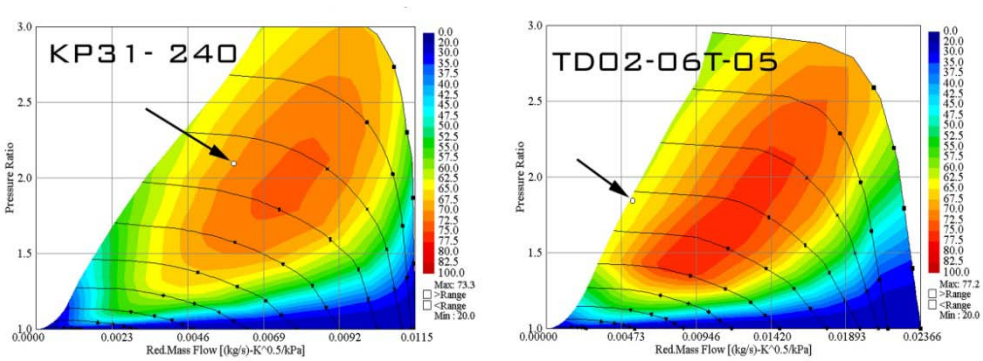

Figure 114: Compressor efficiency contours at 2000 rpm, $IMEP_{net}$ 520 kPa

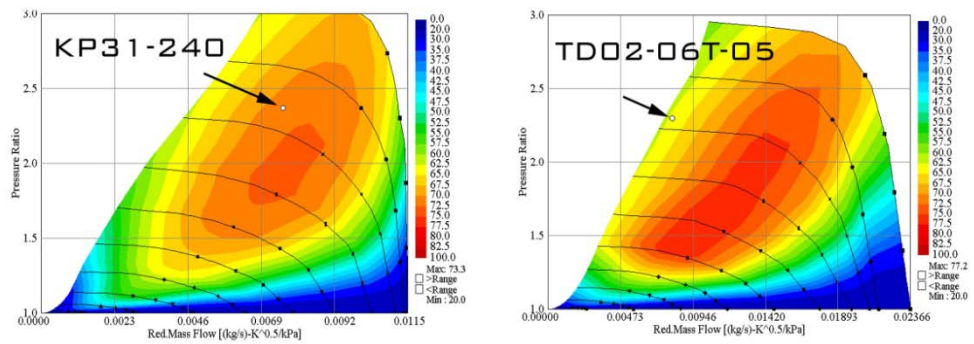

Figure 115: Compressor efficiency contours at 3000 rpm, $IMEP_{net}$ 470 kPa

In experimental tests with the new exhaust camshaft it was revealed that the intake pressure was slightly reduced, compared to the old exhaust camshaft, see Figure 116. At this operating point the boost pressure was reduced up to 5 kPa. This was not identified during the engine simulations shown above since the EVC timing was set to the experimental value. With the new exhaust camshaft, the EVC timing had to be further advanced, compared to the old camshaft, see Figure 117.

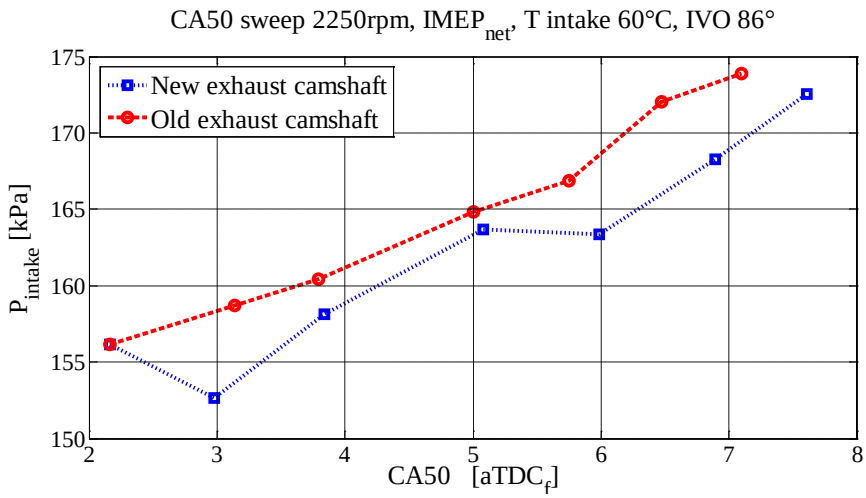

Figure 116: Intake pressure from the two exhaust camshafts

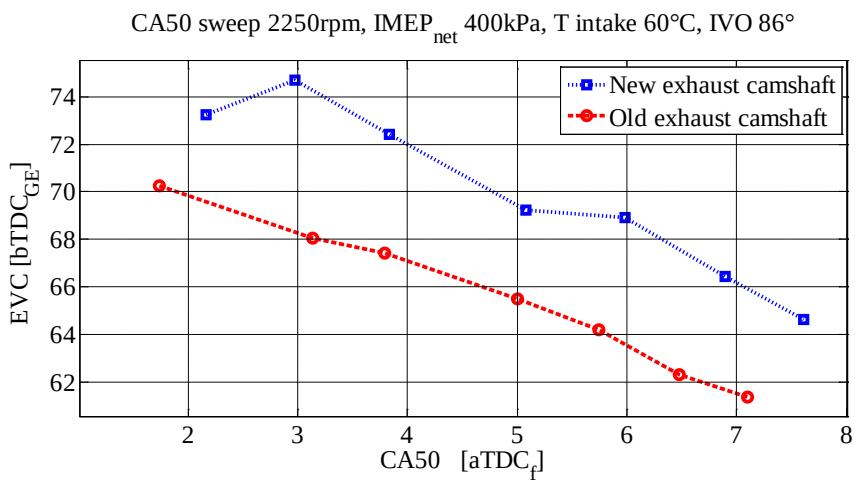

Figure 117: EVC timing from the two exhaust camshafts

The resulting cylinder pressure from the two exhaust camshafts was post-processed in GT-Power at a CA50 timing of 6 degrees, see Figure 118. This showed that the exhaust pressure is reduced at EVC for the new exhaust camshaft leading to an advanced EVC timing compared to the old camshaft. This will reduce the mass flow for the new camshaft, leading to a lower intake pressure.

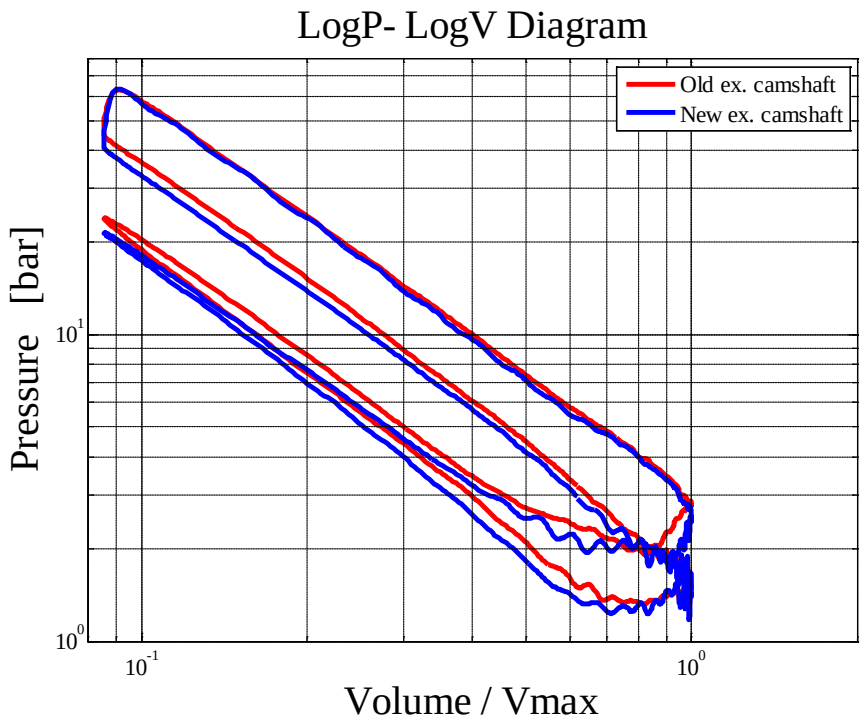

Figure 118: P-V diagram from measured cylinder pressure at 2250 rpm, $IMEP_{net}$ 400 kPa, CA50 at 6 °aTDC_f

6.6.2 Exhaust Valve Closing Timing

In engine simulation of HCCI it is important to set the correct EVC timing, especially if the engine is turbocharged. The EVC position controls the combustion timing, and at the same time it influences the mass flow through the engine.

In simulations it is advisable to have the temperature at TDC as a boundary condition for controlling the EVC position. From the experimental tests, the calculated temperatures at intake valve closing (T_{IVC}) are seen in Figure 119. The temperature is calculated from exhaust -pressure, -temperature and lambda, intake -pressure, -temperature and external EGR level, the fuel flow and its vaporization effect together with a Woschni [95] heat transfer model. In this calculation, the T_{IVC} variation is almost 100 degrees in the operating area.

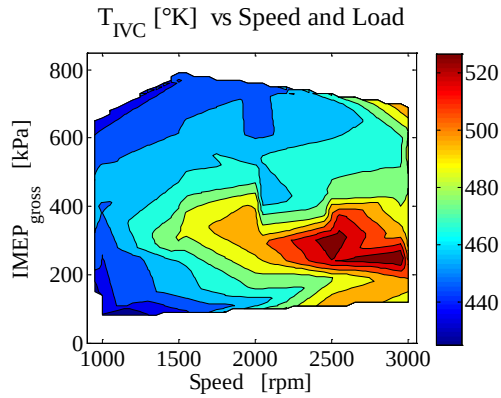

Figure 119: Temperature at intake valve closing

The temperature at IVC starts by calculating the exhaust density at EVC. The main components in exhaust gases is CO_2, N_2 and H_2O. In Figure 120 it is shown how the densities of these species vary with temperature at atmospheric pressure [101].

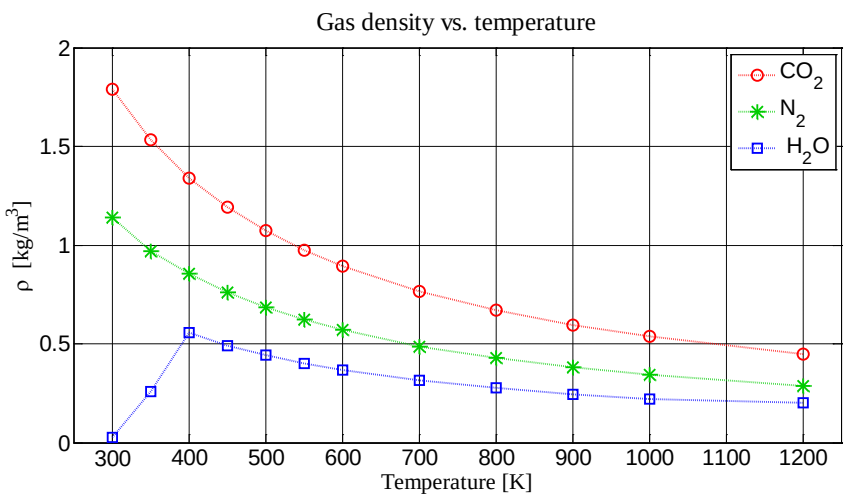

Figure 120: Exhaust species density

The stoichiometric, λ=1, combustion for iso-octane [22] becomes:

$$C_8H_{18} + 12{,}5(O_2+3.773N_2) = 8CO_2 + 9\,H_2O + 47.16\,N_2 \qquad (6.4)$$

Leading to the following mass fraction: CO_2 to 19.1 %, H_20 to 8.8 % and N_2 to 72.1 % in a stoichiometrically burned exhaust gas with iso-octane.

The excess air in combustion when λ>1 can be separated into:

$$(\lambda - 1)\,(12.5(O_2+3.773N_2) \qquad (6.5)$$

For the unburned exhaust, the O_2 mass fraction is 23 % and N_2 at 77 %. In Figure 121, the composed density for the stoichiometrically burned exhaust gas and the unburned part is shown. The unburned exhaust gas has in this example a slightly lower density for a given temperature than the stoichiometrically burned exhaust gas.

By fitting an exponential trend line to these results, the density for the stoichiometrically burned part and unburned part are approximated respectively by:

$$\rho = 297.7T^{-0.9677} \qquad (\lambda=1) \tag{6.6}$$

$$\rho = 367.8T^{-1.0071} \qquad (\lambda > 1) \tag{6.7}$$

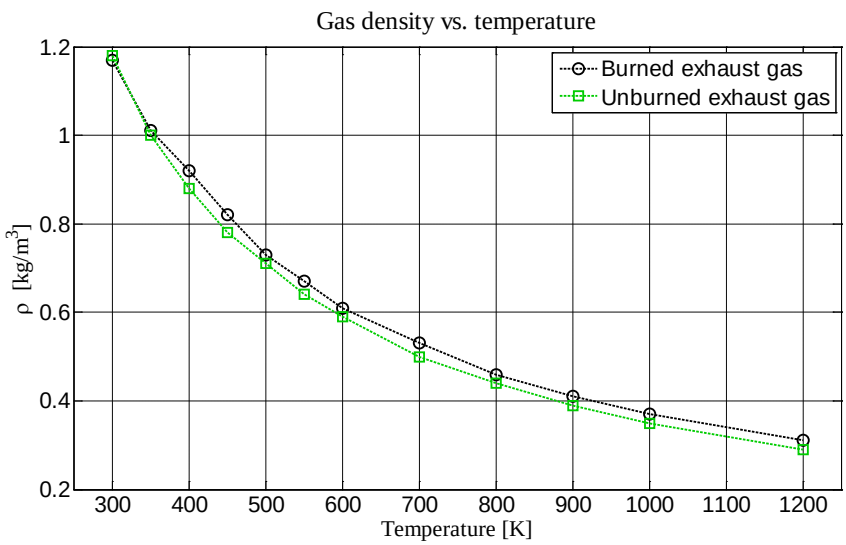

Figure 121: Burned and unburned exhaust density

The EVC timing sets the trapped exhaust volume, as visualized in Figure 122. The mass fractions of the burned ($m_{\lambda=1}$) and unburned ($m_{\lambda>1}$) exhaust gas can be estimated if the exhaust pressure and temperature is known, to get the total mass (m_{NVO}) at EVC:

$$m_{NVO} = m_{\lambda=1} + m_{\lambda>1} \tag{6.8}$$

The temperature drop is calculated from the heat loss (Q_{NVO}) during NVO with a Woschni [95] model, to get the temperature at IVO (T_{IVO}):

$$T_{IVO} = T_{ex} - \frac{Q_{NVO}}{m_{NVO} * c_p} \tag{6.9}$$

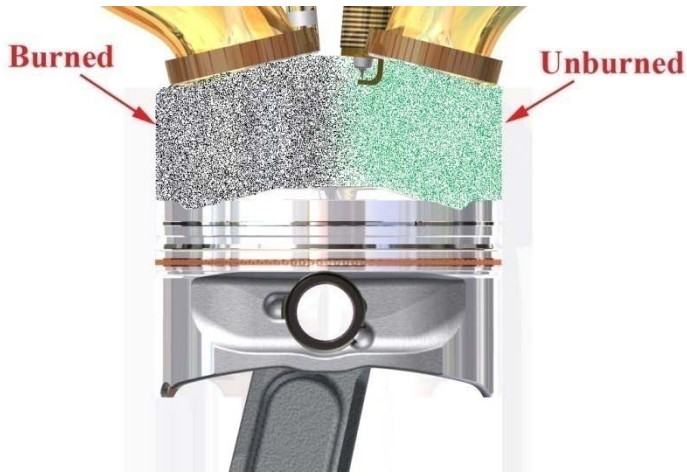

Figure 122: Exhaust gases at an EVC timing of 60 °bTDC$_{GE}$

During the intake stroke, the induced fresh air (m_{air}) can be estimated as:

$$m_{air} = m_{fuel} * \lambda \frac{A}{F_s} \quad (6.10)$$

Where m_{fuel} is the measured or predicted fuel mass per cycle, $\frac{A}{F_s}$ is the stoichiometric air/fuel ratio for the used fuel type, λ is the measured ratio of actual air/fuel ratio to stoichiometric ratio. If external EGR is used and the EGR fraction is known, the EGR mass can be estimated with:

$$m_{EGR} = m_{air} * EGR_{fraction} \quad (6.11$$

If the external EGR is lean, the excessive air is given by:

$$m_{airEGR} = m_{EGR} * \frac{\lambda - 1}{\lambda} \quad (6.12)$$

At the timing for IVC the in-cylinder composition can be estimated as visualized in Figure 123. The temperature at IVC, T_{IVC}, is determined by summarizing the relative mass fractions and their temperatures given by:

$$T_{IVC} = \frac{m_{NVO} * T_{IVO} + m_{air} * T_{air} + m_{EGR} * T_{EGR}}{m_{NVO} + m_{air} + m_{EGR}} \quad (6.13)$$

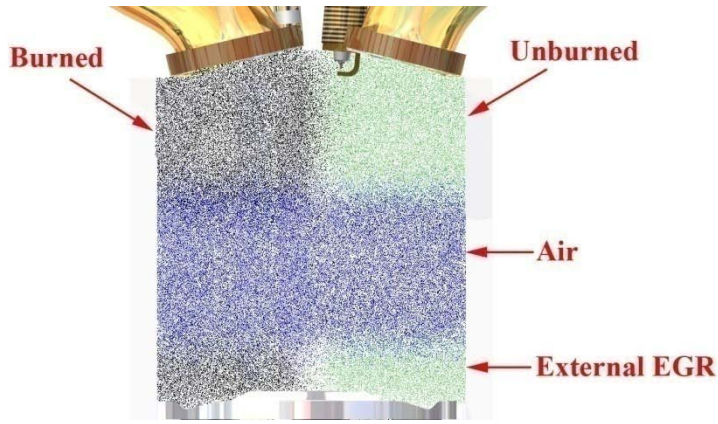

Figure 123: In-cylinder composition at BDC

The same calculation gives the burned gas fraction (x_b). In Figure 124, the calculated burned gas fraction of the experimental data is shown. By setting the specific heat ratio as a function of the burned gas fraction, the specific heat ratio varies between 1.31 and 1.36 (γ_{air} = 1.4, γ_{burned} = 1.3), see Figure 125.

By using the ideal gas law, the predicted Temperature at TDC (T_{TDC}) is calculated with heat losses during compression with the Woschni function [95]. And the fuel vaporization cooling effect is included. If no combustion is regarded, the resulting T_{TDC} is seen in Figure 126. This simplified method for estimating the temperature at TDC is normally an option for controlling the engine and it indicates that a temperature of approximately 1000 K is reached at TDC in most of the test area. This is in agreement with other results [102]. At low load, the engine has more part of the fuel injected in the NVO period for fuel reformation due to limitation in EVC range, in this high load setup. This temperature increase is not reflected in the estimated T_{TDC}. At low engine speed there is also influence from SA, and this is not included in the model for the calculated T_{TDC}.

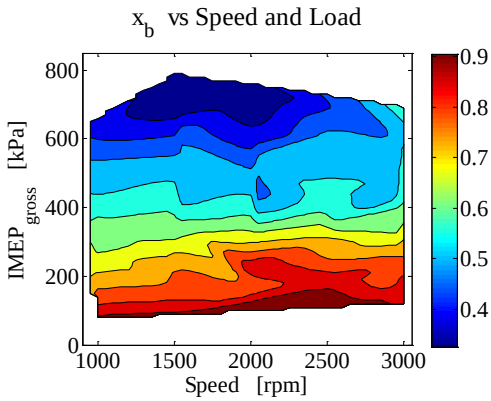

Figure 124: Burned gas fraction, x_b

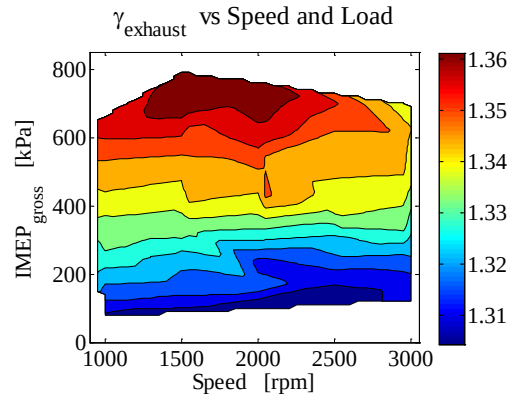

Figure 125: Specific heat ratio, γ

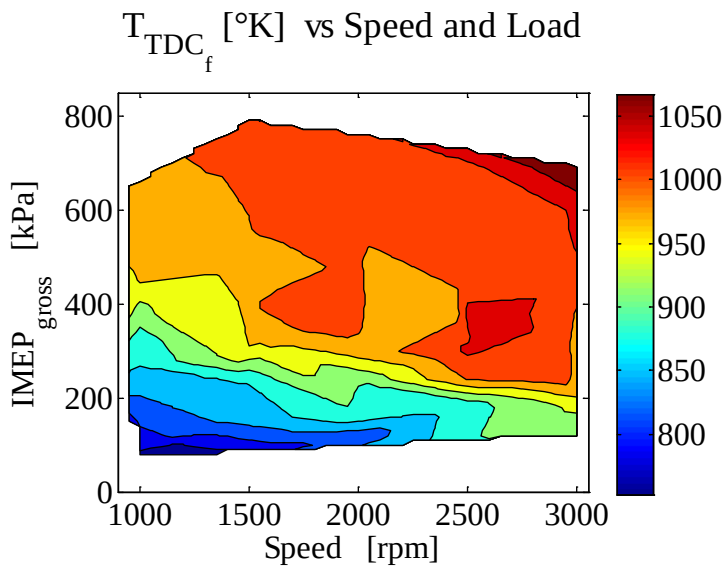

Figure 126: Estimated temperature at TDC, T_{TDC}

When simulating this turbocharged HCCI engine at medium and high load the EVC position is set by the T_{TDC} with appropriate control blocks in the simulating program, as seen in Figure 127. This has shown that the predicted EVC position and therefore the boost pressure follow the real engine tests closely, see Figure 128 to Figure 131.

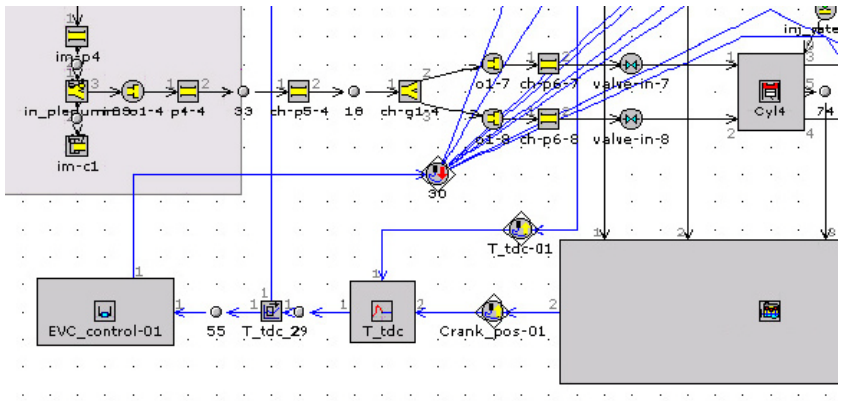

Figure 127: Temperature control in the engine simulating program

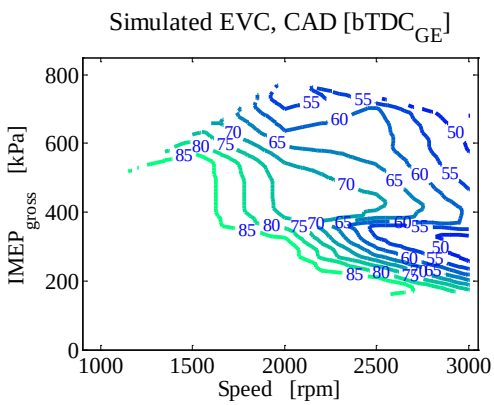

Figure 128: Simulated EVC

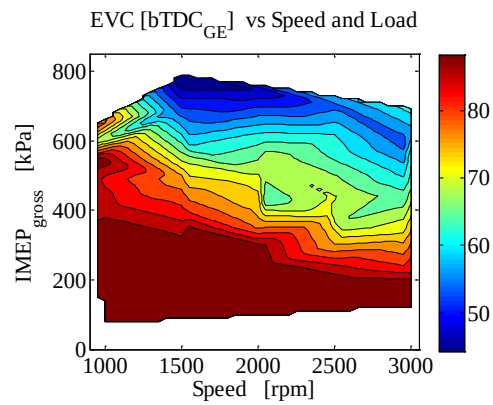

Figure 129: Experimental EVC

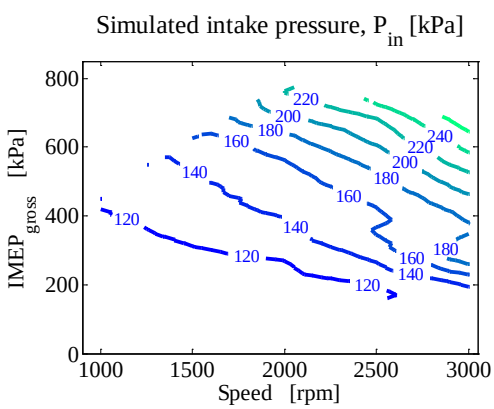

Figure 130: Simulated intake pressure

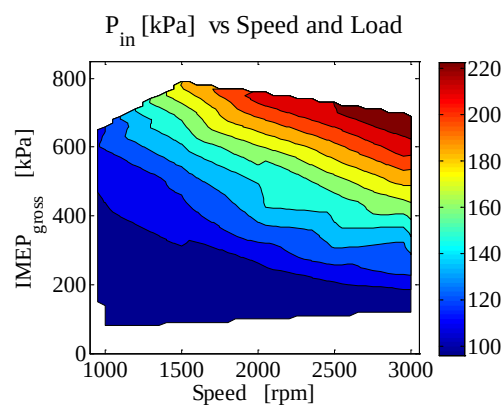

Figure 131: Experimental intake pressure

By using the described EVC control and the combustion parameters in Paper V, it is possible to accurately predict this turbocharged HCCI engine in an engine simulating program. It can be used to evaluate different camshaft profiles and turbochargers etc. before any changes are made to the engine.

6.6.3 Conclusions from HCCI Simulation

In engine simulation of HCCI, it is important to have the right combustion parameters, especially if the engine is turbocharged. The combustion timing and heat release rate have to be predicted as well as appropriate valve timings. If the engine is operated with NVO and short duration valve timings there can be high throttling losses over the valves. This needs to be predicted accurately in the simulation. When boost pressure is used to decrease the combustion noise it is important to predict the turbocharger performance closely.

The exhaust valve closing timing needs to be accurately predicted since it sets the combustion timing and also influences the mass flow through the engine. The calculated temperature at intake valve closing is used in conjunction with the burned gas fraction to predict the temperature at TDC_f by using the ideal gas law. This calculation gives a temperature at TDC_f in the region of 1000 K for most operating conditions. This temperature is used as a boundary condition for controlling the exhaust valve timing in the engine simulation at medium and high load, as it will predict the real exhaust valve closing timing.

6.7 Operating Range after Simulations and Optimization of Valve System and Turbocharger Components

With the knowledge from how different operating variables affects the results together with improvement in hardware and control strategy, the complete operating range for the turbocharged HCCI engine is examined in this section.

6.7.1 Progress

The maximum operating range and the fuel efficiency in this turbocharged HCCI engine has been increased during the research period, due to improvement in hardware and operating strategies. In Figure 132 the maximum load range during at different time steps are shown.

The baseline for comparison is the same engine in NA setup with the same operating limitations as for the turbocharged version. The main improvement in load range has come from increased boost pressure from a better sized turbocharger and reduction of throttling losses with the long duration exhaust camshaft.

The final operating range reached BMEP levels above 500 kPa, from 1000 to 3000 rpm, as seen in Figure 133. There are still many areas left for improvement to extend it further; a turbocharger adapted to HCCI, continuously variable valve lift and duration, increased compression ratio and refinements of the control strategy etc. The final maximum load range was limited for different reasons at low, intermediate and high engine speed, as seen in Figure 134

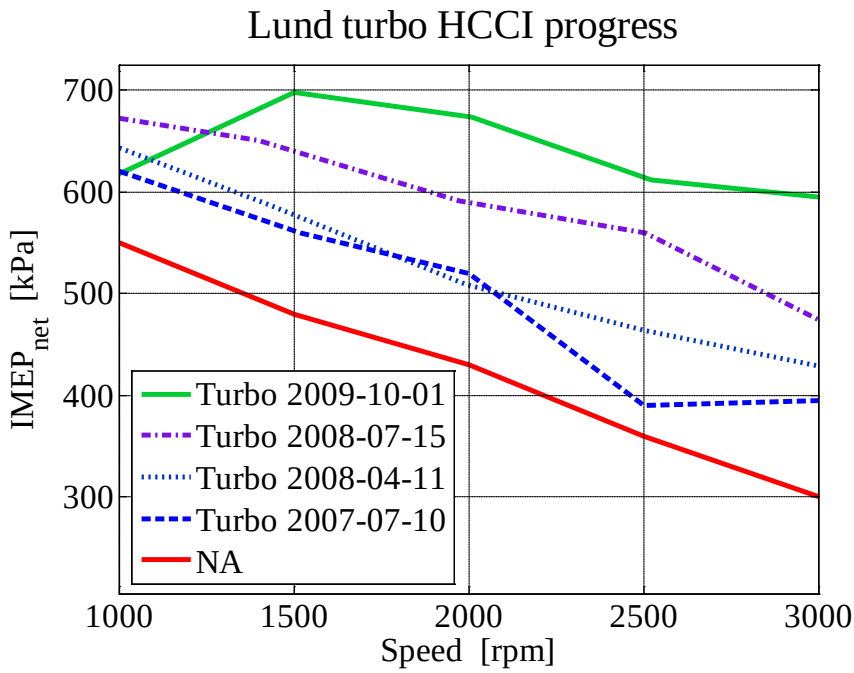

Figure 132: Maximum load range progress

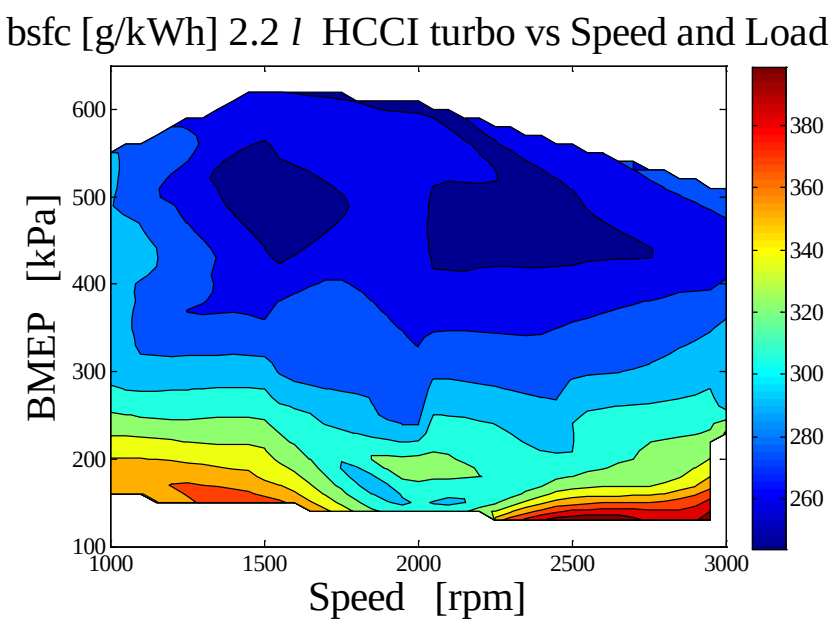

Figure 133: brake specific fuel consumption

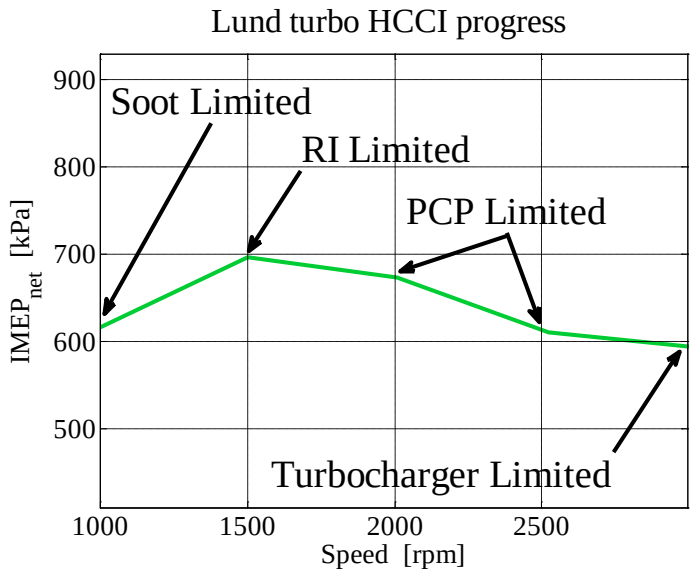

Figure 134: Limitations of operating range

6.7.2 NEDC Test Cycle

The reason to improve the operating range is to reduce the need for mode switch between HCCI and SI and at the same time improve the fuel efficiency in a wider operating range in HCCI mode. Test cycles like the New European Driving Cycle (NEDC) in Figure 135 are used to measure the fuel consumption and exhaust emissions from a vehicle [103]. The NEDC consists of four repeated ECE-15 driving cycles and one Extra Urban Driving Cycle or EUDC test cycle. The ECE-15 cycle is devised to represent the driving conditions in a big city and is characterized by low vehicle speed, low engine load and low exhaust temperature from idle periods. The EUDC is added after the fourth ECE-15 cycle to capture a more aggressive and higher speed driving mode, with a maximum speed of 120 km/h.

In Figure 136 is an example of required positive load and engine speed for the 2.2 *l* engine and a medium size car. The engine speed is below 3000 rpm in the test cycle and if the engine can reach 5 bar BMEP in this engine speed range, almost the entire NEDC test cycle can be covered in HCCI.

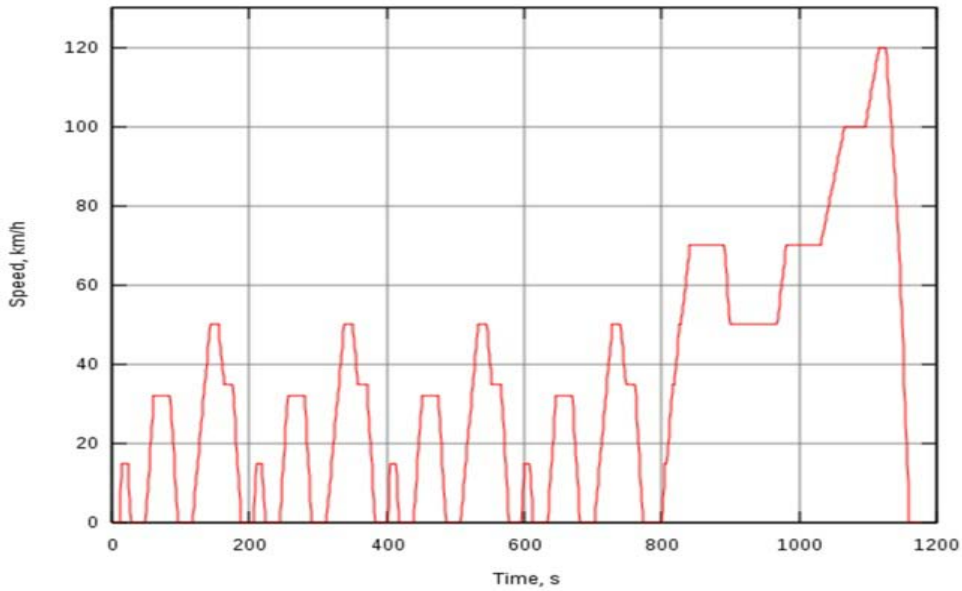

Figure 135: NEDC test cycle

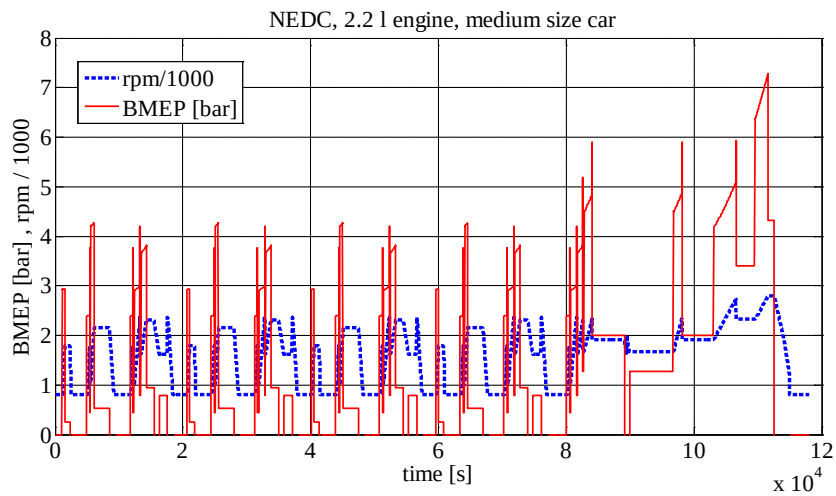

Figure 136: NEDC for the 2.2 *l* engine

6.7.3 Results from Final Operating Range

In order to make a speed and load test, the operating limitations are set out as previously described with limitations for:

- RI below 5 MW/m²
- CoV below 3.0 % or STD of $IMEP_{net}$ below 15 kPA at low load
- EI NOx below 1.0 g/kg_{fuel} if lean, unlimited at stoichiometric
- Soot below 0.10 FSN
- PCP below 9.5 MPa

The turbocharged HCCI engine is tested from 1000 to 3000 rpm in steps of 500 rpm with load steps of 50 kPa. The goal has been to minimize the fuel consumption, nsfc, in all operating points. The injection strategy has been with split injection where the cylinder balancing has been done with the first injection in the NVO period as described in the experimental setup. Both symmetrical and asymmetrical intake valve timing has been used. The final NVO range is from 72 to 172 CAD. The ignition timing and IVO is manually controlled and adjusted to every test point. The cooling temperature and external EGR is also manually controlled. The fuel pressure during these tests are from 12 to 16 MPa. The results are with the final hardware and control settings. This means that the longer duration (155°) new exhaust camshaft and the small KP31 diesel turbocharger are used.

6.7.3.1 Engine Operating Settings

The first fuel injection, SOI1, is used for the cylinder balancing and the average SOI1 timing for all cylinders are shown in Figure 137. The cylinder that needs least advancing of the combustion timing due to the increased heat from the fuel reformation, usually has an SOI timing near 300 °$bTDC_f$. At low engine speed and high load it can be seen that the average injection timing is delayed to reduce the soot emissions. At low load the injection timing is advanced to increase the heat from the fuel reformation. The basic NVO timing is set for the best efficiency at high load. The injection duration is usually set around 3 ms in SOI1, as seen in Figure 138. The second injection timing is usually near 260 °$bTDC_f$, see Figure 139, since the efficiency is highest in this area. At low load, a late SA stratified injection is used to increase the combustion stability with no penalty in NOx or soot emissions. The injection duration in Figure 140, is proportional to load in the entire engine speed range.

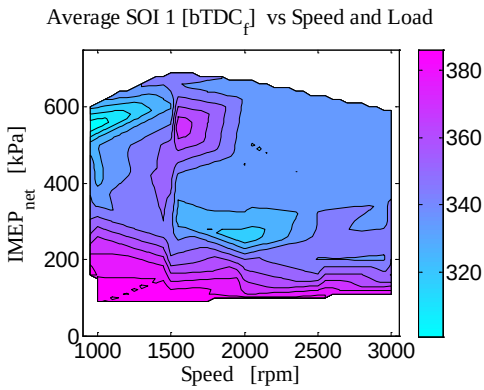

Figure 137: Average SOI 1 injection timing

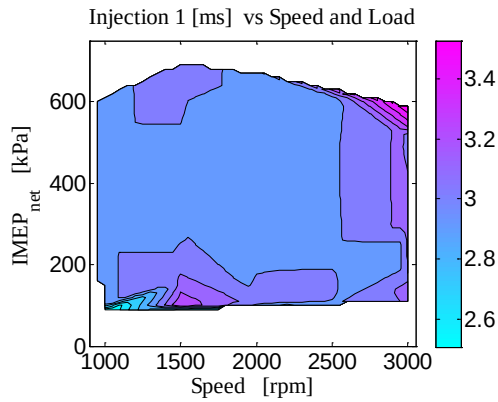

Figure 138: First injection time

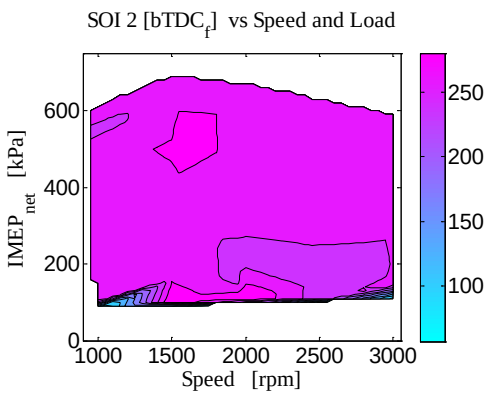

Figure 139: SOI 2 injection timing

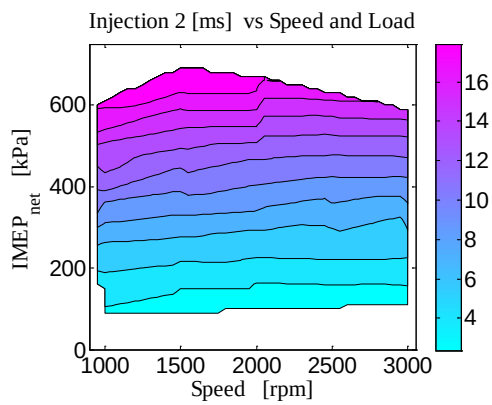

Figure 140: Second injection time

The ignition timing in Figure 141, has a set-point at 29°. At low load the ignition timing is advanced in conjunction to the stratified fuel injection. At low engine speed and high load, the mass flow is low, and efforts are made to improve the mass flow by a delayed combustion timing to increase the boost pressure. This can be assisted by a delayed spark timing.

The EVC position in Figure 142 shows that the entire available timing range are used, and the limited EVC range is visible at the lower load regime.

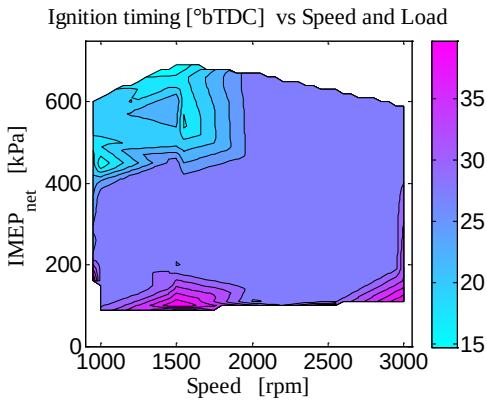

Figure 141: Ignition timing

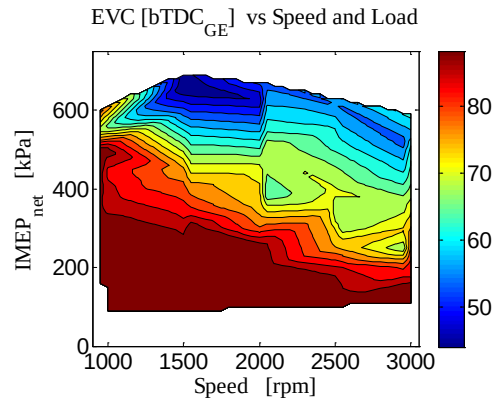

Figure 142: Exhaust valve closing timing

The IVO timing is mostly asymmetrical to the EVC timing, except when the EVC is in the most advanced position, as seen in Figure 143. At high engine speed and high load the turbocharger turbine is choked. The in-cylinder pressure is reduced by a more symmetrical IVO timing, leading to reduced mass flow and higher gas exchange efficiency.

The intake temperature is reduced in the intercooler circuit to reduce the mass flow through the engine at high engine speeds and high load, see Figure 144. When the intake temperature is decreased, there is need for increased internal EGR for a given combustion timing. This can be achieved by an advanced EVC timing, giving improvement in efficiency for this condition.

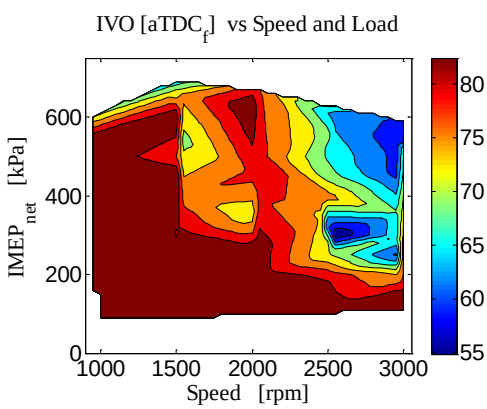

Figure 143: Intake valve opening timing

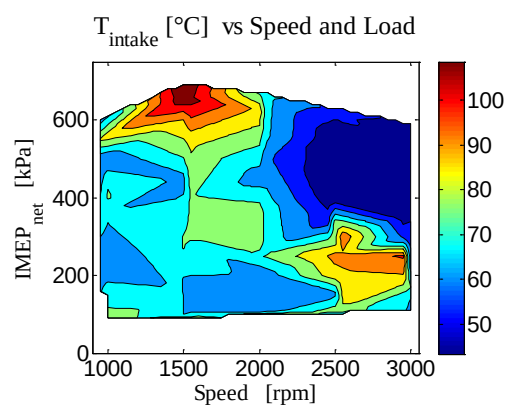

Figure 144: Intake temperature

The intake pressure in Figure 145, is maximized at all operating points as long as the back pressure can be maintained at reasonable levels. The intake pressure scales to load and engine speed. The highest achievable intake pressure is close to 220 kPa. The limiting factor for the boost pressure is the small fixed geometry exhaust turbine that becomes choked at higher engine speeds. On the other hand this turbocharger is suitable to deliver boost at small mass flows. One way to alter the mass flow through the engine is to adjust the cooling temperature with the electrical cooling pump, see Figure 146. At low load the cooling temperature is increased due to limitations in available NVO range. The influence from the coolant temperature on possible intake pressure is almost as strong as adjustment in the intake temperature.

External EGR, see Figure 147, is used when NOx emissions are high, or when the pumping losses are high. At high engine speed the throttling losses can be reduced with EGR, leading to more beneficial valve timings.

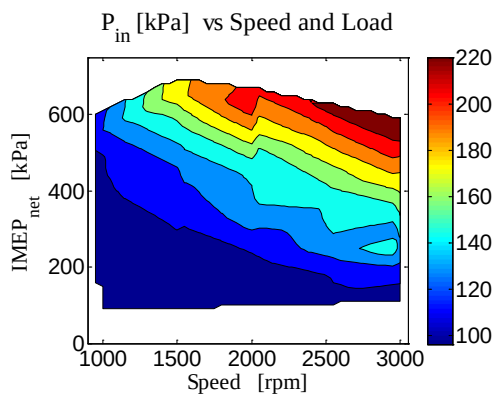

Figure 145: Intake pressure

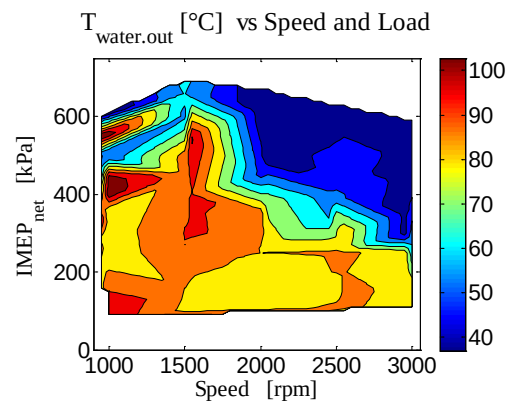

Figure 146: Coolant temperature

The combustion timing, CA50, in Figure 148, is balanced against the resulting combustion noise, combustion stability and efficiency. At low load the CA50 is advanced before TDC_f to stabilize the combustion and also to decrease the load. As a delayed CA50 timing will increase the mass flow and therefore the boost pressure, it has to be weighted against loss of expansion work.

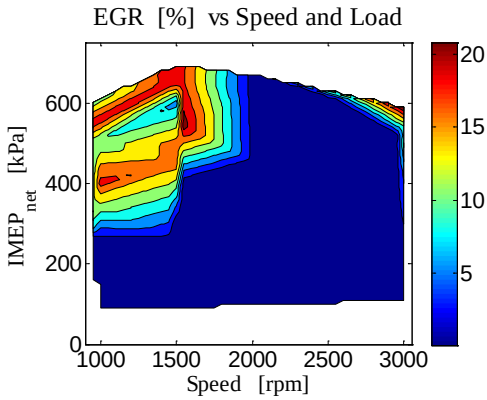

Figure 147: External EGR level

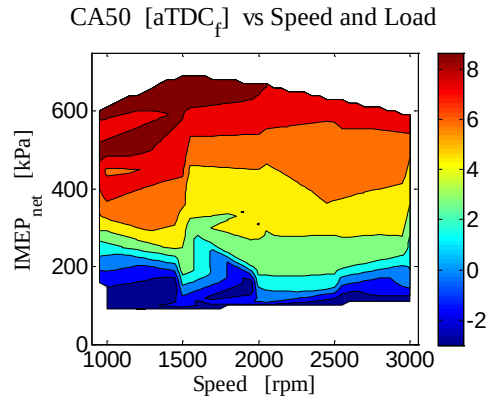

Figure 148: Combustion timing, CA50

6.7.3.2 Results from Speed and Load Testing

The net specific fuel consumption, nsfc, for the entire operating range is shown in Figure 149. To better visualize nsfc, it is divided into two parts; above and below 300 kPa NMEP as seen in Figure 150 and Figure 151. At loads above 300 kPa the nsfc is reduced at low engine speed due to increased heat losses and from stoichiometric operation. At other engine speeds the nsfc stays even at nsfc below 240 g/kWh. The nsfc starts to increase below 200 kPa. Below this load, fuel reformation in NVO is used to increase the in-cylinder heat, leading to increased heat losses. There is also loss of expansion work at low load with the advanced CA50 timing that is used to increase the combustion stability.

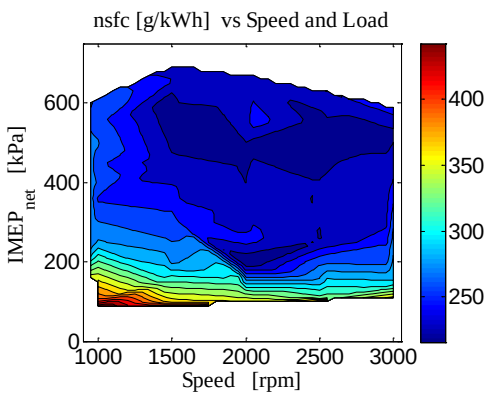

Figure 149: net specific fuel consumption, nsfc

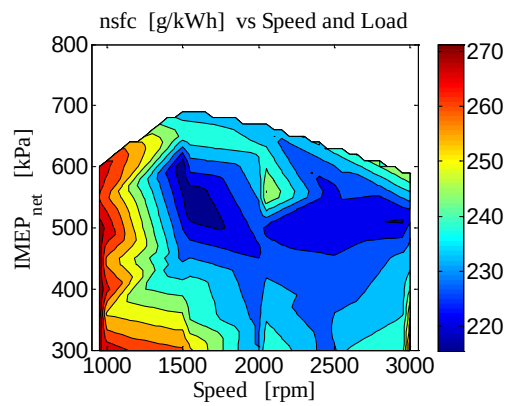

Figure 150: nsfc above 300 kPa $IMEP_{net}$

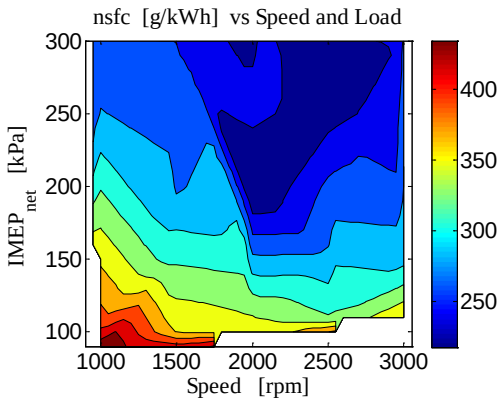

Figure 151: nsfc below 300 kPa $IMEP_{net}$

The combustion noise, RI, is the hardest limitation to fulfill. To keep RI low and efficiency high, the following parameters are optimized; the combustion timing, injection split and timing, intake valve timing, intake temperature, coolant temperature, external EGR usage, fuel pressure and ignition timing, based on experience from the operator. RI scales with load as seen in Figure 152. What cannot be seen, is the steep rise of RI if the combustion timing is slightly off the set position. At low engine speed and high load the influence from SA is high and therefore the combustion timing can be retarded more to reduce RI. At 1500 rpm the RI was the limiting factor.

The easiest way to reduce the combustion noise is to delay the combustion timing, and this normally increases CoV. The turbocharged HCCI has an advantage over a NA HCCI. If there is boost pressure, the turbocharged HCCI engine can operate at a more advanced combustion timing than the NA HCCI engine, and thus increase the efficiency due to higher expansion ratio. A more advanced combustion timing will also decrease the CoV for the turbocharged HCCI engine. The CoV is low in the operating range, except at low load as seen in Figure 153. But at low load the operating limit is set by the standard deviation, STD of $IMEP_{net}$. The CoV can increase drastically at high load or engine speed with just 1 degree change of the combustion timing but this is not presented. In Figure 154 the STD of $IMEP_{net}$ is shown, it increases at low load and engine speed. In most of the operating range the STD is low except at high load and engine speed. This could be connected to the low intake temperature that is used to reduce the mass flow, meaning that the stabilizing effect from the internal EGR is lost. To further complement these combustion stability calculations the STD of CA50 is seen in Figure 155.

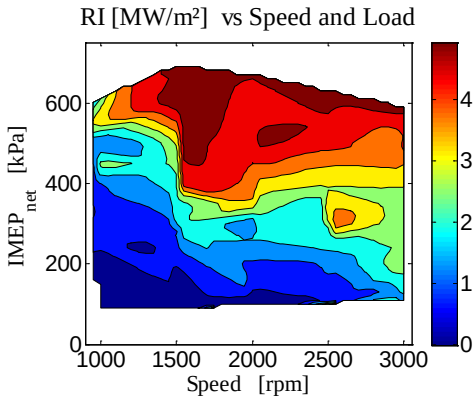

Figure 152: Ringing Intensity, RI

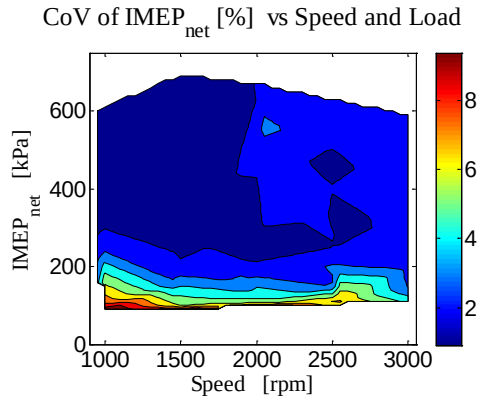

Figure 153: CoV of $IMEP_{net}$

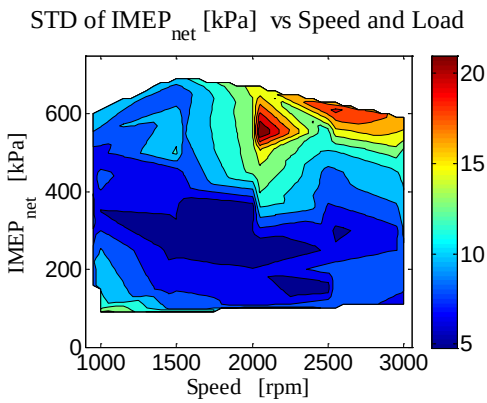

Figure 154: Standard deviation of $IMEP_{net}$

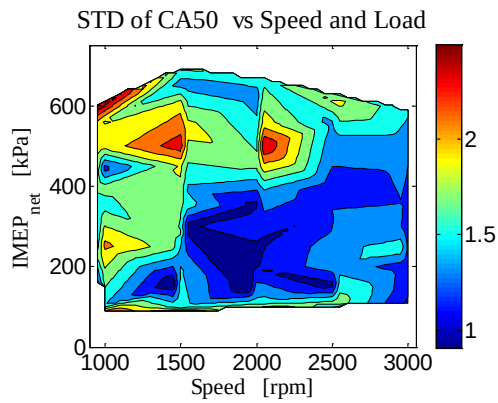

Figure 155: Standard deviation of CA50

The intake pressure directly influences the peak cylinder pressure together with the IVC timing and specific heat ratio. At 2000 to 2500 rpm the PCP is becoming a limiting factor, as seen in Figure 156. The STD of PCP can also be used as an indicator of combustion stability. Here, this scales to load and it is stable at low load, see Figure 157.

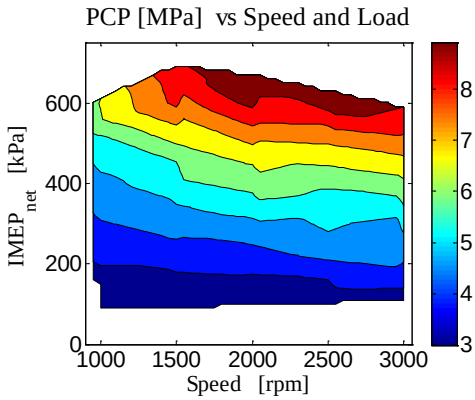

Figure 156: Peak cylinder pressure, PCP

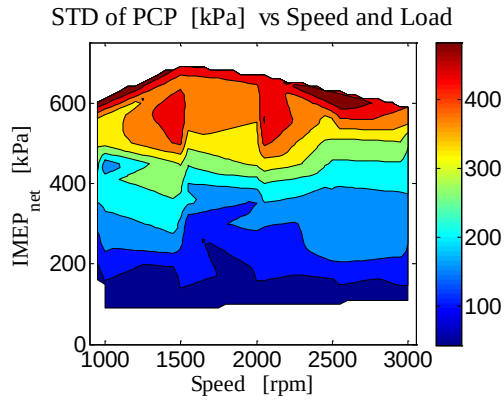

Figure 157: Standard deviation of PCP

With higher intake pressure, the dilution increases and NOx level is reduced. If the NOx level become too high, the engine has to be operated stoichiometric with the aid of a TWC to meet the NOx legislation. The NOx emissions are low in the entire operating range except at 1000 rpm and high load, see Figure 158. To operate the engine stoichiometrically this engine uses a long route EGR system. In Figure 159, lambda is shown. With external EGR an advanced EVC timing is required in order to maintain constant combustion timing. Pumping losses can then be reduced due to more suitable valve timing at high load. The usage of EGR at 3000 rpm and high load is seen as a richer mixture in Figure 159.

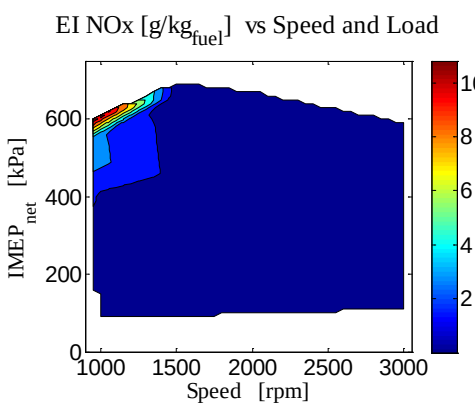

Figure 158: Emission Index Nitrogen oxides, EI NOx

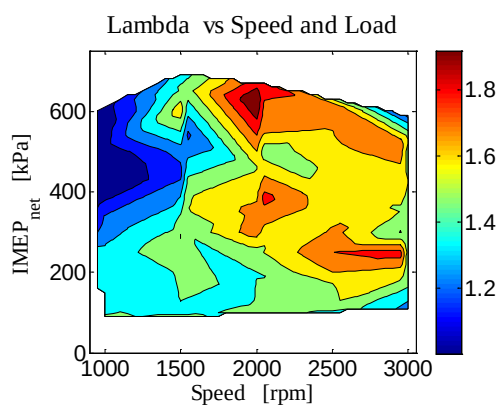

Figure 159: Lambda level

When the dilution is increased in the turbocharged HCCI engine, soot is usually no problem, due to the increased oxygen content. But at low engine speed the mass flow is not enough to increase the intake pressure. This leads to increasing soot emission, as seen in Figure 160. The possible load at 1000 rpm was limited by the high soot level. To reduce the soot level, the first fuel injection was delayed as much as possible and the fuel pressure was increased to 16 MPa, in an effort to reduce the high soot level.

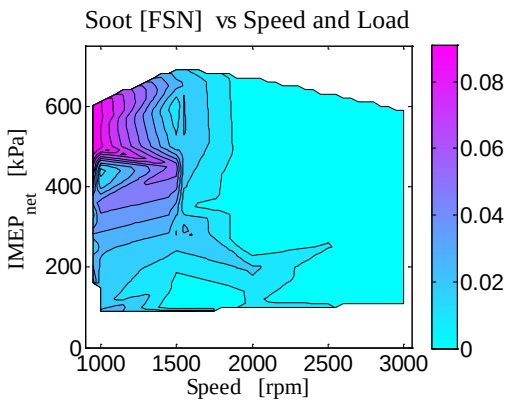

Figure 160: Soot emission, FSN

In this turbocharged setup it is as expected that the pumping losses increases at high load, up to significant levels, as seen in Figure 161. As described earlier, the PMEP is divided into two parts, pressure loss over the engine, P_{ex}-P_{in} and throttling losses over the valves, $Throttling_{valve}$. In Figure 162, the pressure loss over the engine is shown. Even if efforts are made to reduce the mass flow with the engine operating settings, the pressure loss is high due to the small fixed geometry turbine. This turbine size is needed for building boost pressure at low engine speeds but it limits the operating range at high engine speed The resulting throttling over the valves in Figure 163, was reduced substantially with the longer duration exhaust valve timing. The negative numbers for the throttling losses at low load are due to heat release during the NVO, making the engine by definition a two-stroke engine. This was used to circumvent the limitations in NVO range.

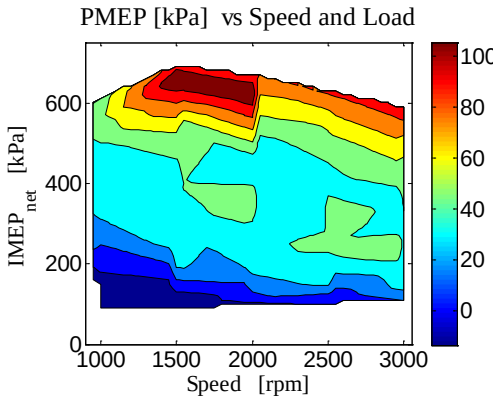

Figure 161: Pumping mean effective pressure, PMEP

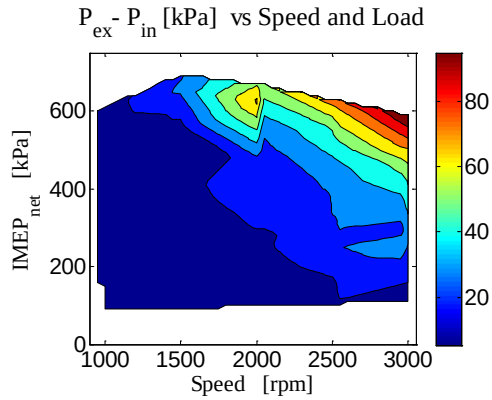

Figure 162: Pressure loss over the engine

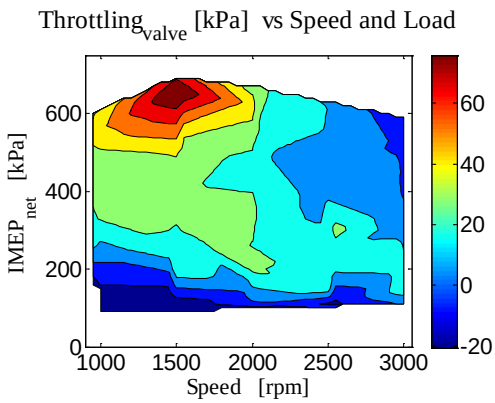

Figure 163: Throttling losses over the valves

6.7.3.3 Speed and Load, Efficiency Breakdown

The combustion efficiency in Figure 164 is even throughout the speed and load range. The thermal efficiency in Figure 165, on the other hand shows the increasing heat losses at low engine speed and low loads. At low engine speed the engine is operated stoichiometrically and this increases the heat losses from the recompression due to the advanced EVC timing. The resulting gross indicated efficiency is above 35 % in most of the operating range with some peaks above 40 % as seen in Figure 166.

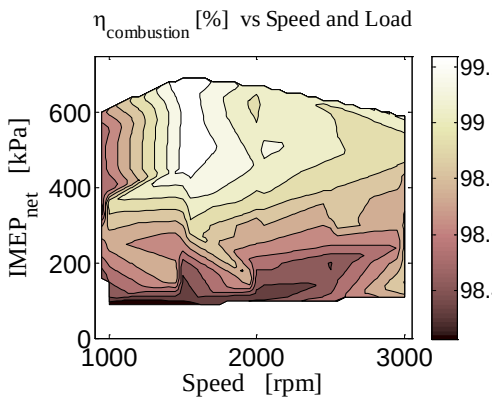

Figure 164: Combustion efficiency

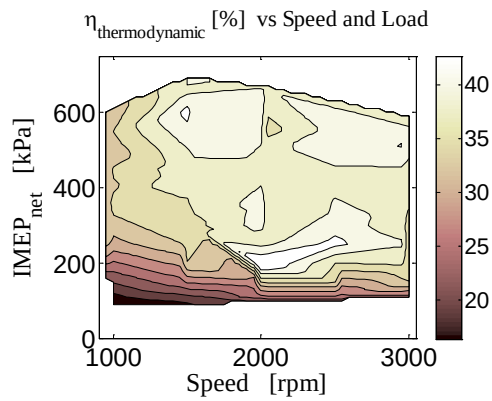

Figure 165: Thermodynamic efficiency

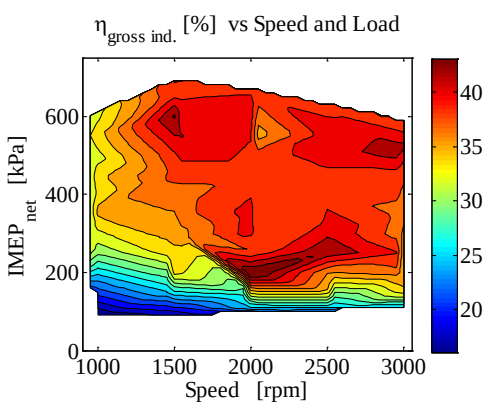

Figure 166: Gross indicated efficiency

The pumping losses in Figure 161 gives the gas exchange efficiency in Figure 167. This part has the most potential to be improved for this turbocharged HCCI setup. This could be done with a turbocharger designed for HCCI operation. The resulting net indicated efficiency in Figure 168, is above 30 % in most of the operating area, except at low engine speed or low loads due to reasons described earlier.

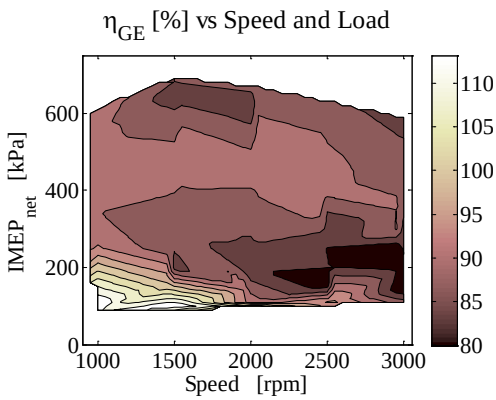

Figure 167: Gas exchange efficiency

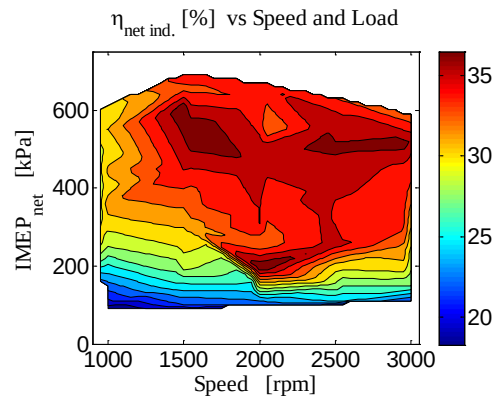

Figure 168: Net indicated efficiency

6.7.4 Discussion

When load is increased for this turbocharged HCCI engine setup the operating parameters have to be balanced against each other. For example, if the load range is to be increased and the pressure rise rate is too high, the combustion timing can be delayed, if the combustion stability stays low. The back pressure goes up from the increased mass flow and therefore the intake pressure and temperature is increased. The valve timing must be changed to keep the combustion timing, which means that a later EVC timing is needed and therefore the EVO timing is later as well. There is then risk for increasing throttling losses as the camshaft has short duration. If the combustion timing is delayed from MBT there will also be loss in thermodynamic efficiency.

The pressure rise rate induced combustion noise is reduced with intake boost, leading to an increase of possible HCCI operating range. The peak cylinder pressure can be a limiting factor when the boost pressure is high. Combustion phasing with cylinder balancing of CA50 with split injection together with cylinder balancing of IMEP improves engine operation and maximizes the load range.

When delaying the combustion phasing to decrease the pressure rise rate, there is risk of high CoV of $IMEP_{net}$. The CoV needs to be at a low level to suppress the risk for misfire. Fuel pressure and injection timing controls soot formation, and liquid film on the piston top should be avoided. At low engine speed and high load the

boost pressure is low, resulting in high NOx emissions. Thus requiring stoichiometric operation. There can be further improvements of fuel efficiency and exhaust emissions with a better sized turbocharger and other valve timings for this turbocharged HCCI engine.

7 Summary and Conclusions

The question is why do we want to operate in HCCI mode? What we are trying to do is to improve the efficiency of the SI engine at low load and still keep the basic SI engine structure.

The gas exchange process was far from optimal with the used valve operation and turbocharger system. This gave significant gas exchange penalty. The pressure loss over the engine due to the turbocharger performance, would be the primary target for improvement of the gas exchange efficiency.

In Figure 169, a comparison of this turbocharged HCCI engine and a direct injected 2.0*l* turbocharged SI engine is shown. The average improvement is 11 % for the turbocharged HCCI engine in this operating range, with a maximum improvement of more than 35 %. At the highest operating load there is no real improvement for this turbocharged HCCI engine setup, mostly due to the low gas exchange efficiency.

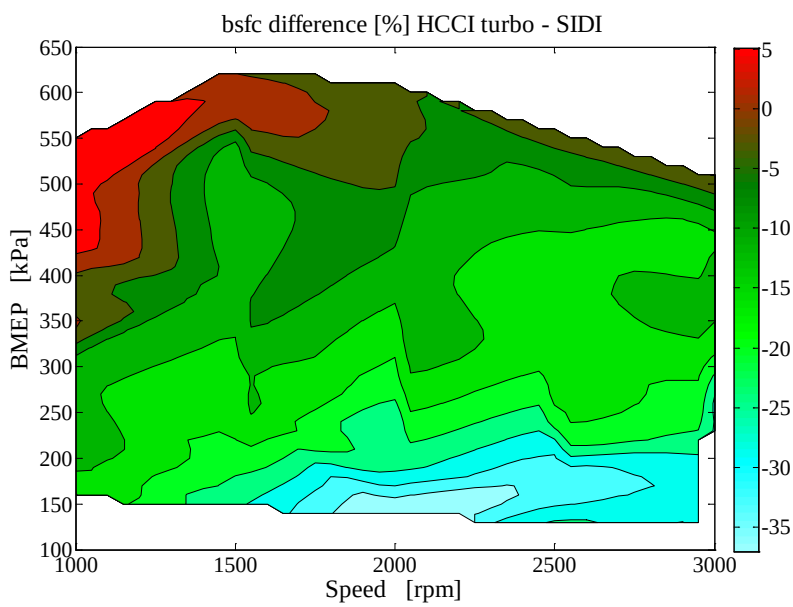

Figure 169: bsfc difference with turbocharged HCCI compared to an SIDI engine

It has been shown that the intake pressure in this turbocharged NVO HCCI engine depends on many variables. The mass flow and therefore the boost pressure can be altered by the fuel injection timing, the combustion timing, the intake valve timing, the intake temperature, the coolant temperature, the ignition timing and with external EGR. This gives the possibility to alter the operating conditions to operate

this turbocharged HCCI engine efficiently in a wide load and engine speed range. The soot emission limited the maximum load range at 1000 rpm. At 1000 rpm the small mass flow was not enough to increase the intake pressure and the NOx emission rise above the set limit, and the engine had to be operated stoichiometric. At higher loads the combustion noise is always a challenge and RI limited operation at 1500 rpm. With the increased intake pressure, the peak cylinder pressure limited the operating range at 2000 to 2500 rpm. At 3000 rpm, the load range was limited by the turbocharger. The combustion stability was the limiting factor for minimum load at all engine speeds. With this turbocharged HCCI engine, the NOx emissions are low when there is boost pressure and does not limit the operating range.

A challenge with turbocharging and HCCI can be a delayed boost pressure during a load transient, leading to increased combustion noise. It is shown that increased fuel reformation during the negative valve overlap increases the mass flow, leading to higher intake pressure. This can be used even before the actual load transient, giving more boost with a penalty in fuel efficiency.

By choosing a better sized turbocharger it was possible to increase the operating range due to higher intake pressure and at the same time reach improvements in fuel efficiency. When the HCCI engine is turbocharged and operated at high load the pumping losses can be high. These could be reduced substantially with an increased exhaust valve duration, further improving the fuel efficiency. It is shown that this turbocharged HCCI engine can have up to 35% improvement in specific fuel consumption when compared to a modern direct injected turbocharged SI engine.

One of the research goals for this thesis was to extend the operating range to more than 500 kPa BMEP, from 1000 to 3000 rpm with the described operating limitations, and this was also fulfilled, as seen in Figure 133.

7.1 Future Work

The turbocharged HCCI engine is very sensitive to the operating settings. This sets high demands on the operating strategies and control system function. The engine sensor signals have to be processed accurately and the control system should have some built in logic.

In this NVO setup, the mass flow through the engine is mainly controlled by the EVC position. The EVC position is at the same time the main controller for the combustion timing. This makes things more complicated since it is important to increase the intake pressure to reduce the combustion noise in high load HCCI mode. Some sort of variable area turbine could be used to overcome this. The turbocharger could be electrically assisted or complemented with a supercharger. The influence on mass flow from the EVC position can be reduced by having a higher compression ratio or by heating up the incoming air. We warmed the incoming air by the heated intake manifold that was used from the beginning of this research. This principle could be extended to other places for the incoming air.

Even if the valve throttling losses were reduced with the longer duration exhaust valve timing, the optimum should be a fully variable valve train for a turbocharged HCCI engine. At low engine speed we want to maximize the expansion ratio with a late EVO timing but we need an early EVC due to increased heat losses. At high engine speed, the EVO needs to be earlier to reduce the pumping work from the blow down process and since the influence from heat losses are reduced a later EVC timing is needed. Together with the influence of increased intake pressure the desired valve timings and duration is changing with the operating conditions.

The soot level at low engine speed and high load might be improved by changing fuel injector type or fuel pressure together with the piston dome design. But the best way to reduce the soot level should be to increase the oxygen concentration by a higher intake pressure.

Since misfires easily become violent at high load these have to be avoided. There was some problems with random misfires during this research, but it was caused by intermittent loss of fuel pressure or due to the IMEP regulation by the control system. To prevent misfires, the ignition system could be made more powerful with microwave assist or similar high power concepts.

With NVO the thermal loading and piston blow-by is increased due to the recompression. This mostly affects the piston assembly. This can be handled by increased oil cooling of the piston crown, or maybe by steel material for the pistons.

To operate in HCCI, the SI engine structure is normally not changed. The combustion chamber might need to be modified to improve HCCI operation.

Generally the HCCI combustion is very beneficial due to the high expansion ratio and low combustion temperature. This lead to high efficiency and low NOx emissions, but the lack of direct combustion control is an issue for a production implementation.

To get a more direct control of the combustion timing, the fuel can be injected in the region of TDC in the same manner as for the diesel engine. This mean that the fuel pressure has to be increased substantially compared to the DI system used today in SI engines, otherwise soot emissions will be an issue.

8 References

1. S. Onishi, S. Hong Jo, K. Shoda, P Do Jo, S Kato: "Active Thermo-Atmosphere Combustion (ATAC) – A New Combustion Process for Internal Combustion Engines", SAE Paper 790501.

2. M. Noguchi, Y. Tanaka, T. Tanaka, Y. Takeuchi: "A study on gasoline engine combustion by observation of intermediate reactive products during combustion", SAE Paper 790840.

3. M. Stockinger, H. Schäpertöns, P. Huhlmann: "Versuche an einem genischansaugenden Verbrennungsmotor mit Selbstzündung" MTZ 53 (1992).

4. T. Aoyama, Y. Hattori, J. Mizuta, Y. Sato: "An experimental study on premixed-charge compression ignition gasoline engine", SAE Paper 960081.

5. M. Christensen, B. Johansson, P. Amnéus, F. Mauss: "Supercharged Homogeneous Charge Compression Ignition", SAE Paper 980787.

6. J-O. Olsson, P. Tunestål, G. Haraldsson, B. Johansson: "A Turbo Charged Dual Fuel HCCI Engine", SAE Paper 2001-01-1896.

7. D. Y., M. L. Wyszynski, A. Megaritis, H. Xu: "Applying Boosting to Gasoline HCCI Operation With Residual Gas Trapping", SAE Paper 2005-01-2121.

8. C. Wildman, R. J. Scaringe, W.Cheng: "On the Maximum Pressure Rise Rate in Boosted HCCI Operation", SAE Paper 2009-01-2727.

9. J. E. Dec, Y. Yang: "Boosted HCCI for High Power Without Engine Knock and With Ultra-Low NOx Emissions~Using Conventional Gasoline", SAE Paper 2010-01-1086.

10. J. Hyvönen, B. Johansson: "HCCI Operating range with VNT Turbo charging", Controlled Auto Ignition, p.217-234.

11. J-O. Olsson, P. Tunestål, J. Ulfvik, B. Johansson: "The effect of cooled EGR on emissions and performance of a turbocharged HCCI engine", SAE Paper 2003-01-0743.

12. C. Wilhelmsson, P. Tunestål, B. Johansson: "Operation Strategy of a Dual-Fuel HCCI Engine With VGT", SAE Paper 2007-01-1855.

13. J. Lavy, J-C. Dabadie, C. Angelberger, P. Duret, J. Willand, A. Juretzka, J. Schaflein, T. Ma, Y. Lendresse, A. Satre, C. Schulz, H. Kramer, H. Zhao, L.

Damiano : "Innovative ulra-low nox controlled auto-ignition combustion process for gasoline engines: the 4-space project", SAE Paper 2000-01-1837.

14. P. M. Najt, D. E. Foster: "Compression-Ignited Homogeneous Charge Combustion", SAE Paper 830264.

15. M. Christensen, P. Einewall, B. Johansson: "Homogeneous Charge Compression Ignition (HCCI) Using Isooctane, Ethanol and Natural Gas – A Comparison to Spark Ignition Operation", SAE Paper 972874.

16. M. Christensen, B. Johansson: "Influence of mixture quality on homogeneous charge compression ignition", SAE Paper 982454.

17. M. Richter, A. Franke, M. Aldén, A. Hultqvist, B. Johansson: "Optical diagnostics applied to a naturally aspirated homogeneous charge compression ignition engine", SAE Paper 1999-01-3649.

18. A. Hultqvist, M. Christensen, B. Johansson, A. Franke, M. Richter, M. Aldén: " A study of the homogeneous charge compression ignition combustion process by chemiluminescence imaging", SAE Paper 1999-01-3680.

19. M. Christensen, B. Johansson: "Homogeneous charge compression ignition with water injection", SAE Paper 1999-01-0182.

20. M. Christensen, A. Hultqvist, B. Johansson: "Demonstrating the multi-fuel capability of a homogeneous charge compression ignition engine with variable compression ratio", SAE Paper 1999-01-3679.

21. J-O. Olsson, P. Tunestål, B. Johansson: "Closed-loop control of an HCCI engine", SAE Paper 2001-01-1031.

22. J. B. Heywood: "Internal Combustion Engine Fundamentals", McGraw-Hill, New York, 1988.

23. P. Flynn, G. Hunter, R. Durrett, L. Farrell, W. Akinyemi: "Minimum engine flame temperature impacts on diesel and spark-ignition engine NOx production", SAE Paper 2000-01-1177.

24. J. Yang, R. W. Anderson: "Fuel injection strategies to increase full-load torque output of a direct-injection SI engine", SAE Paper 980495.

25. R. H. Stanglmaier, J. Li, R. D. Matthews: "The effect of in-cylinder, wall-wetting location on the HC emissions from SI engines", SAE Paper 1999-01-0502.

26. R. H. Muñoz, Z. Han, B. A. VanDerWege, J. Yi: "Effect of Compression Ratio on Stratified-Charge, Direct-Injection Gasoline Combustion", SAE Paper 2005-01-0100.

27. P. Lückert, A. Waltner, E. Rau, G. Vent, U. Schaupp: "Der neue V6-Ottomotor mit Direkteinspritzung von Mercedes-Benz", MTZ 2006 /11.

28. R. Flierl, C. Landerl, R. Hofmann, T. Melcher, H. Steyer: "Der neue BMW Vierzylinder-Ottomotor mit VALVETRONIC", MTZ 62 / 2001.

29. D. Cleary, G. Silvas: "Unthrottled Engine Operation with Variable Intake Valve Lift, Duration, and Timing", SAE Paper 2007-01-1282.

30. J-M. Zaccardi, A. Pagot, F. Vangraefschepe, C. Dognin, S. Mokhtari: "Optimal Design for a Highly Downsized Gasoline Engine", SAE Paper 2009-01-1794.

31. J. E. Dec: "A conceptual model of DI diesel combustion based on laser-sheet imaging", SAE Paper 970873.

32. M. T. Noorman, D. N. Assanis, D. J. Patterson, S. C. Tung, S. I. Tseregounis: "Overview of techniques for measuring friction using bench tests and fired engines" SAE Paper 2000-01-1780.

33. M. Christensen, B. Johansson, A. Hultqvist: "The effect of piston topland geometry on emissions of unburned hydrocarbons from a homogeneous charge compression ignition", SAE Paper 2001-01-1893.

34. A. Hultqvist, M. Christensen, B. Johansson, M. Richter, J. Nygren, J. Hult, M. Aldén: "The HCCI combustion process in a single cycle~High-Speed fuel tracer LIF and chemiluminescence imaging", SAE Paper 2002-01-0424.

35. A. Vressner, A. Lundin, M. Christensen, P. Tunestål, B. Johansson: "Pressure oscillations during rapid HCCI combustion", SAE Paper 2003-01-3217.

36. T. Tsurushima, E. Kunishima, Y. Asaumi, Y. Aoyagi, Y. Enomoto: "The effect of knock on heat loss in homogeneous charge compression ignition engines", SAE Paper 2002-01-0108.

37. S. Hensel, F. Sarikoc, F. Schumann, H. Kubach, U. Spicher: "Investigations on the Heat Transfer in HCCI Gasoline Engines", SAE Paper 2009-01-1804.

38. M. Sjöberg, J.E. Dec, W. Hwang: "Thermodynamic and Chemical Effects of EGR and Its Constituents on HCCI Autoignition", SAE Paper 2007-01-0207.

39. J. E. Dec, M. Sjöberg, W. Hwang: "Isolating the Effects of EGR on HCCI Heat-Release Rates and NOX Emissions", SAE Paper 2009-01-2665.

40. G. M. Rassweiler, L. Withrow: "Motion Pictures of Engine Flames Correlated With Pressure Cards", SAE Paper 380139.

41. P. Strandh, M. Christensen, J. Bengtsson, R. Johansson, A. Vressner, P. Tunestål, B. Johansson: "Ion current sensing for HCCI combustion feedback", SAE Paper 2003-01-3216.

42. G. E. Bogin Jr., J. H. Mack, R. W. Dibble: "Fuel Effects on Ion Sensing in a Homogeneous Charge Compression Ignition (HCCI) Engine", SAE Paper 2009-01-1805.

43. H. Zhang, H. Xie: "Research on Relativity of Knock Sensor Signal and Gasoline HCCI Combustion Obtained With Trapping Residual Gas", SAE Paper 2010-01-1242.

44. I. Andersson, T. McKelvey, M. Thor: "Evaluation of a Closed-Loop Spark Advance Controller Based on a Torque Sensor", SAE paper 2008-01-0987.

45. F. Ponti, V. Ravaglioli, G. Serra, F. Stola: "Instantaneous Engine Speed Measurement and Processing for MFB50 Evaluation", SAE Paper 2009-01-2747.

46. M. J. Andrie: "Non-Intrusive Low Cost Cylinder Pressure Transducer for Internal Combustion Engine Monitoring and Control", SAE Paper 2009-01-0245.

47. J. Martinez-Frias, S. Aceves, D. Flowers, R. Smith, R. Dibble: "HCCI Engine Control by Thermal Management", SAE Paper 2000-01-2869.

48. G. Haraldsson, P. Tunestål, B. Johansson, J. Hyvönen: "HCCI Closed-Loop Combustion Control Using Fast Thermal Management", SAE Paper 2004-01-0943.

49. G. Haraldsson, P. Tunestål, B. Johansson, J. Hyvönen: "HCCI combustion phasing in a multicylinder engine using variable compression ratio", SAE Paper 2002-01-2858.

50. G. Haraldsson, P. Tunestål, B. Johansson, J. Hyvönen: "HCCI combustion phasing with closed-loop combustion control using variable compression ratio in a multi-cylinder engine", SAE Paper 2003-01-1830.

51. Z. Chen, K. Mitsuru: "How to put the HCCI engine to practical use: Control the ignition timing by compression ratio and increase the power output by supercharge", SAE Paper 2003-01-1832.

52. J. Martinez-Frias, S. M. Aceves, D. Flowers, J.R. Smith, R. Dibble: "Equivalence ratio-EGR control of HCCI engine operation and the potential for transition to spark-ignited operation", SAE paper 2001-01-3613.

53. C. D. Marriott, R. D. Reitz: "Experimental investigation of direct injection gasoline for premixed compression-ignited combustion-phasing control", SAE Paper 2002-01-0418.

54. T. Urushihara, K. Hiraya, A. Kakuhou, T. Itoh: "Expansion of Hcci Operating Region By the Combination of Direct Fuel Injection, Negative Valve Overlap and Internal Fuel Reformation", SAE Paper 2003-01-0749.

55. J. E. Dec, W. Hwang, M. Sjöberg: "An Investigation of Thermal Stratification in HCCI Engines Using Chemiluminescence Imaging", SAE Paper 2006-01-1518.

56. L. Cummins: "Internal Fire", dba Carnot Press, USA, 2000.

57. R. H. Thring: "Homogeneous-Charge Compression-Ignition (HCCI) engines", SAE Paper 892068.

58. J. Willand, R-G. Nieberding, G. Vent, C. Enderle: "The Knocking Syndrome - Its Cure and Its Potential", SAE Paper 982483.

59. J. D. Dale, A. K. Oppenheim: "Enhanced ignition for I.C. engines with premixed gases", SAE Paper 810146.

60. J. D. Dale, A. K. Oppenheim: "A rationale for advances in the technology of I. C. Engines", SAE Paper 820047.

61. A. K. Oppenheim: "The knock syndrome~its cures and its victims", SAE Paper 841339.

62. M. Asai, T. Kurosaki, K. Okada: "Analysis on fuel economy improvement and exhaust emission reduction in a two-stroke engine by using an exhaust valve", SAE Paper 951764.

63. Y. Ishibashi, M. Asai: "Improving the exhaust emissions of two-stroke engines by applying the activated radical combustion", SAE Paper 960742.

64. N. Hata, T. Iio: "Improvement of two-stroke engine performance with the Yamaha Power Valve System (YPVS)", SAE Paper 810922.

65. 1998, Hondabladet.

66. N. B. Kaahaaina, A. J. Simon, P. A. Caton, C. F. Edwards: "Use of dynamic valving to achieve residual-affected combustion", SAE Paper 2001-01-0549.

67. J. Li, H. Zhao, N. Ladomatos: "Reserch and Development of Controlled Auto-Ignition (CAI) Combustion in a 4-Stroke Multi-Cylinder Gasoline Engine", SAE Paper 2001-01-3608.

68. L. Koopmans, I. Denbratt: "A Four Stroke Camless Engine, Operated in Homogeneous Charge Compression Ignition Mode with Commercial Gasoline", SAE Paper 2001-01-3610.

69. H. Zhau, J. Li, T. Ma, N. Ladommatos:" Performance and Analysis of a 4-stroke Multi-Cylinder Gasoline Engine with CAI Combustion", SAE paper 2002-01-0420.

70. L. Koopmans, H. Ström, S. Lundgren, O. Backlund, I. Denbratt: "Demonstrating a SI-HCCI-SI Mode Change on a Volvo 5-Cylinder Electronic Valve Control Engine", SAE Paper 2003-01-0753.

71. T. Ibara, M. Iida, D. E. Foster: "Study on Characteristics of Gasoline-Fueled HCCI Using Negative Valve Overlap", SAE Paper 2006-32-0047.

72. K. Inoue, K. Nagahiro, Y. Ajiki, N. Kishi: "A high power, wide torque range, efficient engine with a newly developed variable-valve-lift and timing mechanism", SAE Paper 890675.

73. C. Brüstle, D. Schwarzenthal: "VarioCam Plus~A highlight of the Porsche 911 turbo engine", SAE Paper 2001-01-0245.

74. http://en.wikipedia.org/wiki/Variable_valve_timing.

75. H. Hosoya, H. Yoshizawa, S. Watanabe, N. Tomisawa, K. Abe: "Development of new concept control system for valve timing control", SAE Paper 2000-01-1226.

76. M. Hattori, T. Inoue, Z. Mashiki, A. Takenaka, H. Urushihata, S. Morino, T. Inohara: "Development of Variable Valve Timing System Controlled by Electric Motor", SAE Paper 2008-01-1358.

77. O. Lang, W. Salber, J. Hahn, S. Pischinger, K. Hortmann, C. Bücker: "Thermodynamical and Mechanical Approach Towards a Variable Valve Train for the Controlled Auto Ignition Combustion Process", SAE paper 2005-01-0762.

78. J. T. Wentworth: "More on origins of exhaust hydrocarbons ~ effects of zero oil consumption, deposit location, and surface roughness", SAE Paper 720939.

79. J. Willand, C. Jelitto, J. Jakobs: "Das GCI-Brennverfahren von Volkswagen" MTZ 2008 / 4.

80. J. Hyvönen, G. Haraldsson, B. Johansson: "Operating range in a multi-cylinder HCCI engine using variable compression ratio", SAE Paper 2003-01-1829.

81. P. Strandh, J. Bengtsson, R. Johansson, P. Tunestål, B. Johansson: "Variable Valve Actuation for Timing Control of a Homogeneous Charge Compression Ignition Engine", SAE Paper 2005-01-0147.

82. J. Hyvönen, G. Haraldsson, B. Johansson: "Supercharging HCCI to extend the operating range in a multi-cylinder VCR-HCCI engine", SAE Paper 2003-01-3214.

83. K. Hatamura: "A Study on HCCI (Homogeneous Charge Compression Ignition) Gasoline Engine Supercharged by Exhaust Blow Down Pressure", SAE Paper 2007-01-1873.

84. T. Kuboyama, Y. Moriyoshi, K. Hatamura, T. Yamada, J. Takanashi: "An Experimental Study of a Gasoline HCCI Engine Using the Blow-Down Super Charge System", SAE Paper 2009-01-0496.

85. A. Fuhrhapter, W. F. Piock, G. K. Fraidl: "CSI – Controlled Auto-ignition – The Best Solution for the Fuel Consumption – Versus Emission Trade-Off?", SAE Paper 2003-01-0754.

86. H. Persson, A. Rémon, B. Johansson: "The Effect of Swirl on Spark Assisted Compression Ignition (SACI)", JSAE 20077167, SAE Paper 2007-01-1856.

87. J. Hyvönen, G. Haraldsson, B. Johansson: "Operating Conditions Using Spark Assisted HCCI Combustion During Combustion Mode Transfer to SI in a Multi-Cylinder VCR-HCCI Engine", SAE Paper 2005-01-0109.

88. T. Urushihara, K. Yamaguchi, K. Yoshizawa, T. Itoh: "A Study of a Gasoline-Fueled Compression Ignition Engine~Expansion of HCCI Operation Range Using SI Combustion as a Trigger of Compression Ignition", SAE Paper 2005-01-0180.

89. H. Kopecek, E. Wintner, M. Lackner, F. Winter, A. Hultqvist: "Laser-stimulated ignition in a homogeneous charge compression ignition engine", SAE Paper 2004-01-0937.

90. M. Weinrotter, E. Wintner, K. Iskra, T. Neger, J. Olofsson, H. Seyfried, M. Aldén, M. Lackner, F. Winter, A. Vressner, A. Hultqvist, B. Johansson: "Optical

Diagnostics of Laser-Induced and Spark Plug-Assisted HCCI Combustion", SAE Paper 2005-01-0129.

91. G. Lumsden, H. C. Watson: "Optimum control of an S.I. engine with a Lambda#32 and 5 capability", SAE Paper 950689.

92. W. P. Attard, N. Fraser, P. Parson, E. Toulson: "A Turbulent Jet Ignition Pre-Chamber Combustion System for Large Fuel Economy Improvements in a Modern Vehicle Powertrain", SAE Paper 2010-01-1457.

93. L. Koopmans, R. Ogink, I. Denbratt: "Direct gasoline injection in the negative valve overlap of a homogeneous charge compression ignition engine", SAE Paper 2003-01-1854.

94. N. Wermuth, H. Yun, P. Najt: "Enhancing Light Load HCCI Combustion in a Direct Injection Gasoline Engine by Fuel Reforming During Recompression", SAE Paper 2009-01-0923.

95. G. Woschni: "A Universally Applicable Equation for the instantaneous Heat Transfer Coeffficient in the Internal Combustion Engine", SAE Paper 670931.

96. U. Aronsson, H. Solaka, C. Chartier, Ö. Andersson, B. Johansson: "Impact of Mechanical Deformation due to Pressure, Mass, and Thermal Forces on the In-Cylinder Volume Trace In Optical Engines of Bowditch Design", SAE India paper 119.

97. J. A. Eng: "Characterization of pressure waves in HCCI combustion", SAE Paper2002-01-2859.

98. M. M. Andreae, W. K. Cheng, T. Kenney, J. Yang: "On HCCI Engine Knock," SAE Paper 2007-01-1858.

99. www.DieselNet.com, "Smoke Opacity".

100. W. Schindler, M. Nöst, W. Thaller, T. Luxbacher: "Stationäre und transiente messtechnische Erfassung niedriger Rauchwerte" MTZ 2001 / 10.

101. Y. A. Cengel: " Introduction to thermodynamic and heat transfer", McGraw-Hill, New York, 1997.

102. M. C. Weikl, F. Beyrau, A. Leipertz, A. Loch, C. Jelitto, J. Willand: "Locally Resolved Measurement of Gas-Phase Temperature and EGR Ratio in an HCCI Engine and Their Influence on Combustion ", SAE Paper 2007-01-0182.

103. http://www.dieselnet.com/standards/cycles/ece_eudc.html.

9 Summary of papers

9.1 Paper I

HCCI Operating Range in a Turbo-charged Multi Cylinder Engine with VVT and Spray-Guided DI
T. Johansson, B. Johansson, P. Tunestål, H. Aulin
SAE technical paper 2009-01-0494
Presented at the SAE world congress, April 2009, Detroit, USA

In this first paper it was shown which operating limitations one can expect the HCCI engine has to fulfill and how these affects the operating range. It was suggested that combustion noise, combustion stability, NOx and soot emission together with allowed PCP must be considered to get practical operating points in HCCI mode. The influence of boost pressure on combustion noise and NOx level is shown. The control of combustion timing is fundamental to reduce combustion noise and the Ringing Intensity, RI, is found to correlate to the experienced combustion noise. The effect of to high peak cylinder pressure and the reason of a piston failure is shown with Finite Element Analysis. The influence of the injection timing on combustion phasing is shown together with how single and split injection affects soot and efficiency. When NOx level rises above the limit the engine has to be operated stoichiometric to be able to reduce the NOx emissions in a normal 3-way catalyst but considerations has to be done to increase the combustion stability.

By using the above described results a control strategy is proposed on how to operate this turbocharged HCCI engine for best results by using cylinder balancing of CA50 timing, IMEP and lambda. The possible operating range from 1000 to 3000 rpm is presented by extensive result graphs. Finally is a comparison to a NA setup operated with the same limitations and it is concluded that the operating range could be extended with the turbocharger setup.
The engine is equipped with a VGT turbocharger from a 90hp diesel engine.

The author did the experiments, evaluated the data and wrote the paper. The author designed and modified the experimental apparatus. H. Aulin set up the control system.

9.2 Paper II

Thermodynamic Modeling and Control of a Negative Valve Overlap Turbo Engine
H. Aulin, T. Johansson, P. Tunestål, B. Johansson
IASTED paper 651-071
Presented at Control and Applications congress, July 2009, Cambridge, UK
In this paper the model based CA50 controller is described for the turbocharged HCCI engine. To be able to predict the combustion timing a thermodynamic model

of the engine is described. This model predicts the induced air mass, the trapped residual mass and wall temperature. A black box model is used for the turbocharger function to capture the transient dynamics. With the measured in-cylinder pressure a nonlinear model is linearized to give a five state model of the engine. This model is used for constructing a feed forward controller for the EVC position. Transient result show that the model can predict and control the combustion timing accurately against simulated results. The model is tuned for volumetric efficiency and a fuel variation test needs to be made to describe how the combustion phasing relates to the cylinder temperature, engine speed and fuel amount.

The author did the steady state experiments and provided data for model verification. The results from the thermodynamic model in the paper was compared to authors own thermodynamic model. The author designed and modified the experimental apparatus. H. Aulin wrote the paper.

9.3 Paper III

Control of a Turbo Charged NVO HCCI
Engine using a Model Based Approach
H. Aulin, T. Johansson, P. Tunestål, B. Johansson
IFP paper
Presented at E-COSM congress, November 2009, Rueil-Malmaison, France

This paper describes the thermodynamic model and linearization in the same way as in Paper II. Experimental transient results are included and compared to the set point for combustion timing or load. The strategy for cylinder balancing is described with the split injection operation. The first fuel injection is during the NVO period to balance the CA50 timing between the cylinders to reduce the combustion noise and increase the capable load. The second fuel injection amount is used for cylinder balancing of IMEP. The results with deactivated and activated cylinder balancing shows that the variation in load and CA50 timing is reduced substantially with the cylinder balancing activated.

The author did the steady state experiments and provided data for model verification. The author did the experiments and processed the data for the maximum capable operating range. The author designed and modified the experimental apparatus. H. Aulin wrote the paper.

9.4 Paper IV

The Effect of Intake Temperature in a Turbocharged Multi Cylinder Engine operating in HCCI mode
T. Johansson, B. Johansson, P. Tunestål, H. Aulin
SAE technical paper 2009-24-0060
Presented at the ICE congress, September 2009, Capri, Italy

This paper highlights how important the combustion timing and intake temperature is in HCCI mode. This is done at one operating point, 2250 rpm and $IMEP_{net}$ 400 kPa. This point was chosen due to the wide span of boost levels that can be reached with alteration of the intake temperature. It also has different operating limitations due to combustion stability, high pressure rise rate and turbocharger performance. At any higher load or engine speed it was not possible to have wide variation of combustion timing due to misfire or heavy knocking. At lower load or engine speed the variation of boost pressure was less. It is shown that boost pressure scales directly with intake temperature and combustion timing. The highest efficiency is found where the combustion is most unstable. By adding external EGR the boost pressure is decreased due to the increased heat capacity needs more internal EGR, which result in loss of mass flow to turbocharger. But the external EGR is found to increase the combustion stability and improve the efficiency in a small range. Besides using CoV as a combustion stability indicator it is proposed that it should be complemented with the standard deviation of CA50.

The engine is equipped with a fixed geometry turbocharger from a 47hp diesel engine.

The author did the experiments, evaluated the data and wrote the paper. The author designed and modified the experimental apparatus. H. Aulin set up the control system

9.5 Paper V

HCCI Heat Release Data for Combustion Simulation, based on Results from a Turbocharged Multi Cylinder Engine
T. Johansson,P. Borgqvist, B. Johansson, P. Tunestål, H. Aulin
SAE technical paper 2010-01-1490
Presented at the SAE Brasil congress, May 2010, Rio de Janeiro, Brazil
T. Johansson, P. Borgqvist, B. Johansson, P. Tunestål, H. Aulin

Today it is common to evaluate and optimize engine functions in engine simulating program, and it was felt that data and methods was missing for HCCI combustion in the literature. In this paper the data from the complete operating range was

presented. It is shown that important parameters like combustion timing, combustion duration and Wiebe constant can be set to result dependent functions in the simulating program. When using NVO, the valve timings need to be estimated, especially when the engine is turbocharged to get good correlation on the gas exchange process and turbocharger performance. It is presented how this can be done by controlling the EVC position to have a certain temperature at TDC_f. From the operating range data, it is shown that the temperature at IVC can be predicted by calculations. Even if there is a wide variation on the temperature at IVC the temperature ends up fairly even at TDC_f . The deviation of the temperature, TDC_f is explained by the fuel reformation in the NVO that is used due to limited NVO range, and the spark assist at low engine speed.The engine is equipped with a fixed geometry turbocharger from a 47hp diesel engine and the exhaust valve duration is increased 25%.

The author did the experiments, evaluated the data, did the engine simulation and wrote the paper. The author designed and modified the experimental apparatus. H. Aulin set up the control system. P. Borgqvist did the optimization of the Wiebe constants.

9.6 Paper VI

Turbocharging to extend HCCI Operating Range in a Multi Cylinder Engine-Benefits and Limitations
T. Johansson, B. Johansson, P. Tunestål, H. Aulin
FISITA technical paper F2010-A037
Presented at the FISITA congress, May 2010, Budapest, Hungary

In this paper the effect of intake temperature, boost levels, combustion timing, intake valve timing, residual fraction and injection timing are demonstrated. From the results it can be seen how different settings affect intake pressure and hence combustion noise. The results show that the load range in turbocharged HCCI has been increased substantially compared to a naturally aspirated HCCI engine. The evaluation of different turbochargers and cam profiles has contributed to increased efficiency and load range capability. It can be operated from 1 bar indicated mean effective pressure to more than 6 bar, from 1000 and 3000 rpm. A comparison between a modern SI engine and this turbocharged HCCI engine shows that the HCCI engine can have up to 35 % higher fuel efficiency.

It is shown how the operating limitations influences the possible operating range and how the progress of the maximum operating range has increased during time.

The engine is equipped with both a 90 hp VGT and a 47 hp fixed geometry turbocharger from diesel engines and the exhaust valve duration is both as the original and the extended.

The author did the experiments, evaluated the data and wrote the paper. The author designed and modified the experimental apparatus. The author designed and modified the experimental apparatus. H. Aulin set up the control system..

Paper I

2009-01-0494

HCCI Operating Range in a Turbo-charged Multi Cylinder Engine with VVT and Spray-Guided DI

Thomas Johansson, Bengt Johansson, Per Tunestål
Faculty of engineering, Lund University

Hans Aulin
GM Powertrain AB, Sweden

ABSTRACT

Homogenous charge compression ignition (HCCI) has been identified as a promising way to increase the efficiency of the spark-ignited engine, while maintaining low emissions. The challenge with HCCI combustion is excessive pressure rise rate, quantified here with Ringing Intensity. Turbocharging enables increased dilution of the charge and thus a reduction of the Ringing Intensity. The engine used is an SI four cylinder base with 2.2*L* displacement and is equipped with a turbocharger. Combustion phasing control is achieved with individual intake/ exhaust cam phasing. Fuel injection with spray guided design is used. Cycle resolved combustion state is monitored and used for controlling the engine either in closed or open loop where balancing of cylinder to cylinder variations has to be done to run the engine at high HCCI load. When load is increased the NOx levels rise, the engine is then run in stoichiometric HCCI mode to be able to use a simple three-way catalyst. The fuel used is 95 RON pump gasoline and injection strategies are evaluated in order to maintain low soot levels and high efficiency. Limitations and benefits on operating range are examined between 1000 and 3000 rpm. This paper investigates how to extend the HCCI range and how to reduce the high pressure rise rate with: increased boost from turbocharging, external EGR and different injection strategies. A higher boost pressure was found to extend the load range. It is shown that the limitation from high RI, NOx or soot is not the same in all engine speed and load points. By turbocharging the engine in HCCI mode there is greater flexibility to increase the range of practical operating points.

INTRODUCTION

The HCCI mode offer advantages in high thermal efficiency and low emissions but so far has the possible load range been limited compared to conventional spark ignition (SI) engines. HCCI can be a complement to the throttled SI engine during part load to increase engine efficiency. By boosting the engine in HCCI mode the possible load range can be extended [1, 2, 3, 4] and total efficiency can be improved. The need for mode switches between HCCI and SI is reduced which simplifies the control task. The control of combustion timing in internal combustion engines has always been important to maximize efficiency and avoid damages. The SI engine uses spark to ignite the air/fuel mixture and therefore it relies on a suitable fuel type with high octane number to resist autoignition or knock. The drawback is that in order to use spark ignition the engine must be operated near stoichiometric conditions [5] with a three-way catalyst (TWC). Thus the SI engine has to be throttled at lower loads leading to efficiency losses, alternatively the SI engine can have a stratified charge to reduce the throttling losses but this demands a more complicated exhaust after-treatment if operated lean.

The high temperature in the flame front in the SI engine raises the nitrogen-oxide (NOx) emissions. The NOx emissions can be reduced in a normal TWC if the engine is run stoichiometric. In the HCCI engine the temperature of the fuel/air mixture is raised during the compression stroke until it is autoignited around top dead center (TDC). The combustion temperature is lower than in an SI engine and this reduces NOx emission formation.

Since the heat release rate with autoignition is much higher than from a normal SI flame front the time window is very short for successful timing and all the right conditions have to be set during the intake stroke. The autoignition can be made with lean air/fuel mixtures and therefore throttling losses are reduced.

The implementation of HCCI on a SI engine is usually done with minor modification to the SI engine structure but this might need to be changed to maximize the potential of HCCI. The scope of this paper is to investigate the upper load range limit for a turbocharged HCCI engine by imposing some operating limits. The boost pressure versus back pressure is considered for best efficiency and balanced against the combustion noise reduction the increased boost has.

The HCCI combustion has been researched on the last decades now and there is published a lot of results but the operating limitations is often just a few. This paper shows which limitations one can expect the HCCI has to fulfill and how it influences the operating range.

EXPERIMENTAL SET-UP

ENGINE SYSTEM The test engine is an in-line four cylinder gasoline engine with a total displacement of 2.2L. The cylinder head is a 4-valve design with a pent-roof combustion chamber. There are some small squish areas on the intake and exhaust sides. The piston has a raised piston dome with a small bowl in the center. The intake channel is side-drafted with a low tumble design. The engine is direct injected (DI) with a slightly canted, centrally placed injector and is of the Spray-Guided type. The eight-hole solenoid fuel injector has a cone angle of 60^o. The canted spark plug is located close to the fuel injector and has an extended tip. To achieve HCCI combustion the engine is run with negative valve overlap (NVO), with short lift and short duration camshafts designed for a naturally aspirated (NA) HCCI engine. In Figure 1 the minimum and maximum valve timings is plotted. The variable valve timing (VVT) is controlled by hydraulic actuators at the camshafts, meaning there is a separate 50 crank angle degree (CAD) adjustment on both intake and exhaust valve timings. The engine is turbocharged by a variable geometry turbine (VGT), the VGT position is controlled by an electric actuator. The exhaust manifold is of pulse type with short individual runners straight to the turbine inlet as seen in Figure 2. On the intake side there is a water cooled charge intercooler. The aluminum intake manifold has short intake runners and a small volume, it is mounted tight against the cylinder head as seen in Figure 3.

The cooling system has an electric driven water pump and the coolant temperature is adjusted by the control system. Engine specifications are listed in Table 1.

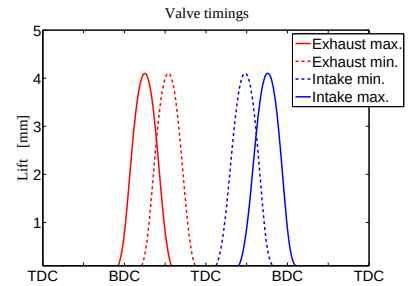

Figure 1: Valve timing range and setup

Figure 2: Exhaust manifold

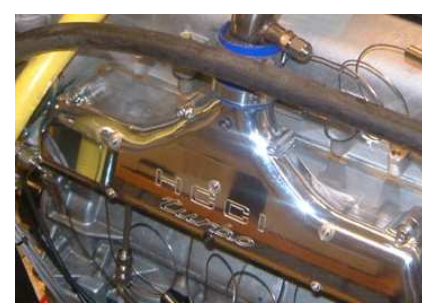

Figure 3: Intake manifold

MEASUREMENT AND CONTROL SYSTEM The control system is a combined data acquisition and engine control unit from dSPACE. The signals from a fully instrumented engine set-up are collected and analyzed. For combustion feedback there are individual cylinder pressure sensors. The control system has an in-cycle resolved heat release calculation where main parameters like timing for 50% heat released (CA50), peak cylinder pressure (PCP) and peak pressure derivative (dP/CAD) etc. are used for cylinder individual control in closed or open loop.

Emission analysis and soot measurement is collected on an external PC and the data is sent to the control unit. Table 2 shows the measurement and control equipment.

Table 1: Engine specifications

Number of cylinders	4
Displacement	2198 cm^3
Bore x Stroke	86 mm x 94.6 mm
Compression Ratio	11.75:1
Camshaft duration	125 CAD
Camshaft lift	4.1 mm
NVO range	44–144 CAD
Turbocharger	B&W BV35
Fuel Supply	DI, up to 20 MPa
Fuel Type	Gasoline, 95 RON

Table 2: Measurement and control system.

ECU and data logging	dSPACE Rapid Pro
Cylinder pressure sensor	Kistler 6043Asp
Charge amplifier	Kistler 5011B
Emission analyzer	Horiba 9100 MEXA
Soot analyzer	AVL 415 S

RESULTS AND DISCUSSION

The maximum load in HCCI is often limited by the fast combustion rate where the combustion induced noise is a major factor. By increasing the air dilution in the cylinder with for example turbocharging the audible noise is suppressed and the HCCI load range can be extended. By increasing possible load range in HCCI the total efficiency can be increased and there will be less need for HCCI-SI mode switching that imposes in itself some challenging control tasks. The mode switching can for example involve mechanical switching between SI and HCCI camshaft profiles. In fairness the boosted mode switches HCCI-SI adds more complexity since the intake manifold pressure is different in HCCI and SI mode.

Normally the pressure rise rate is measured in bar/CAD or MPa/ms [6] and is used to impose some operating limits but neither of these catch the real combustion noise when the engine is supercharged, the Ringing Intensity (RI)– MW/m^2 [7] on the other hand compares the pressure rise rate to peak cylinder pressure and engine speed. In this study RI has been used as a criterion to limit the pressure rise rate. In Figure 4 there is a comparison between these different pressure rise rate expressions when the load is constant and boost pressure is varied.

To be able to increase the load range we want as high intake pressure as possible to keep combustion noise at a low level, meaning we want a low RI number, preferably below 6 MW/m^2, a limit Eng[7] found that Lund used in earlier tests. It is common to operate the NVO HCCI with almost symmetrical valve timings, meaning that the intake valve opening (IVO) follows the exhaust valve closing (EVC). As the load gets higher less EVC is needed to keep the combustion timing and with these short duration camshafts the intake valve closing (IVC) will then be before bottom dead center (BDC). As seen in Figure 5 the boost pressure is increased by delaying IVC with asymmetrical valve timing to increase cylinder filling.

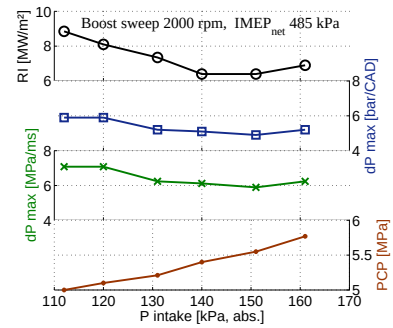

Figure 4: Boost sweep with different pressure rise rate expressions

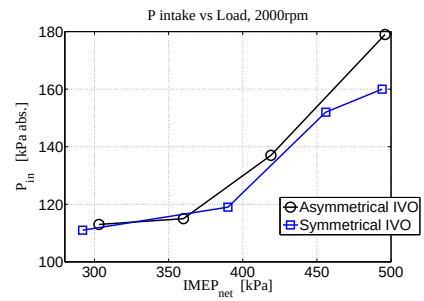

Figure 5: Load sweep with symmetrical valve timing and IVO locked at 72°aTDC

The achievable boost pressure has to be weighted against pumping losses due to turbocharger inefficiency and throttling losses over the valves, to keep engine efficiency as high as possible– see Figure 6. Is there a downfall with high boost pressure beside efficiency concerns?

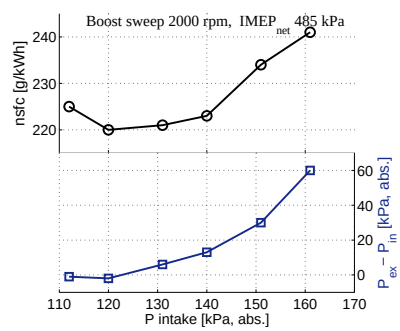

Figure 6: Boost sweep versus nsfc and back pressure

Since PCP scales with the intake pressure– see Figure 4, it can become a limiting factor. There is risk for structural damage of the engine if the design limit is exceeded. An example of consequences of high PCP can be seen in

Figure 7. The engine was operated at 2000 rpm and 600 kPa indicated mean effective pressure (IMEP$_{net}$), intake pressure at 220 kPa (abs.) and PCP at 10.5 MPa, RI at 8, when a piston failure occurred. Finite element analysis

Figure 7: Damaged piston due to high PCP

(FEA) reveals that the piston stress level was above the fatigue limit as seen in Figure 8. A redesign of the piston was made with increased top land height and the PCP limit was reduced to 8.5 MPa.

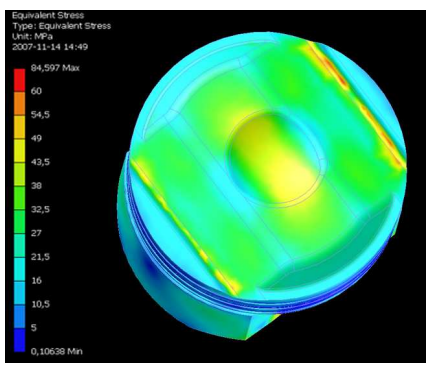

Figure 8: Piston failure FEA

The combustion phasing– CA50 is the main operating parameter when running in HCCI mode, a later CA50 can raise upper load limit by decreasing the RI and PCP as seen in Figure 9, this has to be weighted against an efficiency loss when moving away from the timing for maximum brake torque (MBT). A later CA50 will increase the energy to the turbine with higher boost as a result, here the turbocharger sizing plays an important role. The boosted HCCI engine can on the other hand for a given RI use a better phased combustion and hence improve thermal efficiency compared to a naturally aspirated HCCI engine. The temperature and pressure decreases after TDC, and since the autoignition is dependent on both to start the chemical reactions, there is an increase in cycle to cycle variances (CoV) with late combustion phasing. Is there a risk with too late combustion timing?

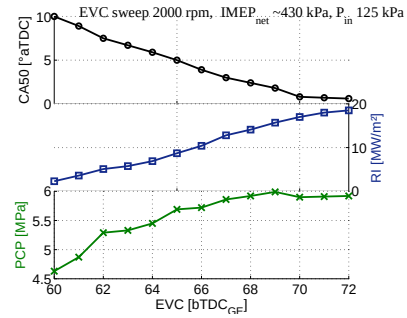

Figure 9: EVC sweep vs. CA50 and PCP

HCCI is known for its low CoV of IMEP$_{net}$ compared to SI engines but when load is maximized with a late CA50 the CoV of IMEP$_{net}$ increases. At higher engine speeds where the time window for proper combustion phasing is reduced, it is more difficult to retard the combustion. We have found that there is less possibility for misfire when the CoV is kept under 3.5%. Misfire at high HCCI load results in violent combustion the following cycles and must be avoided at all times.

To increase the operating range it is vital that all the cylinders operate identically, meaning that they have the same CA50 position, IMEP$_{net}$ and RI. This means that the control system has to perform cylinder balancing (CB). Injection of the fuel in NVO can give a reformation of the fuel with an increase in charge temperature and therefore advances the combustion timing, it will be more advanced if the fuel is injected in the beginning of the NVO than in the end, as seen in Figure 10 where a start of injection (SOI) sweep is done with fixed valve timings. The excess air during NVO injection influences the fuel reformation and the effect of combustion phasing is more pronounced at lean mixtures [8].

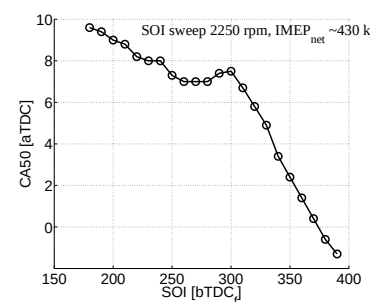

Figure 10: CA50 timing vs. SOI with single injection

The fuel injection timing has an influence on efficiency and soot. For example, injecting the fuel in the NVO sector will require a later EVC to keep the CA50 position correct. This means there will be less energy to the turbine and higher pumping losses from the exhaust blow-down with

this type of short duration camshaft operating at high load. Injecting the fuel too late will also decrease efficiency as seen in Figure 11 due to insufficient time for vaporization. By splitting up the fuel injection and injecting a part of the

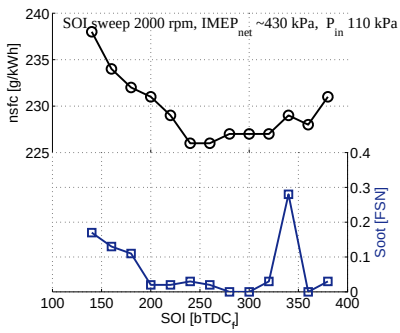

Figure 11: SOI sweep with single fuel injection

fuel in the NVO and the rest later, it is possible to have CB and injection timing with the highest fuel efficiency as seen in Figure 12, here 30% of the fuel is injected in the first injection.

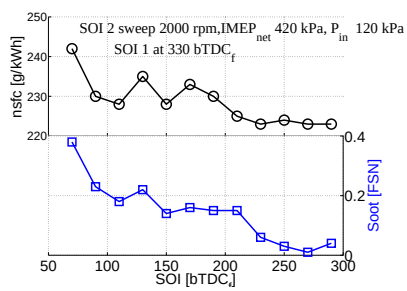

Figure 12: SOI sweep with double fuel injection timings

The control system sets the CA50 position and uses the cylinder with the most advanced CA50 position for EVC set point, the rest of the cylinders are then advanced by adjusting the injection timing and/or fuel amount in the first injection, until all cylinders have the same CA50 position. As there will be some differences in injection timing when using CA50 balancing there will also be some differences in efficiency between the cylinders. This results in different load– IMEP$_{net}$ between the cylinders. If we want to maximize the load range there has to be CB of IMEP$_{net}$ as well, this is done at the main injection event. Obviously this affect the CA50 balancing since increasing the fuel amount will raise the combustion heat– leading to earlier CA50 for that cylinder, so the CB has to be constantly monitored and adjusted by the control system.

Injecting the fuel around TDC when the piston is close to the injector raises the risk for fuel impingement on the piston surface, leaving a liquid fuel film that can lead to an increase in soot levels. As can be seen in Figure 11 and Figure 12, a late injection timing will also increase the soot level and lower the efficiency. These tests were done with 12 MPa fuel pressure. The soot level can be reduced by increasing the fuel pressure to enhance fuel vaporization, the fuel injector design together with piston design [9] will also influence soot formation. To get a FSN limit on soot we look at the Euro 5 and 6 legislation which limits the soot level to 0.005 g/km, if we assume a vehicle with a fuel consumption of 0.06 l/km or 44 g/km and operating at $\lambda = 1.5$ the Smoke opacity arrives roughly at 0.25 %[10] which corresponds to a FSN value of 0.05 [11].

HCCI is known for the low NOx emission levels but as the load increases, NOx emissions increase due to higher temperature and relative less dilution, meaning there will be a NOx limit when operating lean HCCI (and using a normal TWC). The Euro 5 and 6 limits the NOx emissions at 0.06 g/km, if we again assume a fuel consumption of 44 g/km, the corresponding NOx level will be 1.36 g/kg$_{fuel}$. To be on the safe side our NOx limit is set 20% below this value at 1.1 g/kg$_{fuel}$. With higher intake pressure the dilution increases and the NOx level is reduced as seen in Figure 13.

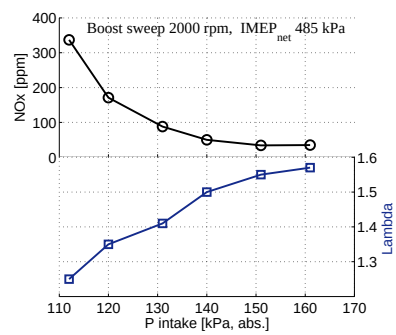

Figure 13: Boost sweep vs. NOx and Lambda

If the NOx level gets too high the engine has to be operated stoichiometric to meet the NOx legislation, there are some concerns about the low temperature in HCCI mode and operating with a TWC but in this engine the need for a TWC is at high load where the light off temperature of the TWC is reached. To run the engine stoichiometrically this engine has external exhaust gas recirculation (EGR). Two types of EGR routing are common; short and long, the short EGR bleeds off exhaust gas before the turbine inlet and route it to the compressor outlet on the intake side. This mean there is a loss of exhaust energy to the turbine– something that is already low in HCCI mode due to the low combustion temperature, leading to an unwanted decrease of intake boost. The long route EGR takes exhaust gas after the turbine and directs it to the compressor inlet. To get a positive displacement of exhaust gas there is a throttle in the exhaust system to increase back pressure. The compressor inlet can be used as an ejector to

enhance the EGR flow, so the needed back pressure is quite small.

The external EGR can be beneficial due to the thermodynamic cooling effect [12]. Advanced EVC timing is required in order to maintain constant CA50. Pumping losses are thus reduced due to more suitable valve timing at high load. On the other hand the advanced EVC timing increases the heat losses during recompression. The result in the end will depend on speed and load. A drawback with EGR in HCCI mode is the relatively slow response in a system that is normally cycle to cycle controlled, especially during transients. Another drawback is the added weight and cost. Instead of using external EGR the boost pressure should be as high as possible to increase the dilution and suppress the NOx emissions but it has to be weighed against the pumping losses.

When operating the engine at a global $\lambda = 1$ in conjunction with above described cylinder balancing of IMEP$_{net}$ there will be local difference in cylinder to cylinder lambda that can lead to increased CoV, and even to misfire from the cylinder running richest. The lambda difference between all the cylinders when balancing with IMEP$_{net}$ or lambda in two tests is shown in Figure 14. So when operating near $\lambda = 1$ there should be lambda balancing [13] instead of IMEP$_{net}$ balancing for stable engine running.

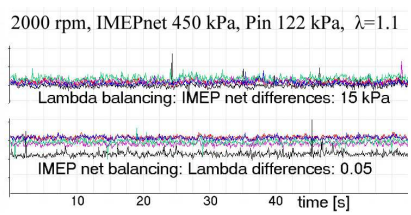

Figure 14: Cylinder balancing with IMEP$_{net}$ and Lambda

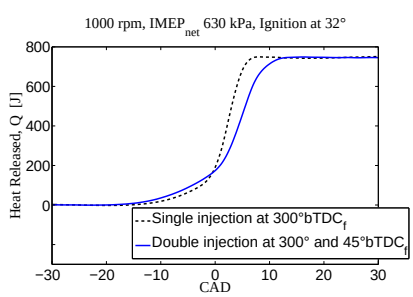

Figure 15: Heat release comparison

The HCCI operating is normally done without a spark to ignite the charge but we have seen that spark assist (SA) can give a lower CoV and thus enable a later combustion phasing. Especially at low engine speed and high load a later phasing is possible with low CoV with SA and thereby increasing possible load, here the NOx emissions is high and thus the engine is already operated stoichiometric. This means that the ignition timing is always adjusted depending on load and engine speed for best result but the influence from SA on the NOx emissions [14] has to be considered. The SA HCCI used in these tests has a normal steep HCCI heat release; in Figure 15 there is a heat release comparison between two injection strategies, the double injection with a small late second injection shows a slow initial heat release, that later becomes steeper. Even if RI is decreased here from 5.5 to 3.5 MW/m^2 with this double injection, the soot level is increased from 0.09 to unacceptable 1.39 FSN.

SPEED AND LOAD TESTING In order to make speed and load sweeps we set some operating limitations outlined previously that one can expect the HCCI engine has to fulfill. The operating limitations are set as following:

– RI below 6 MW/m^2
– CoV below 3.5%
– PCP below 8.5 MPa
– Soot average 0.05 FSN
– EI NOx below 1.1 g/kg$_{fuel}$ if lean, unlimited at stoichiometric

The turbocharged HCCI engine is tested from 1000 to 3000 rpm, from 300 kPa IMEP$_{net}$ and up to the point where operating limitations hinder further increase in possible load. The goal is to have low net specific fuel consumption (nsfc). We used cylinder balancing of combustion phasing and load with late combustion phasing without excessive fluctuations in IMEP$_{net}$. The split injection timings is adapted to every test point. Ignition timing is adjusted for low CoV or late CA50 as long there is no NOx penalty. IVO and EVC timing is most of the time asymmetrical set to increase cylinder filling with this turbo set-up. Fuel pressure during these tests are between 12–16 MPa. Desired fuel amount and VGT position are set manually.

The intake pressure as seen in Figure 16 scales with load and engine speed. Since the turbocharger is a bit large for this HCCI engine the highest intake pressure is around 180 kPa (abs.). The CA50 set-point has to be delayed from MBT timing to maximize exhaust energy and the VGT position is then adjusted for maximum boost. The short duration camshafts on this engine means that for higher loads, less EVC is needed and the exhaust valve opening (EVO) is then close to BDC where the available pressure to the turbine is small. This decreases possible boost pressure and increases pumping losses. When the boost pressure goes up the intake temperature also goes up, as seen in Figure 17. The intake temperature is measured inside the intake channel, 40 mm upstream the intake valve. This temperature is without any intercooler effect during these tests and scales to compressor efficiency plus the intake manifold that is integrated to the cylinder head in this engine set-up.

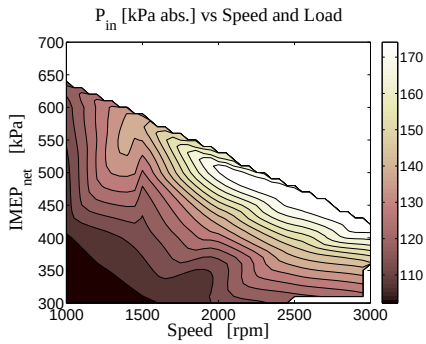

Figure 16: Speed and load testing– Intake pressure

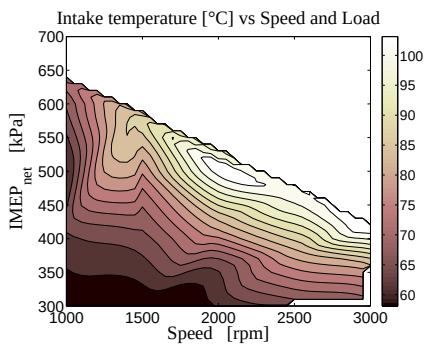

Figure 17: Speed and load testing– Intake temperature

When the emission index (EI) of NOx emission raises above the limitation at 1.1 g/kg$_{fuel}$ the engine is operated with cooled external EGR from the long route system. The EGR percentage is measured as the CO_2 ratio between the exhaust and the intake manifold. In Figure 18 the needed EGR is used to suppress NOx emissions, it is also used to decrease throttling losses over the valves at high engine speed by the increased EVC that is needed with EGR. At low engine speeds the exhaust flow to this turbine is insufficient to increase the boost pressure and therefore the air dilution is low, leading to high NOx levels and then the engine is operated stoichiometric.

The combustion phasing seen in Figure 19 is set for stable engine running without misfires. It is in most cases delayed from MBT to decrease peak pressure rise and to increase available exhaust energy to the turbine. The corresponding EVC position is plotted in Figure 20. When the EVC position is less than 55 CAD, EVO is after BDC.

The resulting nsfc is seen in Figure 21, the efficiency is best at 2000 rpm and up, at low engine speed the engine is run stoichiometric due to high NOx emissions. The increased in-cylinder heat capacity when operating stoichiometric leads to that the EVO phasing has to be advanced, further increasing the heat losses from the recompression. At this engine speed there is no gain in reducing

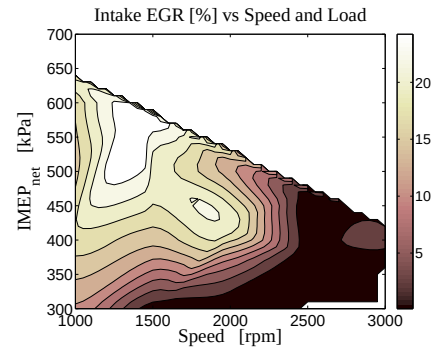

Figure 18: Speed and load testing– Intake EGR %

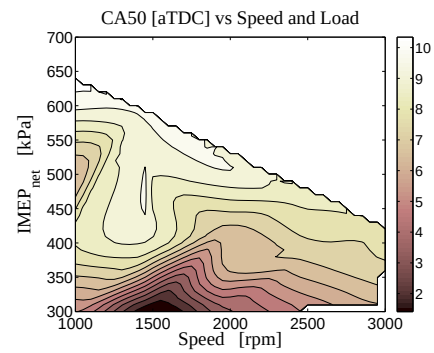

Figure 19: Speed and load testing– CA50 position

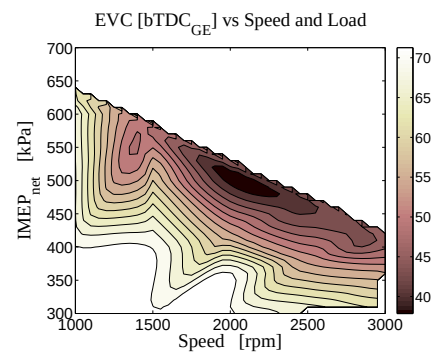

Figure 20: EVC position

pumping losses by advancing the EVC timing. At some low load points the EVC range is not enough to set the combustion phasing right and all the fuel is injected during the NVO. The testing is done so RI scales with load, meaning that there is room for improvement in nsfc at the cost of a higher RI.

The high pressure rise rate is the main limiting factor during these tests and is presented as RI in Figure 22. The

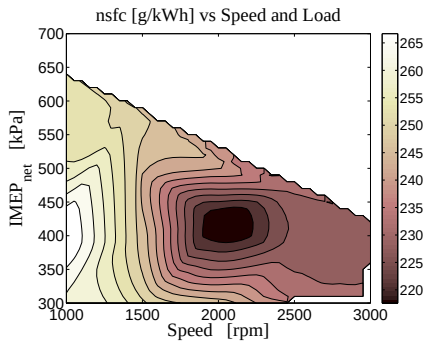

Figure 21: Speed and load testing– nsfc

maximum pressure rise in MPa/ms in Figure 23 has a similar shape as the RI. The corresponding maximum dP in bar/CAD is shown in Figure 24. The peak cylinder pressure is not a limiting factor in these tests, as seen in Figure 25.

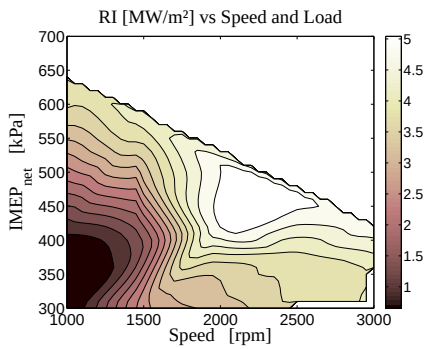

Figure 22: Speed and load testing– RI

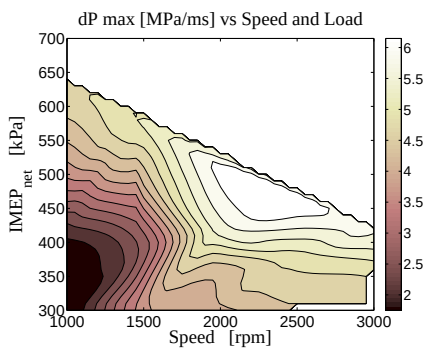

Figure 23: Speed and load testing– dP in Mpa/ms

In the highest speed range the CoV is a major factor against a late combustion timing even if is not obvious by

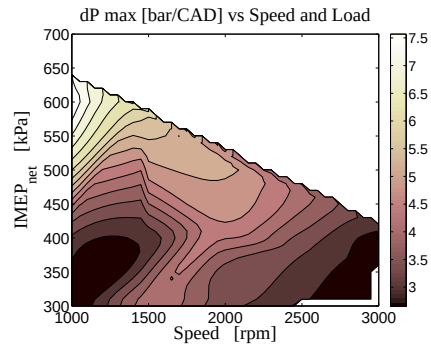

Figure 24: Speed and load testing– dP in bar/CAD

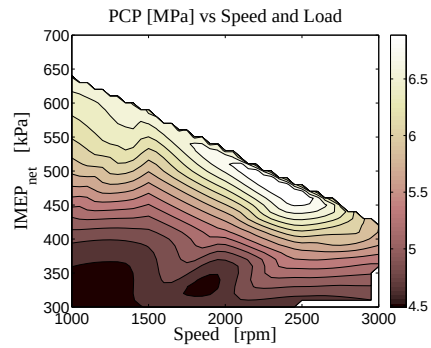

Figure 25: Speed and load testing– Peak cylinder pressure

looking at the Figure 26, here a tiny change of CA50 can drastically increase the CoV. The CoV is quite low except at 1500rpm/ 300 kPa IMEP$_{net}$, where both fuel injections had to be advanced into the NVO to get desired combustion phasing. At Figure 27 the CA10 to CA90 duration in that test point is short so here the cycle to cycle variations is high with all the fuel injected in the NVO. The area with longer CA10 to CA90 duration coincides also where the external EGR is used.

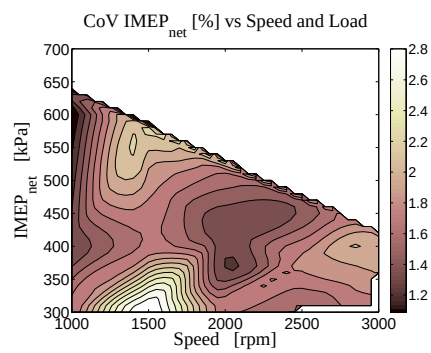

Figure 26: Speed and load testing– CoV of IMEP$_{net}$

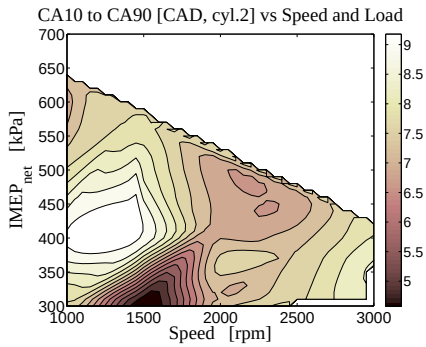

Figure 27: Speed and load testing– CA10 to CA90 duration

At high load and low engine speed the NOx emission as seen in Figure 28 increases and the engine is operated stoichiometric, see Figure 29, with cooled EGR from the long route system. The soot level in Figure 30 limited the possible load at 1000 rpm even if the fuel pressure here was increased from 12 MPa to 16 MPa.

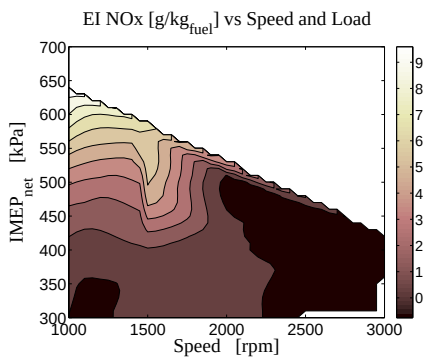

Figure 28: Speed and load testing– NOx emissions

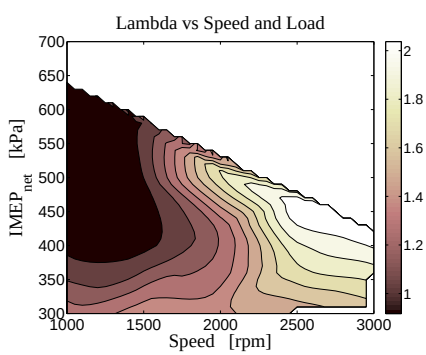

Figure 29: Speed and load testing– Lambda

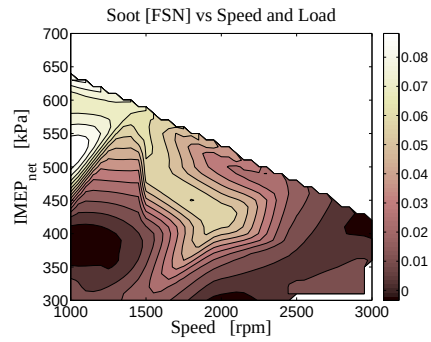

Figure 30: Speed and load testing– Soot

SPEED AND LOAD TESTING, EFFICIENCY BREAKDOWN The engine efficiency can be divided into small fractions as seen in Figure 31. The combustion efficiency is defined as the relationship between heat released (Q_{hr}MEP) and normalized fuel energy/ cycle (FuelMEP). The thermodynamic efficiency is then the relationship between IMEP$_{gross}$ and Q_{hr}MEP. Gas exchange efficiency is defined as the relationship between IMEP$_{gross}$ and IMEP$_{net}$. Indicated efficiency is the relationship between IMEP$_{net}$ and FuelMEP.

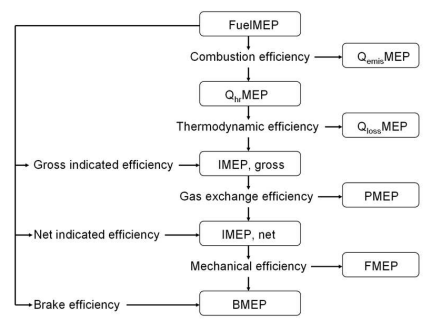

Figure 31: Engine efficiency break-down

The combustion efficiency in Figure 32 is stable throughout the speed and load test. The thermal efficiency in Figure 33 on the other hand show the increasing heat losses at low engine speed. Here the engine is operated stoichiometric which increases the recompression losses when the EVC timing has to be advanced due to the higher heat capacity from the increased external EGR.

Looking at the gas exchange efficiency in Figure 34, this turbocharged engine set-up can be improved on. By separating the pumping losses in two parts the reason to the low efficiency can be seen:
a. The pressure loss over turbine/compressor: $P_{ex} - P_{in}$ in Figure 35.
b. The pressure loss over inlet and exhaust valves: valve throttling in Figure 36.
With a turbocharger one usually encounters higher back

pressure than boost pressure, here the turbocharger is a bit large and therefore the VGT position has to be controlled for highest possible boost. The high throttling losses originates from the short duration exhaust camshaft, since late EVC is needed at high HCCI load the EVO can be close to BDC, leading to increased pumping work from the blow-down process. The resulting indicated efficiency is seen in Figure 37 for this turbocharged engine.

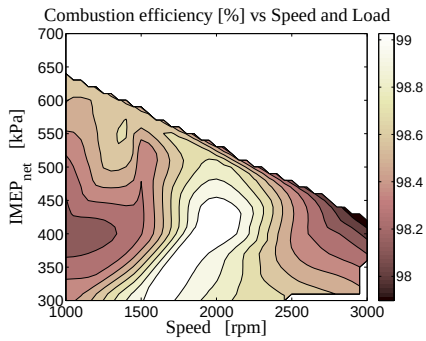

Figure 32: Combustion efficiency

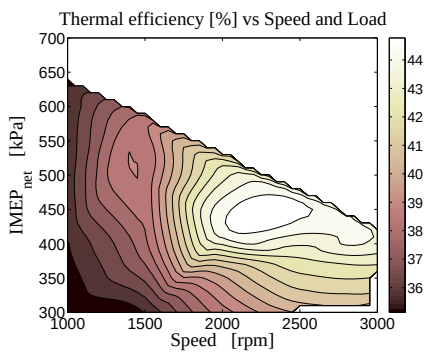

Figure 33: Thermal efficiency

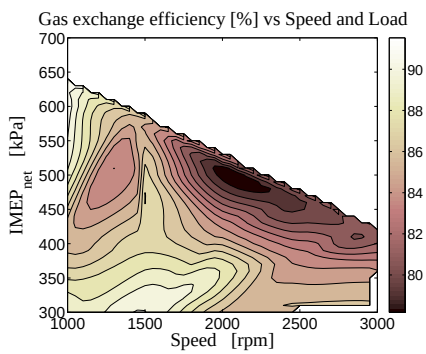

Figure 34: Gas exchange efficiency

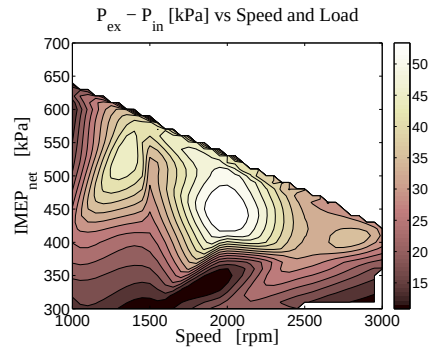

Figure 35: Pressure loss over turbine/compressor: $P_{ex} - P_{in}$

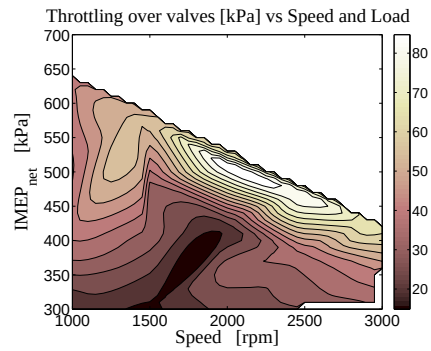

Figure 36: Pressure loss over inlet and exhaust valves: valve throttling

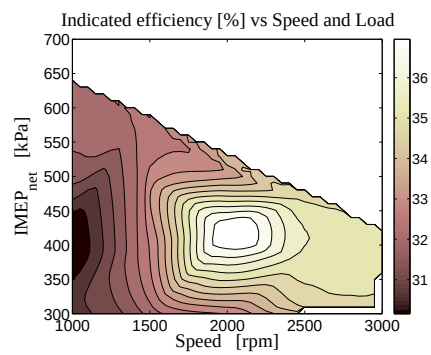

Figure 37: Indicated efficiency

DISCUSSION

When load is increased by this turbocharged HCCI engine the operating parameters all the time has to be balanced against each other. For example if we need to increase the load range where the pressure rise rate is too high the CA50 can be delayed if the CoV is stays low, the back pressure goes up from the delayed combustion timing and therefore the intake pressure and temperature is increased. The camshaft timing has to be changed to keep CA50 position meaning a later EVC is needed and therefore EVO comes later and there is risk for increasing throttling losses with these short duration camshafts. If the CA50 is delayed from MBT there will also be a loss in efficiency. On the other hand if we compare to a NA HCCI engine, we can operate on a combustion timing closer to MBT at high load with this boosted HCCI engine for the same RI number, leading to improved efficiency with right turbocharger sizing.

Finally in Figure 38 there is a comparison of possible load range between our turbocharged set-up and a naturally aspirated HCCI set-up; with an OEM style exhaust manifold. The limitations are the same and the control strategy and operating is the same, by turbocharging the possible load range is increased in the whole speed range.

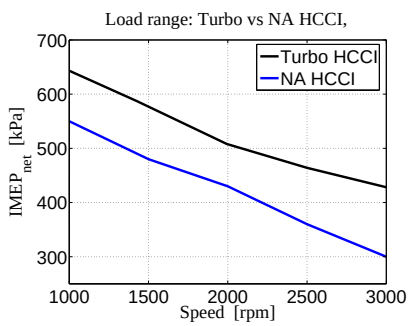

Figure 38: Maximum load: turbocharged vs. NA HCCI

CONCLUSIONS

- The pressure rise induced combustion noise is reduced with intake boost, leading to an increase of the capable HCCI operating range.
- The peak cylinder pressure can be a limiting factor when the boost pressure is high.
- Combustion phasing with cylinder balancing of CA50 with split injection together with cylinder balancing of IMEP$_{net}$ improve engine operating and maximize the load range.
- By delaying the combustion phasing to decrease the pressure rise rate there is risk of high CoV of IMEP$_{net}$ and the CoV has to be kept on a low level to suppress the possibility of misfire.
- Fuel pressure and injection timing control soot formation, and liquid film on the piston top should be avoided.
- When operating with a normal three-way catalyst the NOx emission at high load leads to that the engine must be operated stoichiometric with external EGR. Due to the slow response in the EGR system the air dilution by higher boost pressure should be preferred to suppress NOx formation.
- There is scope to increase the efficiency with better turbocharger sizing and valve timings that is better suited for this turbocharged HCCI engine.

ACKNOWLEDGMENTS

This project is supported by GM Powertrain and the Swedish Energy Agency

REFERENCES

[1] Christensen, M., Johansson, B., Amnéus, P. Mauss, F., "Supercharged homogeneous charge compression ignition," *SAE Paper 980787*.

[2] Christensen, M., Johansson, B., "Supercharged homogeneous charge compression ignition (hcci) with exhaust gas recirculation and pilot fuel," *SAE Paper 2000-01-1835*.

[3] Hyvönen, J., Haraldsson, G., Johansson, B., "Supercharging HCCI to extend the operating range in a multi-cylinder VCR-HCCI engine," *SAE Paper 2003-01-3214* .

[4] Olsson, J-O., Tunestål, P., Johansson, B., "Boosting for high load HCCI," *SAE Paper 2004-01-0940*.

[5] Heywood, J. B., "Internal Combustion Engine Fundamentals," McGraw-Hill, New York, 1988.

[6] Andreae, M.M, Cheng, W.K., Kenney, T., Yang, J., "On HCCI Engine Knock," *SAE Paper 2007-01-1858*.

[7] Eng, J.A., "Characterization of pressure waves in HCCI combustion," *SAE Paper 2002-01-2859*.

[8] Koopmans, L., Ogink, R., Denbratt, I., "Direct gasoline injection in the negative valve overlap of a homogeneous charge compression ignition engine," *SAE Paper 2003-01-1854*.

[9] Yang, J., Kenney, T., "Some concepts of DISI engine for high fuel efficiency and low emissions," *SAE Paper 2002-01-2747*.

[10] www.DieselNet.com," *Smoke Opacity*.

[11] Schindler, W., Nöst, M., Thaller, W., Luxbacher, T., "Stationäre und transiente messtechnische Erfassung niedriger Rauchwerte," *MTZ 2001 / 10*.

[12] Sjöberg, M., Dec, J.E., Hwang, W., "Thermodynamic and Chemical Effects of EGR and Its Constituents on HCCI Autoignition," *SAE Paper 2007-01-0207*.

[13] Yamaoka, S., Kakuya, H., Nagakawa, S., Okada, T., Shimada, A., Kihara, Y., "HCCI Operation Control in a Multi-Cylinder Gasoline Engine," *SAE Paper 2005-01-0120*.

[14] Persson, H., Pfeiffer, R., Hultqvist, A., Johansson, B., Strm, H., "Cylinder-to-Cylinder and Cycle-to-Cycle Variations at HCCI Operation With Trapped Residuals," *SAE Paper 2005-01-0130*.

CONTACT

Thomas Johansson, M.Sc.ME

E-mail:Thomas.Johansson@energy.lth.se

Lund University, Faculty of Engineering, Department of Energy Sciences, Division of Combustion Engines, P.O. Box 118, SE-221 00 Lund, Sweden

DEFINITIONS AND ABBREVIATIONS

abs.:	Absolute
BDC:	Bottom Dead Center
BMEP:	Brake Mean Effevtive Pressure
CA10:	Crank angle 10% burned
CA50:	Crank angle 50% burned
CA90:	Crank angle 90% burned
CB:	Cylinder Balancing
CAD:	Crank Angle Degrees
COV:	Coefficient of Variation
DI:	Direct Injection
dP:	Pressure derivate
EI:	Emission Index
EGR:	Exhaust Gas Recirculation
EVC:	Exhaust Valve Closing
EVO:	Exhaust Valve Open
FEA:	Finite Element Analysis
FMEP:	Friction Mean Effevtive Pressure
FSN:	Filter Smoke Number
FuelMEP:	Fuel Mean Effective Pressure
HCCI:	Homogeneous Charge Compression Ignition
$IMEP_{gross}$:	Indicated Mean Effective Pressure, gross
$IMEP_{net}$:	Indicated Mean Effective Pressure, net
IVC:	Intake Valve Closing
IVO:	Intake Valve Opening
NA:	Naturally Aspirated
NOx:	Nitrogen Oxide
nsfc:	Net Specific Fuel Consumption
NVO:	Negative Valve Overlap
MBT:	Maximum Brake Torque
OEM:	Original Equipment Manufacturer
P ex:	Pressure Exhaust
P in:	Pressure Intake
PCP:	Peak Cylinder Pressure
PMEP:	Pumping Mean Effevtive Pressure
Q_{emis}MEP:	Emission Mean Effevtive Pressure
Q_{hr}MEP:	Heat Release Mean Effevtive Pressure
Q_{loss}MEP:	Heat losses Mean Effevtive Pressure
RON:	Research Octane Number
RI:	Ringing Intensity
SA:	Spark Assist
SI:	Spark Ignition
SOI:	Start of Injection
TDC:	Top Dead Center
TDC_f:	Top Dead Center, firing
TDC_{GE}:	Top Dead Center, gas exchange
TWC:	Three-Way Catalyst
VGT:	Variable Geometry Turbine
VVT:	Variable Valve Timing

Paper II

THERMODYNAMIC MODELLING AND CONTROL OF A NEGATIVE VALVE OVERLAP TURBO HCCI ENGINE

Hans Aulin
GM Powertrain Sweden
Trollhättan Sweden
email: hans.aulin@gm.com

Thomas Johansson, Per Tunestål,
Bengt Johansson
Div. of Combustion Engines
Lund Institute of Technology
Sweden

ABSTRACT
It is tractable to increase the torque for an HCCI engine and one way is to add a turbocharger. Operating in HCCI mode requires accurate control of the combustion phasing, CA50. The higher the engine torque, the narrower the CA50 window becomes where HCCI operation is maintained. As the CA50 varies stochastically between cycles this requires improved CA50 control for turbo HCCI engines. The main factors affecting CA50 is the mass/temperature of the inducted air and the residuals kept from last engine cycle. The residuals can be controlled by advancing or retarding the timing for exhaust valve closure, EVC. A turbo adds to the overall complexity due to temperature and pressure dynamics introduced over the intake and exhaust manifold. A model based CA50 controller is proposed consisting of a feed-forward and a feedback part. A linear state space model is derived from a nonlinear thermodynamic model predicting five states in the cylinder (cylinder temperature, mass oxygen, mass residuals, wall temperature and pressure). The state space model is used for constructing a feed forward filter and a LQG controller for EVC. The controller was successfully tested and evaluated in simulations.

KEY WORDS
Turbo HCCI, Modeling, simulation, LQG Control, Kalman filtering, NVO.

1 Introduction

A large challenge to take the HCCI engine from a test bed environment to real production vehicles is CA50 control. The combustion concept does not really have any direct means to control when combustion starts such as the spark for the SI engine or the time of injection as for the diesel engine. The right temperature must be set at IVC to achieve compression ignition at the right time instant. This is achieved by controlling EVC before top dead center, TDC to capture more or less hot residuals that will mix with the fresh charge. As the pressure rise rate depends on the amount of available air and residual gas fraction a turbo is mounted to the engine yielding an increase in operating range [1]. The higher the engine load for this engine configuration, the narrower the CA50 window becomes where HCCI operation can be maintained. Too early combustion will lead to high pressure rise rate and noise. Too late combustion will lead to misfires. As the CA50 varies stochastically between cycles this requires precise control of EVC. The intake, exhaust pressure and temperature dynamics introduced by the turbo system add to the overall complexity for managing sufficient control. These challenges are handled using a model based approach. Two models are constructed, one four state black box model to handle the turbo pressure dynamics and one physical engine model based on well known thermodynamic equations. The physical model has been linearized to a five state model. The two models were used to construct an LGQ feedback controller and a feedforward filter. The controller was successfully tested in simulations. The results show a promising and intuitive approach for negative valve overlap (NVO) controllers on Turbo HCCI engines.

2 The Nonlinear HCCI Model

The nonlinear engine state space model is updated once every cycle. For every cycle a state vector X (descibing the in cylinder relations) is calculated

$$X = \begin{bmatrix} m_a & m_e & T & P & T_w \end{bmatrix}^T \tag{1}$$

The states m_a and m_e describe the two species mass air and exhaust mass residuals. To be able to compute a complete engine cycle three other states describing mixture temperature, T, wall temperature, T_w and cylinder pressure, P are required. The relations describing the dynamics for one cycle to another are, for the purpose of readability, divided into several processes according to Fig.1. A complete cycle is defined as going from the process ”combustion” to the process ”heat transfer” in the figure. The equations used for each process is presented in Sections 2.1 to 2.8. Fig.2 illustrates the steps using a cylinder pressure trace. The numbers in the figure denote each process. The main objective for the model is to predict CA50 using an equation describing how it relates to estimated mixture temperature, speed and fuel mass.

.

$$
\begin{array}{l}
Inputs \\
\downarrow \\
Combustion \rightarrow Expansion \rightarrow Blowdown \rightarrow EVC \\
\uparrow \qquad\qquad\qquad\qquad\qquad\qquad\qquad\qquad \downarrow \\
Heattransfer \leftarrow Compression \leftarrow IVC \leftarrow IVO \\
\downarrow \\
CA50\ estimation
\end{array}
$$

Figure 1. Process flow describing the nonlinear model. One cycle is defined as the calculations needed to go from combustion to heat transfer.

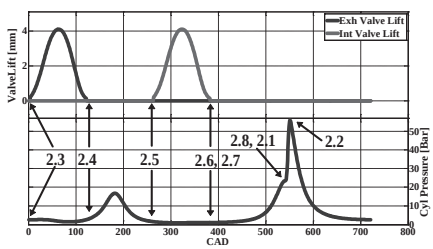

Figure 2. Valve lift and cylinder pressure trace for a cycle with process numbers according to the section numbers in the text. A complete cycle is defined as going from the point combustion (2.1) to heattransfer (2.8).

2.1 Combustion

The model assumes instantaneous combustion at top dead center (see arrow 2.1 in Fig. 2). The calculations started from here are based on the states calculated from previous cycle (See Eq.1). The temperature increase depends on the amount of energy released during combustion and the total mass in the cylinder

$$T_2 = \frac{m_{fuel} Q_{LHV}}{(m_a + m_e) C_v} + T \tag{2}$$

T_x, m_{ax}, m_{ex} and C_v denotes the temperature, mass air, mass exhaust and specific heat. With known temperature T_2 and constant volume at combustion the cylinder pressure, P_2 can be calculated using the ideal gas law

$$P_2 = \frac{PT_2}{T} \tag{3}$$

Assuming that all needed oxygen for complete combustion is used the amount of unused air left is given by

$$m_{a2} = m_a - m_{fuel} \left(\frac{A}{F}\right)_s \tag{4}$$

where $\left(\frac{A}{F}\right)_s$ is the stoichiometric air to fuel mass ratio. Due to the closed valves the total mass in the cylinder is constant. The mass of exhaust is then increased according to

$$m_{e2} = m_e + m_{fuel} \left(\frac{A}{F}\right)_s \tag{5}$$

The wall temperature is unchanged

$$T_{w2} = T_w \tag{6}$$

2.2 Expansion

If the heat losses are ignored isentropic relations can be used to describe how temperature, T_3 and pressure P_3 relate to T_2 and P_2. Expansion to cylinder volume at exhaust valve opening is therefore given by

$$T_3 = T_2 \left(\frac{V_{tdc}}{V_{evo}}\right)^{\gamma - 1} \tag{7}$$

and

$$P_3 = P_2 \left(\frac{V_{tdc}}{V_{evo}}\right)^{\gamma} \tag{8}$$

where V_{tdc} and V_{evo} are the cylinder volumes directly after combustion and at exhaust valve opening respectively. γ is the polytropic exponent and is assumed constant. The other parameters are changed according to

$$m_{a3} = m_{a2},\ m_{e3} = m_{e2},\ T_{w3} = T_{w2} \tag{9}$$

2.3 Blowdown

After exhaust valve opening blowdown occurs when the exhausts expands to manifold pressure. The temperature after expansion can be calculated according to

$$T_4 = T_3 \left(\frac{P_{exh}}{P_3}\right)^{\frac{\gamma - 1}{\gamma}} \tag{10}$$

where P_{exh} is the exhaust manifold pressure. The other parameters are changed according to

$$m_{a4} = m_{a3},\ m_{e4} = m_{e3},\ P_4 = P_{exh},\ T_{w4} = T_{w3} \tag{11}$$

2.4 Exhaust Valve Closing

The early closing of the exhaust valves will cause the cylinders to capture a significant amount of hot residuals. The temperature and the amount of these residuals will have a large impact on temperature, equivalence ratio and combustion phasing for the following cycle. Using the ideal gas law just before EVO and at EVC and combining the two will give

$$m_{a5} = \frac{m_{a2} V_{evc} P_{exh} T_3}{(\eta V_{evo} P_3 T_4)} \tag{12}$$

and

$$m_{e5} = \frac{m_{e3} V_{evc} P_{exh} T_3}{(\eta V_{evo} P_3 T_4)} \quad (13)$$

The tuning parameter η is statically mapped in the model and depends on speed and cam phasing. It is used to compensate for the higher pressure in the cylinder compared to the manifold due to throttling over the low lift valves. η is at high boost/load quite low (minimum is approx 0.5). Obviously, the low lift valves, introduce throttling lossses and remove part of the advantage that HCCI otherwise is well known for. The other parameters are unchanged.

$$P_5 = P_{exh},\ T_{w5} = T_{w4},\ T_5 = T_4 \quad (14)$$

2.5 Expansion to Intake Manifold Pressure

The exhaust residual mixture captured in the negative valve overlap is recompressed and then expanded to manifold pressure. The temperature T_6 of the residuals at intake pressure is given by

$$T_6 = T_4 \left(\frac{P_{in}}{P_{exh}} \right)^{\frac{\gamma-1}{\gamma}} \quad (15)$$

Where P_{in} is the intake manifold pressure. The other parameters are changed according to

$$m_{a6} = m_{a5},\ m_{e6} = m_{e5},\ P_6 = P_{in},\ T_{w5} = T_{w4} \quad (16)$$

2.6 Mixing of Residuals at Intake Valve Closure

The hot residuals are mixed together with the intake manifold air yielding a lower mixture temperature, T_7 at IVC. By combining

$$T_7 = \frac{P_{in} V_{ivc} \eta}{(m_{a7} + m_{a5} + m_{e5}) R} \quad (17)$$

and

$$T_7 = \frac{(m_{a5} + m_{e5}) T_6 + m_{a7} T_{in}}{m_{a5} + m_{e5} + m_{a7}} \quad (18)$$

(where specific heat is assumed to be equal for the residuals and the fresh air) and solving for m_{a7}, the amount of inducted air gives the following expression

$$m_{a7} = \frac{P_{in} V_{ivc} \eta - R T_6 m_{e5} - R T_6 m_{a5}}{R T_{in}} \quad (19)$$

Throttling over the intake valves is assumed to be similar during exhaust and intake hence the same η is used in both Eq.12 and Eq.13. The other parameters are changed according to

$$m_{e7} = m_{e6},\ P_7 = P_6,\ T_{w7} = T_{w6} \quad (20)$$

2.7 Compression to TDC

As during expansion the heat losses are ignored and the isentropic relations can be used

$$T_8 = T_7 \left(\frac{V_{ivc}}{V_{tdc}} \right)^{\gamma-1} \quad (21)$$

$$P_8 = P_7 \left(\frac{V_{ivc}}{V_{tdc}} \right)^{\gamma} \quad (22)$$

The other parameters are changed according to

$$m_{a8} = m_{a7},\ m_{e8} = m_{e7},\ T_{w8} = T_{w7} \quad (23)$$

2.8 Heat Transfer From the Walls

A slow drift of CA50 is typically seen after an increase or decrease in injected fuel amount, with all actuators steady directly after the transient. This drift is caused by changes in intake and cylinder wall temperatures. The influence from the walls can be accounted for by using equations as follows [2]

$$\frac{\partial T_h}{\partial t} = A T_h + B T_{Coolant} \quad (24)$$

Where

$$A = \begin{bmatrix} -\frac{h_c A_c}{m C_v} & \frac{h_c A_c}{m C_v} \\ 2\frac{h_c A_c}{m_c C_p} & -2\frac{h_c A_c + \frac{k_c A_c}{L_c}}{m_c C_p} \end{bmatrix} \quad (25)$$

$$B = \begin{bmatrix} 0 \\ \frac{2 k_c A_c}{L_c m_c C_p} \end{bmatrix} \quad (26)$$

and

$$T_h = \begin{bmatrix} T \\ T_w \end{bmatrix} \quad (27)$$

The heat transfer coefficient, h_c is given by Woschni's correlation [3]

$$h_c = \frac{3.26 P^{0.8} w^{0.8}}{B^{0.2} T^{0.55}} \quad (28)$$

m and m_c are the gas mixture and cylinder wall masses respectively. A_c, L_c represent cylinder wall area and thickness. C_p is the wall heat capacity and k_c is the conduction coefficient. T_w is the wall temperature. w and B denote engine speed and bore respectively. The described model is continuous and is therefore converted to discrete time by using zero order hold. The discrete model is used to update the parameters T and T_w. The other parameters are changed according to

$$m_a = m_{a8},\ m_e = m_{e8},\ P = P_8 \quad (29)$$

This process step completes a cycle and the state vector is updated. It is time to start over again with combustion for the next cycle.

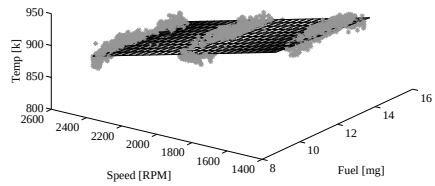

Figure 3. Approximated temperatures required to initiate combustion with a CA50 of 5 at different loads and speed. Gray stars denote experimental results.

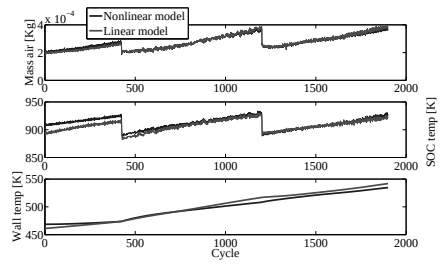

Figure 4. Comparison between the linear and the original, nonlinear model for a fuel sweep from 3 to 5 bar at cycle 1 to 500 @1500RPM, cycle 500 to 1300 @2000RPM and cycle 1300 to 1800 @2500RPM. The linear model follows the nonlinear successfully but has some small deviation for the first 500 cycles.

2.9 CA50 Estimation

The most important part of the model is to predict the combustion phasing, CA50. A link from the states estimated after the heattransfer process step is needed to calculate CA50 (Fig.1). The main parameters affecting the combustion phasing are the mixture temperature, the oxygen concentration and pressure/temperature history. In similar work different approaches involving the Arrhenius knock integral model have been used to take these factors into account [4], [5], [6]. The Arrhenius model is based on an exponential correlation between the temperatures and pressures in the cylinder. Here a simple approach suitable for controller design has been taken. It is assumed that the main combustion trigger is the temperature at TDC. This temperature may differ depending on speed and fuel mass. Using the nonlinear engine model estimated temperatures for different load, speed, measured CA50 and correlating them against Eq. 30 yields a simple model for estimating combustion phasing.

$$CA50 = K_1 T + K_2 m_{fuel} + K_3 w + K_4 \qquad (30)$$

Given experimental data, a least-squares estimation of the parameters K_1 to K_4 can easily be achieved [7]. The equation is the last part of the engine model (see CA50 Estimation in Fig.1) The complete engine model can now be used for estimating mass air, mass exhaust, mixture temperature, wall temperature , pressure and finally combustion phasing during transients. Fig.3 illustrates estimated temperatures needed to initiate combustion with a CA50 of 5 CAD after top dead center,ATDC.

2.10 Combining the Process Equations

By combining Eq.2 to Eq.29 five nonlinear equations are given describing the states, X in the cylinder (see 1).

3 Linearization

Making Taylor approximations of the nonlinear equations at an operating point preferably around the middle of the speed load range yields a linear discrete state space model of the form

$$\begin{bmatrix} m_a(k) \\ m_e(k) \\ T(k) \\ P(k) \\ T_w(k) \end{bmatrix} = A \begin{bmatrix} m_a(k-1) \\ m_e(k-1) \\ T(k-1) \\ P(k-1) \\ T_w(k-1) \end{bmatrix} + B \begin{bmatrix} \eta \\ m_{fuel} \\ V_{evo} \\ V_{evc} \\ V_{ivc} \\ T_{in} \\ P_{in} \\ P_{exh} \\ w \\ T_{coolant} \end{bmatrix}$$
$$Y = \begin{bmatrix} 0 & 0 & 1 & 0 & 0 \end{bmatrix} \begin{bmatrix} m_a(k) \\ m_e(k) \\ T(k) \\ P(k) \\ T_w(k) \end{bmatrix} \qquad (31)$$

This linear model is very similar to the original model over a wide operating range (Fig. 4). Evaluation of the model proved it to be both controllable and observable, making it suitable for controller design.

4 Exhaust and Intake Pressure Turbo Models

The proposed engine model predicts the states inside the cylinders. The model needs a number of inputs but some of these, intake and exhaust pressure are greatly affected by the turbo and must therefore also be modelled. This is done by making a system identification of the pressure dynam-

Figure 5. The turbo model with the look up table for compensation of nonlinearities.

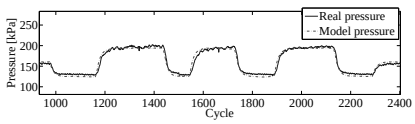

Figure 6. Results for the turbo intake pressure model compared to experimental data for load steps between 3 to 5.2 Bar. Results were similar for the exhaust pressure

ics in the intake and exhaust, Yielding a black box model. The experimental data used for this work was excited by perturbing the load with a pseudorandom binary sequence. In total two four state models were identified for the turbo model, one for the exhaust and one for the intake pressure using the N4SID function with Matlab system identification toolbox. To compensate for some of the nonlinearities, the model uses a lookup table used for estimation of steady state pressure at different speed and load. The black box model is only used to capture the transient dynamics (see Fig. 5). A future work would be to replace this model using a mean value model strategy of the turbo and the intake/exhaust.

5 Model Validation

The models are implemented in Simulink and a set of experimental engine transient data are compared to simulated data. Fig.6 illustrates simulated versus measured intake manifold pressure. The turbo model captures the dynamics well. Fig. 7 and 8 illustrate step responses for estimated and real experimental results during load steps from 3 to 5 to 3 bar. In these experiments EVC was mapped against fuel. Fig. 7 shows estimated versus measured air to fuel ratio, lambda. The rapid increase in fuel causes the air to fuel ratio spikes during the transients. After a while the turbo starts to build up pressure and the air to fuel ratio settles to a steady-state value. The opposite occurs at high to low load. The lambda sensor is too slow and is also mounted too far away from the exhaust valves to capture these dynamics. Fig. 8 illustrates how simulated, measured CA50 and wall temperature change during the load steps. The figure shows how CA50 starts to drift after the load changes and how well the model captures this behavior. The drift is caused by changes of intake air temperature and wall temperature dynamics. The described behavior is a good

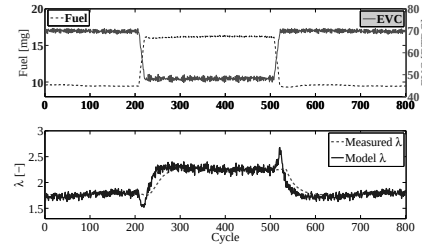

Figure 7. Estimated versus measured lambda during a load transient. The model captures dynamics that the sensor is unable to resolve.

example describing why simple mapping is not enough to handle control during transients.

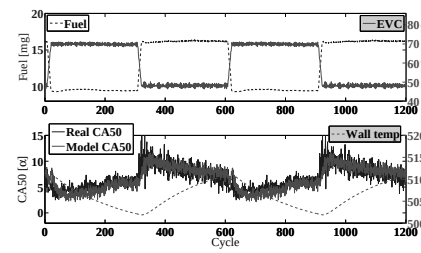

Figure 8. Simulated and measured CA50 during a set of load steps. The model captures the drifting CA50 due to changes in intake and wall temperature.

6 The Resulting CA50 Controller for EVC

The controller is designed based on the turbo and the linearized engine models. Fig. 9 gives a brief introduction describing the signal flow surrounding the controller. The different parts describing the controller are the CA50 to temperature calculations, the Kalman filter, the feedback controller and the feedforward.

6.1 CA50 to Temperature

This part of the controller converts CA50 to a temperature estimate. The estimation is used for temperature feedback and reference calculations for the controller (See Fig. 9). Inverting Eq. 30 to

$$T = \frac{CA50 - K_2 m_{fuel} - K_3 w - K_4}{K_1} \qquad (32)$$

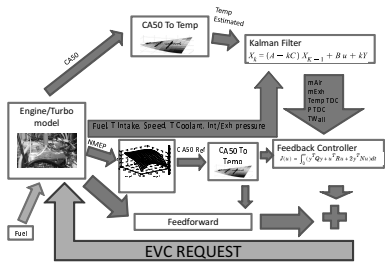

Figure 9. Overview describing the flow of signals as it looks when running the model against the controller. The turbo and the engine models are here combined as Engine/Turbo model.

Yields the expression describing the conversion.

6.2 Kalman Filter for Engine State Estimation

The controller uses the engine states for feedback however most of these states are not measurable and must therefore be estimated. This is done using the engine model together with a Kalman filter

$$\begin{bmatrix} \hat{m_a}(k) \\ \hat{m_e}(k) \\ \hat{T_c}(k) \\ \hat{P}(k) \\ \hat{T_w}(k) \end{bmatrix} = [A - KC] \begin{bmatrix} m_a(k-1) \\ m_e(k-1) \\ T(k-1) \\ P(k-1) \\ T_w(k-1) \end{bmatrix} + .. \\ B \begin{bmatrix} \eta \\ m_{fuel} \\ V_{evo} \\ V_{evc} \\ V_{ivc} \\ T_{in} \\ P_{in} \\ P_{exh} \\ w \\ T_{coolant} \end{bmatrix} + kY(k-1) \tag{33}$$

The measured output, Y is the temperature of the mixture at TDC. It is calculated using the CA50 measurements, current fuel and speed using Eq.32.

6.3 State Feedback Controller

The feedback controller is a MISO LQG controller with the control law $u = -K\hat{x}$ where $\hat{x}$ contains the estimated states from the Kalman filter and an additional integrator state. The values of the feedback gain matrix, K are estimated by optimizing the quadratic cost function

$$J(U) = \int_0^\infty (Y^T QY + U^T RU + 2Y^T NU)dt \tag{34}$$

Where Q and R are weighting matrices, Y the output (Tmix) and U the vector of inputs for the engine model. The additional integrator state was implemented by augmenting the model according to

$$\begin{bmatrix} x(k+1) \\ x_i(k+1) \end{bmatrix} = \begin{bmatrix} A & 0 \\ C & I \end{bmatrix} X(k) + \begin{bmatrix} B \\ 0 \end{bmatrix} U(k) + .. \\ \begin{bmatrix} 0 \\ I \end{bmatrix} r(k) \tag{35}$$

In this way error free tracking can be accomplished. Due to the CA50 to temperature conversion the controller believes that it controls the mixture temperature.

6.4 Inverted Engine Model For Feedforward

The model's capability to predict the engine behaviour is used for feedforward. Transfer functions for mass fuel to mixture temperature/pressure and for EVC to temperature are derived from the discrete engine and turbo state space models

$$\begin{array}{ll} P_{exh}(z) = \frac{b_1(Z)}{a_1(Z)} m_{fuel}(z) & T(z) = \frac{b_2(Z)}{a_2(Z)} P_{exh}(z) \\ V_{evc}(z) = \frac{a_3(Z)}{b_3(Z)} T(z) & P_{in}(z) = \frac{b_4(Z)}{a_4(Z)} m_{fuel}(z) \\ T(z) = \frac{b_5(Z)}{a_5(Z)} P_{in}(z) & T(z) = \frac{b_6(Z)}{a_6(Z)} m_{fuel}(z) \end{array} \tag{36}$$

Inverting the transfer function for EVC to temp and combining the other transfer functions yields an expression for feed forward during reference temperature and load steps with the following structure

$$V_{evc} = \frac{a_3(z)T(z)}{b_3(z)} + \frac{a_3(z)b_5(z)b_4(z)m_{fuel}(z)}{b_3(z)a_5(z)a_4(z)} + ... \\ \frac{a_3(z)b_2(z)b_1(z)m_{fuel}(z)}{b_3(z)a_2(z)a_1(z)} + \frac{a_3(z)b_6(z)m_{fuel}(z)}{b_3(z)a_6(z)} \tag{37}$$

Where T is the reference value, fuel is the requested fuel amount. The filter that is given by this expression is the feed forward for exhaust valve closure. If the engine would behave exactly according to the model this would give very precise feedforward.

7 Simulations

The LQG controller was implemented in Simulink and tested against the HCCI model. Simulations were used to tune the controller that was subsequently used in the real control system. Fig. 10 shows the results of different load steps at 2000 RPM when using the LQG controller but without feedforward. Note the large deviations during the transients. In Fig.11 the same steps are shown but with the feedforward activated the system follows the reference trajectory very well.

8 Conclusion

A nonlinear HCCI model has been developed and linearized to give a 5 state model of the engine. The model

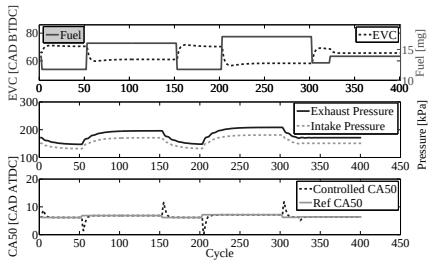

Figure 10. Load transients using the LQG controller to stabilize CA50. The controller error is quite large during the transient.

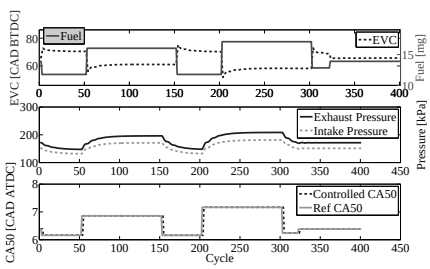

Figure 11. Load transients using the LQG controller together with the feedforward filter to stabilize CA50. The CA50 follows the reference very precise. Note the different scale for the CA50 axis compared to the transient without feedforward.

does a good job predicting the combustion phasing. It takes the intake and exhaust pressures into account something particularly important when running HCCI with Turbo. Even though a number of simplifications have been made, the model is precise enough to capture the general trends and dynamics of the engine. To tune the model, two tuning procedures must be performed. First, the tuning parameter, η describing the throttling losses must be calibrated against experimental mass air flow, speed and mass fuel. Second, Experimental data from at least two fuel sweeps at minimum to maximum load, at lowest and highest speed are needed to adapt Eq. 30 to describe how the combustion phasing relates to the cylinder temperature, speed and fuel. A simple model is fitted using least-squares estimation. The low complexity in the proposed strategy makes the model straight forward to implement and tune. Evaluation of the model proved it to be both controllable and observable, making it well suited for its main purpose of being used for controller design. The engine model predicts the states inside the cylinder but the external states, the exhaust and intake pressure are modelled using a black box model derived from experimental data. The two models were used to design an LQG controller and feedforward filter. Simulations and some initial real engine experiments using the controller have shown promising results. Future work on this topic is to evaluate the controller on the real engine, Investigate combined speed and load transients and improve the turbo model using a mean value model based approach.

9 Acknowledgement

The author would like to thank Per Andersson from GM Powertrain Sweden for proof reading.

10 Abbreviations and Acronyms

HCCI Homogeneous Charge Compression Ignition
NA Naturally Aspirated
NVO Negative Valve Overlap
EVC Exhaust Valve Closure
EVO Exhaust Valve Opening
IVO Intake Valve Opening
IVC Intake Valve Closure
TDC Top Dead Centre
SI Spark Ignition
NMEP Neat Mean Effective Pressure
SOI Start Of Injection
CA50 Crank Angle 50 burnt
BTDC Before Top Dead Centre
ATDC After Top Dead Centre
RI Ringing Index

References

[1] J.Hyvönen, B.Johansson. HCCI operating range with vnt turbo charging. *Haus der Technik*, 2005.

[2] A.Widd, P.Tunestål, R.Johansson. Physical modeling and control of homogeneous charge compression ignition (hcci) engines. *47th IEEE Conference on Decision and Control*, 2005.

[3] J. B. Heywood. *Internal Combustion Engine Fundamentals*. (McGraw-Hill International, London, 1988).

[4] G.Shaver. Modelling cycle-to-cycle dynamics and mode transition in hcci engines with variable valve actuation. *Control Engineer Practice 14*, pages 213–222, May 2006.

[5] F. Agrell. Control of hcci during engine transients by aid of variable valve timings through the use of model based non-linear compensation. *SAE Paper No. 2005-01-0131*, 2005.

[6] M. Shahbakhti. Predicting HCCI auto-ignition timing by extending a modified knock-integral. *SAE Paper No. 2007-01-0222*, 2007.

[7] A.Bjerhammar. *Theory of errors and generalized matrix inverses*. (Elsevier publishing company, Stockholm Sweden, 1973).

[8] K.Åström, B.Wittenmark. *Computer controlled systems: Theory and design*. (Prentice-Hall International Editions, 1984).

Paper III

Control of a Turbo Charged NVO HCCI Engine using a Model Based Approach

Hans Aulin *
Thomas Johansson,Per Tunestål, Bengt Johansson **

* *GM Powertrain Sweden, (e-mail: hans.aulin@gm.com).*
** *Div. of Combustion Engines, Lund Institute of Technology Sweden)*

Abstract: By using a turbo the operating range of the HCCI engine can be increased, but at the expense of increased controller complexity. The dynamics the turbo introduces in the intake and the exhaust manifolds, have a large impact on the in-cylinder mixture temperature, pressure and finally the combustion phasing. To compensate for this and to maintain desired combustion phasing, precise control of the negative valve overlap is required. A physical model is therefore developed and linearized to yield a state space model, used for Kalman filter and main feedback controller design. The original nonlinear model is inverted to provide feedforward. The main actuators for the controller are the intake and exhaust cam phasing, fuel amount and timing of the injections. The main sensor signals used by the controller are the cylinder pressure, intake exhaust pressure, and intake temperature. The model is validated against experimental data, simulated with the controller and finally the controller was tested on the real engine. The article shows the big picture of how a control system for a spray guided, turbo charged, negative valve overlap HCCI engine can be developed.

Keywords: Turbo HCCI, Modeling, Simulation, Kalman filtering, NVO

1. INTRODUCTION

The low NOx, particle matter and high efficiency of the HCCI engine makes it a contender for being part of the propulsion system in the worlds future vehicle fleet. The engine concept does not have any direct ignition trigger such as the spark for the SI or the time of injection for the diesel engine. Instead the internal conditions in the cylinder such as temperature, pressure, mass fuel and residual gas fraction are the ignition triggers (Stanglmaier (1999)). Due to the lack of a direct ignition trigger, closed loop cycle to cycle control is needed. The combustion can be controlled by using strategies such as dual fuel (Strand (2006)) or by using variable compression ratio (Haraldsson (2003)). An other approach is changing the effective compression ratio through intake valve closure, IVC timing (Agrell (2003)). The approach used by the authors, controls the amount of hot residuals (Johansson (2009)). By controlling exhaust valve closure, EVC before top dead centre more or less hot residuals are captured into the next cycle (see Fig. 1) These hot residuals are used in the next cycle to heat up the mixture and, if EVC is controlled correctly, the temperature will reach the right conditions for self ignition at the desired CA50.

The typical NA NVO HCCI engine suffers from a small operating region due to high pressure rise rate and ringing intensity with increased load. A turbo is therefore used to increase the load for the HCCI engine and to suppresses the ringing by diluting the mixture with more oxygen (Hyvonen (2005)). Fig. 2 illustrates how the load

⋆ The authors would like to thank GM Powertrain and the Swedish Energy Agency for the financial support.

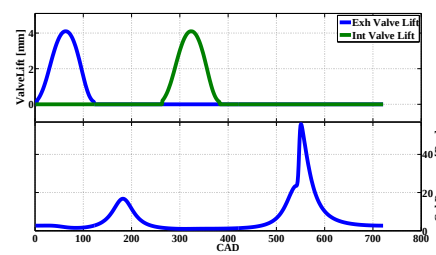

Fig. 1. Valve lift and pressure trace for a NVO HCCI engine

is increased for a given set of limitations in ringing index, emissions, combustion stability etc for the engine used in this study.

Using the overlap strategy with early closing of EVC pressure changes over the exhaust manifold have a direct coupling to the mass of the captured residuals and hence CA50. Due to the turbo charger dynamics, control becomes a challenge.

Initial HCCI controller attempts were based on non model based PID controllers. The trend has over time changed into more model based controllers. (Souder (2004)) et al presented an LQG controller designed using a model derived from system identification methods. (G.Shaver (2006)) developed physical models working in a crank angle resolved resolution. A critical part of all HCCI engine models is the prediction of start of combustion.

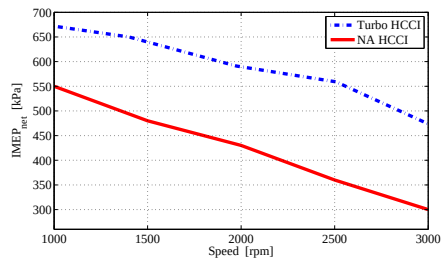

Fig. 2. Possible increase in load using turbo charging

Some authors incorporate different derivates of Arrhenius knock integral model (G.Shaver (2006); Agrell (2005); Shahbakhti (2007)). To further capture the dynamics of the engine behavior, Blom (2008) incorporated a wall temperature model to capture the slow dynamics of a drifting CA50. In this work, a mathematical nonlinear model similar to Gerdes (2004) and Aulin (2009) working in a cycle to cycle basis was constructed to be able to design improved combustion phasing controllers. The model gives a very simple understanding of the process from one cycle to another. Using Maple an analytical expression describing the engine was linearized to yield a four state linear model. The original model was inverted for feedforward control and the simplified four state linear model was used for Kalman filter and feedback controller design.

2. EXPERIMENTAL SETUP

The engine used in this study is an in-line four cylinder gasoline spray guided General Motors engine. The engine is equipped with hydraulic cam phasers with low lift cams timed for negative valve overlap (Fig. 1). The engine is also equipped with cylinder individual pressure transducers, intake, exhaust pressure/temperature sensors and a small fixed geometry turbo. The control system is a fully Simulink-based dSpace Rapid Pro system. The dynamometer can be operated from the dSpace System.

3. ENGINE MODELING AND LINEARIZATION

A brief introduction of the main controller is shown in Fig. 3 describing the flow of the main signals. The model presented below is used for designing the engine Kalman filter, the combustion feedback controller, the feedforward and to estimate a CA50 to temperature correlation.

The key factors influencing the combustion in the cylinder i.e. temperatures, pressure and in cylinder masses are described in the model using a thermodynamic approach.

3.1 Model structure

The engine model is updated once each cycle. For every cycle, ending at TDCf, a state vector describing the in cylinder conditions is calculated. These states are described as two species: mass air, state m_a, which is the unburnt part and mass burned gas, state m_e, which is considered an inert residual gas. To be able to compute a complete

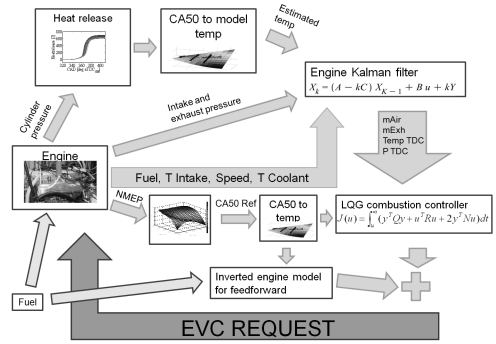

Fig. 3. Controlscheme describing flow of control signals

engine cycle, two additional states are needed, the mixture temperature, T, and cylinder pressure, P. The main goal for the model is to predict the temperature at TDC. This temperature is correlated against CA50 for different fueling/speed levels. A function describing this correlation is then used for predicting the combustion phasing. For each new simulation of a cycle the initial conditions are taken from environmental inputs and previous cycles according to:

$$T_1(k) = T_9(k-1)$$

$$P_1(k) = P_9(k-1)$$

$$m_{a1}(k) = m_{a9}(k-1)$$

$$m_{e1}(k) = m_{e9}(k-1)$$

The different processes describing the dynamics for a cycle will now be presented.

3.2 Combustion

The model assumes instantaneous combustion at top dead center. The temperature increase depends on the amount of energy released during combustion and the total mass in the cylinder. The temperature after combustion is then given by

$$T_2(k) = \frac{m_{fuel} Q_{LHV}}{(m_{a1}(k) + m_{e1}(k)) C_v} + T_1(k) \tag{1}$$

m_{fuel} and Q_{LHV} represent mass of injected fuel and lower heating value for the fuel respectively.

With known temperature and constant volume during combustion the cylinder pressure, $P_2(k)$ can be calculated using the ideal gas law

$$P_2(k) = \frac{P_1(k) T_2(k)}{T_1(k)} \tag{2}$$

Assuming that all required oxygen for complete combustion is used, the amount of unused air left is given by

$$m_{a2}(k) = m_{a1}(k) - m_{fuel} \left(\frac{A}{F}\right)_s \tag{3}$$

where $\left(\frac{A}{F}\right)_s$ is the stoichiometric air to fuel mass ratio. Due to the closed valves the total mass in the cylinder

is constant. The mass of burned gas is then increased accordingly

$$m_{e2}(k) = m_{e1}(k) + m_{fuel}\left(\frac{A}{F}\right)_s \quad (4)$$

3.3 Expansion

If the heat losses are ignored during expansion, isentropic relations can be used to describe how temperature, T_3 and pressure P_3 relate to T_2 and P_2. Expansion to cylinder volume at exhaust valve opening is therefore given by

$$T_3(k) = T_2(k)\left(\frac{V_{tdc}}{V_{evo}}\right)^{\gamma-1} \quad (5)$$

and

$$P_3(k) = P_2(k)\left(\frac{V_{tdc}}{V_{evo}}\right)^{\gamma} \quad (6)$$

where V_{tdc} and V_{evo} are the cylinder volume directly after combustion and at exhaust valve opening. γ is the polytropic exponent and is assumed constant. The other parameters are updated according to

$$m_{a3}(k) = m_{a2}(k),\ m_{e3}(k) = m_{e2}(k) \quad (7)$$

3.4 Blowdown

After exhaust valve opening the burned gas expand to manifold pressure. The temperature after expansion can be calculated according to

$$T_4(k) = T_3(k)\left(\frac{P_{exh}}{P_3(k)}\right)^{\frac{\gamma-1}{\gamma}} \quad (8)$$

where P_{exh} is the exhaust manifold pressure. The other parameters are changed according to

$$m_{a4}(k) = m_{a3}(k), m_{e4}(k) = m_{e3}(k), P_4(k) = P_{exh}(k) \quad (9)$$

3.5 Exhaust Valve Closing

The early closing of the exhaust valves will cause the cylinders to trap some of the hot residuals. These residuals will later mix with the fresh charge during the intake stroke. The temperatures and the amount of the residuals will therefore have an impact on equivalence ratio and combustion phasing in the following cycle. Using the ideal gas law just before EVO and at EVC and combining the two will give the amount of residuals and fresh charge at EVC.

$$m_{a5}(k) = \frac{m_{a4}(k)V_{evc}P_{exh}T_3(k)}{(\eta V_{evo}P_4(k)T_4(k))} \quad (10)$$

and

$$m_{e5}(k) = \frac{m_{e4}(k)V_{evc}P_{exh}T_3(k)}{(\eta V_{evo}P_4(k)T_4(k))} \quad (11)$$

The tuning parameter η is statically mapped in the model and depends on speed and cam phasing, it is used to compensate for the higher pressure in the cylinder compared to manifold due to the throttling over the low lift valves. η is at high boost/load quite low (minimum is approx 0.5). Obviously, the low lift valves introduce throttling losses and remove part of the efficiency advantage that HCCI is otherwise so well known for. The other parameters are changed according to

$$P_5 = P_{exh},\ T_5 = T_4 \quad (12)$$

3.6 Expansion to intake manifold pressure

The exhaust residual mixture captured in the negative valve overlap will be recompressed and then expanded to the manifold pressure. The temperature T_6 of the residuals at intake pressure is given by

$$T_6(k) = T_5(k)\left(\frac{P_{in}}{P_{exh}}\right)^{\frac{\gamma-1}{\gamma}} \quad (13)$$

Where P_{in} is the intake manifold pressure. The other parameters are changed according to

$$m_{a6} = m_{a5},\ m_{e6} = m_{e5},\ P_6 = P_{in} \quad (14)$$

3.7 Mixing of residuals at Intake Valve Closure

The hot residuals are mixed together with the intake manifold air yielding a lower mixture temperature, T_7 at IVC. By combining

$$T_7(k) = \frac{P_{in}V_{ivc}\eta}{(m_{a7}(k) + m_{a6}(k) + m_{e6}(k))R} \quad (15)$$

and

$$T_7(k) = \frac{(m_{a6} + m_{e6})T_6 + m_{a7}T_{in}}{m_{a6} + m_{e6} + m_{a7}} \quad (16)$$

(where specific heat is assumed to be equal for the residuals and the fresh air) and solving for m_{a7}, the amount of inducted air gives the following expression

$$m_{a7}(k) = \frac{P_{in}V_{ivc}\eta - RT_6m_{e5} - RT_6m_{a5}}{RT_{in}} \quad (17)$$

Throttling over the valves is assumed to be similar during exhaust and intake, hence the same η is used for compensation. The other parameters are changed according to

$$m_{e7} = m_{e6},\ P_7 = P_6 \quad (18)$$

3.8 Compression to TDC

During the compression the heat losses are ignored and the isentropic relations can be used

$$T_8(k) = T_7(k)\left(\frac{V_{ivc}}{V_{tdc}}\right)^{\gamma-1} \quad (19)$$

$$P_8(k) = P_7(k)\left(\frac{V_{ivc}}{V_{tdc}}\right)^{\gamma} \quad (20)$$

The other parameters are changed according to

$$m_{a8} = m_{a7},\ m_{e8} = m_{e7} \quad (21)$$

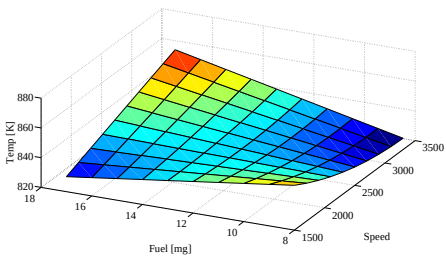

Fig. 4. Temperatures for different load and speed

3.9 Heat Transfer

The heat transfer to the cylinder walls is estimated using Newton's law of cooling. The resulting equation for the temperatures is then

$$T_9(k) = \frac{-h_c A_c (T_8 - T_w)\Delta t}{mC_v} + T_8(k) \tag{22}$$

The heat transfer coefficient, hc is given by Woschni's formula (see Heywood (1988))

$$h_c = \frac{3.26 P_8(k)^{0.8} w^{0.8}}{B^{0.2} T_8(k)^{0.55}} \tag{23}$$

m is the total gas mixture mass ($m_{e8} + m_{a8}$). A_c is the cylinder wall area. T_w is the wall temperature and B is the cylinder bore and w is the engine speed.

Combining the presented equations (Eq.1-23) yields four equations describing each state from cycle to cycle on the following form

$$m_a(k+1) = f_1(u(k+1), m_a(k), m_e(k), T(k), P(k)) \tag{24}$$

$$m_e(k+1) = f_2(u(k+1), m_a(k), m_e(k), T(k), P(k)) \tag{25}$$

$$T(k+1) = f_3(u(k+1), m_a(k), m_e(k), T(k), P(k)) \tag{26}$$

$$P(k+1) = f_4(u(k+1), m_a(k), m_e(k), T(k), P(k)) \tag{27}$$

where $u(k)$ is the engine inputs according to

$u(k) = [\eta, m_{fuel}, V_{evo}, V_{evc}, V_{ivc}, T_{in}, P_{in}, P_{exh}, w, T_{coolant}]^T$

and where $m_a(k), m_e(k), T(k), P(k), T_w$ are the states from previous cycle. A number of simplifications have been made in the described model but it is precise enough to capture the general trends and the dynamics of the engine behavior.

3.10 Linearization

Making a Taylor approximation of the nonlinear equations Eq.24-Eq.27 at an operating point, preferably in the middle of the speed load range, yields a linear discrete state space model of the form $x(k) = Ax(k-1) + Bu(k-1)$, $y(k) = Cx(k)$:

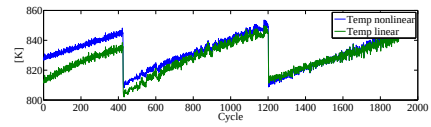

Fig. 5. Linearization results: 3 to 5 bar NMEP at 1500RPM during cycle 0-410, at 2000 RPM during cycle 500 to 1200 and 2500 RPM during cycle 1200 To 1900

$$\begin{bmatrix} m_a(k) \\ m_e(k) \\ T(k) \\ P(k) \end{bmatrix} = A \begin{bmatrix} m_a(k-1) \\ m_e(k-1) \\ T(k-1) \\ P(k-1) \end{bmatrix} + B \begin{bmatrix} \eta \\ m_{fuel} \\ V_{evo} \\ V_{evc} \\ V_{ivc} \\ T_{in} \\ P_{in} \\ P_{exh} \\ w \end{bmatrix} \tag{28}$$

$$Y = [\,0\ 0\ 1\ 0\,] \begin{bmatrix} m_a(k) \\ m_e(k) \\ T(k) \\ P(k) \end{bmatrix}$$

Where the states in x are mass air, mass residuals, mean temperature and pressure in the cylinder at TDC just before combustion. The inputs used are the filling efficiency, mass of fuel, cylinder volume at EVO, EVC and IVC, the manifold intake/exhaust pressure and finally speed. The generated linear model has properties of being both controllable, observable and fairly similar to the original model. A comparison between the linear and the original nonlinear model at different speeds and fuel amounts can be seen in Fig. 5.

3.11 Predicting CA50

The model presented so far does not estimate the combustion phasing. The main parameters affecting the combustion phasing is the mixture temperature, the oxygen concentration and pressure/temperature history. In similar studies the Arrhenius knock integral model has been used in various ways to take these factors into account (G.Shaver (2006); Ågrell (2005); Shahbakhti (2007)). The Arrhenius expression is based on an exponential correlation between reaction rate, temperature and pressure in the cylinder. A different approach, suitable for controller design, has been taken in this work where (Eq.29) has been fitted to experimental data.

$$CA50(k) = f(\omega, m_{fuel}, T(k)) \tag{29}$$

The inputs are engine speed, fuel mass and temperature. In Fig. 4 a map is generated from this function showing how the estimated start of combustion temperature relates to speed and fuel mass for a CA50 of 5 CAD aTDC.

4. MODEL VERIFICATION

The models are implemented in Simulink and a set of experimental data points are compared to simulations. Fig. 6 illustrate a load sweep at 2000 RPM with oscillating exhaust cam. The model shows good agreement with the real test data. Similar performance was achieved

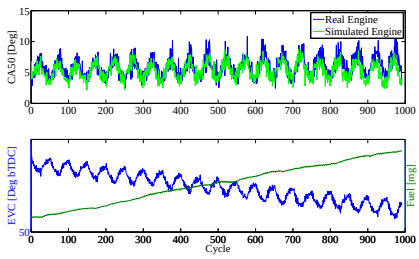

Fig. 6. Validation of model for sweep from low to high load at 2000RPM

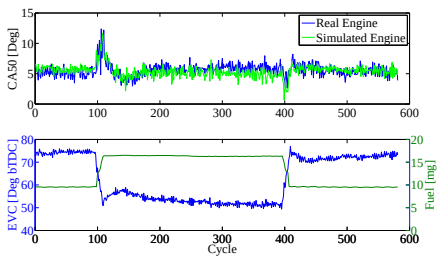

Fig. 7. Validation of model for load steps from low to high to low load at 2000RPM

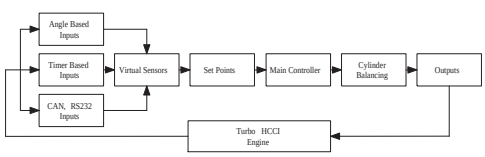

Fig. 8. Overview describing the flow of signals from input to output

at 1500 and 2500 rpm. Fig. 7 shows the result from a series of load steps at 3 to 5 to 3 bar NMEP. It can be concluded that also here a good match between experimental and simulated data is achieved. Compared to system identification methods as described in Bengtsson (2006) et al, this approach yields good understanding of the process during each engine cycle and the model states achieved have a physical meaning. But likely similar model accuracy can be achieved using the system identification approach.

5. THE CONTROL SYSTEM

A brief introduction of the signal in the controller is illustrated in Fig. 8. The inputs are divided into angle based, time based, and CAN/RS232 based inputs. The $Virtualsensors$ part performs the NMEP, RI, dP/dCa and heatrelease calculations. This is also where various observers and filters are located. *Setpoints* takes care of some map based feedforward. The *maincontroller* consists of a Kalman filter, an LQG controller and a feedforward controller. The *cylinderbalancing* uses the main controller's injection signals as feedforward but offsets some of the cylinders to maintain equal phasing and load. In the output block the controllers for throttles, fuel pump, cam phasing, water pump etc are placed to keep the actuator according to the control system demands.

5.1 Kalman Filter for Predicting the States

Since the states describing the engine are not directly measurable they are estimated using a Kalman filter. The Kalman filter is described according to

$$\begin{bmatrix} \hat{m}_a(k) \\ \hat{m}_e(k) \\ \hat{T}_c(k) \\ \hat{P}(k) \end{bmatrix} = [A - KC] \begin{bmatrix} \hat{m}_a(k-1) \\ \hat{m}_e(k-1) \\ \hat{T}(k-1) \\ \hat{P}(k-1) \end{bmatrix} + .. \\ B \begin{bmatrix} \eta \\ m_{fuel} \\ V_{evo} \\ V_{evc} \\ V_{ivc} \\ T_{in} \\ P_{in} \\ P_{exh} \\ w \\ T_{coolant} \end{bmatrix} + Ky(k-1) \tag{30}$$

The filter minimizes the mean square error $E\{|x(k) - \hat{x}(k)|\}$ where $\hat{x}$ and $x(k)$ are the estimated and real state vectors respectively. For the design of the gain matrix (K), the process noise and measurement noise have been set to zero. The measured output, y, is the temperature of the mixture at TDC. It is estimated from the CA50 measurements using the inverse of Eq.29.

5.2 The Feedback

An LQG controller is used for feedback. This controller is acting on estimated states from the Kalman filter. To handle modeling errors and accomplish error free tracking an integrator state is used to augment the state space model:

$$\begin{bmatrix} x(k) \\ x_i(k) \end{bmatrix} = \begin{bmatrix} A & 0 \\ -C & I \end{bmatrix} x_a(k-1) + \begin{bmatrix} B \\ 0 \end{bmatrix} u(k-1) + .. \\ \begin{bmatrix} 0 \\ 1 \end{bmatrix} r(k-1)$$

$$y(k) = [\, C_y \;\; 0 \,]$$

Where x is the original states, x_i the integrator state, x_a the augmented state vector, r the reference temperature and u the model inputs.

5.3 The Feedforward

The model's capability to predict the engine behavior is used for the feedforward. This is done by inverting Eg.29 and Eq.24-Eq.27 and combining them to yield a mathematical expression from CA50 reference to the feed forward action for exhaust valve closure.

5.4 Cylinder balancing

At loads above 4 bar NMEP the margins are small and it is vital that the four cylinders have equal NMEP and

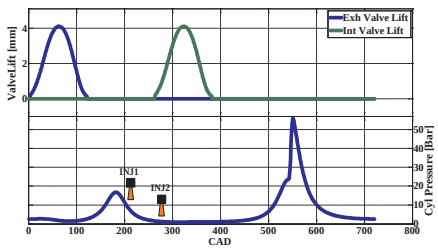

Fig. 9. Injection strategy: Inj1 for CA50 balancing and the Inj2 (the main injection) for NMEP balancing

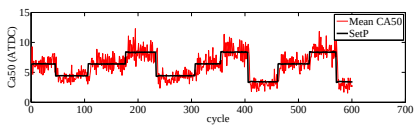

Fig. 10. CA50 stepresponses at 4 bars NMEP

combustion phasing. With equal actuator settings for all cylinders, heavy ringing may occur in some cylinders while others may be close to misfiring. Therefore cylinder balancing is vital with increased load. This is achieved by individually changing the start of injection and fuel amount for two injections for each cylinder and cycle. The two injections are, one small injection during the negative valve overlap and one main injection during the intake stroke (Fig. 9). The combustion phasing controller is acting on the first injection. By letting a PI-controller advance or retard this injection individual control of combustion phasing is possible. The injection timing for the cylinder with the earliest combustion is set to the reference value from the main feedforward. The other injections are allowed to float around within the reference value and a predefined maximum limit to maintain equal phasing.

The NMEP balancing works in a similar way but acts on the main injection. The total fuel amount is for this injection kept according to the reference value from the feedforward but the controller individually distributes the fuel for the four cylinders. To compensate for the differences between the injectors the controller is adaptive and remembers the injector settings from history. The two described cylinder balancing methods are tuned for maximum stability rather than speed.

6. EXPERIMENTAL RESULTS

6.1 Transient performance

Rise time for CA50 step responses is of little importance for a real engine application but it gives some indication of the performance of the controller. Fig. 10 illustrate step responses at 4 bar NMEP. The mean rise time for a CA50 step is about 3 cycles.

The engine is able to run at lower loads than 3 bar NMEP but this study is limited to investigate HCCI using Turbo at loads above 3 bar. Fig. 11 shows NMEP steps between

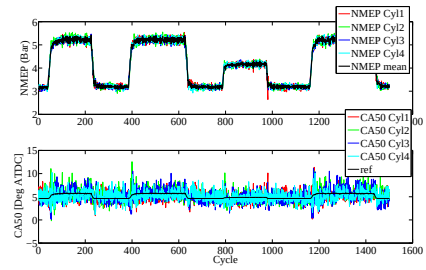

Fig. 11. CA50 during load steps

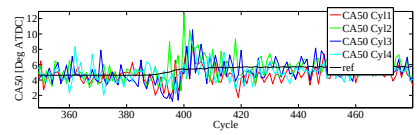

Fig. 12. CA50 during a load step (zoomed in from Fig. 11 at cycle 350 to 470)

3 and 5.2 bar and how the phasing for the four cylinders follow the reference. Cycles 350 to 470 are in Fig. 12 zoomed in from Fig. 11. There is some small deviation from the reference during cycle 390 to 410 but the controller settles quite fast. A challenge with running the engine at higher load is that the engine has a very narrow band where the engine actually runs. A later CA50 timing than 8 to 9 CAD ATDC almost instantly causes misfires. This requires very precise control of the cams.

The main challenge running this NVO turbo HCCI engine is the turbo lag during transients, heavily affecting the mixture temperature for the next cycle. During a load step from high to low load the exhaust pressure will rapidly decrease but the manifold pressure lags a couple of cycles. This leads to a sudden decrease of hot residuals yielding lower mixture temperature at IVC and finally a later CA50 and possibly misfires. To maintain the correct mixture temperature, the action that must be taken is increased EVC during the transient compared to steady state. During an increase in load the reverse occurs. The increase in fuel will lead to exhaust pressure/temperature increase and lagging intake pressure. This will lead to higher temperature at IVC and hence to early combustion. This is compensated for by using less EVC compared to steady state. Fig. 13 illustrates how the camshafts move during a 3 to 5.2 to 3 bar step series. The described phenomenon is obvious at Cycles 230 to 240 when going from 5.2 bar to 3 bar in Fig. 13.

6.2 Combustion noise

The ringing intensity, RI is used as a measure of the noise level for the engine. Above 6 MW/m^2, the noise level starts to become rough for the human ear. It is with the current setup difficult to make large load transients without loud noise before enough pressure is built up from the Turbo (see Fig. 14). The noise problem can be avoided by defining a constraint in RI but this would result in a slower response from the driver NMEP request which is not desirable.

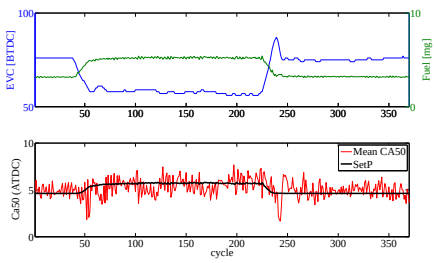

Fig. 13. EVC during load transient 3 to 5.2 Bar NMEP

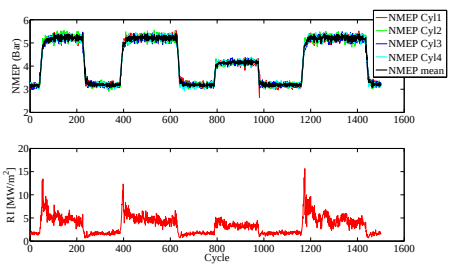

Fig. 14. RI during transients

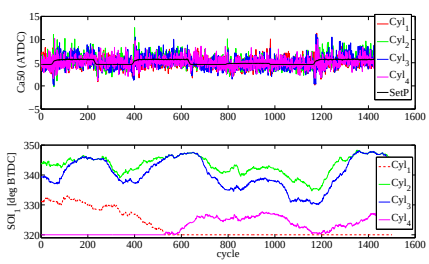

Fig. 15. CA50 balancing by changing SOI1. Note how SOI_1 for cylinder four is kept at the reference from Cycle 0 to 470 and how it changes to keep Cylinder one at the reference value. The reference value is in this case 320 Deg BTDC.

6.3 Cylinder Balancing

In Fig. 15 the start of injection is displayed together with the combustion phasing. Note how SOI_1 for Cylinder 4 is kept at the reference from Cycle 0 to 470 and how it subsequently changes to keep Cylinder 1 at the reference value. The reference value is in this case 320 Deg BTDC.

The controller remembers the differences between the injectors for different load points this can be seen in Fig. 16.

Fig. 17 illustrates the difference between deactivated and activated cylinder balancing. The controller is started at Cycle 210. It settles fast and reduces the risk of misfire.

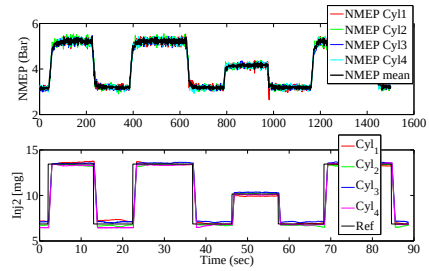

Fig. 16. NMEP balancing by controlling fuel distribution

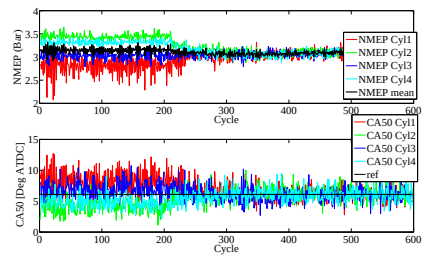

Fig. 17. Activation of cylinder balancing at cycle 210

At high load the engine behaves nervously. This cannot be seen in the CoV NMEP calculations but in the CA50 measurements. The cause could be the large pressure oscillations in the intake and the exhaust pressure having a direct impact on the mixture relation and hence the combustion phasing.

7. CONCLUSION

An HCCI model has been developed and linearized to give a state space model of the engine. A number of generalizations have been made but still the model manages to capture the general trends and dynamics of the engine. The model takes the intake and exhaust pressures into account. That is something particularly important when running HCCI with Turbo. The model was used to design feedback and feedforward controllers as well as a Kalman filter. During transients the turbo lag introduces some problems but engine experiments conducted have shown that the proposed approach works fine to handle control at fast load transients. Drawbacks with this kind of engine concept are throttling losses and loud combustion noise during fast transients that most likely would be difficult to avoid. At high load the engine shows nervous cycle to cycle behavior that is difficult to predict and control. The controller still has some areas for improvements so for future work it remains to test and tune the model/controller to handle combined speed and load transients. The second thing is to develop a physical mean value model of the turbo system for use together with a Kalman filter for improved exhaust and intake pressure feedback. This will likely improve the controllers. The question one must ask when considering the engine concept as a whole is whether

the advantages make up for the disadvantages to make it worth putting into production?

8. ABBREVIATIONS AND ACRONYMS

NA Naturally Aspirated

NVO Negative Valve Overlap

EVC Exhaust Valve Closure

EVO Exhaust Valve Opening

IVO Intake Valve Opening

IVC Intake Valve Closure

TDC Top Dead Centre

TDC Top Dead Centre Firing

SI Spark Ignition

NMEP Neat Mean Effective Pressure

SOI Start Of Injection

CA50 Crank Angle 50 % Burnt

BTDC Before Top Dead Centre

ATDC After Top Dead Centre

RI Ringing Index

CAD Crank Angle Degrees

CoV Coefficient of variation

REFERENCES

Agrell, F. (2003). Transient control of hcci through combined intake and exhaust valve actuation. *SAE Paper No. 2003-01-3172*.

Agrell, F. (2005). Control of hcci during engine transients by aid of variable valve timings through the use of model based non-linear compensation. *SAE Paper No. 2005-01-0131*.

Aulin, H. (2009). Thermodynamic modeling and control of a turbo hcci engine. *Iasted Controls and application*.

Bengtsson, J. (2006). Multi-output control of a heavy duty hcci engine using variable valve actuation and model predictive control. *SAE Paper No. 2006-01-0873*.

Blom, D. (2008). Hcci engine modeling and control using conservation principles. *SAE Paper No. 2008-01-0789*.

Gerdes, J.C. (2004). Cycle-tocycle control of hcci engines with variable valve actuation. *Homogenus Charge Compression Ignition Symposium*.

G.Shaver (2006). Modelling cycle-to-cycle dynamics and mode transition in hcci engines with variable valve actuation. *Control Engineer Practice 14*, 213–222.

Haraldsson, G. (2003). Hcci combustion phasing with closed-loop combustion control using variable compression ratio in a multi cylinder engine. *SAE Paper No. 2003-01-1829*.

Heywood, J.B. (1988). *Internal Combustion Engine Fundamentals*. McGraw-Hill International, London.

Hyvonen, J. (2005). Hcci operating range with vnt turbo charging. *Haus der Technik*.

Johansson, T. (2009). Hcci operating range in a turbocharged multi cylinder engine with vvt and spray-guided di. *SAE Paper No. 2009-01-0494*.

Shahbakhti, M. (2007). Predicting hcci auto-ignition timing by extending a modified knock-integral. *SAE Paper No. 2007-01-0222*.

Souder, S. (2004). Closed-loop control of a multi-cylinder hcci engine. *Homogenus Charge Compression Ignition Symposium*.

Stanglmaier, D.S. (1999). Homogenous charge compression ignition (hcci). *SAE Paper No. 1999-01-3682*.

Strand, P. (2006). *HCCI Operation - Closed loop combustion control using VVA or dual fuel*. Lund University, Lund.

Paper IV

2009-24-0060

The Effect of Intake Temperature in a Turbocharged Multi Cylinder Engine operating in HCCI mode

Thomas Johansson, Bengt Johansson, Per Tunestål
Faculty of engineering, Lund University

Hans Aulin
GM Powertrain AB, Sweden

ABSTRACT

The operating range in HCCI mode is limited by the excessive pressure rise rate and therefore high combustion induced noise. The HCCI range can be extended with turbocharging which enables increased dilution of the charge and thus a reduction of combustion noise. When the engine is turbocharged the intake charge will have a high temperature at increased boost pressure and can then be regulated in a cooling circuit. Limitations and benefits are examed at 2250 rpm and 400 kPa indicated mean effective pressure. It is shown that combustion stability, combustion noise and engine efficiency have to be balanced since they have optimums at different intake temperatures and combustion timings. The span for combustion timings with high combustion stability is narrower at some intake temperatures and the usage of external EGR can improve the combustion stability. It is found that the standard deviation of combustion timing is a useful tool for evaluating cycle to cycle variations. One of the benefits with HCCI is the low pumping losses, but when load and boost pressure is increased there is an increase in pumping losses when using negative valve overlap. The pumping losses can then be circumvented to some extent with a low intake temperature or EGR, leading to more beneficial valve timings at high load.

INTRODUCTION

The homogenous charge compression ignition (HCCI) combustion offers high thermal efficiency, low throttling losses and low emissions. The limited operating range in HCCI mode makes it to an alternative to the spark ignited (SI) engine at low load to improve the efficiency. On the other hand the diesel engine has shown some favorable properties when operated with fuels with long ignition delay like gasoline [1] leading to low soot and nitrogen oxides (NOx) levels. Here the HCCI mode or a mix of it can be attractive to cover the whole operating range. In HCCI mode the air-fuel charge is auto ignited by controlling the temperature and pressure history inside the engine cylinder to initiate and time the combustion phasing at the right moment.

When operating with a homogenous charge the right conditions for the combustion timing has to be set before intake valve closing (IVC). With the introduction of direct injection (DI) of the fuel there is an increased control space [2, 3] and even a possibility to change the operating conditions after IVC, so the preferred charge composition does not have to, or will be homogenous [4].

To reach auto ignition in a four-stroke engine the in-cylinder temperature is normally increased by exhaust gas recirculation (EGR), air heating or both as outlined in the eighties by Thring [5]. The compression ratio can also be used to control the HCCI combustion timing [6, 7]. The concept with negative valve overlap (NVO) with early exhaust valve closing to trap a certain amount of hot residuals is widely accepted to control combustion timing. Here the variable valve timing (VVT) is accurately controlled either mechanically or electrically.

The concept of re-breathing [8] might be more mechanically complicated but has an advantage in reduced heat losses since it can be operated without recompression. The combustion timing in HCCI can also be adjusted with the intake temperature by a thermal management system [9, 10], but this need a heat recovery system.

The combination of intake heating and NVO [11] in a naturally aspirated (NA) engine showed that the intake temperature had a low impact on engine operating but increased temperature could be used to extend the low load limit. By boosting the engine in HCCI mode to extend the possible load range [12, 13, 14, 15, 16], the intake temperature will be elevated and can therefore be cooled down to a suitable level with an intercooler. The boost pressure can be controlled directly by the intake valve timing [16] which gives large freedom to operate the engine with optimum efficiency, emissions, combustion noise, cyclic variations and control strategies. With NVO the intake temperature directly control how much internal EGR is needed for a given combustion timing and therefore the in-cylinder relative burn gas fraction. The chemical and thermodynamic properties of the EGR [17] will influence the combustion. In addition to the residual gas, external cooled EGR can be used and it was found that it could improve combustion efficiency while there seem to be low influence on the combustion duration [18] in HCCI mode.

The main operating parameter in HCCI mode is the combustion timing here represented by the crank angle of 50% heat released (CA50). The CA50 timing will effect the engine performance substantially and need to be controlled exactly to run the HCCI engine successfully. If engine speed goes up or if load is increased the CA50 window for stable engine running will be narrowed, making the engine control more challenging.

The scope of this paper is to investigate how combustion timing, intake temperature and EGR influence a turbocharged NVO HCCI engine performance. This is done by dividing the result in small fractions. By doing this the understanding on how to operate a turbocharged HCCI engine is expanded. Since the application of HCCI has to meet consumer demand, emission legislation and control capability the real operating range is always a balance between these. The result is also applicable to some extent for a NA HCCI engine.

EXPERIMENTAL SET-UP

ENGINE SYSTEM The test engine is an in-line four cylinder gasoline engine with a total displacement of 2.2*l*. The cylinder head is a 4-valve design with a pent-roof combustion chamber. There are some small squish areas on the intake and exhaust sides. The piston has a raised piston dome with a small bowl in the center. The intake channel is side-drafted with a low tumble design. The engine has DI with a slightly canted, centrally placed injector of the Spray-Guided type. The eight-hole solenoid fuel injector has a cone angle of 60^{o}. The spark plug is located close to the fuel injector and has an extended tip. The spark is always operated as a safety measurement against misfires and it can also improve the combustion stability at late combustion timings. To achieve HCCI combustion the engine is operated with NVO with low lift and short duration camshafts designed for a NA HCCI engine. In Figure 1 the minimum and maximum valve timings are plotted.

The VVT is controlled by hydraulic actuators at the camshafts giving a separate 50 crank angle degree (CAD) adjustment on both intake and exhaust valve timings. The engine is turbocharged by a fixed geometry turbine. The exhaust manifold is of pulse type with short individual runners straight to the turbine inlet. On the intake side there is a water cooled intercooler. The heated aluminum intake manifold has short intake runners and a small volume. The cooling system has an electric driven water pump and the coolant temperature is adjusted by the control system. Engine specifications are listed in Table 1.

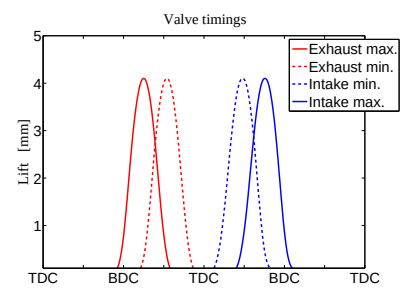

Figure 1: Valve timing range and setup

Table 1: Engine specifications

Number of cylinders	4
Displacement	2198 cm^3
Bore x Stroke	86 mm x 94.6 mm
Compression Ratio	11.75:1
Valve duration	125 CAD
Valve lift	4.1 mm
NVO range	74–174 CAD
Turbocharger	B&W KP31
Fuel Supply	DI, up to 20 MPa
Fuel Type	Gasoline, 95 RON

Figure 2: Exhaust manifold

Figure 3: Intake manifold

MEASUREMENT AND CONTROL SYSTEM The control system is a combined data acquisition and engine control unit from dSPACE. The signals from a fully instrumented engine set-up are collected and analyzed. For combustion feedback there are individual cylinder pressure sensors. The control system has an in-cycle resolved heat release calculation where main parameters like CA50, peak cylinder pressure (PCP) and peak pressure derivative (dP/CAD) etc. are used for cylinder individual control in closed loop. Emission analysis and soot measurement are collected on an external PC and the data is sent to the control unit.

To increase the operating range it is important that all the cylinders operate identically, meaning that they have the same CA50 position, indicated mean effective pressure (IMEP$_{net}$) and peak pressure rise rate. This means that the control system has to perform cylinder balancing (CB). Injection of the fuel in NVO can give a reformation of the fuel with an increase in charge temperature and reduction in effective octane number leading to advanced combustion timing. The combustion timing will be more advanced if the fuel is injected in the beginning of the NVO than in the end. The control system sets the CA50 position and uses the cylinder with the most advanced CA50 position for the exhaust valve closing (EVC) set point. The other cylinders are then advanced by adjusting the injection timing and/or fuel amount in the first injection, until all cylinders have the same CA50 position. Since there will be some differences in injection timing when using CA50 balancing there will also be some differences in efficiency between the cylinders. This results in different load, IMEP$_{net}$ in the cylinders. To maximize the load range there has to be CB of IMEP$_{net}$ as well. This is done at the main injection event. Obviously this affect the CA50 balancing since increasing the fuel amount will raise the combustion heat, leading to earlier CA50 for that cylinder. Therefore the CB has to be constantly monitored and adjusted by the control system. Table 2 shows the measurement and control equipment.

Table 2: Measurement and control system.

ECU and data logging	dSPACE Rapid Pro
Cylinder pressure sensor	Kistler 6043Asp
Charge amplifier	Kistler 5011B
Emission analyzer	Horiba 9100 MEXA
Soot analyzer	AVL 415 S

TEMPERATURE AND EGR CONTROL SYSTEM The intake temperature is controlled by an electrical throttle in the bypass routing to the water-cooled intercooler circuit, see Figure 4. When the throttle is fully open the main air flow goes through the bypass routing due to less flow discharge compared to the intercooler circuit. By closing the throttle the airflow is forced through the intercooler circuit.

The long route EGR system takes exhaust gas after the turbine and route it to the compressor inlet. To get a positive displacement of exhaust gas there is a throttle in the exhaust system to increase back pressure. The compressor inlet can be used as an ejector to enhance the EGR flow, so the needed back pressure is quite small. The external EGR routing is cooled by the engine cooling circuit and is controlled by an EGR valve near the turbocharger, see Figure 4.

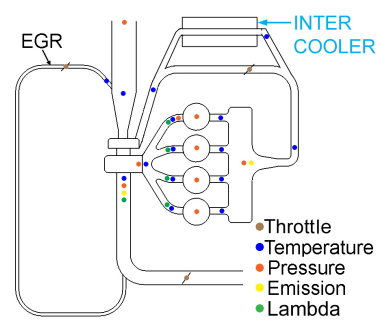

Figure 4: Engine layout

The presented results are based on average results from all four cylinders during 1000 cycles The deviation in engine load between measured test points is $\pm$ 3 kPa and in engine speed $\pm$ 2 rpm. Engine coolant temperature is $\sim 80^{\circ}\ C$ out from the engine.

RESULTS AND DISCUSSION

The combustion phasing in HCCI mode is vital for stable engine running and efficiency. In the NVO concept the EVC timing is the major control variable for the combustion phasing since it controls the amount of trapped hot residual gas. The intake valve timing can also be used to control the combustion timing but the influence is weaker and not as predictive as the EVC timing which makes it less suitable for cycle to cycle combustion control. It is normal to operate with almost symmetrical valve timings on the intake and exhaust. With these short duration valve timings, a late intake valve closing will increase the available in-cylinder pressure when the engine is turbocharged. The combustion timing is even more important due to the direct influence it has on boost pressure and therefore the intake temperature. A later combustion timing will increase the available exhaust enthalpy for the exhaust turbine leading to higher boost pressure. This means that the intake temperature will also increase. There is then the freedom to adjust the intake charge temperature by the cooling circuit to obtain best overall performance depending on load and engine speed.

The maximum load in HCCI is often limited by the fast combustion rate where the combustion induced noise is a major factor. By increasing the air dilution in the cylinder with turbocharging the audible noise is suppressed and therefore the operating range can be extended. The pressure rise rate can be measured in bar/CAD or MPa/ms [19] and is used to impose a operating limit. But neither of these catch the real combustion noise when the engine is supercharged. The Ringing Intensity (RI)– MW/m^2 [20], on the other hand compares the pressure rise rate to peak cylinder pressure and engine speed and is therefore used in these tests.

The engine tests in this study are performed at 2250 rpm and 400 kPa IMEP$_{net}$. This load and speed point was chosen due to the wide span of boost levels that can be reached here with alteration of the intake temperature. It also has different operating limitations due to combustion stability, high pressure rise rate and turbocharger performance. Even if it is possible to operate this turbocharged HCCI engine at a higher load at this engine speed, it is unsuitable for a wide CA50 sweep due to the high pressure rise rate at early combustion timings. In the first set of results the CA50 position and intake temperature are swept. Then there is an external EGR and intake temperature sweep at locked CA50 timing, and finally, there is a CA50 sweep with and without EGR at the same intake temperature. During these tests the intake valve timing is constrained to latest possible opening position to increase available in-cylinder pressure.

CA50 AND INTAKE TEMPERATURE SWEEP AT 2250 RPM AND 400 KPA IMEP$_{NET}$ From this test there are some additional graphs that can be found in the APPENDIX. In Figure 5 the intake manifold pressure (P$_{in}$) is shown at the possible operating range in this test point. The temperature can be altered from $110^\circ\ C$ down to $45^\circ\ C$ with the throttle controlled intercooler routing. The timing for CA50 can not be set to more than $\sim 7^o$ aTDC$_f$ for stable engine operating at this test point. The importance for robust CA50 control is evident when operating this turbocharged HCCI engine since it is dependent on the boost pressure to decrease RI to manage high load. The resulting PCP reflects the wide intake pressure variations and span from 6.6 to 8.2 MPa, see Figure 6.

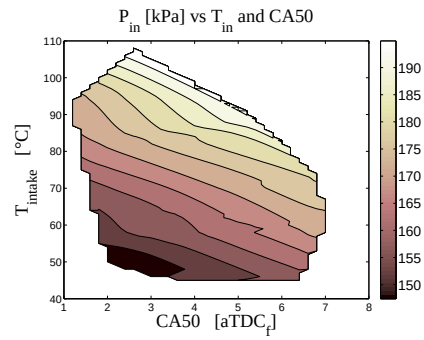

Figure 5: Intake pressure, absolute

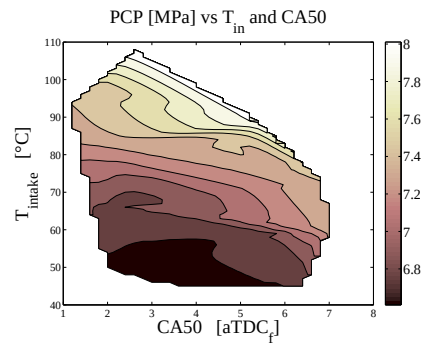

Figure 6: Peak cylinder pressure

The influence of the intake temperature is strong on achievable boost level. Since less burned gas fraction (x_b) is needed, see Figure 7, at higher intake temperatures for a given combustion phasing, the specific heat capacity in the charge is reduced and thus the mass flow rate is increased. This increased mass flow to the turbocharger increase the boost pressure.

The corresponding charge temperature at intake valve closing (T$_{IVC}$) is plotted in Figure 8. To shift the CA50 one degree, the T$_{IVC}$ changes approximately 8^o, except at low temperatures where the CA50 timing is very sensitive and changes rapidly to the T$_{IVC}$. The corresponding EVC position that is used to set the combustion phasing is seen in Figure 9.

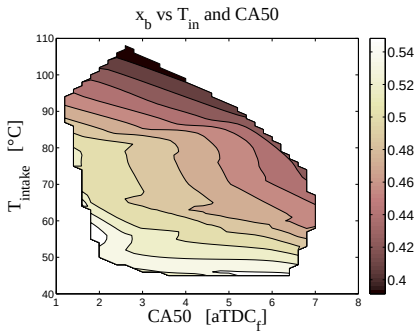

Figure 7: Burned gas fraction, x_b

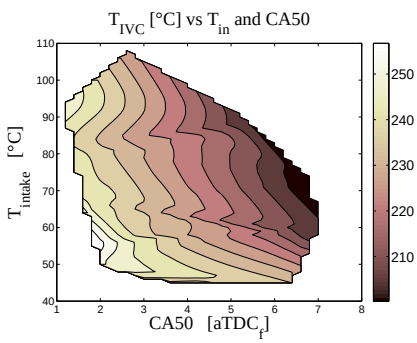

Figure 8: Temperature at IVC

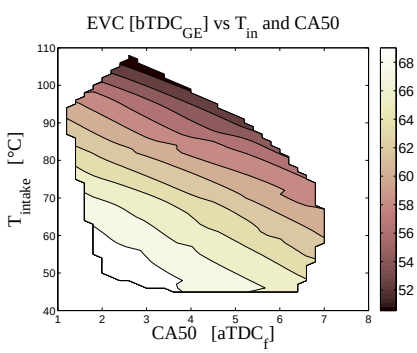

Figure 9: EVC position

When the boost level is increased it often comes at a cost, in the form of increased pumping losses that is represented as pumping mean effective pressure (PMEP) in Figure 10. The achievable boost pressure has to be weighted against the pumping losses from the turbocharger inefficiency and throttling losses over the valves, to keep engine efficiency as high as possible.

By separating the pumping losses in two parts further information is available: PMEP= Throttling$_{valve}$ + ($P_{ex} - P_{in}$)

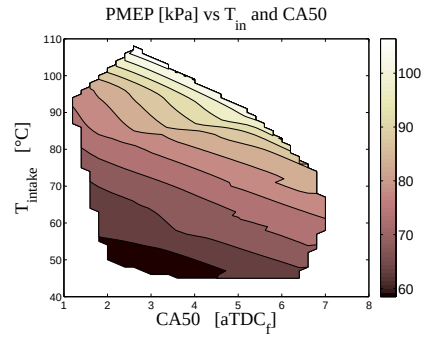

Figure 10: Pumping losses

$P_{ex} - P_{in}$: The pressure loss over turbine/compressor is shown in Figure 11.
Throttling$_{valve}$: The pressure loss over inlet and exhaust valves is shown in Figure 12.
With a turbocharger one usually encounters higher back pressure than boost pressure. Since the turbocharger is on the small side here, it was not possible to have a later CA50 timing than 3^o (aTDC$_f$) the highest intake temperature. The reason to this is that the back pressure increased considerable which led to reduced possible load range. The high throttling losses originates from the short duration valve timings. For example, at high HCCI load a late EVC is needed which lead to that the exhaust valve opening (EVO) can be close to BDC. This will increase the pumping work from the blow-down process.

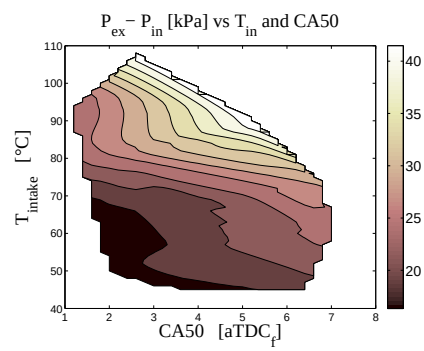

Figure 11: Pressure loss over turbine/ compressor

To decrease the engine noise the combustion timing can be delayed but this can increases the probability for misfire. The coefficient of variance (CoV) of IMEP$_{net}$ as seen in Figure 13 can be used as an indicator of combustion stability. Since the nature of HCCI combustion inhibits some cycle to cycle variations of combustion timing, the CoV of IMEP$_{net}$ need to be complemented by variations in combustion phasing as well. In Figure 14 the standard deviation (STD) of CA50 is plotted. Looking at the CoV graph, a later CA50 timing is the major influence of low

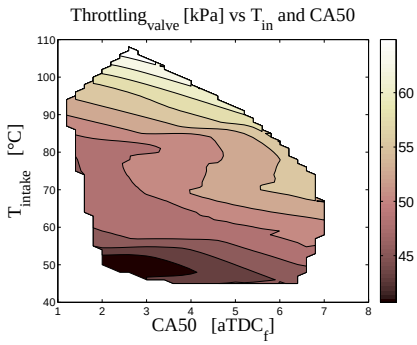

Figure 12: Valve throttling losses

combustion stability. But the STD of CA50 reveals that there is an issue when the intake temperature is low as well. This is also noticeable when listening to the engine running. It has a more ruff engine sound at low intake temperatures. At the lowest temperatures the burned gas fraction, as seen in Figure 7, is highest and the dilution from boost pressure is lowest, making the influence from small variations in T_{IVC} more pronounced, see Figure 8.

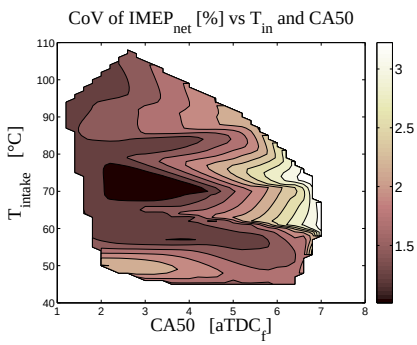

Figure 13: CoV of IMEP$_{net}$

The high pressure rise rate is the main limiting factor when the load is increased. In Figure 15 it can be seen that the CA50 position is the major control variable for the pressure rise rate. Recall that the intake pressure (Figure 5) increases with later CA50 position and high intake temperature. The pressure rise rate scale to the amount of dilution but the effect of this is masked to some extent because there is a need to burn more fuel at constant load when the pumping losses increases.

In Figure 16 the combustion duration for CA10 to CA90 is shown. The CA50 timing is the most important factor but there is some influence from the increased dilution with higher boost pressures as well. The residual gas (Figure 7) level has no direct influence on the combustion duration

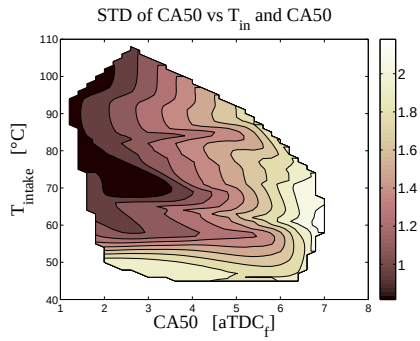

Figure 14: Standard deviation of CA50

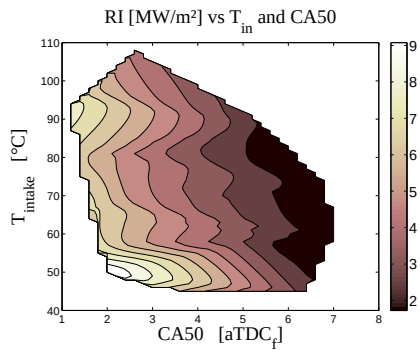

Figure 15: Ringing Intensity

here.

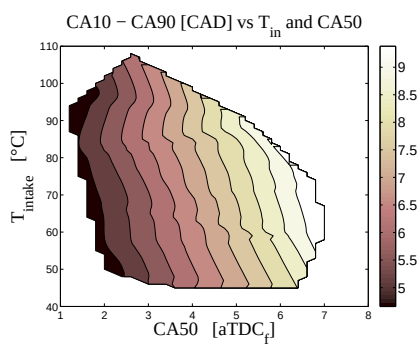

Figure 16: Combustion duration, CA10 to CA90

The NOx emissions can be an issue when the load is increased in HCCI mode but the NOx level at this engine speed and load is very low as seen in Figure 17. A later combustion timing decreases the combustion temperature with further reduction in the NOx level. The increased dilution from increased intake pressure is also a

reason for the low NOx levels. In Figure 18 the corresponding lambda is plotted. Normally when the NOx level is increased above a set limit [16] the lambda level is used to operate the engine stoichiometric on cylinder to cylinder basis.

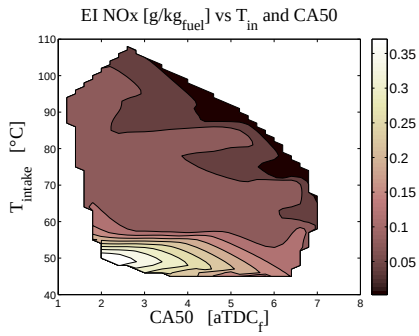

Figure 17: NOx emissions

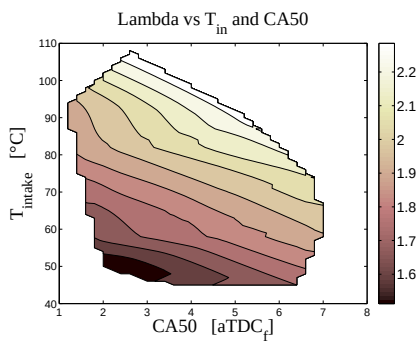

Figure 18: Lambda

The engine total efficiency can be divided into fractions [21] as seen in Figure 19. The combustion efficiency is defined as the relationship between heat released (Q$_{hr}$MEP) and normalized fuel energy/ cycle (FuelMEP). The thermodynamic efficiency is then the relationship between IMEP$_{gross}$ and Q$_{hr}$MEP. Gas exchange efficiency is defined as the relationship between IMEP$_{gross}$ and IMEP$_{net}$. Indicated efficiency is the relationship between IMEP$_{net}$ and FuelMEP.

By using suitable injection timings the combustion efficiency in Figure 20 is high at this test point. The main deviation is from the combustion timing. The thermal efficiency in Figure 21 on the other hand show its highest efficiency at low intake temperatures where the mass flow is low. At this low intake temperature there is a need for advanced exhaust valve timing. The heat losses during the recompression phase can be an issue but this is more

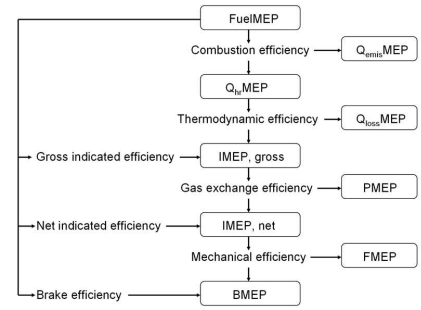

Figure 19: Engine efficency break-down

pronounced at low engine speeds. There is also an increase in thermal efficiency around $80^\circ\ C$. The gas exchange efficiency in Figure 22 scales to the intake pressure and originates from the turbocharger performance (Figure 11) and throttling losses (Figure 12) associated with these type of short duration valve lifts at increased load. The indicated efficiency Figure 23 is then the sum of the combustion, thermal and gas exchange efficiency. It is apparent that the intake temperature has strong influence on total efficiency where the operating temperature has to be balanced against combustion noise and stability.

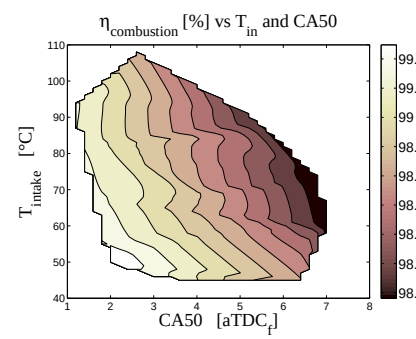

Figure 20: Combustion efficiency

The next test is on how external EGR influences engine operation. The EGR fraction is measured as the CO_2 ratio between the exhaust and the intake manifold.

EGR AND INTAKE TEMPERATURE SWEEP AT 2250 RPM AND 400 KPA IMEP$_{NET}$ The combustion timing during these tests has a CA50 position at 4^o (aTDC$_f$) except at the highest temperatures where no more than 3^o (aTDC$_f$) could be used due to increasing back pressure as described earlier. From this test there are some additional graphs that can be found in the APPENDIX.

In Figure 24 the available boost pressure decreases with

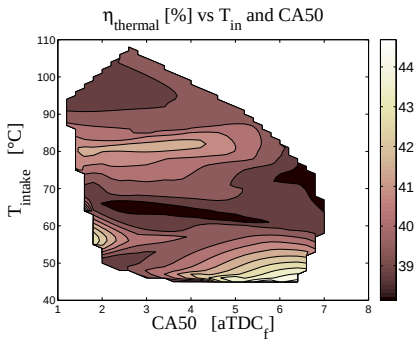

Figure 21: Thermal efficiency

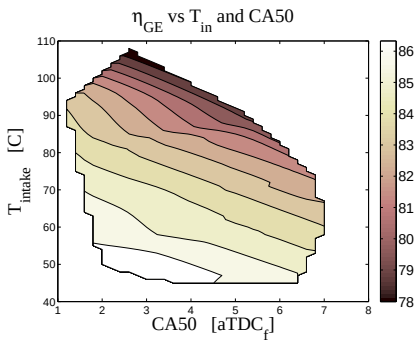

Figure 22: Gas exchange efficiency

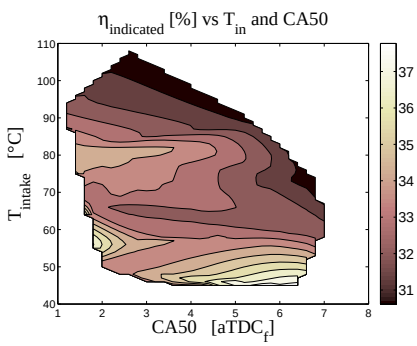

Figure 23: Indicated efficiency

increasing EGR levels. This is a function of the increased burned gas fraction, see Figure 25, where the charge will have an increased heat capacity. This leads to a decreased mass flow rate for a given combustion timing as seen in Figure 26.

The pumping losses are divided in two parts as described earlier. In Figure 27 the influence of increased EGR show some variation in turbocharger performance at lower in-

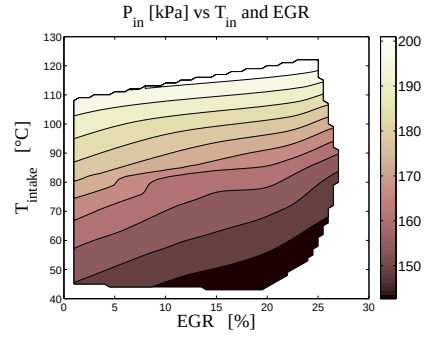

Figure 24: EGR sweep, Intake pressure

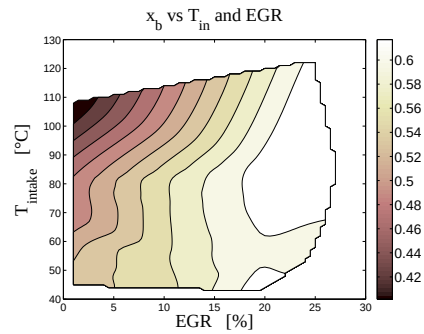

Figure 25: EGR sweep, Burned gas fraction

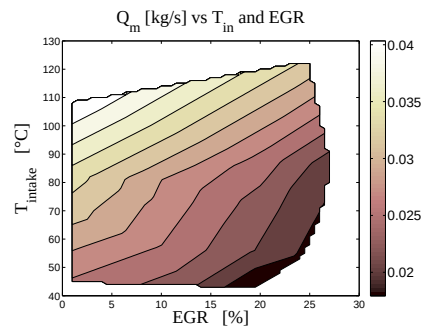

Figure 26: EGR sweep, Mass flow

take temperatures. The largest decrease in throttling losses occur at low intake temperatures and high EGR levels, see Figure 28. Here the mass flow is reduced which suites current valve timings.

The combustion stability seems to have an optimum around an intake temperature of 60° C when looking at the CoV of IMEP$_{net}$ in Figure 29. On the other hand, if we look at the standard deviation of CA50 in Figure 30 the picture broadens. Here an increase of EGR leads to less combustion fluctuations except at low intake temper-

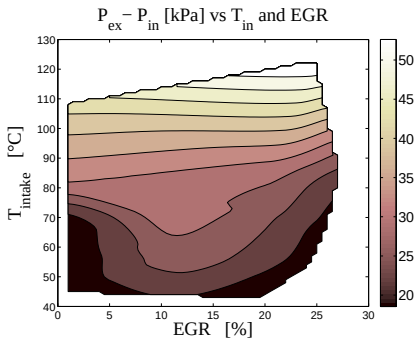

Figure 27: EGR sweep, Pressure losses over turbine–compressor

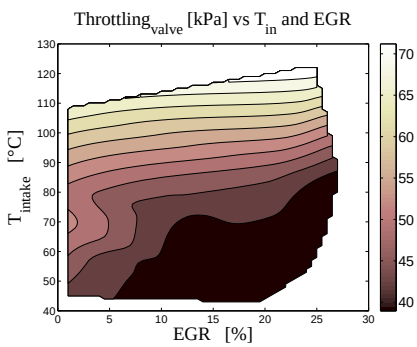

Figure 28: EGR sweep, Throttling losses

atures.

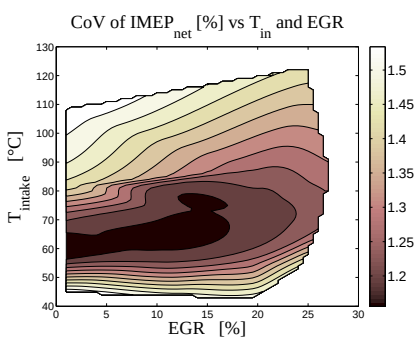

Figure 29: EGR sweep, CoV of IMEP$_{net}$

Since the combustion noise, quantified here with RI, is of major interest during turbocharged HCCI operation, it is seen that increased external EGR has different effects on RI depending on intake temperature, see Figure 31. At higher intake temperatures the RI level is stable even if the intake pressure is decreasing at the same time, see Figure 24. At lower temperatures RI is increasing with higher EGR levels. The corresponding combustion duration in Figure 32 reflects this behavior. There is no clear connection between the combustion duration and the burned gas fraction shown in Figure 25. In normal engine operating an increase of EGR level will delay the combustion timing due to increased in-cylinder heat capacity, but here the combustion timing is kept constant. In Figure 16 it could be seen that the combustion timing is the main parameter for the combustion duration.

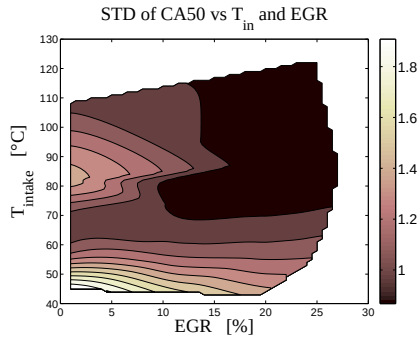

Figure 30: EGR sweep, Standard deviation of CA50

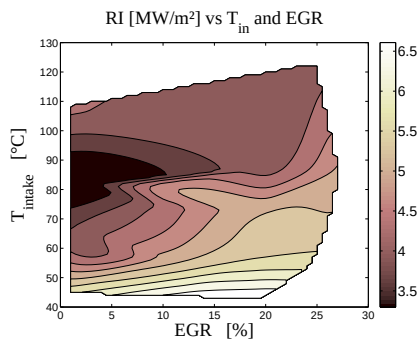

Figure 31: EGR sweep, Ringing Intensity

Finally the indicated efficiency in Figure 33 shows no real gain to operate with external EGR at this load and speed point (and these CA50 timings) except at the point with low intake temperature and high EGR level. But recall that the RI level and the cycle to cycle variations are high here.

Since the combustion timing is fixed during these tests the question rises of what happens if the combustion timing is swept with and without external EGR and the intake temperature is kept constant.

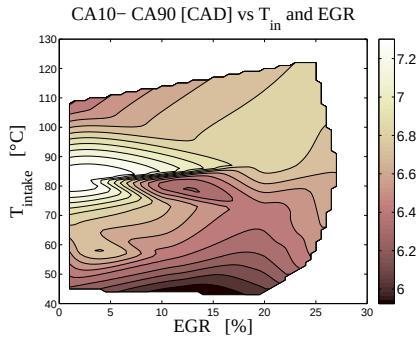

Figure 32: EGR sweep, Combustion duration, CA10 to CA90

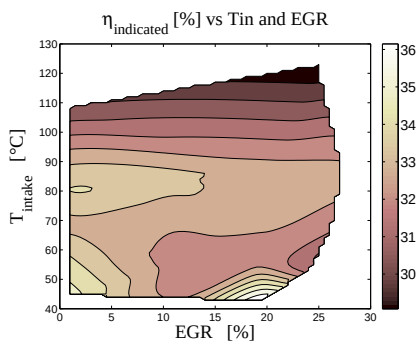

Figure 33: EGR sweep, Indicated efficiency

CA50 SWEEP WITH AND WITHOUT EGR AT 2250 RPM AND 400 KPA IMEP$_{NET}$ To further expand this load and speed point, a CA50 sweep is done with and without EGR at an intake temperature of $60^\circ\ C$. This intake temperature was chosen since it has acceptable RI levels, low cycle to cycle variations, a broad combustion timing range and rather high total efficiency. The EGR level is set around 19%, this range of positive displacement could be reached without any increase in backpressure. In Figure 34 the boost pressure is decreasing with EGR and so is also the throttling losses. The pressure differential between the intake and exhaust ($P_{ex} - P_{in}$) is not really affected by the increased EGR here.

In Figure 35 the CoV of IMEP is reduced with EGR at late CA50 timings, this trend is even more pronounced when looking at the STD of CA50. Notable is also that the operating range is wider with EGR. The combustion duration, CA10 to CA90, shows no real influence of EGR.

The RI is higher at early CA50 positions when using EGR which reflects the relative lower dilution level, see Figure 36. The other pressure rise expressions, dP/CAD and dP/ms, also reflect this at a smaller scale.

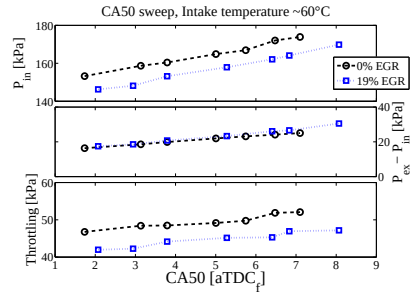

Figure 34: CA50 sweep, with and without EGR

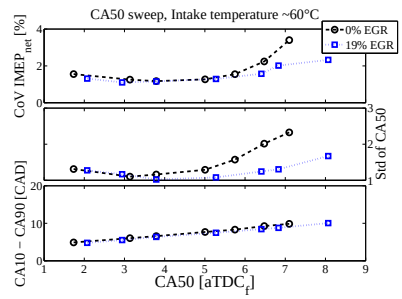

Figure 35: CA50 sweep, with and without EGR

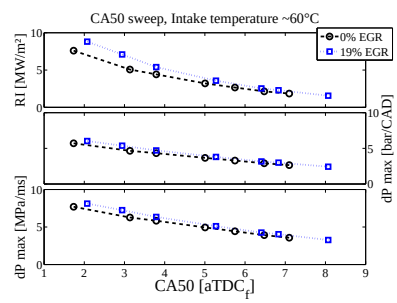

Figure 36: CA50 sweep, with and without EGR

In Figure 37 the combustion efficiency is higher with EGR but this effect is counteracted at early CA50 timings where the thermal efficiency is lower. The rise in thermal efficiencies at late CA50 timings reflects the more stable combustion position with EGR which has less cyclic fluctuations than without EGR. The gas exchange efficiency is improved slightly with EGR due to reduced throttling losses as shown in Figure 34. Finally the indicated efficiency shows that it can be beneficial to operate with EGR due to better combustion stability at late combustion timings.

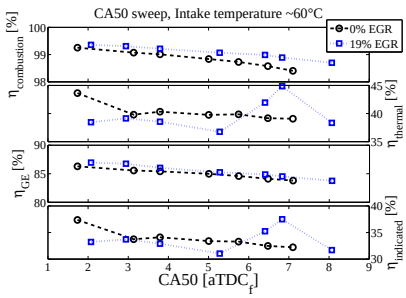

Figure 37: CA50 sweep, with and without EGR

DISCUSSION

When operating a turbocharged HCCI engine with NVO, the extra freedom to adjust the intake temperature is attractive from a combustion perspective where one can operate the engine at the most beneficial temperature. For example if the pressure rise rate is high we want a high intake pressure. Choosing a higher intake temperature leads to higher intake pressure and the combustion noise can be reduced. However, this has to be weighted against the increased pumping losses with reduction in efficiency. Too high intake pressure can result in loss of turbocharger performance and this was the case at the highest intake temperatures where the increasing backpressure limited the available combustion timing range. This can be circumvented by appropriate intake valve timing which is constrained in these tests. A shrinking combustion timing range puts even higher demands on the control system, especially during transients where a broad combustion timing range is wanted.

At this speed and load point, 2250 rpm and IMEP$_{net}$ 400 kPa, the best efficiency was reached with low intake temperatures but at the same time there is a loss of combustion stability. The loss of combustion stability is not really obvious when only using the CoV of IMEP$_{net}$ as a measurement. The standard deviation of CA50 visualizes the combustion stability more clearly. By using external EGR the combustion range and stability can be increased. EGR show no big influence on combustion duration and efficiency. The usage of an external EGR systems added weight, cost and control complexity, has to be considered.

The combustion timing is the major variable during these tests since it directly control the dilution level and the intake temperature level that can be reached. This gives the combustion timing a huge impact on test results in HCCI mode. This further emphasizes the importance of robust combustion timing control in turbocharged HCCI mode. The prediction of the in-cylinder charge temperature and properties at IVC can be used by the control system. Combined with a DI fuel system there is a possibility to influence the combustion timing at a late stage.

To find the optimum operating intake temperature and combustion timing one has to balance factors like pressure rise rate, efficiency, combustion stability/ range and emissions level against each other. This study is only performed at one engine speed and load point so the question is how the results are at other speed/ load points, how changes in turbocharger, valve timings etc. influences the result. This need to be investigated in future work.

CONCLUSIONS

From this test point at 2250 rpm and 400 kPa IMEP$_{net}$

- Available intake pressure scales directly with intake temperature and combustion timing, it can therefore be modulated with charge cooling and valve timings.
- An increase of intake pressure decreases peak pressure rise rate but has to be weighed against increasing pumping losses.
- The highest indicated efficiency at this study was found with the lowest intake temperature, but in practice, the high pressure rise rate and cyclic variations makes it an unsuitable working area.
- Standard deviation of the combustion phasing is a good measurement of combustion stability that can complement CoV of IMEP$_{net}$ for the cycle to cycle behavior.
- The usage of external EGR is shown to improve combustion stability and extend usable combustion timing range.
- Turbocharger performance and appropriate valve timings are vital for improving efficiency and operating range in a NVO HCCI engine.
- Test results are heavily influenced by the combustion timing.

ACKNOWLEDGMENTS

This project is supported by GM Powertrain and the Swedish Energy Agency

REFERENCES

[1] Kalghatgi, G. T, Risberg, P., Ångström, H-E., "Advantages of fuels with high resistance to auto-ignition, low temperature, compression ignition combustion," *SAE Paper 2006-01-3385*.

[2] Marriot, C. D., Reitz, R. D., "Experimental investigation of direct injection- gasoline for premixed compression ignited combustion phasing control," *SAE Paper 2002-01-0418*.

[3] Urushihara, T., Hiraya, K., Kakuhou, A., Itoh, T., "Expansion of HCCI operating region by the combination of direct fuel injection, negative valve overlap and internal fuel reformation," *SAE Paper 2003-01-0749*.

[4] Dec, J. E., Hwang, W., Sjöberg, M., "An investigation of thermal stratification in HCCI engines using chemiluminescence imaging," *SAE Paper 2006-01-1518*.

[5] Thring, R. H., "Homogeneous-charge compression-ignition (HCCI) engines," *SAE Paper 892068*.

[6] Christensen, M., Hultqvist, A., Johansson, B.,, "Demonstrating the multi-fuel capability of a homogeneous charge compression ignition engine with variable compression ratio," *SAE Paper 1999-01-3679*.

[7] Haraldsson, G., Tunestål, P. , Johansson, B., Hyvönen, J., "HCCI combustion phasing in a multi-cylinder engine using variable compression ratio," *SAE Paper 2002-01-2858*.

[8] Lang, O., Salber, W., Hahn, J., Pischinger, S., Hortmann, K., Bücker, C., "Thermodynamical and mechanical approach towards a variable valve train for the controlled auto ignition combustion Process," *SAE Paper 2005-01-0762*.

[9] Martinez- Frias, J., Aceves, S. M., Flowers, D., Smith, R., Dibble, R., "HCCI engine control by thermal management," *SAE Paper 2000-01-2869*.

[10] Haraldsson, G., Tunestål, P. , Johansson, B., Hyvönen, J.,"HCCI closed- loop combustion control using fast thermal management," *SAE Paper 2004-01-0943*.

[11] Persson, H., Agrell, M., Olsson, J-O. ,Johansson, B., Ström, H.,"The effect of intake temperature using negative valve overlap," *SAE Paper 2004-01-0944*.

[12] Christensen, M., Johansson, B., Amnéus, P. Mauss, F., "Supercharged homogeneous charge compression ignition," *SAE Paper 980787*.

[13] Christensen, M., Johansson, B., "Supercharged homogeneous charge compression ignition (hcci) with exhaust gas recirculation and pilot fuel," *SAE Paper 2000-01-1835*.

[14] Hyvönen, J., Haraldsson, G., Johansson, B., "Supercharging HCCI to extend the operating range in a multi-cylinder VCR-HCCI engine," *SAE Paper 2003-01-3214*.

[15] Olsson, J-O., Tunestål, P., Johansson, B., "Boosting for high load HCCI," *SAE Paper 2004-01-0940*.

[16] Johansson, T., Johansson, B., Tunestål, P., Aulin, H., "HCCI operating range in a turbo-charged multi cylinder with VVT and spray- guided DI," *SAE Paper 2009-01-0494*.

[17] Sjöberg, M., Dec, J.E., Hwang, W., "Thermodynamic and Chemical Effects of EGR and Its Constituents on HCCI Autoignition," *SAE Paper 2007-01-0207*.

[18] Olsson, J-O., Tunestål, P., Ulfvik, J., Johansson, B., "THe effect of cooled EGR on emissions and performance of a turbocharged HCCI engine," *SAE Paper 2003-01-0743*.

[19] Andreae, M.M, Cheng, W.K., Kenney, T., Yang, J., "On HCCI Engine Knock," *SAE Paper 2007-01-1858*.

[20] Eng, J.A., "Characterization of pressure waves in HCCI combustion," *SAE Paper 2002-01-2859*.

[21] Hyvönen, J., Wilhelmsson, K., Johansson, B., "The effect of displacement on air-diluted, multi-cylinder HCCI engine performance," *SAE Paper 2006-01-0205*.

CONTACT

Thomas Johansson, M.Sc.ME

E-mail: Thomas.Johansson@energy.lth.se

Lund University, Faculty of Engineering, Department of Energy Sciences, Division of Combustion Engines, P.O. Box 118, SE-221 00 Lund, Sweden

DEFINITIONS AND ABBREVIATIONS

aTDC$_f$:	After Top Dead Center, firing
BDC:	Bottom Dead Center
CA10:	Crank angle 10% burned
CA50:	Crank angle 50% burned
CA90:	Crank angle 90% burned
CB:	Cylinder Balancing
CAD:	Crank Angle Degrees
CoV:	Coefficient of Variation
DI:	Direct Injection
dP:	Pressure derivate
EI:	Emission Index
EGR:	Exhaust Gas Recirculation
EVC:	Exhaust Valve Closing
EVO:	Exhaust Valve Open
$\eta_{combustion}$:	Efficiency, combustion
η_{GE}:	Efficiency, gas exchange
$\eta_{indicated}$:	Efficiency, indicated
$\eta_{thermal}$:	Efficiency, thermal
FuelMEP:	Fuel Mean Effective Pressure
HCCI:	Homogeneous Charge Compression Ignition
IMEP$_{gross}$:	Indicated Mean Effective Pressure, gross
IMEP$_{net}$:	Indicated Mean Effective Pressure, net
IVC:	Intake Valve Closing
IVO:	Intake Valve Opening
NA:	Naturally Aspirated
NOx:	Nitrogen Oxide
NVO:	Negative Valve Overlap
P$_{ex}$:	Pressure Exhaust
P$_{in}$:	Pressure Intake
PCP:	Peak Cylinder Pressure
PMEP:	Pumping Mean Effevtive Pressure
Q$_{emis}$MEP:	Emission Mean Effevtive Pressure
Q$_{hr}$MEP:	Heat Release Mean Effevtive Pressure
Q$_{loss}$MEP:	Heat losses Mean Effevtive Pressure
RI:	Ringing Intensity
SI:	Spark Ignition
STD:	Standard deviation
TDC:	Top Dead Center
TDC$_f$:	Top Dead Center, firing
TDC$_{GE}$:	Top Dead Center, gas exchange
T$_{IVC}$;	Temperature, intake valve closing
VVT:	Variable Valve Timing
x$_b$:	Burned gas fraction

APPENDIX

Complementary graphs from CA50 and intake temperature sweep at 2250 rpm and 400 kPa IMEP$_{net}$

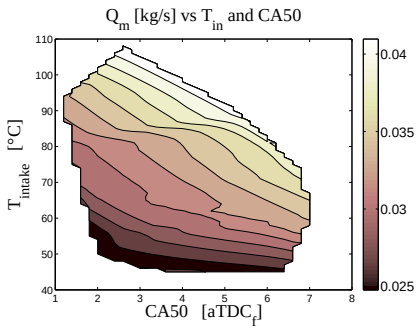

Figure 38: Mass flow

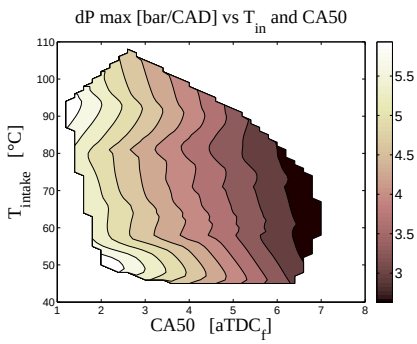

Figure 39: Pressure rise, bar/ CAD

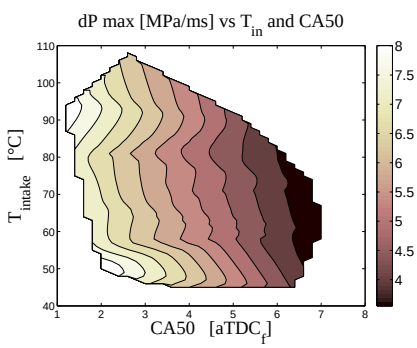

Figure 40: Pressure rise, MPa/ ms

Complementary graphs from EGR sweep at 2250 rpm and 400 kPa IMEP$_{net}$

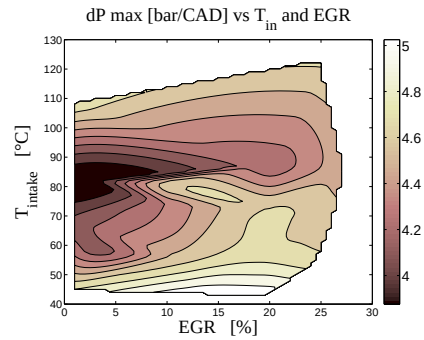

Figure 41: EGR sweep, Pressure rise dP/ CAD

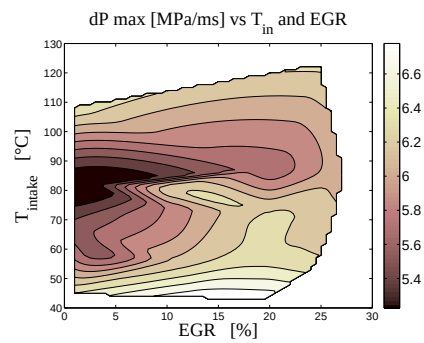

Figure 42: EGR sweep, Pressure rise dP/ ms

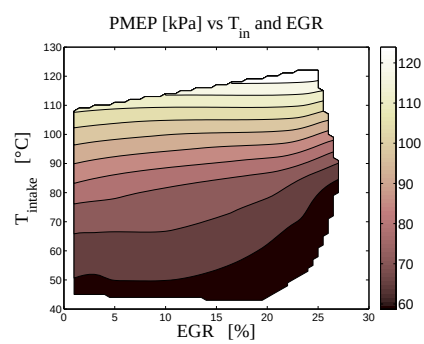

Figure 43: EGR sweep, Pumping losses

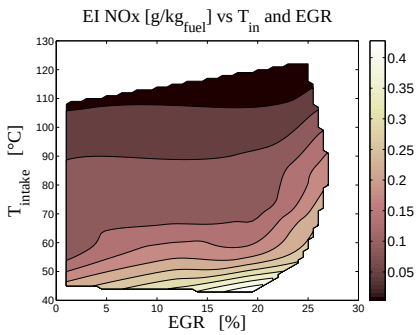

Figure 44: EGR sweep, NOx emissions

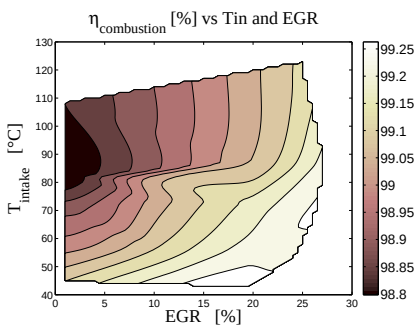

Figure 45: EGR sweep, Combustion efficiency

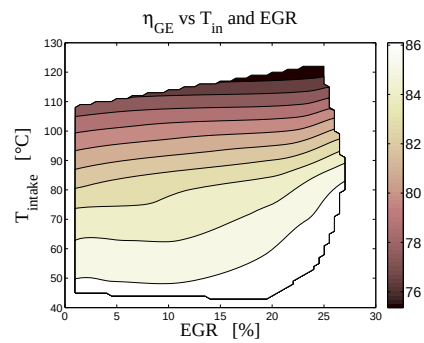

Figure 47: EGR sweep, Gas exchange efficiency

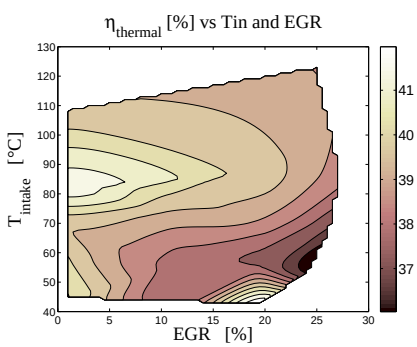

Figure 46: EGR sweep, Thermal efficiency

Paper V

2010-01-1490

HCCI Heat Release Data for Combustion Simulation, based on Results from a Turbocharged Multi Cylinder Engine

Thomas Johansson, Patrick Borgqvist, Bengt Johansson, Per Tunestål
Lund University

Hans Aulin
SAAB Automobile Powertrain AB

Copyright © 2010 SAE International

ABSTRACT

When simulating homogenous charge compression ignition or HCCI using one-dimensional models it is important to have the right combustion parameters. When operating in HCCI the heat release parameters will have a high influence on the simulation result due to the rapid combustion rate, especially if the engine is turbocharged. In this paper an extensive testing data base is used for showing the combustion data from a turbocharged engine operating in HCCI mode. The experimental data cover a wide range, which span from 1000 rpm to 3000 rpm and engine loads between 100 kPa up to over 600 kPa indicated mean effective pressure in this engine speed range. The combustion data presented are: used combustion timing, combustion duration and heat release rate. The combustion timing follows the load and a trend line is presented that is used for engine simulation. The combustion duration in time is fairly constant at different load and engine speeds for the chosen combustion timings here. The heat release rate is fitted to a Wiebe function where the heat release parameter *m* is found. It is shown that this parameter *m* scale to the load and the presented trend line is used for simulating the heat release. When the engine is operated with negative valve overlap the mass flow is reduced through the engine. In an engine simulation the valve timings has to be estimated for different intake temperatures and boost pressure levels. By using the intake temperature at intake valve closing as a prediction tool for the temperature at top dead center, the exhaust valve closing timing can be estimated and will then follow the real test results closely as shown in a GT-Power simulation. The turbocharged test engine is an in-line four cylinder gasoline engine with a total displacement of 2.2 *l*. The engine is direct injected of spray-guided type. To achieve HCCI combustion the engine is operated with low lift and short duration valve timings where the variable negative valve overlap is used for combustion control.

INTRODUCTION

The homogenous charge compression ignition (HCCI) combustion can offer high thermodynamic efficiency, low throttling losses and low emissions. The limited operating range in HCCI mode makes it an alternative to the spark ignited (SI) engine at low load to improve the efficiency of the SI engine. In HCCI mode the air-fuel charge is auto ignited by controlling the temperature and pressure history inside the engine cylinder to initiate and time the combustion phasing at the right moment.

To reach auto ignition in a four-stroke engine the in-cylinder temperature is normally increased by exhaust gas recirculation (EGR), air heating or both as outlined in the eighties by Thring [1]. The compression ratio can also

be used to control the HCCI combustion timing [2,3] The concept with negative valve overlap (NVO) uses early exhaust valve closing to trap a certain amount of hot residuals is widely accepted to control combustion timing. Here the variable valve timing (VVT) is accurately controlled either mechanically or electrically.

The concept of re-breathing [4] might be more mechanically complicated but has an advantage in reduced heat losses since it can be operated without recompression. The combustion timing in HCCI can also be adjusted with the intake temperature by a thermal management system [5,6], but this requires a heat recovery system.

By boosting the engine in HCCI mode the possible load range can be extended [7,8,9,10,11]. The boost pressure can be controlled directly by the intake valve timing [11] which gives large freedom to operate the engine with optimum efficiency, emissions, combustion noise, cyclic variations and control strategies. With NVO the intake temperature directly affects how much internal EGR is needed for a given combustion timing and therefore the in-cylinder relative burn gas fraction. By increasing the intake temperature, less internal EGR is needed which lead to increased mass flow that can lead to higher boost pressure [12]. In addition to the internal EGR, external cooled EGR can be used and it was found that it could improve combustion efficiency while there seem to be low influence on the combustion duration [13] in HCCI mode.

The main operating parameter in HCCI mode is the combustion timing here represented by the crank angle of 50 % heat released (CA50). The CA50 timing will affect the engine performance substantially and need to be controlled exactly to run the HCCI engine successfully. If engine speed goes up or if load is increased the CA50 window for stable engine operating will be narrowed [12], making the engine control more challenging.

When simulating HCCI it is vital to have the right combustion parameters, especially if the engine is turbocharged. The combustion timing and heat release rate has to be predicted together appropriate valve timings. If the engine is operated with NVO and short duration valve timings there can be high throttling losses over the valves [12] and this need to be predicted when simulating the engine performance. Since the boost pressure is used to decrease the combustion noise it is vital that the turbocharger performance is predicted accurately. The scope of this paper is to present data from extensive engine testing and show how it can be used in an engine simulating program.

EXPERIMENTAL SET-UP

ENGINE SYSTEM

The test engine is an in-line four cylinder gasoline engine with a total displacement of 2.2 *l*. The cylinder head is a 4-valve design with a pent-roof combustion chamber. There are some small squish areas on the intake and exhaust sides. The piston has a raised piston dome with a small bowl in the center. The intake channel is side-drafted with a low tumble design. The engine has direct injection (DI) of a Spray-Guided type slightly with a centrally placed injector. The eight-hole solenoid fuel injector has a cone angle of 60°. The spark plug is located close to the fuel injector and has an extended tip. The spark is always operated as a safety measurement against misfires and it can also improve the combustion stability at late combustion timings.

To achieve HCCI combustion the engine is operated with NVO with low lift and short duration camshafts as seen in Figure 1 where the minimum and maximum valve timings are plotted. The variable valve timing (VVT) is controlled by hydraulic actuators at the camshafts giving a separate 50 crank angle degree (CAD) adjustment on both intake and exhaust valve timings. The engine is turbocharged by a fixed geometry turbine. The exhaust manifold is of pulse type with short individual runners straight to the turbine inlet as seen in Figure 2. On the intake side there is a water cooled intercooler. The heated aluminum intake manifold has short intake runners

and a small volume as seen in Figure 3. The cooling system has an electric driven water pump and the coolant temperature is adjusted by the control system. Engine specifications are listed in Table 1.

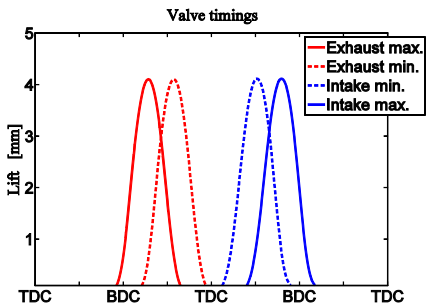

Figure 1: Valve timing range

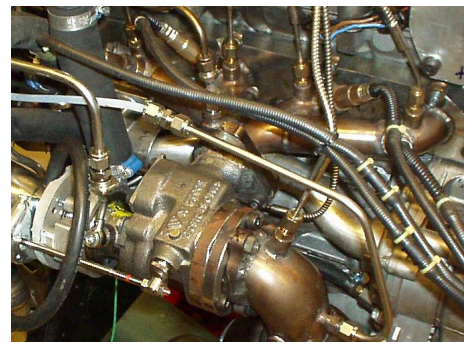

Figure 2: Exhaust manifold

Figure 3: Intake manifold

MEASUREMENT AND CONTROL SYSTEM

The control system is a combined data acquisition and engine control unit from dSPACE. The signals from a fully instrumented engine set-up are collected and analyzed. For combustion feedback there are individual cylinder pressure sensors. The control system has an in-cycle resolved heat release calculation where main parameters like CA50, peak cylinder pressure (PCP) and peak pressure derivative (dP/CAD) etc. are used for cylinder individual control in closed loop. The crank angle decoder has a resolution of 0.2 CAD. Emission analysis and soot measurement are collected on an external PC and the data is sent to the control unit.

To increase the operating range it is important that all the cylinders operate identically, meaning that they have the same CA50 position, indicated mean effective pressure (IMEP) and peak pressure rise rate. This means that the control system has to perform cylinder balancing. Injection of the fuel in NVO can give a reformation of the fuel, resulting in an increase of charge temperature and a reduction in effective octane number leading to more

advanced combustion timing. The combustion timing will be more advanced if the fuel is injected in the beginning of the NVO than in the end. The control system sets the CA50 position and uses the cylinder with the most advanced CA50 position for the exhaust valve closing (EVC) set point. The other cylinders are then advanced by adjusting the injection timing and/or fuel amount in the first injection, until all cylinders have the same CA50 position. Since there will be some differences in injection timing when using CA50 balancing there will also be some differences in efficiency between the cylinders. This results in different load, IMEP in the cylinders. To maximize the load range there has to be cylinder balancing of IMEP as well. This is done at the main injection event. Obviously this affect the CA50 balancing since increasing the fuel amount will raise the combustion heat, leading to earlier CA50 for that cylinder. Therefore the cylinder balancing has to be constantly monitored and adjusted by the actuator set points. Table 2 shows the measurement and control equipment.

Table 1: Engine specifications

Number of cylinders	4
Displacement	2198 cm³
Bore x Stroke	86 mm x 94.6 mm
Compression Ratio	11.75:1
Valve duration IN	125 CAD
Valve duration EX	155 CAD
NVO range	90 -190 CAD
Turbocharger	B&W KP31
Fuel Supply	DI, up to 20 MPa pressure
Fuel Type	Gasoline, 95 RON

Table 2: Measurement and control system

ECU and data logging	dSPACE Rapid Pro
Cylinder pressure sensor	Kistler 6043Asp
Charge amplifier	Kistler 5011B
Emission analyzer	Horiba 9100 MEXA
Soot analyzer	AVL 415 S

TEMPERATURE AND EGR CONTROL SYSTEM

The intake temperature is controlled by an electrical throttle in the bypass routing to the water-cooled intercooler circuit, see Figure 4. When the throttle is fully open the main air flow goes through the bypass routing since it has less flow resistance than the intercooler circuit. By closing the throttle the airflow is forced through the intercooler circuit.

The long route EGR system takes exhaust gas after the turbine and route it to the compressor inlet. To get a positive displacement of exhaust gas there is a throttle in the exhaust system to increase back pressure. The compressor inlet can be used as an ejector to enhance the EGR flow, so the needed back pressure is quite small. The external EGR routing is cooled by the engine cooling circuit and is controlled by an EGR valve near the turbocharger, see Figure 4. The external EGR is used when the engine is operated stoichiometric or when the pumping losses need to be reduced. The pumping losses can be reduced with these types of short duration valve timings by adding cooled EGR to get more beneficial valve timings. If the turbocharger builds more back pressure than boost pressure due to a choked turbine, addition of external EGR will reduce the mass flow. The reason to this is that more internal EGR is needed for a given combustion timing when the heat capacity of the intake charge is increased.

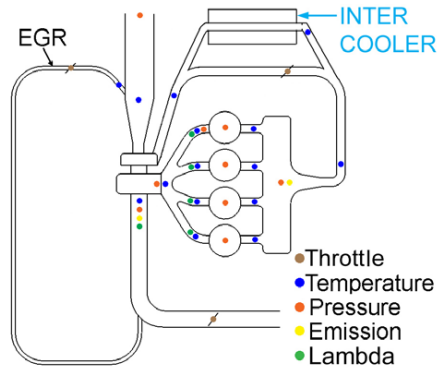

Figure 4: Engine layout

RESULTS AND DISCUSSION

OPERATING LIMITATIONS

When operating in HCCI mode one has to consider operating limitations due to combustion noise, combustion stability, soot level, emission level and peak cylinder pressure. These are outlined in author's previous paper [11] but here is a short background.

Combustion Noise: The maximum load in HCCI is often limited by the fast combustion rate where the combustion induced noise is a major factor. By increasing the air dilution in the cylinder using for example a turbocharger, the audible noise is suppressed and the HCCI load range can be extended. Normally the pressure rise rate is measured in bar/CAD or MPa/ms [14] and is used to impose some operating limits but neither of these catch the real combustion noise when the engine is supercharged. The Ringing Intensity (RI)- MW/m^2 [15] on the other hand compares the pressure rise rate to peak cylinder pressure and engine speed and therefore gives an good indication of the combustion noise. The RI level should be less than 6 MW/m^2.

Coefficient of variation (CoV): HCCI is known for its low CoV of IMEP compared to SI engines but with a late combustion timing the CoV of IMEP increases rapid in HCCI. At higher engine speeds where the time window for proper combustion phasing is reduced, it is more difficult to retard the combustion. We have found that there is less risk for misfire when the CoV is kept under 3.5 %. Misfire at high HCCI load results in violent combustion the following cycles and must be avoided at all times. At low load ie IMEP around 100 kPa the standard deviation (STD) of IMEP is used as limitation instead of CoV and the limit is set to 15 kPa.

Soot level: To get a filter smoke number (FSN) limit on soot we look at the Euro 5 and 6 legislation which limits the soot level to 0.005 g/km, if we assume a vehicle with a fuel consumption of 0.06 l/km or 44 g/km and operating at λ=1.5 the Smoke opacity arrives roughly at 0.25 [16] which corresponds to a FSN value of 0.05 [17].

Nitrogen oxides (NOx) level: HCCI is known for the low NOx emission levels but as the load increases, NOx emissions increase due to higher temperature and relative less dilution, meaning there will be a NOx limit when

operating lean HCCI (and using a normal TWC). The Euro 5 and 6 limits the NOx emissions at 0.06 g/km, if we again assume a fuel consumption of 44 g/km, the corresponding NOx level will be 1.36 g/kg_{fuel}. To be on the safe side our NOx limit is set 20 % below this value at 1.1 g/kg_{fuel}. If this limit is reached the HCCI engine is operated stoichiometric with external EGR.

Peak cylinder pressure (PCP): Since PCP scales with the intake pressure it can become a limiting factor when the engine is turbocharged. There is risk for structural damage of the engine if the design limit is exceeded and for this engine the maximum limit is set to 9.5 MPa.

The results from the above described limitations can be found in the Appendix where also the intake pressure and peak pressure rise is included, since the RI is a function of these.

RESULTS FROM SPEED AND LOAD TEST

The engine is tested from lowest to highest possible load between 1000 to 3000 rpm. The load is represented here with $IMEP_{gross}$ since this is the input for the engine simulations. The test is done in load steps of 50 kPa and engine speed steps of 500 rpm. It is done with the limitations as seen in Table 3. The goal is to have highest possible efficiency in the whole operating range. When the gas exchange efficiency is included for this engine the maximum $IMEP_{net}$ stays above 600 kPa and the resulting BMEP is above 500 kPa between 1000 to 3000 rpm.

Table 3: Engine operating limitations

Combustion noise	RI	6 MW/m²
Combustion stability	CoV of IMEP or STD of IMEP	3.5% or 15 kPa
Soot emission	FSN	0.05 average
NOx emission	EI NOx	1.1 g/kg_{fuel}
Peak cylinder pressure	PCP	9.5 Mpa

COMBUSTION TIMING

The combustion timing- CA50 is the main operating parameter when running in HCCI mode, a later CA50 can raise the upper load limit by decreasing the RI and PCP. This has to be weighted against an efficiency loss when moving away from the timing for maximum brake torque (MBT). A later CA50 will increase the energy to the turbine with higher boost as a result. This is the result from the increased mass flow since less EVC is needed for a later CA50 timing, therfore the turbocharger sizing plays an important role. The boosted HCCI engine can on the other hand for a given RI at high load use a better phased combustion and hence improve thermal efficiency compared to a naturally aspirated (NA) HCCI engine. In Figure 10 the used CA50 timing can be seen. At low load the CA50 timing is advanced before TDC to stabilize the combustion and as load gets higher the CA50 timing is retarded. The ignition timing is adjusted when it has some influence on combustion stability, both at low and high load as seen in Figure 6. The combustion timing is chosen for maximum efficiency and turbocharger performance. In Figure 11 the CA50 is plotted against the load and a trend line is fitted. The trend line equation for CA50 can then be used as a result dependent function in the simulation program. At high load and engine speed the CA50 timing could not be retarded more due choking of the rather small turbine in this set-up. A later CA50 would mean that the EVC timing has to be retarded, this will increase the mass flow which here leads to an increase in pumping losses (backpressure goes up with no gain in boost pressure).

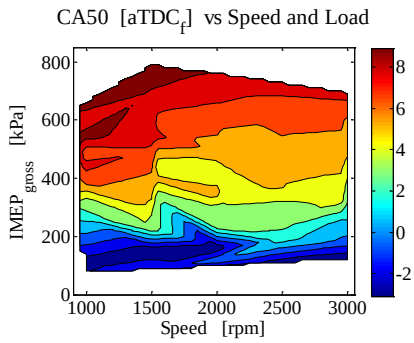

Figure 5: Combustion timing, CA50

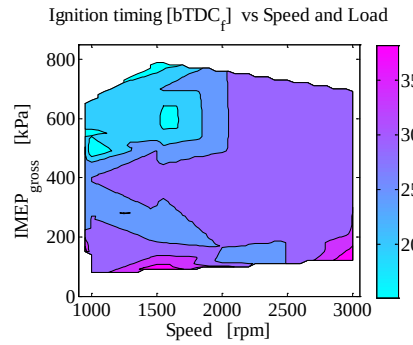

Figure 6: Ignition timing

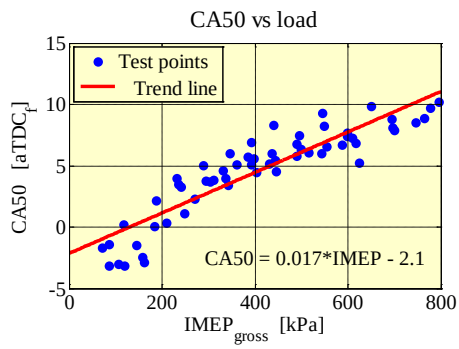

Figure 7: Combustion timing vs. load

COMBUSTION DURATION

The combustion duration between CA10 to CA90 is seen in Figure 8 and it scales to the engine speed. As engine speed is increased the combustion duration is increased in crank angle degrees but in time it stays fairly constant as seen in Figure 9. At low engine speed the combustion time is increased which reflects the stronger influence from spark assisting that is used here. The average time for the combustion duration (CA10 to CA90) in most of the operating range is around 0.7 ms and this can then be used in the simulation program.

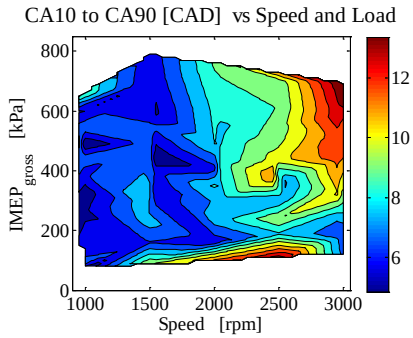

Figure 8: Combustion duration in crank angle degrees

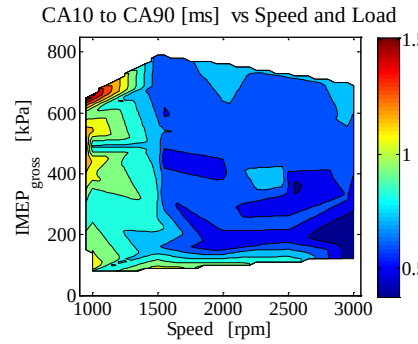

Figure 9: Combustion duration in time

THE WIEBE FUNCTION, FOR HEAT RELEASE SIMULATION

When simulating with single zone combustion models the heat release rate is fitted over the combustion duration and can give a good approximating of the heat release rate. The most common function is the Wiebe function that can be used for the heat release rate in HCCI mode. As seen in Equation 1 there is two unknown parameters, *a* and *m*.

$$x_b = 1 - \exp[-a(\frac{\theta - \theta_{SOC}}{\Delta\theta})^{m+1}] \qquad (1)$$

The parameter *a* estimates the completeness of the combustion process. Typically *a* is set to 5 CAD [18] which corresponds to 99.3 % of burned mass in the function. The parameter *m* depends on the heat release rate, meaning that a small value of *m* will have a high initial heat release rate. A common value of *m* is 2 [18] which give an S-shaped heat release. From this engine testing results, the real heat release is fitted with a Wiebe function where the *a* parameter is set to 5 and the *m* parameter is found by a non linear least square function between 0 and 10 for best fit between the heat release and the Wiebe function. This is done to the heat release from 0.5 % to 99.3 % burned. An example of a real heat release and the corresponding *m* constant in the Wiebe function can be seen in Figure 10. This optimized single Wiebe function does follow the real heat release closely. The result of the *m* parameter for the whole operating range can be seen in Figure 11. The *m* constant is scaling to the load and in Figure 12 the trend line for *m* is plotted against the load. The trend line equation for *m* can then be used as a result dependent function in the simulation program.

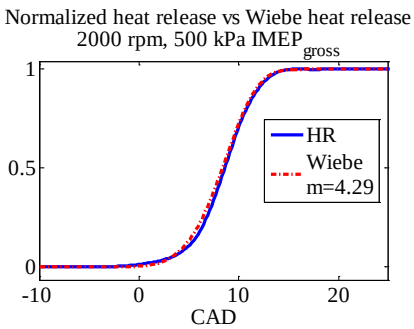

Figure 10: Heat release comparison

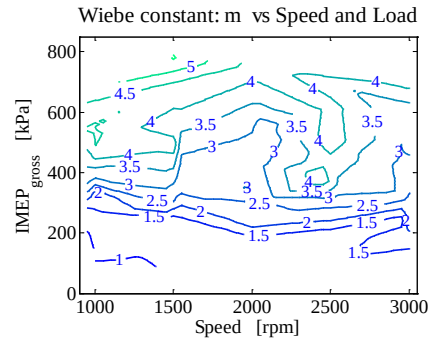

Figure 11: Wiebe constant *m* vs speed and load

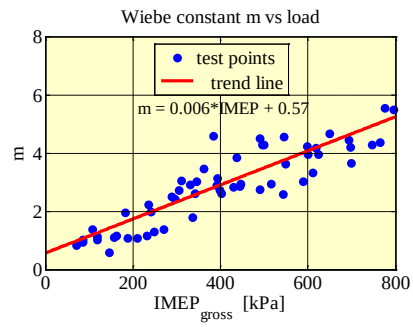

Figure 12: Wiebe constant *m* vs load

ESTIMATING THE EVC POSITION

To set the right condition for auto ignition with NVO some exhaust gases are kept in the cylinder by appropriate exhaust valve timing. The charge is then heated during compression until combustion around TDC. The EVC position controls the combustion timing but at the same time it also influences the mass flow in the engine. To be able to simulate a turbocharged HCCI engine it is important to set the EVC position correct as seen in Figure 13. Here an EVC sweep is done in GT-Power and a change of EVC position of 3 CAD makes the boost pressure differ 12 kPa at this load and speed (2250 rpm and $IMEP_{net}$ 400 kPa). Since the combustions noise relates to the RI level it is vital to predict the boost pressure to choose a suitable sized turbocharger.

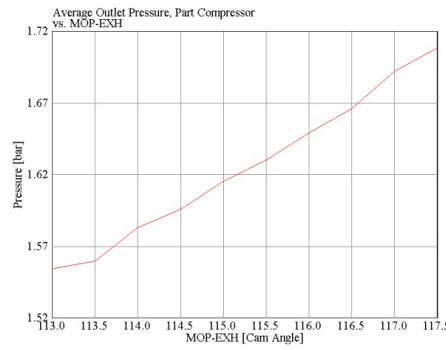

Figure 13: Intake pressure vs. EVC (MOP-EXH) in an engine simulation program

For simulating it is advisable to have the temperature close to TDC as a boundary condition for controlling the EVC position. From the engine testing the calculated temperature at intake valve closing (T_{IVC}) is seen in Figure 14. To estimate this temperature- T_{IVC}, the EVC position sets the trapped volume of internal EGR. The exhaust density is calculated from the lambda level that gives the chemical composition, these species is then adjusted by the exhaust temperature and pressure to calculate the internal EGR mass. The inducted mass is estimated using the intake temperature and pressure together with the lambda level, the measured fuel flow and the external EGR ratio. The mass fractions of the internal EGR and the inducted mass with their respective temperatures are then summarized. By adding the fuel vaporization cooling effect and Woschni heat transfer model the T_{IVC} can be estimated by an ideal cycle calculation. As can be seen the T_{IVC} variation is almost 100 degrees.

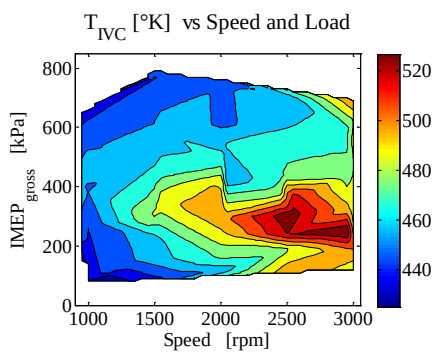

Figure 14: Temperature at intake valve closing, T_{IVC}

The same calculation gives the burned gas fraction (x_b) since the T_{IVC} calculation gives the respective mass ratio. This ratio can be seen in Figure 15. At low load it might look like there is no oxygen left to burn with a burned gas fraction around 90 % but the engine is operated lean here and the internal oxygen level is about 8 %. By setting the specific heat ratio as a function of the burned gas fraction as seen in Figure 16, the specific heat

ratio varies between 1.30 to 1.36. By using the law of ideal gases, the predicted temperature at TDC (T_{TDC}) is calculated without regard to combustion as seen in Figure 17. This simplified method for estimating the temperature at TDC is normally an option for controlling the engine and it indicates that a temperature of ~ 1000 K is reached at TDC in most of the test area. This is also in line with earlier findings. At low load the engine has more part of the fuel injected in NVO period for fuel reformation due to limitation in EVC range in this high load set-up. This temperature increase is not reflected in the estimated T_{TDC}. At low engine speed there is also influence from the spark assisting, which is not reflected in the T_{TDC}. In Figure 18 the used EVC timing from this engine testing is seen.

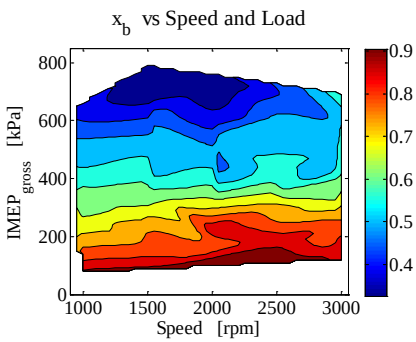

Figure 15: Burned gas fraction, x_b

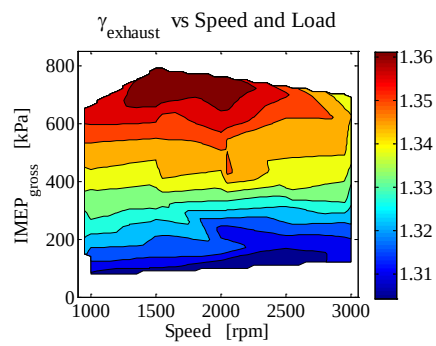

Figure 16: Specific heat ratio, γ

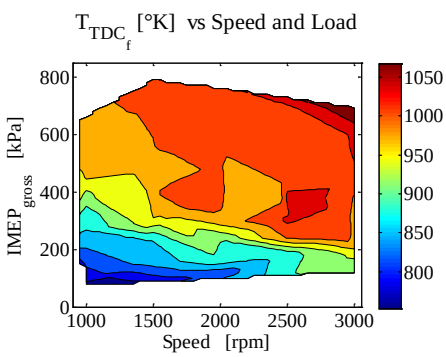

Figure 17: Temperature at TDC, T_{TDC}

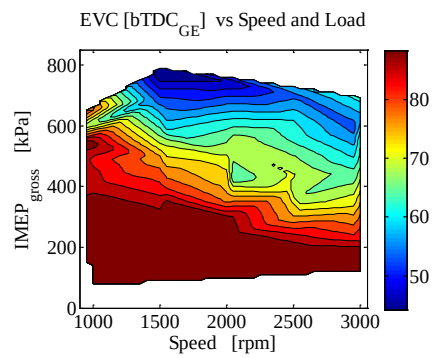

Figure 18: Exhaust valve closing timing, EVC

When simulating this turbocharged HCCI engine at normal and high load, the EVC position is set by the T_{TDC} by simple control blocks in the GT-Power simulating program as seen in Figure 19. This has shown that the predicted EVC position and therefore the boost pressure follow the real engine tests closely.

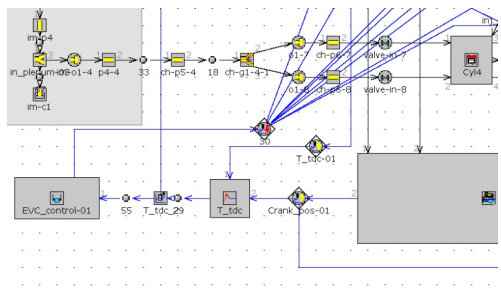

Figure 19: Temperature control in the engine simulating program

By using the combustion parameters shown above from this extensive operating range, it is possible to accurately predict this turbocharged HCCI engine using an engine simulating program as seen in Figure 20 and Figure 21. In this GT-Power simulation, the CA50 timing, the CA10 to CA90 duration and Wiebe constant follows the result dependent functions described above. The EVC position is controlled to have 1000 K at 5 CAD before TDC_f. The simulation is a full factorial [19] run where the engine speed and fuel amount are varied. The only variable that was map based from real engine testing was an imposed intake temperature. The difference at highest intake pressures (compared to Figure A-7) is due to simulation outside the turbocharger map range. These combustion functions have been used to evaluate different camshaft profiles and turbochargers etc. before any changes have been made to the test engine. Even if the presented data is unique for this engine set-up it can be used as a starting point for simulation of other HCCI concepts until enough data is collected to calibrate a suitable model. In this paper it is described how it can be done and it might then serve as a guideline for other HCCI simulations.

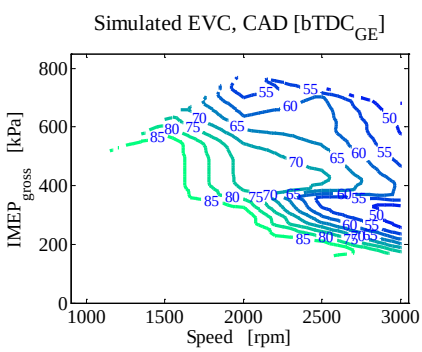

Figure 20: Simulated exhaust valve closing angle, EVC

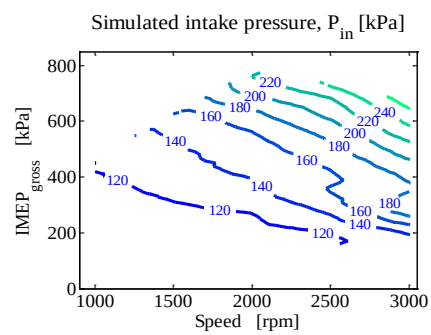

Figure 21: Simulated intake pressure, Pin

SUMMARY/CONCLUSIONS

In this paper it has been shown which limitations one can expect a HCCI engine will operate under. The results showed that it was the high soot level that limited the high load range at low engine speed. At medium speed it was limited by the combustion noise and peak cylinder pressure, at high engine speed the load range was limited by the turbocharger performance.

The combustion timing is an important parameter when operating in HCCI mode and it is even more important in a turbocharged engine since it also controls the mass flow in the engine for a given load. If the combustion timing is advanced for a given load more internal EGR is needed by an advanced exhaust valve closing timing and therefore the mass flow is reduced. It has been shown that the used CA50 timing scales to load and a trend line is presented that is used for simulation. Since the load and burned gas fraction are directly connected here, the CA50 could also been made to scale to the burned gas fraction but in a simulations it is usually easier to predict what kind of load that is going to be simulated.

The combustion duration is shown to increase with engine speed when looking at crank angle degrees but in the time domain it stays fairly constant for the used combustion timings in this test. The heat release from this operating range is used to find the Wiebe function constant; *m*, that can be used to describe the heat release rate for this turbocharged HCCI engine. The *m* constant is found by a non linear least square function which gives a Wiebe heat release that closely follows the real heat release. It is shown that the *m* constant a scale to load and a trend line is presented that is used for one-dimensional heat release simulations.

The exhaust valve closing timing needs to be closely predicted since it sets the combustion timing and also influences the mass flow in the engine by setting how much internal EGR is used. The calculated temperature at intake valve closing is used together with the burned gas fraction to predict in a simple way the temperature at TDC by using the ideal gas law. This calculation shows a temperature at ~1000 K at TDC. This temperature is used as a boundary condition for controlling the exhaust valve timing in the engine simulation and it will then predict the exhaust valve closing timing and therefore the intake pressure accurately.

REFERENCES

1. Thring, R. H., "Homogeneous-charge compression- ignition (HCCI) engines," SAE Technical Paper 892068, 1989.
2. Christensen, M., Hultqvist, A., Johansson, B.,, "Demonstrating the multi-fuel capability of a homogeneous charge compression ignition engine with variable compression ratio," SAE Technical Paper 1999-01-3679, 1999.
3. Haraldsson, G., Tunestål, P. , Johansson, B., Hyvönen, J., "HCCI combustion phasing in a multi-cylinder engine using variable compression ratio," SAE Technical Paper 2002-01-2858, 2002.
4. Lang, O., Salber, W., Hahn, J., Pischinger, S., Hortmann, K., Bücker, C., "Thermodynamical and mechanical approach towards a variable valve train for the controlled auto ignition combustion Process," SAE Technical Paper 2005-01-0762, 2005.
5. Martinez- Frias, J., Aceves, S. M., Flowers, D., Smith, R., Dibble, R., "HCCI engine control by thermal management," SAE Technical Paper 2000-01-2869, 2000.
6. Haraldsson, G., Tunestål, P. , Johansson, B., Hyvönen, J.,"HCCI closed- loop combustion control using fast thermal management," SAE Technical Paper 2004-01-0943, 2004.

7. Christensen, M., Johansson, B., Amnéus, P. Mauss, F., "Supercharged homogeneous charge compression ignition," SAE Technical Paper 980787, 1998.
8. Christensen, M., Johansson, B., "Supercharged homogeneous charge compression ignition (hcci) with exhaust gas recirculation and pilot fuel," SAE Technical Paper 2000-01-1835, 2000.
9. Hyvönen, J., Haraldsson, G., Johansson, B., "Supercharging HCCI to extend the operating range in a multi-cylinder VCR-HCCI engine," SAE Technical Paper 2003-01-3214, 2003.
10. Olsson, J-O., Tunestål, P., Johansson, B., "Boosting for high load HCCI," SAE Technical Paper 2004-01-0940, 2004.
11. Johansson, T., Johansson, B., Tunestål, P., Aulin, H., "HCCI operating range in a turbo-charged multi cylinder with VVT and spray- guided DI," SAE Technical Paper 2009-01-0494, 2009.
12. Johansson, T., Johansson, B., Tunestål, P., Aulin, H., "The effect of Intake Temperature in a Turbocharged Multi Cylinder Engine operating in HCCI mode," SAE Technical Paper 2009-24-0060, 2009.
13. Olsson, J-O., Tunestål, P., Ulfvik, J., Johansson, B., "The effect of cooled EGR on emissions and performance of a turbocharged HCCI engine," SAE Technical Paper 2003-01-0743, 2003.
14. Andreae, M.M, Cheng, W.K., Kenney, T., Yang, J., "On HCCI Engine Knock," SAE Paper 2007-01-1858, 2007.
15. Eng, J.A., "Characterization of pressure waves in HCCI combustion," SAE Technical Paper 2002-01-2859, 2002.
16. DieselNet, “Smoke Opacity,” http://www.dieselnet.com, Feb.2009.
17. Schindler, W., Nöst, M., Thaller, W., Luxbacher, T., "Stationäre und transiente messtechnische Erfassung niedriger Rauchwerte," MTZ 2001/10, October 2001.
18. Heywood, J. B., "Internal Combustion Engine Fundamentals," McGraw-Hill, New York, ISBN 0-07-028637-X: 390, 1988.
19. Box, G.E.P., Hunter, J.S., Hunter, W.G., “Statistics for Experimenters,” John Wiley & Sons, New Jersey, ISBN 0-471-71813-0, 2005

CONTACT INFORMATION

Thomas Johansson, M.Sc.ME

E-mail:Thomas.Johansson@energy.lth.se,Lund University, Faculty of Engineering, Department of Energy Sciences, Division of Combustion Engines P.O. Box 118, SE-221 00 Lund, Sweden

ACKNOWLEDGMENTS

This project is supported by SAAB Automobile Powertrain AB and the Swedish Energy Agency

DEFINITIONS/ABBREVIATIONS

BMEP	Brake Mean Effective Pressure
CA10	Crank angle 10 % burned
CA50	Crank angle 50 % burned
CA90	Crank angle 90 % burned
CB	Cylinder Balancing
CAD	Crank Angle Degrees
CoV	Coefficient of Variation
DI	Direct Injection
dP	Pressure derivate
EI	Emission Index
EGR	Exhaust Gas Recirculation
EVC	Exhaust Valve Closing
FSN	Filter Smoke Number
HCCI	Homogeneous Charge Compression Ignition
$IMEP_{gross}$	Indicated Mean Effective Pressure, gross
$IMEP_{net}$	Indicated Mean Effective Pressure, net
IVC	Intake Valve Closing
NA	Naturally Aspirated
NOx	Nitrogen Oxide
NVO	Negative Valve Overlap
MBT	Maximum Brake Torque
PCP	Peak Cylinder Pressure
RON	Research Octane Number
RI	Ringing Intensity
SI	Spark Ignition
STD	Standard Deviation
TDC	Top Dead Center
TDC_f	Top Dead Center, firing
TDC_{GE}	Top dead center, gas exchange
T_{IVC}	Temperature at IVC
T_{TDC}	Temperature at TDC
TWC	Three Way Catalyst
VVT	Variable Valve Timing
x_b	Burned gas fraction

APPENDIX

RESULTS FROM SPEED AND LOAD TESTING

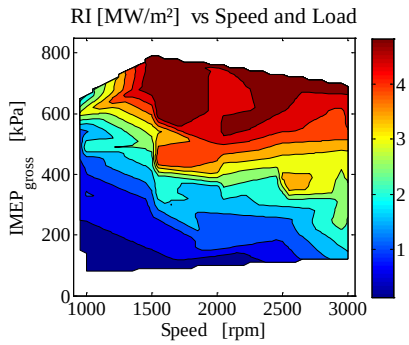

Figure A-1: Combustion noise, RI

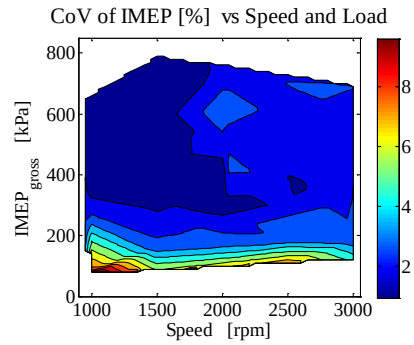

Figure A-2: Combustion stability, CoV of IMEP

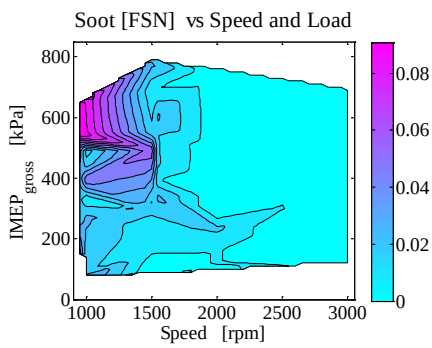

Figure A-3: Soot level, FSN

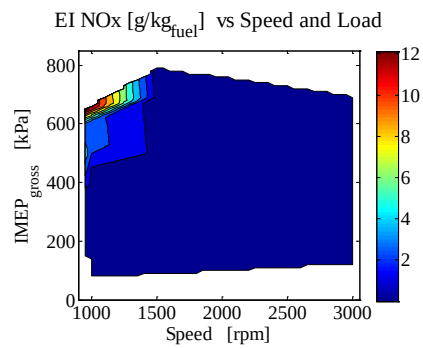

Figure A-4: Nitrogen oxides emission, EI NOx

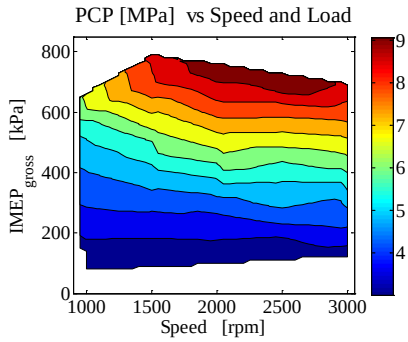

Figure A-5: Peak cylinder pressure, PCP

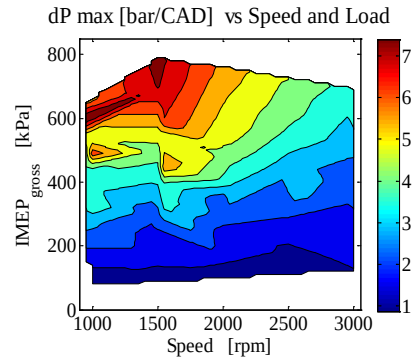

Figure A-6: Maximum pressure rise rate

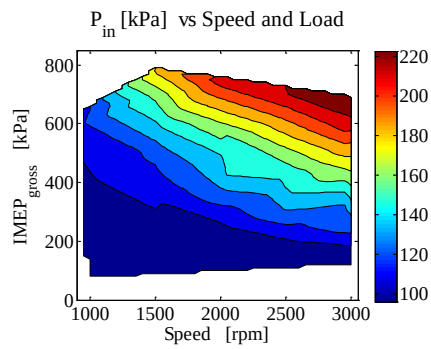

Figure A-7: Intake pressure, P_{in}

Paper VI

F2010A037

TURBOCHARGING TO EXTEND HCCI OPERATING RANGE IN A MULTI CYLINDER ENGINE- BENEFITS AND LIMITATIONS

[1]Johansson, Thomas[*], [1]Johansson, Bengt, [1]Tunestål, Per, [2]Aulin, Hans
[1]Division of Combustion Engines, Faculty of Engineering, Lund University, Sweden, [2]SAAB Automobile Powertrain AB, Sweden

KEYWORDS Direct injection, HCCI, Limitations, Negative valve overlap, Turbo charging

ABSTRACT

In the last decade there has been interest in Homogenous Charge Compression Ignition- HCCI as a way to increase the efficiency of the gasoline engine. The attractive properties are increased fuel efficiency due to reduced throttling losses, increased expansion ratio and higher thermodynamic efficiency. The main drawback of HCCI is the absence of direct combustion timing control. Therefore all the right conditions for auto ignition have to be set before combustion starts. The operating range in HCCI mode is restricted to relatively low load due to rapid combustion which results in high pressure rise rates and thus high combustion induced noise. In the last couple of years different car manufactures have shown concept engines operating in HCCI mode. General Motors has showcased a naturally aspirated HCCI engine operating in the low load regime. To evaluate if the load range in HCCI can be extended with increased inlet pressure our objective was to turbocharge an engine in HCCI mode. Through turbocharging the in-cylinder dilution is increased and the relative pressure rise rate can be decreased leading to a reduction of the combustion noise for a given load. The turbocharged test engine is an in-line four cylinder gasoline engine with a total displacement of 2.2 *l*. The engine is direct injected with spray-guided design. To achieve HCCI combustion the engine is operated with negative valve overlap by low lift and short duration valve timings where variable valve timing is used for combustion control. The effect of intake temperature, boost levels, combustion timing, intake valve timing, residual fraction and injection timing are demonstrated. From the results it can be seen how different settings affect intake pressure and hence combustion noise. The results show that the load range in turbocharged HCCI has been increased substantially compared to a naturally aspirated HCCI engine. The evaluation of different turbochargers and cam profiles has contributed to increased efficiency and load range capability. It can be operated from 1 bar indicated mean effective pressure to more than 6 bar, between 1000 and 3000 rpm. A comparison between a modern SI engine and this turbocharged HCCI engine shows that the HCCI engine can have up to 35 % higher fuel efficiency.

INTRODUCTION

In HCCI mode the air-fuel charge is auto ignited by controlling the temperature and pressure history inside the engine cylinder to initiate and phase the combustion phasing correctly. To reach auto ignition in a four-stroke engine the in-cylinder temperature is normally increased by exhaust gas recirculation (EGR), air heating or both. The concept with negative valve overlap (NVO) with early exhaust valve closing to trap a certain amount of hot residuals is widely

accepted to control combustion timing. Here the variable valve timing (VVT) is accurately controlled either mechanically or electrically. By boosting the engine in HCCI mode the acceptable load range can be extended (1,2,3,4,5) due to reduced combustion noise with more dilution. This makes the turbocharger performance vital to be able to cover a wide operating range. With NVO the intake temperature directly controls how much internal EGR is needed for a given combustion timing and therefore the in-cylinder residual fraction. By increasing the intake temperature, less internal EGR is needed. This leads to an increased exhaust mass flow that can lead to higher boost pressure (6). In addition to the internal EGR, external cooled EGR can be used.

The main operating parameter in HCCI mode is the combustion timing, here represented by the crank angle of 50 % heat released (CA50). The CA50 timing will affect the engine performance substantially and needs to be controlled exactly to run the HCCI engine successfully. If engine speed goes up or if load is increased the CA50 window for stable engine running will be narrowed, making the engine control more challenging. In this paper the results from parameters that affect the intake pressure and the capable load range in turbocharged HCCI mode is shown with the conditions that needs to be fulfilled. Since the application of HCCI has to meet consumer demand, emission legislation and control capability the real operating range is always a balance between these.

EXPERIMENTAL SET-UP

Engine system

The test engine is an in-line four cylinder gasoline engine with a total displacement of 2.2 *l*. The cylinder head is a 4-valve design with a pent-roof combustion chamber. The piston has a raised piston dome with a small bowl in the center. The engine has direct injection (DI) of a spray-guided type with a centrally placed injector. The spark plug is located close to the fuel injector and has an extended tip. The spark is always operated as a safety measure against misfires and it can also improve the combustion stability with late combustion timing.

To achieve HCCI combustion the engine is operated with NVO with low lift and short duration camshafts as seen in Figure 1. The VVT is controlled by hydraulic actuators at the camshafts giving a separate 50 crank angle degree (CAD) adjustment on both intake and exhaust valve timings. The turbocharged engine has an exhaust manifold of pulse type with short individual runners straight to the turbine inlet as seen in Figure 2. On the intake side there is a water cooled intercooler. The heated aluminum intake manifold has short intake runners and a small volume as seen in Figure 3. The cooling system has an electric water pump and the coolant temperature is adjusted by the control system. Engine specifications are listed in Table 1.

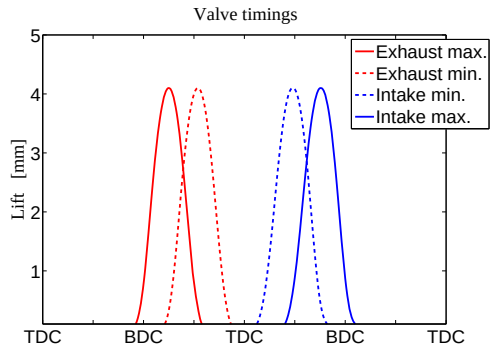

Figure 1: Valve timing range

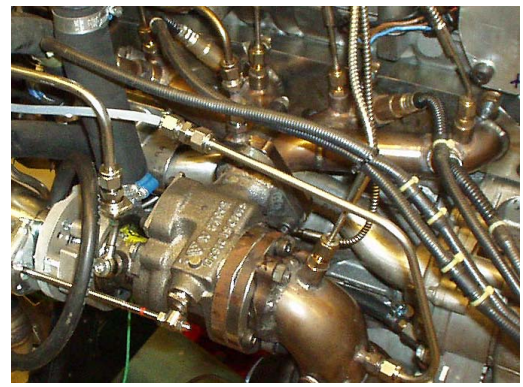

Figure 2: Exhaust manifold

Figure 3: Intake manifold

Table 1: Engine specifications

Number of cylinders	4
Displacement	2198 cm^3
Bore x Stroke	86 mm x 94.6 mm
Compression Ratio	11.75:1
Turbocharger	BorgWarner BV35, KP31
Fuel Supply	DI, up to 20 MPa pressure
Fuel Type	Gasoline, 95 RON

Measurement and control system

The control system is a combined data acquisition and engine control unit from dSPACE. The signals from a fully instrumented engine set-up are collected and analyzed. For combustion feedback there are individual cylinder pressure sensors. The control system has an in-cycle resolved heat release calculation where main parameters like CA50, peak cylinder pressure (PCP) and peak pressure derivative (dP/CAD) etc. are used for cylinder individual control in closed loop. Emission analysis and soot measurement are collected on an external PC and the data is sent to the control unit. To increase the operating range it is important that all the cylinders operate identically, meaning that they have the same CA50 position, indicated mean effective pressure ($IMEP_{net}$) and peak pressure rise rate. This means that the control system has to perform cylinder balancing. Injection of the fuel in NVO can give a reformation of the fuel with an increase in charge temperature and a reduction in effective octane number leading to more advanced combustion timing. The combustion timing will be more advanced if the fuel is injected in the beginning of the NVO than in the end. The control system sets the CA50 position and uses the cylinder with the most advanced CA50 position for the exhaust valve closing (EVC)

set point. The other cylinders are then advanced by adjusting the injection timing and/or fuel amount in the first injection, until all cylinders have the same CA50 position. Since there will be some differences in injection timing when using CA50 balancing there will also be some differences in efficiency between the cylinders. This results in different load, IMEP in the cylinders. To maximize the load range there has to be cylinder balancing of IMEP as well. This is done at the main injection event. Obviously this affects the CA50 balancing since increasing the fuel amount will raise the combustion heat, leading to earlier CA50 for that cylinder. Therefore the cylinder balancing has to be constantly monitored and adjusted by the control system. Table 2 shows the measurement and control equipment.

Table 2: Measurement and control system

ECU and data logging	dSPACE Rapid Pro
Cylinder pressure sensor	Kistler 6043Asp
Charge amplifier	Kistler 5011B
Emission analyzer	Horiba 9100 MEXA
Soot analyzer	AVL 415 S

Temperature and control system

The intake temperature is controlled by an electrical throttle in the bypass routing to the water-cooled intercooler circuit, see Figure 4. When the throttle is fully open the main air flow goes through the bypass routing due to less flow resistance compared to the intercooler circuit. By closing the throttle the airflow is forced through the intercooler circuit. The engine cooled long route EGR system takes exhaust gas after the turbine and route it to the compressor inlet, see Figure 4. To get a positive displacement of exhaust gas there is a throttle in the exhaust system to increase the back pressure. The external EGR is used when the engine is operated stoichiometric or when the pumping losses need to be reduced. The pumping losses can be reduced by adding cooled EGR to get more beneficial valve timings.

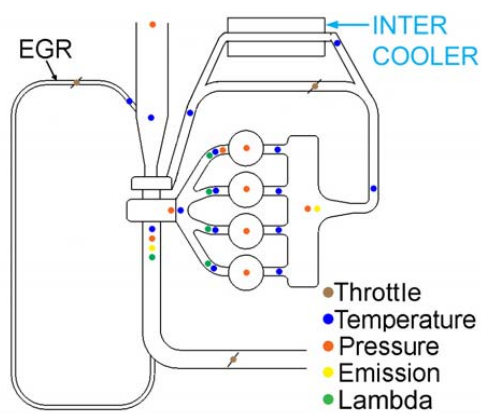

Figure 4: Engine layout

RESULTS AND DISCUSSION

Turbocharging

To increase the maximum load range in HCCI the combustion noise has to be controlled. When operating with NVO the mass flow through the engine is reduced since hot exhaust gas is trapped in the cylinder to initiate the auto ignition. Controlling the combustion timing with the amount of internal residuals influences the mass flow and therefore available boost pressure. In Figure 5, a CA50 sweep is performed with constant load at 2500 rpm. A later CA50 timing needs less internal residuals due to later EVC timing. As a result the mass flow is increased and hence boosts pressure.

Normally in a NVO HCCI engine the intake valve opening (IVO) timing is almost symmetrical to the EVC timing to reduce the pumping work during the gas exchange process. When load and boost pressure is increased, the exhaust and intake temperature are increased meaning that required EVC timing is delayed substantially. With this type of short duration valve timings the intake valve closing (IVC) can therefore be before bottom dead center (BDC). This will reduce the volumetric efficiency and reduce the in-cylinder pressure. In Figure 6, an IVO sweep is performed with a symmetrical starting point to latest possible IVO timing when the CA50 timing is kept constant. This also means that the EVC timing has to be changed continuously as the IVO timing is delayed to keep the chosen combustion timing as seen in Figure 6.

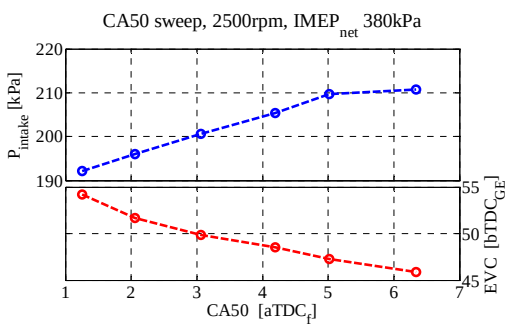

Figure 5: Intake pressure vs. combustion timing

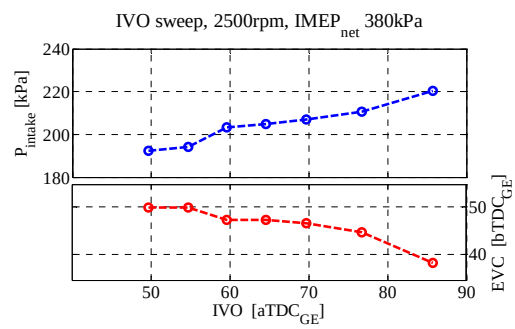

Figure 6: Intake pressure vs. intake valve opening timing

When the boost pressure is increased the intake temperature will increase. A higher intake temperature means that less internal EGR is needed for a set combustion timing. This will lead to an increased mass flow and higher intake pressure as seen in Figure 7. The intake temperature is measured 40mm from the intake valve and the temperature is regulated in the intercooler circuit. The thermal property of the intake system influences the mass flow. Keeping the intake charge hot with for example the heated intake manifold as seen in Figure 3 will increase the mass flow.

External cooled EGR can be used when the engine is operated stoichiometric due to high nitrogen oxide (NOx) emissions or to influence the pumping losses. When the external EGR is increased the mass flow through the engine is reduced due to the increased heat capacity of the

intake charge and more internal EGR is then needed to keep the combustion timing constant as seen in Figure 8.

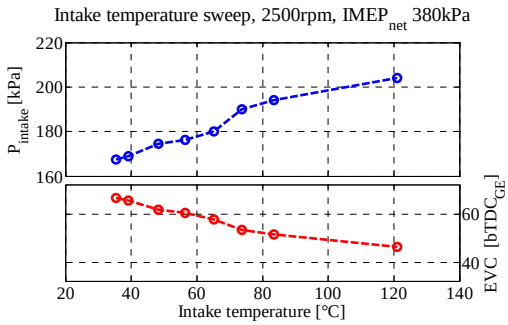

Figure 7: Intake pressure vs. intake temperature

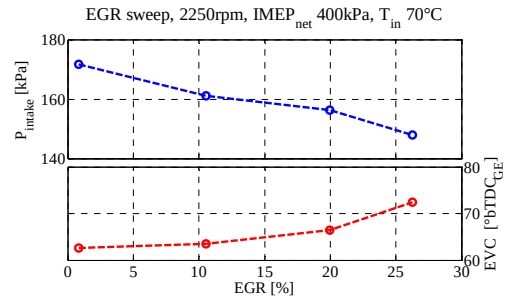

Figure 8: Intake pressure vs. external EGR

The engine coolant temperature will also directly control the intake pressure. A hot coolant temperature will have less heat losses and therefore less internal EGR is needed for a given combustion timing than at cold temperature. This means that a hot coolant temperature will have a higher mass flow than a cold one.

Normally the pressure rise rate is measured in bar/CAD or MPa/ms (7) and is used to impose some operating limits but neither of these catch the real combustion noise when the engine is supercharged, the Ringing Intensity (RI)- MW/m^2 (8) on the other hand compares the pressure rise rate to peak cylinder pressure and engine speed. In this study RI has been used as a criterion to limit the pressure rise rate. A higher intake pressure will not always automatically reduce the combustion noise for a given load since the pumping losses normally increase as well. With increasing pumping losses there is a need to burn more fuel to keep the load and this can counteract the effect of increased intake pressure. The Figure 9 shows a boost sweep done at 2500 rpm by actuating the wastegate. Here the RI is reduced by 8 MW/m^2 when going from low to high intake pressure.

To increase the load range of HCCI there is a need for high boost pressure at very low mass flows. There has not been a demand for this kind of small turbocharger so far which limits the availability of units in production. Our testing has mostly been with off the shelf diesel turbochargers. Figure 10 shows a comparison between two turbochargers, the BV35 is a 90 hp unit with variable geometry turbine (VGT) and the KP31 is a 47 hp unit with fixed turbine. As can be seen the smaller turbocharger is capable to deliver higher boost pressure all the way up to the maximum load here at 2000 rpm. The limitation for the small turbocharger starts at higher engine speeds where the turbine can get choked which leads to increasing pumping losses. But as described above, the mass flow can then be adjusted by appropriate settings for the combustion timing, IVO timing, intake temperature, cooling temperature and external EGR level.

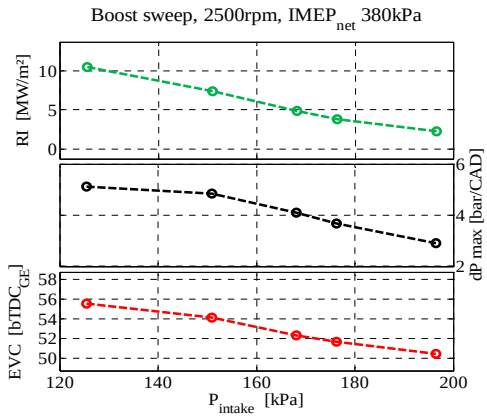

Figure 9: Ringing Intensity and peak pressure rise vs. intake pressure

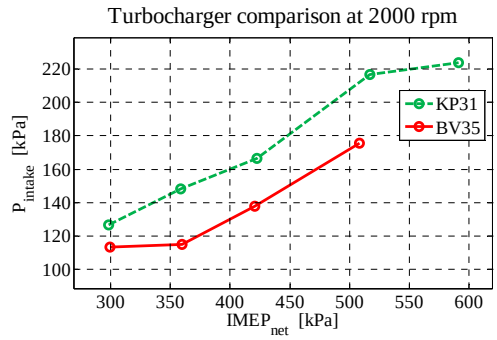

Figure 10: Turbocharger type vs. intake pressure

A challenge during a load transient with a turbocharger is that the boost pressure is normally lagging. This delayed boost pressure can then lead to an increase of the combustion noise reducing available practical load range. So the question is how to get something that we do not have (boost pressure). Recall that there is cylinder balancing by the control system where part of the fuel is injected during the NVO for fuel reformation. Normally we try to minimize this fuel reformation quantity to increase the efficiency and reduce engine out soot emissions. But for a load transient we can increase this fuel reformation quantity by advancing the injection timing for the first fuel is injection as seen in Figure 11. At this operating point, 2000 rpm and $IMEP_{net}$ of 400 kPa, the mass flow increased more than 25 % with the more advanced injection timing. This leads to an increase of boost pressure by 20 kPa (the combustion timing is constant at 6° $aTDC_f$ here). The increased fuel reformation with more advanced injection has to be counteracted by a reduction of the EVC timing to keep the combustion timing at the right position. As the EVC timing directly controls the mass flow the boost pressure can then be increased even before the actual load transient. As there is a limited amount of fuel that can be used for this reformation depending on exhaust conditions together with the EVC timing, the right fuel quantity has to be set to these conditions to counteract the fuel vaporization cooling effect.

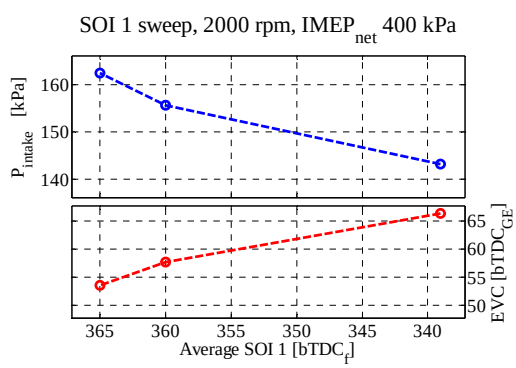

Figure 11: First injection timing vs. intake pressure

Pumping losses

The HCCI mode is known for its low pumping losses mainly due to the possibility to operate the engine unthrottled. With the addition of a turbocharger there is usually an increase of the pumping losses depending on the efficiency of the turbine and the compressor. In Figure 12 it can be seen that the pumping losses increase with load at a fairly high rate in this particular turbocharged HCCI setup with the low duration exhaust camshaft (125° duration).

By separating the pumping losses in two parts further information is available:

- PMEP= $\text{Throttling}_{valve}$ + (P_{ex} - P_{in})
- P_{ex} - P_{in}: The pressure loss over turbine/compressor, shown in Figure 12
- $\text{Throttling}_{valve}$: The pressure loss over inlet and exhaust valves, shown in Figure 12

The throttling losses originate from the short duration valve timings. For example, at high HCCI load, a late EVC timing is needed which can lead to that the exhaust valve opening (EVO) is after BDC. This will increase the pumping work from the blow-down process. To reduce the throttling losses a wide span of valve timings was evaluated in 1-D simulation to improve efficiency at all operating points. From the simulation result a new exhaust camshaft was manufactured with 25% longer duration. In Figure 13 it can be seen that the new longer duration camshaft manages to reduce the throttling losses substantially. The negative throttling losses at low load for the short duration camshaft are due to the extra fuel reformation with some heat release at TDC_{GE}. At high load the throttling losses were reduced by more than 40 kPa at 2000 rpm, the results at other engine speeds were similar.

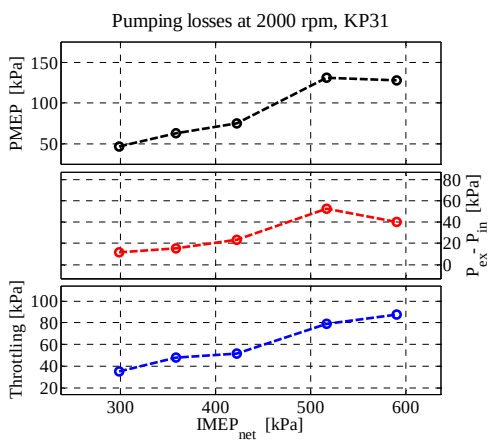

Figure 12: PMEP, P_{ex}-P_{in}, Valve throttling vs. Load

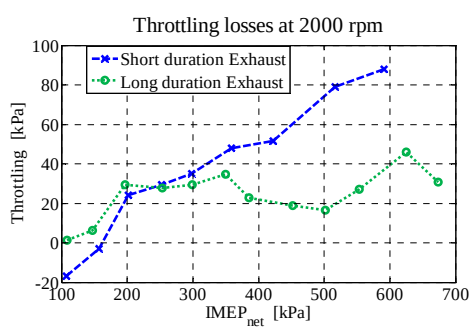

Figure 13: Throttling losses, new vs. old camshaft

OPERATING RANGE LIMITATIONS

By increasing the possible load range in HCCI the total efficiency can be increased and there will be less need for HCCI-SI mode switching that imposes in itself some challenging control tasks. The mode switching can for example involve mechanical switching between SI and HCCI camshaft profiles. In fairness the boosted HCCI to SI adds more complexity since the intake manifold pressure is different in HCCI and SI mode.
The possible operating range in HCCI mode is examined with following operating limitations applied (5).

- Combustion noise, RI below 6 MW/m^2
- Peak cylinder pressure, PCP below 9.5 MPa
- Combustion stability, CoV of $IMEP_{net}$ below 3.5 % (for low load- STD of $IMEP_{net}$ below 15 kPa)
- Soot emission, 0.05 FSN average
- Nitrogen oxides, Emission Index of NOx below 1.1 g/kg_{fuel} if lean, unlimited at stoichiometric

The load range between 1000 and 3000 rpm for this turbocharged engine can be seen in Figure 14. This is with the KP31 turbocharger and the long duration exhaust camshaft. Even if the focus for this turbocharged HCCI engine is to extend the load range upwards it is still possible to operate at low load as well. Since the VVT timing is limited to 50 degrees the low load points are performed with additional fuel reformation in the NVO or late injection with spark assist. The combustion noise here represented by RI is the hardest limitation to fulfill. To keep RI down and efficiency up the following parameters are optimized: the combustion timing, injection split and timing, intake valve timing, intake temperature, coolant temperature, external EGR usage, fuel pressure and ignition timing. The RI scales with load and what cannot be seen in this figure is the steep rise of RI if the combustion timing is slightly off the set position.

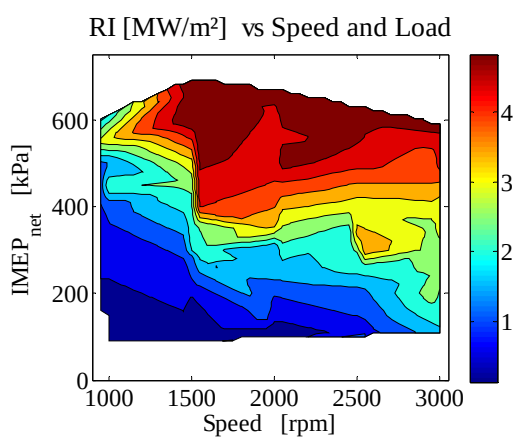

Figure 14: Combustion noise, Ringing Intensity, RI

The intake pressure scales with load and engine speed, as seen in Figure 15. The highest intake pressure is around 220 kPa (abs.). The limiting factor for the boost pressure is the small exhaust turbine which becomes choked at higher engine speeds, but on the other hand it is suitable to deliver boost at small mass flows. The boost pressure directly influences the peak cylinder pressure together with the IVC timing and specific heat ratio. At 2000 to 2500 rpm the PCP is a limiting factor as seen in Figure 16

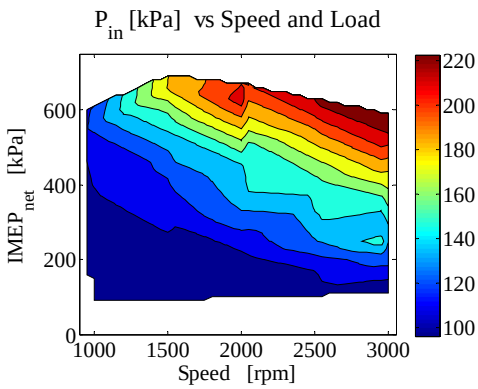

Figure 15: Intake pressure

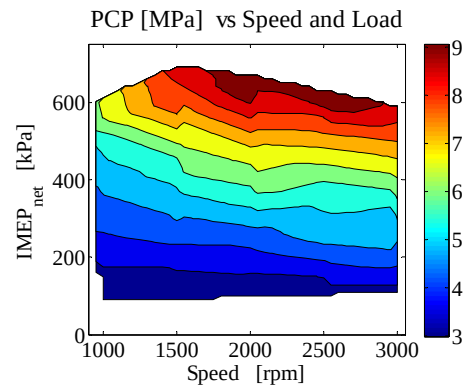

Figure 16: Peak cylinder pressure, PCP

HCCI is known for its low Coefficient of Variation (CoV) but normally CoV increases at late combustion timings. When load is increased the easiest way to reduce the combustion noise is to delay the combustion timing and here the turbocharged HCCI has an advantage over the NA HCCI. If there is boost pressure, the turbocharged HCCI engine can operate at a more advanced combustion timing than the NA HCCI engine and thus can increase the efficiency due to higher expansion ratio. This advanced combustion timing will also decrease the CoV for the turbocharged HCCI engine. In Figure 17, the CoV is seen and it is stable except at lowest load but here the operating limit is set by the standard deviation of IMEP instead. At high load or engine speed the CoV can increase drastically with just 1 degree change of the combustion timing which further increases the demand on the control system.

Injecting the fuel around TDC when the piston is close to the injector increases the risk for fuel impingement on the piston surface. This leaves a liquid fuel film that can lead to an increase in soot formation. A late injection timing will also increase the soot level and lower the efficiency. The soot level can be reduced by increasing the fuel pressure to enhance fuel vaporization, the fuel injector design together with piston design will also influence soot formation. When the dilution is increased as in the turbocharged HCCI engine soot is usually no problem due to the increased oxygen content. But at low engine speed the mass flow is not enough to increase the intake pressure. This leads to increasing soot emission as seen in Figure 18. The possible load at 1000 rpm was limited by the soot level.

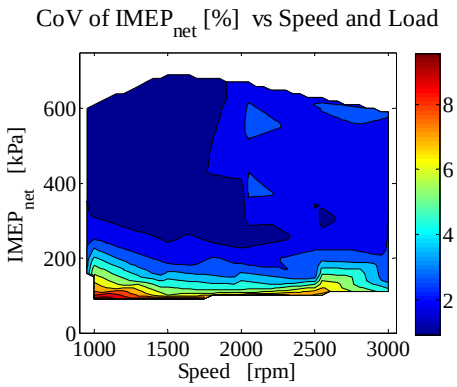

Figure 17: Combustion stability, CoV of IMEP$_{net}$

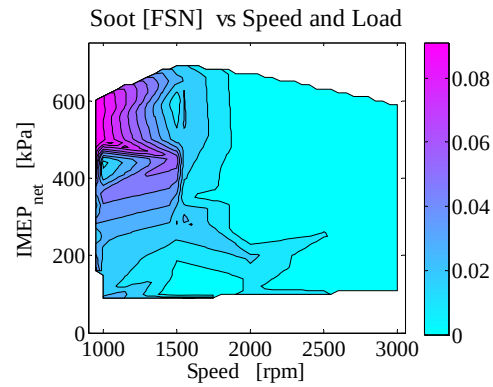

Figure 18: Soot emission, FSN

In HCCI mode the NOx emission is usually very low but when the load is high the NOx emissions can increase due to higher temperature and less dilution. With higher intake pressure the dilution increases and the NOx level is reduced. If the NOx level gets too high the engine need to be operated stoichiometric to meet the NOx legislation with a normal TWC. The NOx emission is low in the whole operating range except at 1000 rpm and high load as seen in Figure 19. To operate the engine stoichiometric, this engine uses external EGR. In Figure 20 the lambda is shown. The external EGR can be beneficial due to the thermodynamic cooling effect. With external EGR an advanced EVC timing is required in order to maintain constant combustion timing. Pumping losses can then be reduced due to more suitable valve timing at high load. The usage of EGR at 3000 rpm and high load is seen as reduced lambda level here. A drawback with EGR in HCCI mode is the relatively slow response in a system that is normally cycle to cycle controlled, especially during transients. Another drawback is the added weight and cost. Instead of using external EGR the boost pressure should be as high as possible to increase the dilution and suppress the NOx emissions but it has to be weighed against increasing pumping losses.

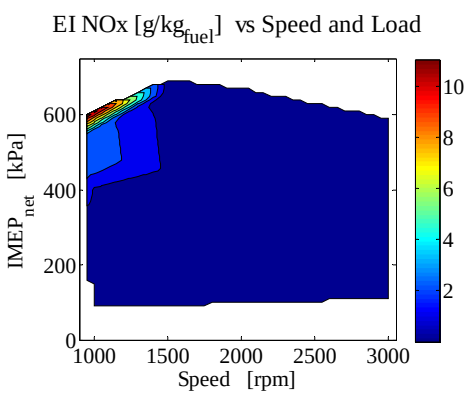

Figure 19: Emission Index Nitrogen oxides, EI NOx

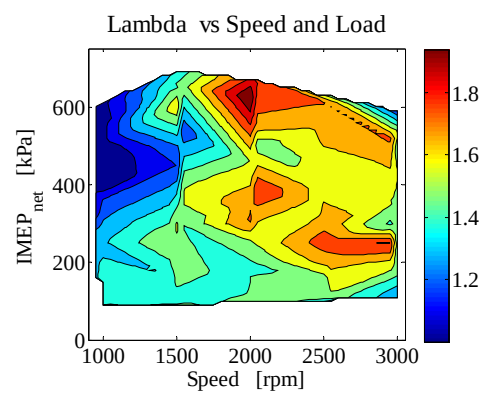

Figure 20: Lambda level

PROGRESS

The maximum operating range in this turbocharged HCCI engine has been increased during the project time due to improvement in hardware and operating strategies. In Figure 21 this evolution is seen. A baseline for comparison is the same engine in NA setup with the same operating limitations as for the turbocharged version. The main improvement in load range has come with a suitable turbocharger and reduction of the throttling losses by the long duration exhaust camshaft. There are still many areas left for improvement of this operating range, for example with a turbocharger adapted to HCCI, modification of the engine hardware and refinements of the control strategy.

The question is then why do we want to operate in HCCI mode? What we are trying to do is to improve the efficiency of the SI engine at low load and still keep the basic SI engine structure. When looking at the brake specific fuel consumption in Figure 22, the efficiency is rather even in the whole operating range except at low load and engine speed. One of this turbocharged HCCI project goals was to extend the operating range to a BMEP level above 500 kPa between 1000 and 3000 rpm with described operating limitations and this was also fulfilled. The area left for most improvement in this turbocharged HCCI engine is the gas exchange process as seen in Figure 23. At low load the efficiency is over 100 % due to some heat release during the NVO. The main pumping loss is from the turbocharger and the rest is then the valve throttling losses. In Figure 24 there is a comparison of this turbocharged HCCI engine and a direct injected 2.0 *l* turbocharged engine. The improvement can be up to 35% at low load. At the highest operating load there is no real improvement for this turbocharged set-up mostly due to the low gas exchange efficiency.

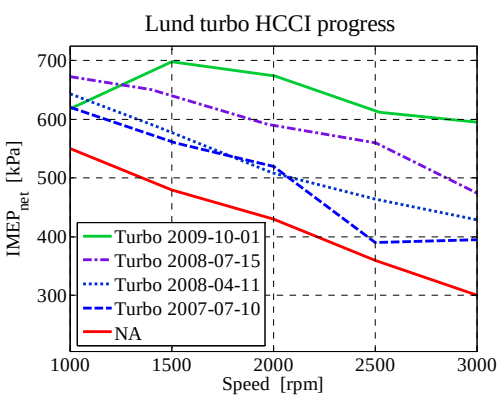

Figure 21: Maximum load range progress

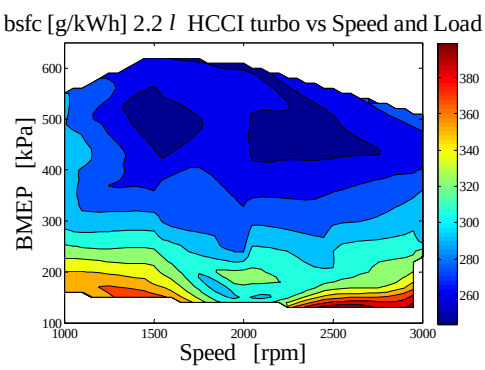

Figure 22: Brake specific fuel consumption, bsfc

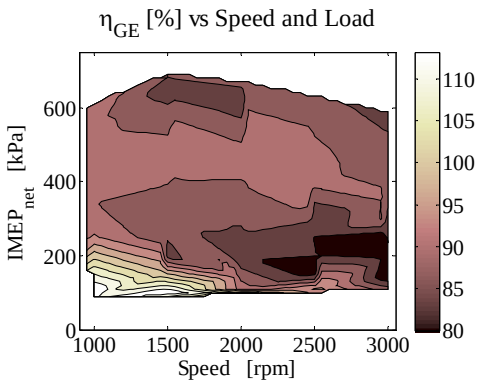

Figure 23: Gas exchange efficiency

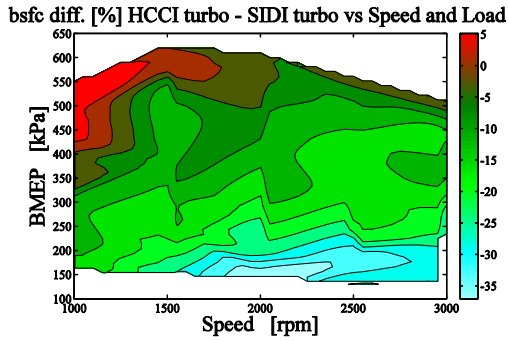

Figure 24: HCCI vs. SI engine, bsfc difference

SUMMARY AND CONCLUSIONS

In this paper it has been shown that the intake pressure in this turbocharged NVO HCCI engine depends on many variables. The mass flow and therefore the boost pressure can be altered by the combustion timing, the intake valve timing, the intake temperature and external EGR. This multi-dimension possibility gives the opportunity to operate turbocharged HCCI efficiently in a wide load and engine speed range. The soot emission limited the load range at 1000 rpm. At higher loads the combustion noise is always a challenge and RI limited operation at 1500 rpm. With the increased intake pressure the peak cylinder pressure limited the operating range at 2000 to 2500 rpm. At 3000 rpm the load range was limited by the turbocharger. The combustion stability was the limiting factor for minimum load at all engine speeds. With this turbocharged HCCI engine the NOx emission is low when there is boost pressure and did not limit operating range. At 1000 rpm the small mass flow was not enough to increase the intake pressure and the NOx emission rose above the set limit and the engine had to be operated stoichiometric.

A challenge with turbocharging and HCCI can be the delayed boost pressure during a load transient increasing the combustion noise. It is shown that by increasing the fuel reformation during the negative valve overlap the mass flow is increased leading to higher intake pressure. This can be used even before the actual load transient.

By choosing a better sized turbocharger it was possible to increase the operating range due to higher intake pressure leading to a reduction of the combustion noise. When the HCCI engine is turbocharged and operated at high load the pumping losses can be high, but these could be reduced substantially with the increased exhaust valve duration. It is shown that this turbocharged HCCI engine can have up to 35 % improvement in specific fuel consumption when compared to a modern direct injected turbocharged SI engine.

REFERENCES

(1) Christensen, M., Johansson, B., Amnéus, P. Mauss, F., "Supercharged homogeneous charge compression ignition," SAE Technical Paper 980787, 1998.
(2) Christensen, M., Johansson, B., "Supercharged homogeneous charge compression ignition (hcci) with exhaust gas recirculation and pilot fuel," SAE Technical Paper 2000-01-1835, 2000.
(3) Hyvönen, J., Haraldsson, G., Johansson, B., "Supercharging HCCI to extend the operating range in a multi-cylinder VCR-HCCI engine," SAE Technical Paper 2003-01-3214, 2003.
(4) Olsson, J-O., Tunestål, P., Johansson, B., "Boosting for high load HCCI," SAE Technical Paper 2004-01-0940, 2004.
(5) Johansson, T., Johansson, B., Tunestål, P., Aulin, H., "HCCI operating range in a turbo-charged multi cylinder with VVT and spray- guided DI," SAE Technical Paper 2009-01-0494, 2009.
(6) Johansson, T., Johansson, B., Tunestål, P., Aulin, H., "The effect of Intake Temperature in a Turbocharged Multi Cylinder Engine operating in HCCI mode," SAE Technical Paper 2009-24-0060, 2009.
(7) Andreae, M.M, Cheng, W.K., Kenney, T., Yang, J., "On HCCI Engine Knock," SAE Paper 2007-01-1858, 2007.
(8) Eng, J.A., "Characterization of pressure waves in HCCI combustion," SAE Technical Paper 2002-01-2859, 2002.